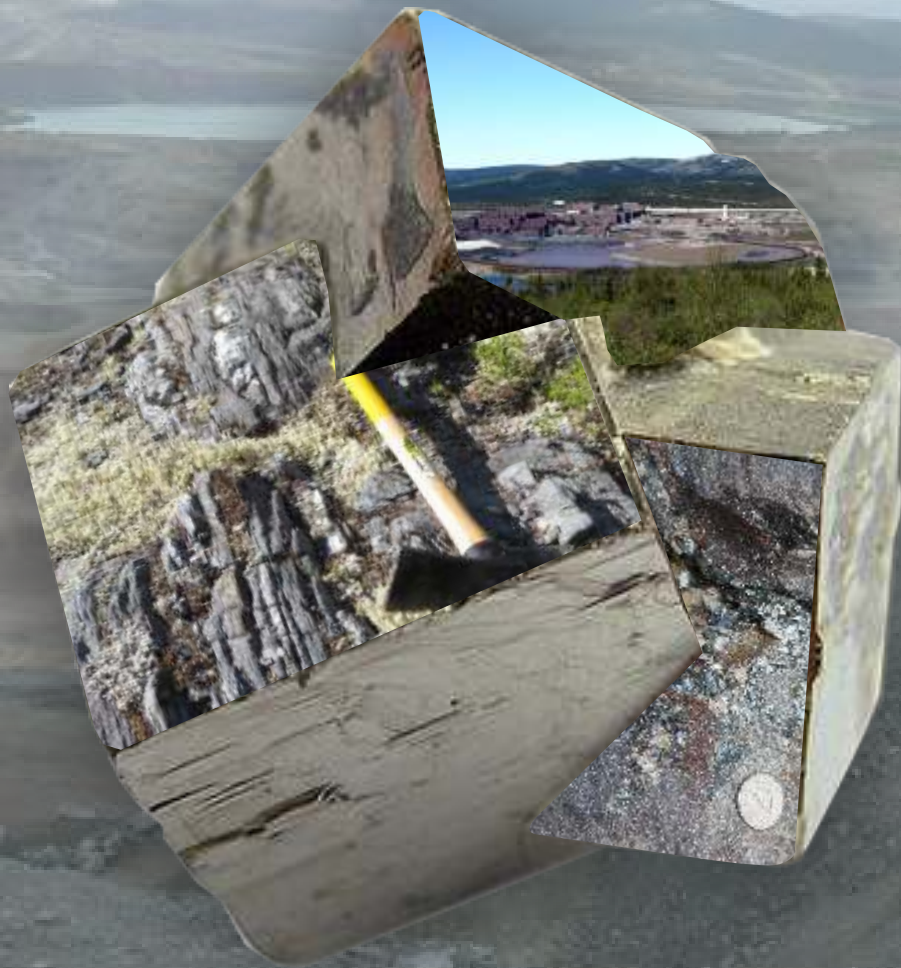


# IRON-ORE DEPOSITS OF SOUTHWESTERN LABRADOR



**J. Conliffe**

Occasional Paper 2019-01

St. John's, Newfoundland

2019







Mines

# IRON-ORE DEPOSITS OF SOUTHWESTERN LABRADOR

J. Conliffe

Occasional Paper 2019-01



St. John's, Newfoundland  
2019

## **NOTE**

The purchaser agrees not to provide a digital reproduction or copy of this product to a third party. Derivative products should acknowledge the source of the data.

## **DISCLAIMER**

The Geological Survey, a division of the Department of Natural Resources (the “authors and publishers”), retains the sole right to the original data and information found in any product produced. The authors and publishers assume no legal liability or responsibility for any alterations, changes or misrepresentations made by third parties with respect to these products or the original data. Furthermore, the Geological Survey assumes no liability with respect to digital reproductions or copies of original products or for derivative products made by third parties. Please consult with the Geological Survey in order to ensure originality and correctness of data and/or products.

### *Recommended citation:*

Conliffe, J.

2019: Iron-ore deposits of southwestern Labrador. Government of Newfoundland and Labrador, Department of Natural Resources, Geological Survey, St. John’s, Occasional Paper 2019-01, 210 pages.

### *Author Address*

J. Conliffe  
Mineral Deposits Section  
Department of Natural Resources  
P.O. Box 8700  
St. John’s, NL  
A1B 4J6  
(Email: jamesconliffe@gov.nl.ca)

# CONTENTS

	Page
<b>ABSTRACT</b> .....	xiii
<b>PART A</b>	
<b>INTRODUCTION</b> .....	1
PURPOSE AND SCOPE .....	1
PREVIOUS WORK .....	1
<b>HISTORY OF EXPLORATION</b> .....	1
<b>REGIONAL GEOLOGY</b> .....	11
LITHOTECTONIC ZONES AND METAMORPHIC TERRANES IN WESTERN LABRADOR .....	13
<b>GEOLOGY OF THE GAGNON TERRANE</b> .....	16
STRATIGRAPHY .....	16
Ashuanipi Complex .....	16
Le Fer (Attikamagen) Formation .....	16
Denault Formation .....	17
Dolly Formation .....	17
McKay River Formation .....	17
Wishart Formation .....	18
Ruth Formation .....	18
Menihek Formation .....	18
Shabogamo Gabbro .....	18
Michel Lake Pluton .....	19
Restoration of the Sedimentary Basin .....	19
Distinguishing between Metamorphosed Rock Units .....	19
STRUCTURAL GEOLOGY .....	19
LITHOTECTONIC DOMAINS .....	20
REGIONAL METAMORPHISM .....	22
<b>SOKOMAN FORMATION</b> .....	24
IRON FORMATION FACIES AND MINERALOGY .....	25
Oxide Facies .....	25
Carbonate Facies .....	26
Silicate Facies .....	27
STRATIGRAPHY .....	28
Carol Lake Basin .....	28
Wabush Basin .....	30
Scully Deposit .....	30
Rose Deposit .....	32
Other Occurrences .....	33
Mills Lake Basin .....	33
Other Occurrences .....	33
GRENVILLIAN DEFORMATION AND METAMORPHISM .....	34
LATE-STAGE ALTERATION .....	35
<b>GEOCHEMISTRY</b> .....	37
SAMPLING AND METHODOLOGY .....	37
MAJOR-ELEMENT GEOCHEMISTRY .....	39

Carol Lake Basin . . . . .	39
Wabush Basin . . . . .	40
Mills Lake Basin . . . . .	40
TRACE-ELEMENT GEOCHEMISTRY . . . . .	40
Carol Lake Basin . . . . .	40
Wabush Basin . . . . .	40
Mills Lake Basin . . . . .	42
RARE-EARTH-ELEMENT (REE) GEOCHEMISTRY . . . . .	44
Carol Lake Basin . . . . .	45
Wabush Basin . . . . .	46
Mills Lake Basin . . . . .	46
DISCUSSION . . . . .	47
Depositional Environment of Oxide-facies Iron Formation . . . . .	47
Depositional Environment of the Basal Silicate Iron Formation . . . . .	48
Late-stage Alteration . . . . .	49
<b>SUMMARY AND CONCLUSIONS . . . . .</b>	<b>49</b>

**PART B**

<b>INTRODUCTION . . . . .</b>	<b>51</b>
<b>NOTES ON THE STRUCTURE OF PART B . . . . .</b>	<b>51</b>
<b>PROSPECT/DEPOSIT DESCRIPTIONS . . . . .</b>	<b>54</b>
1. CANNING . . . . .	54
2. CAROL LAKE NORTH . . . . .	57
3. D’AIGLE BAY 1 . . . . .	60
4. D’AIGLE BAY 2 NORTH . . . . .	62
5. D’AIGLE BAY 2 SOUTH . . . . .	66
6. DULEY . . . . .	69
7. EMMA LAKE . . . . .	73
8. FLATROCK LAKE . . . . .	75
9. GOETHITE BAY . . . . .	78
10. GOETHITE BAY NORTH . . . . .	81
11. GREEN WATER LAKE . . . . .	83
12. HUGUETTE LAKE . . . . .	85
13. HUMPHREY . . . . .	87
14. IRONSTONE . . . . .	92
15. JULIENNE 1 . . . . .	94
16. JULIENNE 2 . . . . .	97
17. JULIENNE LAKE . . . . .	100
18. KNIGHT . . . . .	104
19. KNIGHT NORTH . . . . .	108
20. KNIGHT SOUTH . . . . .	110
21. LORRAINE 4 . . . . .	113
22. LUCE . . . . .	115
23. MILL BASIN . . . . .	119
24. MILLS LAKE . . . . .	122
25. NEAL 1 . . . . .	126
26. POLLY LAKE . . . . .	128
27. ROSE . . . . .	132

	Page
28. SCULLY . . . . .	137
29. SHABO HILL . . . . .	142
30. SHABO PENINSULA NORTH . . . . .	144
31. SHABOGAMO . . . . .	146
32. SITTING BEAR . . . . .	149
33. SMALLWOOD NORTH . . . . .	151
34. SQUID . . . . .	154
35. WABUSH 1 . . . . .	156
36. WABUSH 3 . . . . .	159
37. WABUSH 4 . . . . .	163
38. WABUSH 6 . . . . .	166
39. WABUSH MOUNTAIN . . . . .	169
40. WHITE LAKE . . . . .	171
<b>ACKNOWLEDGMENTS</b> . . . . .	174
<b>REFERENCES</b> . . . . .	174
<b>APPENDICES</b> . . . . .	191
APPENDIX A: Sample Descriptions	
APPENDIX B: Major and Trace Element Data for Outcrop, Drillcore and Pulp Samples	
APPENDIX C: Major-element ICP-OES-FUS Standards and Duplicate Data	
APPENDIX D: Trace-element ICP-OES Standards and Duplicate Data	
APPENDIX E: Trace-element ICP-MS-FUS Standards and Duplicate Data	
APPENDIX F: Exploration Drill-log Database (post-2000)	



## FIGURES

Figure 1.	Map showing the location of the Labrador Trough. . . . .	2
Figure 2.	Simplified topographic map of the study area, showing location of the main geographical features. . . . .	3
Figure 3.	Location of the major iron-ore occurrences in the study area . . . . .	4
Figure 4.	Lithological map, showing the location of schematic restored cross-sections through the continental margin prior to Grenvillian deformation (A-A*, B-B*; Figure 10) and structural cross-sections (C-C', D-D', E-E'; Figure 13). Geological map adapted from unpublished company data (IOC and Alderon) and published maps of the study area (Rivers 1985a, b; Rivers and Massey, 1985; van Gool, 1992) . . . . .	6
Figure 5.	Regional aeromagnetic map of the study area (2 <sup>nd</sup> vertical derivative colour-shade image, shaded from the northwest). Adapted from Cotnoir <i>et al.</i> (2002). . . . .	7
Figure 6.	Aerial photograph showing the location of current, past and future mining activity in the Carol Project area (image courtesy of IOC) . . . . .	9
Figure 7.	Simplified stratigraphy of the Kaniapiskau Supergroup and the underlying Archean basement in the Schefferville Zone . . . . .	12
Figure 8.	Location of major lithotectonic zones in the Labrador Trough and limits of deformation associated with the Hudsonian and Grenville orogenies. Compiled from Wardle and Bailey (1981); Clark and Wares (2005) and van Gool <i>et al.</i> (2008) . . . . .	14
Figure 9.	Schematic stratigraphy of the Kaniapiskau Supergroup in the Tamarack and Schefferville zones in the central Labrador Trough . . . . .	15
Figure 10.	Schematic restored cross-sections through the continental margin in the study area prior to Grenvillian deformation (from van Gool, 1992). Location of cross-sections shown in Figure 4 . . . . .	17
Figure 11.	Schematic tectonic model for the development of the dual-level, fold-thrust belt in the Gagnon terrane, with open and filled triangles as control points. A) The extended Archean basement with inactive Paleoproterozoic normal faults and Knob Lake Group prior to the Grenvillian Orogeny; B) Emplacement of the Molson Lake terrane as a thrust wedge on top of the extended Paleoproterozoic continental margin; C and D) Progressive development of the thin-skinned, upper-level thrust stack; E) Formation of the lower, thick-skinned, level of the thrust stack, with local out-of-sequence thrusting in the upper system. Normal faulting at the top of the wedge occurred after formation of the lower thrust system. Adapted from van Gool <i>et al.</i> (2008); <i>see</i> text and van Gool <i>et al.</i> ( <i>op. cit.</i> ) for detailed discussion . . . . .	21
Figure 12.	Lithotectonic domains in the study area, as defined by van Gool (1992) and van Gool <i>et al.</i> (2008). C-C', D-D', E-E' refer to cross-sections shown in Figure 13. Adapted from van Gool <i>et al.</i> (2008) . . . . .	22
Figure 13.	Geological cross-sections through the Gagnon terrane ( <i>see</i> Figures 4 and 12 for locations). FLSZ, Flora Lake Shear Zone; GF, Grenville Front; MLT, Molson Lake terrane; EL, erosion level; Lr and Ur, lower and upper levels of the thrust belt. Adapted from van Gool <i>et al.</i> (2008). . . . .	23
Figure 14.	Map showing metamorphic zones and isograds in pelitic and semipelitic rocks in the Gagnon terrane (after Rivers, 1983b) with estimated P-T conditions from garnet and coexisting matrix minerals in quartz-garnet-biotite ± kyanite ± plagioclase ± muscovite ± leucosome assemblages (after van Gool, 1992). Adapted from van Gool <i>et al.</i> (2008). Bt = Biotite; Chl = Chlorite; Grt = Garnet; Ky = Kyanite; Ms = Muscovite; St = Staurolite. . . . .	24
Figure 15.	Location of the Carol Lake, Wabush and Mills Lake basins described in the text. Refer to Figure 3 for locations of individual iron-ore occurrences mentioned in the text . . . . .	28
Figure 16.	Stratigraphic column for the Sokoman Formation in the Carol Lake area (after Muwais, 1974) . . . . .	29
Figure 17.	Stratigraphic column for the Sokoman Formation in the Scully deposit (Wabush Mines) and Rose deposit. Compiled from unpublished company data and lithological descriptions in O'Leary (1973); Farquharson and Thalenhorst (2006) and Lyons <i>et al.</i> (2013) . . . . .	31

Figure 18.	Map showing alignment of zones of strong secondary alteration in the Sokoman Formation in the Scully deposit, Canning prospect and eastern part of the White Lake prospect. Also shown is the location of the strongly altered Wishart Formation quartzite in a quarry north of the Trans-Labrador Highway. Broken black line indicates location of major northwest–south-east-trending reverse fault in the Scully deposit, broken red line indicates likely extension of this fault to the northwest through the Canning prospect and broken pink line indicates possible continuation of this fault to the eastern portion of the White Lake prospect. . . . .	37
Figure 19.	Bivariate plots of $\text{Fe}_2\text{O}_3$ vs. select major elements for samples of oxide-facies iron formation in the Carol Lake, Wabush and Mills Lake basins . . . . .	41
Figure 20.	Bivariate plots of $\text{Fe}_2\text{O}_3$ vs. select major elements for samples of BSIF in the Wabush and Mills Lake basins. Also included are the average values of oxide-facies iron formation samples from the same basins . . . . .	42
Figure 21.	A) Trace-element composition of oxide-facies iron formation and BSIF from the Carol Lake, Wabush and Mills Lake basins; B) Trace-element composition of oxide-facies iron formation from the Carol Lake, Wabush and Mills Lake basins normalized against the average value of taconite from the Schefferville area (data from Conliffe, 2016a). . . . .	43
Figure 22.	The REE distribution patterns normalized to Post-Archean average Australian Shale (PAAS) for weakly altered oxide-facies iron formation in the Carol Lake, Wabush and Mills Lake basins. Samples from the Carol Lake Basin separate into deposits from the mine area of the Carol Project, samples from south of the mine area (Polly Lake and Knight prospects) and samples from north and west of the mine area (D’Aigle Bay 2 North prospect and Squid showing). <i>See text for details.</i> . . . . .	44
Figure 23.	Bivariate plots of $\text{Pr}/\text{Yb}_{(\text{SN})}$ and $\text{Y}/\text{Ho}$ against total REE ( $\Sigma\text{REE}$ ) concentration of oxide-facies iron formation in the Carol Lake and Wabush basins. Samples from the Carol Lake Basin separate into deposits from the mine area of the Carol Project, samples from south of the mine area (Polly Lake and Knight prospects) and samples from north and west of the mine area (D’Aigle Bay 2 North prospect and Squid showing). <i>See text for details</i> . . . . .	45
Figure 24.	Bivariate plots of $\text{Ce}/\text{Ce}^*_{(\text{SN})}$ vs. $\text{Pr}/\text{Pr}^*_{(\text{SN})}$ (showing true Ce anomalies) and $\text{Eu}/\text{Eu}^*_{(\text{SN})}$ vs. $\text{Sm}/\text{Sm}^*_{(\text{SN})}$ (showing true Eu anomalies) from oxide-facies iron formation in the Carol Lake, Wabush and Mills Lake basins. Grey areas indicate no significant anomalies. <i>See text for details.</i> . . . . .	46
Figure 25.	A) Model of ocean redox structure in the late Paleoproterozoic based on REE analyses from iron formations (adapted from Planavsky <i>et al.</i> , 2010). The model shows a mechanism for the transport of metal and Ce oxides from oxic-shallow seawater across the redoxcline, with dissolution of Mn-oxides in anoxic waters lowering Y/Ho ratios and increasing LREE to HREE ratios ( <i>see schematic REE profiles</i> ); B) Average REE distribution patterns normalized to Post-Archean average Australian Shale (PAAS) for weakly altered oxide-facies iron formation in the Carol Lake (mine area) and Wabush basins, showing increased LREE to HREE ratios in the Wabush Basin related to deposition in deeper water below the redoxcline . . . . .	48
Figure 26.	Overview map showing location of individual showings, prospects and deposits discussed in detail. Number refers to deposit number listed in Table 1. For detailed location of showing, prospects and deposits in the area indicated by the black box outline, <i>see</i> Figure 27 . . . . .	52
Figure 27.	Map showing location of individual showings, prospects and deposits. Numbers refer to deposits in Table 1. . . . .	53
Figure 28.	A) Geological map of the Canning prospect (adapted from Cotnoir <i>et al.</i> , 2002), showing location of drillholes from 1971, 2010 and 2011 exploration programs (Muwais and Broemling, 1971; Carter, 2011a; Marshall, 2012a); B) Airborne magnetics (second vertical derivative) showing the extent of iron formation (data from Cotnoir <i>et al.</i> , 2002) . . . . .	54
Figure 29.	A) Geological map of the Carol Lake North area (adapted from Cotnoir <i>et al.</i> , 2002), showing location of drillholes from 2010, 2011 and 2012 drilling programs (Hovis and Goldner, 2011a; Goldner and Sauve, 2012; Goldner <i>et al.</i> , 2013); B) Airborne magnetics (second vertical derivative) showing extent of iron formation (data from Cotnoir <i>et al.</i> , 2002) . . . . .	57

Figure 30.	A) Geological map of the D'Aigle Bay area (adapted from Cotnoir <i>et al.</i> , 2002), showing location of drillhole from 2006 drilling program (Clark, 2006); B) Airborne magnetics (second vertical derivative) showing extent of iron formation (data from Cotnoir <i>et al.</i> , 2002) . . . . .	61
Figure 31.	Geological maps and aeromagnetic data from the D'Aigle Bay 2 North prospect in the Bondurant Lake area, showing location of drillhole from 2010 drilling program (Carter, 2011b). A) Geological map of Rivers and Massey (1985); B) Geological map based on IOC mapping (adapted from Cotnoir <i>et al.</i> , 2002); C) Airborne magnetics (second vertical derivative) in the Bondurant Lake area, showing extent of iron formation (data from Cotnoir <i>et al.</i> , 2002) . . . . .	63
Figure 32.	A) Geological map of the D'Aigle Bay 2 South prospect (adapted from Cotnoir <i>et al.</i> , 2002), showing location of drillholes from 2005 and 2010 exploration programs (Darch, 2005a; Carter, 2011b); B) Airborne magnetics (second vertical derivative) showing extent of iron formation (data from Cotnoir <i>et al.</i> , 2002) . . . . .	66
Figure 33.	A) Geological map of the Duley prospect (adapted from Cotnoir <i>et al.</i> , 2002), showing location of drillholes from 2010 exploration programs (Carter, 2011c); B) Airborne magnetics (second vertical derivative) showing extent of iron formation (data from Cotnoir <i>et al.</i> , 2002) . . . . .	69
Figure 34.	A) Geological map of the Emma Lake showing (adapted from Cotnoir <i>et al.</i> , 2002), showing location of drillholes from 2012 exploration programs (Steele, 2013); B) Airborne magnetics (second vertical derivative) showing extent of iron formation (data from Cotnoir <i>et al.</i> , 2002). . . . .	73
Figure 35.	A) Geological map of the Flatrock Lake area (adapted from Cotnoir <i>et al.</i> , 2002), showing location of drillholes from 2010 and 2011 drilling programs (Hovis and Goldner, 2011b, 2012); B) Airborne magnetics (second vertical derivative) showing extent of iron formation (data from Cotnoir <i>et al.</i> , 2002) . . . . .	75
Figure 36.	A) Geological map of the Goethite Bay area (adapted from Cotnoir <i>et al.</i> , 2002), showing location of drillholes from 2010, 2011 and 2012 drilling programs (Hovis and Goldner, 2011b; 2012; Goldner <i>et al.</i> , 2013); B) Airborne magnetics (second vertical derivative) showing extent of iron formation (data from Cotnoir <i>et al.</i> , 2002). . . . .	78
Figure 37.	A) Geological map of the Goethite Bay North area (adapted from Cotnoir <i>et al.</i> , 2002), showing location of drillhole 10LB0011 from 2010 drilling program (Hovis and Broadbent, 2010); B) Airborne magnetics (second vertical derivative) showing extent of iron formation (data from Cotnoir <i>et al.</i> , 2002) . . . . .	81
Figure 38.	A) Geological map of the Green Water Lake showing (adapted from Cotnoir <i>et al.</i> , 2002), showing location of drillhole from 2012 exploration program (Goldner <i>et al.</i> , 2013); B) Airborne magnetics (second vertical derivative) showing extent of iron formation (data from Cotnoir <i>et al.</i> , 2002). . . . .	83
Figure 39.	A) Geological map of the Huguette Lake showing (adapted from Cotnoir <i>et al.</i> , 2002), showing location of drillholes from 2010 and 2011 exploration programs (Hovis and Goldner, 2011b; Wallace, 2012b); B) Airborne magnetics (second vertical derivative) showing extent of iron formation (data from Cotnoir <i>et al.</i> , 2002) . . . . .	85
Figure 40.	Aerial photograph of the Humphrey deposit, showing location of the active and dormant pits discussed in text (image courtesy of IOC) . . . . .	87
Figure 41.	A) Geological map of the Humphrey deposit showing location of active and dormant pits discussed in text and of former Smallwood mine (adapted from Cotnoir <i>et al.</i> , 2002); B) Airborne magnetics (second vertical derivative) showing extent of iron formation (data from Cotnoir <i>et al.</i> , 2002). . . . .	88
Figure 42.	A) Geological map of the Ironstone showing (adapted from Cotnoir <i>et al.</i> , 2002), showing location of drillholes from 2010 exploration program (Carter, 2011d); B) Airborne magnetics (second vertical derivative) showing extent of iron formation (data from Cotnoir <i>et al.</i> , 2002) . . . . .	92
Figure 43.	A) Geological map of the Julienne 1 prospect (adapted from Cotnoir <i>et al.</i> , 2002) showing location of drillholes from 2006 and 2012 exploration programs (Clark, 2007a; Goldner <i>et al.</i> , 2013); B) Airborne magnetics (second vertical derivative) (data from Cotnoir <i>et al.</i> , 2002) . . . . .	94

Figure 44.	A) Geological map of the Julienne 2 prospect (adapted from Cotnoir <i>et al.</i> , 2002), showing location of drillholes from 2001 and 2010 exploration programs (Cotnoir <i>et al.</i> , 2002; Carter, 2011d); B) Airborne magnetics (second vertical derivative) showing extent of iron formation (data from Cotnoir <i>et al.</i> , 2002) . . . . .	97
Figure 45.	A) Geological map of the Julienne Lake deposit (adapted from Cotnoir <i>et al.</i> , 2002), showing location of drillholes from 2010 and 2012 exploration programs (Coates <i>et al.</i> , 2012; Seymour <i>et al.</i> , 2012); B) Airborne magnetics (second vertical derivative) of Julienne Lake Peninsula, showing extent of iron formation and extension of the deposit into Julienne Lake (data from Cotnoir <i>et al.</i> , 2002). . . . .	100
Figure 46.	A) Geological map of the Knight prospect (adapted from Cotnoir <i>et al.</i> , 2002), showing location of drillholes from 2001 and 2006 exploration programs (Cotnoir <i>et al.</i> , 2002; Clark, 2007b); B) Airborne magnetics (second vertical derivative) showing extent of iron formation (data from Cotnoir <i>et al.</i> , 2002). . . . .	104
Figure 47.	A) Geological map of the Knight North showing (adapted from Cotnoir <i>et al.</i> , 2002), showing outcrop sample locations from 2001 exploration programs (Cotnoir <i>et al.</i> , 2002); B) Airborne magnetics (second vertical derivative) showing extent of iron formation (data from Cotnoir <i>et al.</i> , 2002). . . . .	108
Figure 48.	A) Geological map of the Knight South prospect (adapted from Cotnoir <i>et al.</i> , 2002), showing location of drillholes from 2002 exploration program (Darch and Goodman, 2003); B) Airborne magnetics (second vertical derivative) showing extent of iron formation (data from Cotnoir <i>et al.</i> , 2002). . . . .	110
Figure 49.	A) Geological map of the Lorraine 4 prospect (adapted from Cotnoir <i>et al.</i> , 2002), showing location of drillholes from 1985 exploration program (Simpson <i>et al.</i> , 1985); B) Airborne magnetics (second vertical derivative) showing extent of iron formation (data from Cotnoir <i>et al.</i> , 2002) . . . . .	113
Figure 50.	Aerial photograph of the Luce deposit, showing location of the Luce South, Luce Main and Luce Basin pits (image courtesy of IOC) . . . . .	115
Figure 51.	A) Geological map of the Luce deposit (adapted from Cotnoir <i>et al.</i> , 2002); B) Airborne magnetics (second vertical derivative) showing extent of iron formation (data from Cotnoir <i>et al.</i> , 2002) . . . . .	117
Figure 52.	A) Geological map of the Mill Basin prospect (adapted from Cotnoir <i>et al.</i> , 2002), showing location of drillholes from 2002 exploration programs (Darch <i>et al.</i> , 2003a); B) Airborne magnetics (second vertical derivative) showing extent of iron formation (data from Cotnoir <i>et al.</i> , 2002) . . . . .	119
Figure 53.	Geological maps and aeromagnetic data from the Mills Lake deposit ( <i>see text for discussion</i> ). A) Geological map based on Alderon mapping and diamond drilling (adapted from Lyons and Velcic, 2013); B) Geological map based on IOC mapping and interpretation of regional airborne magnetic surveys (adapted from Cotnoir <i>et al.</i> , 2002); C) Airborne magnetics (second vertical derivative) showing extent of iron formation (data from Cotnoir <i>et al.</i> , 2002). . . . .	123
Figure 54.	A) Geological map of the Neal 1 showing (adapted from Cotnoir <i>et al.</i> , 2002), showing location of drillholes from 2012 exploration programs (Steele, 2013); B) Airborne magnetics (second vertical derivative), showing extent of iron formation (data from Cotnoir <i>et al.</i> , 2002). . . . .	126
Figure 55.	A) Geological map of the Polly Lake prospect (adapted from Cotnoir <i>et al.</i> , 2002), showing location of drillholes from 2001, 2005 and 2011/2012 exploration programs (Cotnoir <i>et al.</i> , 2002; Darch, 2005b; Bineli Betsi, 2012); B) Airborne magnetics (second vertical derivative) showing extent of iron formation (data from Cotnoir <i>et al.</i> , 2002) . . . . .	128
Figure 56.	Geological maps and aeromagnetic data from the Rose deposit ( <i>see text for discussion</i> ). A) Geological map based on Alderon mapping and diamond drilling (adapted from Lyons and Velcic, 2013); B) Geological map based on IOC mapping and interpretation of regional airborne magnetic surveys (adapted from Cotnoir <i>et al.</i> , 2002); C) Airborne magnetics (second vertical derivative) showing extent of iron formation (data from Cotnoir <i>et al.</i> , 2002). . . . .	133



	Page
Figure 57. Geological map of the Scully deposit (adapted from Cotnoir <i>et al.</i> , 2002) . . . . .	137
Figure 58. Google Earth image of mining operations at Scully deposit, showing location of active pits as well as undeveloped area (The Boot) and plant site. Images taken in 2002 (west) and 2004 (east). . . . .	138
Figure 59. A) Geological map of the Shabo Hill showing (adapted from Cotnoir <i>et al.</i> , 2002), showing location of drillholes from 2010 exploration program (Hovis and Broadbent, 2010; Hovis and Goldner, 2011b); B) Airborne magnetics (second vertical derivative) showing extent of iron formation (data from Cotnoir <i>et al.</i> , 2002) . . . . .	142
Figure 60. A) Geological map of the Shabo Peninsula North showing (adapted from Cotnoir <i>et al.</i> , 2002), showing location of drillholes from 2010 and 2011 exploration programs (Hovis and Broadbent, 2010; Hovis and Goldner, 2011c); B) Airborne magnetics (second vertical derivative) showing extent of iron formation (data from Cotnoir <i>et al.</i> , 2002) . . . . .	144
Figure 61. A) Geological map of the Shabogamo prospect (adapted from Cotnoir <i>et al.</i> , 2002), showing location of drillholes from 2001, 2006, 2010 and 2011 exploration programs (Cotnoir <i>et al.</i> , 2002; Clark, 2007; Carter, 2011d; Hovis and Goldner, 2011c); B) Airborne magnetics (second vertical derivative) showing extent of iron formation (data from Cotnoir <i>et al.</i> , 2002) . . . . .	146
Figure 62. A) Geological map of the Sitting Bear showing (adapted from Cotnoir <i>et al.</i> , 2002), showing outcrop sample locations from 2008, 2009 and 2010 exploration programs (Reynolds and Mitchell, 2008; Downing, 2009; Hovis and Goldner, 2011c); B) Airborne magnetics (second vertical derivative) showing extent of iron formation (data from Cotnoir <i>et al.</i> , 2002). . . . .	149
Figure 63. Aerial photograph of the Smallwood North prospect, showing location of the former Smallwood Mine (image courtesy of IOC) . . . . .	151
Figure 64. A) Geological map of the Smallwood North prospect (adapted from Cotnoir <i>et al.</i> , 2002), showing location of drillholes from 2017 exploration programs (IOC, personal communication); B) Airborne magnetics (second vertical derivative) showing extent of iron formation (data from Cotnoir <i>et al.</i> , 2002). . . . .	152
Figure 65. A) Geological map of the Squid showing (adapted from Cotnoir <i>et al.</i> , 2002), showing location of drillholes from 2011 exploration programs (Duvergier, 2012); B) Airborne magnetics (second vertical derivative) showing extent of iron formation (data from Cotnoir <i>et al.</i> , 2002) . . . . .	154
Figure 66. A) Geological map of the Wabush 1 prospect (adapted from Cotnoir <i>et al.</i> , 2002), showing location of drillholes from 2002 exploration program (Darch <i>et al.</i> , 2003a); B) Airborne magnetics (second vertical derivative) showing extent of iron formation (data from Cotnoir <i>et al.</i> , 2002) . . . . .	156
Figure 67. Aerial photograph of the Wabush 3 and Luce deposits, showing outline of the proposed Wabush 3 pit (image courtesy of IOC) . . . . .	159
Figure 68. A) Geological map of the Wabush 3 deposit (adapted from Cotnoir <i>et al.</i> , 2002), showing location of drillholes from 2007 and 2010-2012 exploration programs (Pond, 2013); B) Airborne magnetics (second vertical derivative) showing extent of iron formation (data from Cotnoir <i>et al.</i> , 2002). . . . .	160
Figure 69. A) Geological map of the Wabush 4 prospect (adapted from Cotnoir <i>et al.</i> , 2002); B) Airborne magnetics (second vertical derivative) showing extent of iron formation (data from Cotnoir <i>et al.</i> , 2002) . . . . .	163
Figure 70. A) Geological map of the Wabush 6 deposit (adapted from Cotnoir <i>et al.</i> , 2002), showing location of drillholes from 2002 and 2007-2012 exploration programs (Darch <i>et al.</i> , 2003a; Marshall, 2012b); B) Airborne magnetics (second vertical derivative) showing extent of iron formation (data from Cotnoir <i>et al.</i> , 2002) . . . . .	166
Figure 71. Geological map of the Wabush Mountain area (adapted from Cotnoir <i>et al.</i> , 2002), showing approximate location of drillholes from 1962 drilling programs (Hartopp, 1962a) . . . . .	169
Figure 72. A) Geological map of the White Lake prospect (adapted from Cotnoir <i>et al.</i> , 2002), showing location of drillholes from 2010, 2011 and 2012 IOC exploration programs (Duvergier, 2012); B) Airborne magnetics (second vertical derivative) showing extent of iron formation (data from Cotnoir <i>et al.</i> , 2002) . . . . .	171



## PLATES

Plate 1.	IOC concentrator and pellet plant, Carol Project . . . . .	10
Plate 2.	Humphrey Main pit, Carol Project . . . . .	10
Plate 3.	View of the Luce pit from observation deck. . . . .	11
Plate 4.	Aerial view of Wabush Mines concentrator, with Scully Mine in background . . . . .	11
Plate 5.	Silicate Carbonate Iron Formation (SCIF) facies at the base of the Sokoman Formation, showing characteristic orange weathering of Fe-silicates . . . . .	13
Plate 6.	Outcrop of the Upper Red Cherty (URC) facies of the Middle Iron Formation of the Sokoman Formation in the central Labrador Trough . . . . .	13
Plate 7.	Lower Red Cherty (LRC) facies of the Middle Iron Formation of the Sokoman Formation. . . . .	13
Plate 8.	Fissile and carbon-rich shales of the Ruth Formation at the base of the Sokoman Formation in the central Labrador Trough . . . . .	13
Plate 9.	Folded iron formation, with alternating layers of magnetite and of Fe-silicates and quartz (from outcrop along Trans-Labrador Highway close to the Québec border) . . . . .	25
Plate 10.	Mixed oxide-carbonate-facies iron formation with alternating bands of magnetite and carbonate-rich iron formation (from Wabush 3 deposit, drillhole W3-11-101 @ 212 m). . . . .	25
Plate 11.	Oxide-facies iron formation, with coarse-grained specularite and quartz filling vug (from boulder in Carol Project). . . . .	25
Plate 12.	Moderately altered, hematite-rich iron formation, with bands of specular hematite and quartz (from Duley Prospect, drillhole DU-10-03 @ 131.7 m). . . . .	26
Plate 13.	A) Photomicrograph of typical banded oxide-facies iron formation, with bands of fine-grained magnetite–hematite and quartz (from Polly Lake prospect, plane-polarized light); B) Same view as A, in reflected light. . . . .	26
Plate 14.	Photomicrograph of specular hematite and magnetite replacing possible ooliths in parent iron formation (from Humphrey deposit; drillhole HS-10-72 @ 218 m, reflected light) . . . . .	26
Plate 15.	Photomicrograph of specular hematite and quartz, with elongate specular hematite imparting schistosity to sample (from Duley prospect; drillhole DU-10-03 @ 131.7 m, reflected light) . . . . .	26
Plate 16.	Carbonate-facies, with alternating bands of siderite–dolomite and quartz (from D’Aigle Bay 2 North prospect; drillhole DB-10-14 @ 165.9 m). . . . .	27
Plate 17.	Photomicrograph of carbonate-facies iron formation with bands of coarse-grained carbonate and medium-grained quartz (from Knight prospect; drillhole KN-06-A @ 204.7 m, cross-polarized light). . . . .	27
Plate 18.	Silicate-facies iron formation, with abundant brown-weathering grunerite (from Carol Lake area) . . . . .	27
Plate 19.	Silicate-facies iron formation with discontinuous bands of quartz (mantled by biotite) and Fe-silicates (actinolite, grunerite) . . . . .	27
Plate 20.	Garnet-bearing BSIF from the base of the Sokoman Formation in the Duley prospect (drill-hole DU-10-03 @ 147 m) . . . . .	30
Plate 21.	A) Photomicrograph of BSIF from the base of the Sokoman Formation, with a quartz-carbonate matrix and large brown grunerite, green chlorite and transparent garnet crystals (from Duley prospect; drillhole DU-10-03 @ 147 m, plane-polarized light); B) Same view as A, in cross-polarized light. . . . .	30
Plate 22.	Mixed silicate and oxide (hematite) facies iron formation, with pink rhodochrosite (from Mills Lake deposit, drillhole K-10-95 @ 76.3 m). . . . .	33
Plate 23.	Photomicrograph of silicate-facies iron formation, with brown manganese aegirine and pink to transparent rhodochrosite (from Mills Lake deposit; drillhole K-10-95 @ 76.3 m, plane-polarized light). . . . .	33
Plate 24.	Photomicrograph of co-existing euhedral to subhedral hematite and magnetite (from Humphrey deposit; drillhole HS-10-72 @ 218 m, reflected light) . . . . .	34

	Page
Plate 25. Photomicrograph of hematite replacing an euhedral grain of magnetite (forming martite and kenomagnetite), with secondary goethite infilling space around the grain (from Julienne 2 prospect; drillhole J2-10-08 @ 153.2 m, reflected light) . . . . .	34
Plate 26. Photomicrograph of moderately altered oxide-facies iron formation, and hematite grains mantled by brown goethite (from Julienne 2 prospect; drillhole J2-10-08 @ 153.2, plane-polarized light) . . . . .	35
Plate 27. Photomicrograph of moderately altered oxide-facies iron formation, and magnetite partially replaced by hematite and mantled by secondary goethite (from Julienne 2 prospect; drillhole J2-10-08 @ 153.2 m, reflected light) . . . . .	36
Plate 28. Photomicrograph of strongly altered oxide-facies iron formation, with magnetite and hematite completely replaced by secondary goethite (from Julienne Lake deposit; drillhole JL-10-17B @ 2.5 m, reflected light) . . . . .	36
Plate 29. Photomicrograph of strongly altered oxide-facies iron formation, with vein of remobilized Mn-oxides (from Julienne Lake deposit, reflected light) . . . . .	36
Plate 30. A) Typical lean quartz–specularite schist with moderate hematite alteration (drillhole CA-10-02 @ 241.8 m); B) Strongly altered quartz–specularite schist, with secondary goethite replacing carbonates (drillhole CA-10-02 @ 227 m) . . . . .	55
Plate 31. A) Banded oxide-facies iron formation with dark-grey magnetite-rich layers, white–light-grey chert-rich layers and lesser yellow carbonate-rich layers (drillhole DB-10-14 @ 162.9 m); B) Photomicrograph of banded, magnetite-rich ore with magnetite (minor hematite) and quartz-rich bands (drillhole DB-10-14 @ 163.1 m, reflected light) . . . . .	64
Plate 32. A) Interlayered magnetite-rich and hematite-rich oxide-facies iron formation, correlating with RC2 at the Rose deposit (drillhole DU-10-03 @ 84.5 m); B) Quartz–specularite schist correlating with RC1 at the Rose deposit (drillhole DU-10-03 @ 131.7 m); C) Photomicrograph of quartz–specularite schist (drillhole DU-10-03 @ 131.7 m, reflected light); D) Basal silicate iron formation with abundant garnet (drillhole DU-10-03 @ 146.9 m); E) Photomicrograph of garnet-bearing basal silicate iron formation (drillhole DU-10-03 @ 147 m, cross-polarized light); F) Probable F <sub>2</sub> folding in the Sokoman Formation, located on the eastern limb of the syncline (view looking south) . . . . .	71
Plate 33. A) View of the Humphrey Main pit, looking north from observation point; B) Silicate-facies iron formation; C) Magnetite-rich oxide-facies iron formation with gangue carbonate and quartz (drillhole SW-10-69 @ 48.5 m); D) Oxide-facies iron formation, with medium- to coarse-grained magnetite and hematite and cream-coloured carbonate (drillhole SP-11-27 @ 77 m); E) Oxide-facies iron formation, with coarse-grained specular hematite and quartz-filling vug; F) Hematite-rich oxide-facies iron formation with gangue quartz (jasper) (drillhole HW-10-45 @ 13.3 m) . . . . .	89
Plate 34. A) Photomicrograph of specular hematite and magnetite replacing possible ooliths in parent iron formation (drillhole HS-10-72 @ 218 m, reflected light); B) Photomicrograph of co-existing euhedral to subhedral hematite and magnetite (drillhole HS-10-72 @ 218 m, reflected light); C) Oxide-facies iron formation, with disseminated magnetite (light grey) and hematite (pink grey) and gangue quartz (drillhole LO-10-04 @ 60.3 m); D) Same view as (C), in cross-polarized light . . . . .	90
Plate 35. A) LIF close to the contact with Wishart Formation quartzite, with large euhedral garnets (drillhole J2-06-05 @ 117.3 m); B) Quartz–hematite oxide-facies iron formation (drillhole J2-06-05 @ 103.1 m) . . . . .	95
Plate 36. Quartz–hematite oxide-facies iron formation (drillhole J2-10-08 @ 153.2 m) . . . . .	98
Plate 37. A) Aerial view of the Julienne Lake peninsula, looking south. Historic trench (T62-01) exposed on hilltop and Pleistocene-raised beach clearly visible; B) Historical trench (T62-01), with large boulder of folded oxide-facies iron formation; C) Massive, friable oxide-facies iron formation; D) Banded oxide-facies iron formation, with quartz-rich and hematite-rich layers (drillhole JL10-16 @ 53.6 m); E) Gently dipping bed of Mn-rich iron formation, from north end of Trench 10-01; F) Strongly altered Basal Silicate member, with large altered garnets (drillhole JL12-08 @ 85.6 m) . . . . .	102

Plate 38.	A) Typical carbonate–silicate-facies iron formation from the LIF (drillhole KN-06-A @ 227.7 m); B) Typical quartz–magnetite oxide-facies iron formation (drillhole KN-06-A @ 161.5 m); C) Quartz–magnetite oxide-facies iron formation with very coarse-grained clots of magnetite (drillhole KN-06-A @ 219.5 m); D) Quartz–carbonate–magnetite–hematite oxide-facies iron formation (drillhole KN-06-A @ 166.5 m); E) Photomicrograph of oxide-facies iron formation with magnetite and hematite and gangue quartz, carbonate and minor Fe-silicates (drillhole KN-06-A @ 166.5 m, reflected light); F) Same view as (E), in cross-polarized light . . . . .	106
Plate 39.	A) View of the Luce deposit, looking north from observation point above Luce South pit; B) Typical fine-grained, magnetite-rich oxide-facies iron formation (drillhole LU-10-62 @ 91 m); C) Medium-grained, friable hematite-rich oxide-facies iron formation (drillhole LU-10-77 @ 62 m); D) Photomicrograph of hematite-rich oxide-facies iron formation, with hematite (light grey) and magnetite (pink grey) crystals (drillhole LU-10-77 @ 62 m); E) Strongly altered, goethite-rich iron formation from west wall of Luce Main pit (drillhole LU-13-364 @ 207 m) . . . . .	116
Plate 40.	A) Banded, magnetite-rich oxide-facies iron formation from the lower domain of the lower oxide member (drillhole K-10-95 @ 93.6 m); B) Hematite-rich oxide-facies iron formation with pink rhodonite, from middle domain of lower oxide member (drillhole K-10-95 @ 76.25 m); C) Photomicrograph of hematite replacing a euhedral grain of magnetite, forming martite (rim) and kenomagnetite (core) (drillhole K-10-95 @ 76.25 m, reflected light); D) Photomicrograph of gangue carbonate and Mn-rich aegirine with minor hematite (drillhole K-10-95 @ 76.25 m, plane-polarized light) . . . . .	124
Plate 41.	A) Overview of the Polly Lake area, overlooking Polly Lake; B) Outcrop of banded quartz–hematite–actinolite–carbonate iron formation (close to collar of drillhole PL-11-05); C) Banded magnetite-rich oxide-facies iron formation (drillhole PL-11-14 @ 41.2 m); D) Folded oxide-facies iron formation, with quartz-rich and magnetite-rich layers (drillhole PL-11-14 @ 71.2 m) . . . . .	129
Plate 42.	A) View of the Rose Central Zone of the Rose deposit, looking west; B) Banded quartz–hematite from RC-1 member (drillhole K-11-171 @ 232 m); C) Quartz–magnetite–hematite iron formation from RC-2 member (drillhole K-11-171 @ 205.6 m); D) Moderately altered quartz–hematite from RN-2 member (drillhole K-11-115 @ 329.2 m); E) Quartz–magnetite–carbonate iron formation from RC-3 member (drillhole K-11-171 @ 140.6 m); F) Strongly altered basal silicate-facies iron formation from Rose North Zone (drillhole K-11-115 @ 401.4 m) . . . . .	134
Plate 43.	A) Photomicrograph of quartz–hematite–magnetite schist from RC-2, with hematite replacing magnetite and gangue quartz and carbonate (drillhole K-11-171 @ 205.1 m, reflected light); B) Same view as (A), in cross-polarized light . . . . .	135
Plate 44.	A) Strongly altered basal silicate-facies iron formation from West pit; B) Banded quartz–hematite–pyrolusite schist (Unit 53) from East pit (east); C) Quartz–hematite–pyrolusite schist with circular pits after leached carbonate minerals (Unit 53); East pit (east); D) Quartz–goethite waste unit (Unit 52) from East pit (east); E) Middle quartzite marker horizon from West pit; F) Banded quartz–hematite schist from West pit (Unit 31) . . . . .	139
Plate 45.	A) Outcrop of friable, hematite-rich oxide facies iron formation with folded band of Fe-silicates; B) Outcrop of folded oxide-facies iron formation, with magnetite-rich bands (dark grey) and quartz-rich bands (light grey); C) Banded magnetite-rich oxide-facies iron formation, with band of Fe-silicate–quartz and minor coarse-grained hematite (drillhole W3-11-101 @ 215.5 m); D) Photomicrograph of oxide-facies iron formation, with magnetite (pink grey) and tabular coarse-grained hematite crystals (light grey) (drillhole W3-11-101 @ 215.5 m) . . . . .	161

	Page
Plate 46. A) Outcrop of folded quartz–magnetite–hematite oxide-facies iron; B) Quartz–magnetite–hematite oxide-facies iron formation with coarse-grained magnetite (drillhole W4-10-01 @ 12.8 m); C) Photomicrograph of oxide-facies iron formation with coarse-grained magnetite bands and fine-grained hematite and quartz (drillhole W4-10-01 @ 12.8 m); D) Moderately altered, friable oxide-facies iron formation with abundant Mn-oxides (drillhole W4-10-01 @ 74.1 m) . . . . .	164
Plate 47. A) Hematite-rich oxide-facies iron formation (drillhole W6-10-135 @ 31.2 m); B) magnetite-rich oxide-facies iron formation with gangue quartz and carbonate (drillhole W6-10-135 @ 50.5 m) . . . . .	167

## TABLES

Table 1. Main iron-ore deposits and occurrences in the study area discussed, in detail, in this publication . . . . .	5
Table 2. Major active and dormant mines and developed prospects in the study area, including mineral reserves and resources . . . . .	10
Table 3. Stratigraphic correlations between the formations of the Gagnon Group (as defined by Clarke, 1965) and those of the Kaniapiskau Supergroup in the central Labrador Trough (Adapted from Rivers, 1980d) . . . . .	16
Table 4. Summary statistics for major-element, trace-element, and REE concentrations of oxide-facies iron formation and Basal Silicate Iron Formation in the Labrador City/Wabush area . . . . .	38

## ABSTRACT

*The iron-ore deposits of southwestern Labrador have been mined continuously since 1962, and in 2016 they accounted for more than half of the annual gross value of mineral shipments for Newfoundland and Labrador. These deposits, classified as metataconite deposits, are a distinct group of iron-ore deposits only described from this region. They are hosted in the Sokoman Formation iron formation, and were metamorphosed and deformed during the Grenville Orogeny at ca. 1.0 Ga. Three broadly defined end-member facies describe the Sokoman Formation: oxide facies (the main ore-bearing unit), silicate facies, and carbonate facies. The iron formation recrystallized during regional metamorphism, and the oxide-facies iron formation consists of medium- to coarse-grained magnetite, specular hematite, and quartz, and is easily beneficiated into iron concentrates (approximately 65% Fe) ideal for pellet production. Deformation and associated structural thickening during the Grenville Orogeny were also important in the development of mineable thicknesses of oxide-facies iron formation.*

*Forty individual iron-ore occurrences have been described from the study area (NTS 23B/14, 23B/15, 23G/02, 23G/03 and part of 23G/07). These are subdivided into a number of distinct basins, which based on stratigraphic correlations between individual occurrences and geochemical variations, may represent separate depositional centres. The Carol Lake Basin, which hosts all occurrences in the Iron Ore Company of Canada's Carol Lake Project, is subdivided into a Lower Iron Formation (LIF) dominated by carbonate-facies iron formation, a Middle Iron Formation (MIF) predominantly of oxide-facies iron formation, and an Upper Iron Formation (UIF) with carbonate- and silicate-facies iron formation, and rare oxide-facies bands. The Wabush Basin, hosting the idled Scully Mine and developed prospects at the Julienne Lake and Rose deposits, is composed of a distinctive Basal Silicate Iron Formation (BSIF) that is overlain by a thick sequence of oxide-facies iron formation; carbonate-facies LIF is absent. A smaller third basin, the Mills Lake Basin, is located in the southwest of the study area, whilst a number of occurrences on the western margin of the study area are not included in any basin due to the lack of detailed stratigraphic information.*

*Geochemical data indicate that the oxide-facies iron formation represents the local ocean chemistry during deposition, and samples from the Wabush and Mills Lake basins generally have elevated Mn and Ba, lower Y/Ho ratios, and are relatively enriched in LREE compared to samples from the Carol Lake Basin. These geochemical trends indicate that deposition in the Wabush and Mills Lake basins occurred in deeper water than that in the Carol Lake Basin, below the redoxcline in a stratified ocean (having an oxic upper layer and reduced lower layer).*

*Some iron-ore occurrences have been extensively altered, resulting in magnetite in oxide-facies iron formation being partially to completely oxidized to secondary martite with common goethite, and Mn being remobilized into discrete layers and veins. The close spatial association between altered iron formation and brittle faults suggests that these faults may have been reactivated during tectonic activity, and late-stage fluid movement may have focussed along these structures. This late-stage fluid flow is not associated with any iron enrichment, unlike high-grade supergene deposits in the Schefferville area, where late-stage fluid flow, intense alteration and transformation of magnetite to hematite and goethite are responsible for upgrading the iron formation from ~30% Fe to >55% Fe. This may be due to the chemistry of the fluids or the larger quartz grain size in the metamorphosed iron formation, which would impede dissolution.*





# PART A

## INTRODUCTION

### PURPOSE AND SCOPE

The Labrador City and Wabush areas have had a long history of mining and exploration, with iron-ore deposits first discovered in the 1940s and mining commencing in the 1960s. Today, mining forms the backbone of the economy of western Labrador, and in 2016 the iron-ore occurrences accounted for more than half of the annual gross value of mineral shipments for Newfoundland and Labrador (2016 GNL statistics). The iron ores occur in the Paleoproterozoic Sokoman Formation, within a sequence of sedimentary and volcanic rocks commonly referred to as the Labrador Trough, which extends for over 1100 km, from Lac Pléti in the south to Ungava Bay in the north (Figure 1). In southwestern Labrador, the Sokoman Formation was deformed and metamorphosed during the Grenville Orogeny, resulting in the formation of a class of deposits known as metataconites. Metataconites form from strongly metamorphosed and recrystallized iron formation, with 25–40 wt. % Fe. The term metataconite is exclusively used in the Labrador Trough. Despite their relatively low grade (<40% Fe), the coarse grain-size and low degree of impurities (*e.g.*, Al, P) allow for easy beneficiation into iron concentrates (~65% Fe) that can be used to produce high-quality iron-ore pellets.

In response to increased exploration activity in southwest Labrador, driven by an increase in iron-ore prices, the Survey initiated a study of known iron-ore deposits in southwestern Labrador in 2012. The study area covers NTS map areas 23B/14, 15, 23G/02, 03 and the southern part of NTS map area 23G/07 (Figure 2), and includes 40 named iron-ore occurrences (Figure 3; Table 1). This report is a synthesis, based on deposit-scale mapping, logging of diamond-drill core and visits to active mines and known occurrences, and incorporates data from recent industry-assessment reports and a number of academic studies. It represents the first such report since Gross (1968), and is intended as a reference document to assist future exploration and development. It also includes new geochemical data from 25 individual occurrences, as well as detailed descriptions of the geology and previous work carried out on all 40 named iron-ore occurrences (*see* Part B).

### PREVIOUS WORK

The following is a brief summary of some of the geological work conducted since the 1930s, including bedrock-geology mapping, and studies on the structural and metamorphic history of the Gagnon Terrane. This is not intended to be a complete description of past works and studies; information on the discovery and development of the iron-ore occurrences in southwestern Labrador is summarized in Part B.

The first geological mapping of present day Labrador City and Wabush was carried out in the early 1930s as part of investigations into the gold potential of the region (Gill *et al.*, 1937). Significant iron-ore resources were discovered in the late 1940s and this was followed by systematic mapping of the region by exploration companies (Neal, 1950a, 1951; Beemer, 1952; Almond, 1953; Jackson, 1954; Gross, 1955; Knowles, 1955, summarized in Jackson, 1963), who focussed on the extent and economic potential of iron occurrences. The first description of the regional stratigraphy and structure was published by Knowles and Gastil (1959) and Gastil and Knowles (1960). More detailed, regional-scale mapping by the Geological Survey of Canada (Fahrig, 1960, 1967; Jackson, 1976), and the Newfoundland Department of Mines and Energy resulted in the publication of a series of maps at 1:50 000 and 1:100 000 scales (Rivers, 1980a, b, c; 1985a, b; Rivers and Massey, 1985). Parts of the study area were remapped, in detail, by van Gool (1992). Additionally, Iron Ore Company of Canada (IOC) geologists refined the regional maps with detailed localized mapping and interpretation of a regional aeromagnetic survey completed in 2001 (Cotnoir *et al.*, 2002). The geological map shown in Figure 4 is a result of the compilation of previous published maps, unpublished IOC geological maps, and interpretation of the regional aeromagnetic data (Figure 5).

A number of studies have also investigated the metamorphic and structural history of the study area. Rivers (1983a) showed that the structural history is dominated by Grenvillian deformation (~1.0 Ga), and by Paleoproterozoic sediments, thrust over Archean basement, in a foreland-directed fold and thrust belt. Subsequent studies described a complex history of deformation in the region, with at least three generations of folding, and multiple stacked thin- and thick-skinned thrust systems (van Gool, 1992; Rivers *et al.*, 1993; van Gool *et al.*, 2008). Klein (1966, 1973, 1978) studied the mineral assemblages in the metamorphosed iron formation. These studies focussed on the silicate and carbonate facies of the Sokoman Formation, and showed that the metamorphic reactions within the iron formations are complex where mineral assemblages are controlled by mobility of H<sub>2</sub>O and CO<sub>2</sub> (Klein, 1978). Subsequent research investigated mineral assemblages in metapelites and quartzofeldspathic rocks, and identified consistent metamorphic zones throughout the region (Rivers, 1983b; van Gool, 1992).

### HISTORY OF EXPLORATION

The first reference to iron ore in Labrador was by Father Pierre Babel, a Jesuit missionary, who travelled in the region in the 1860s. In the 1890s, A.P. Low, of the Geological Survey of Canada, first reported on the iron formations near Menihék Lake and Astray Lake, and noted the potential for large deposits. However, the region attracted little interest at the time,

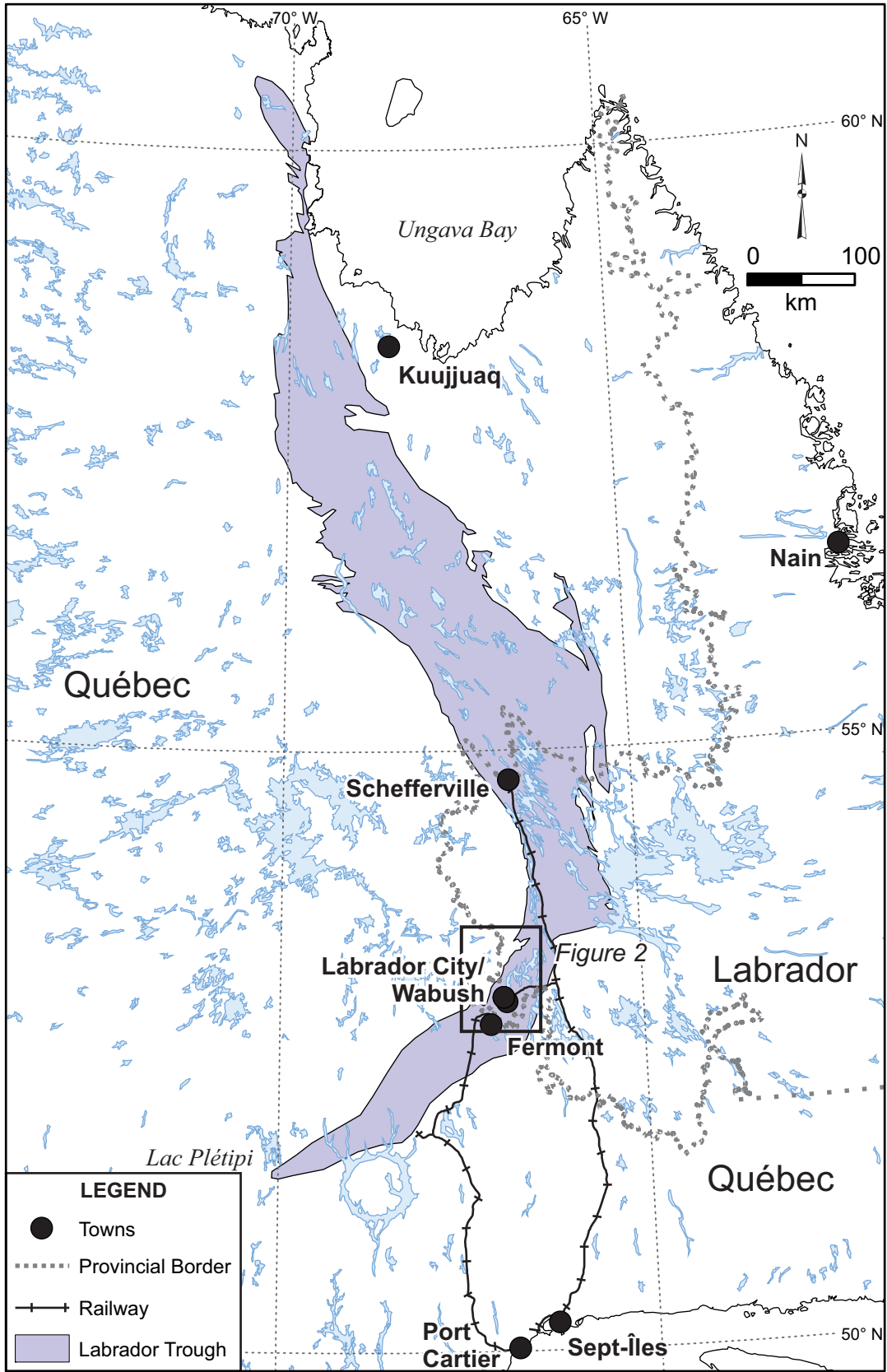


Figure 1. Map showing the location of the Labrador Trough.

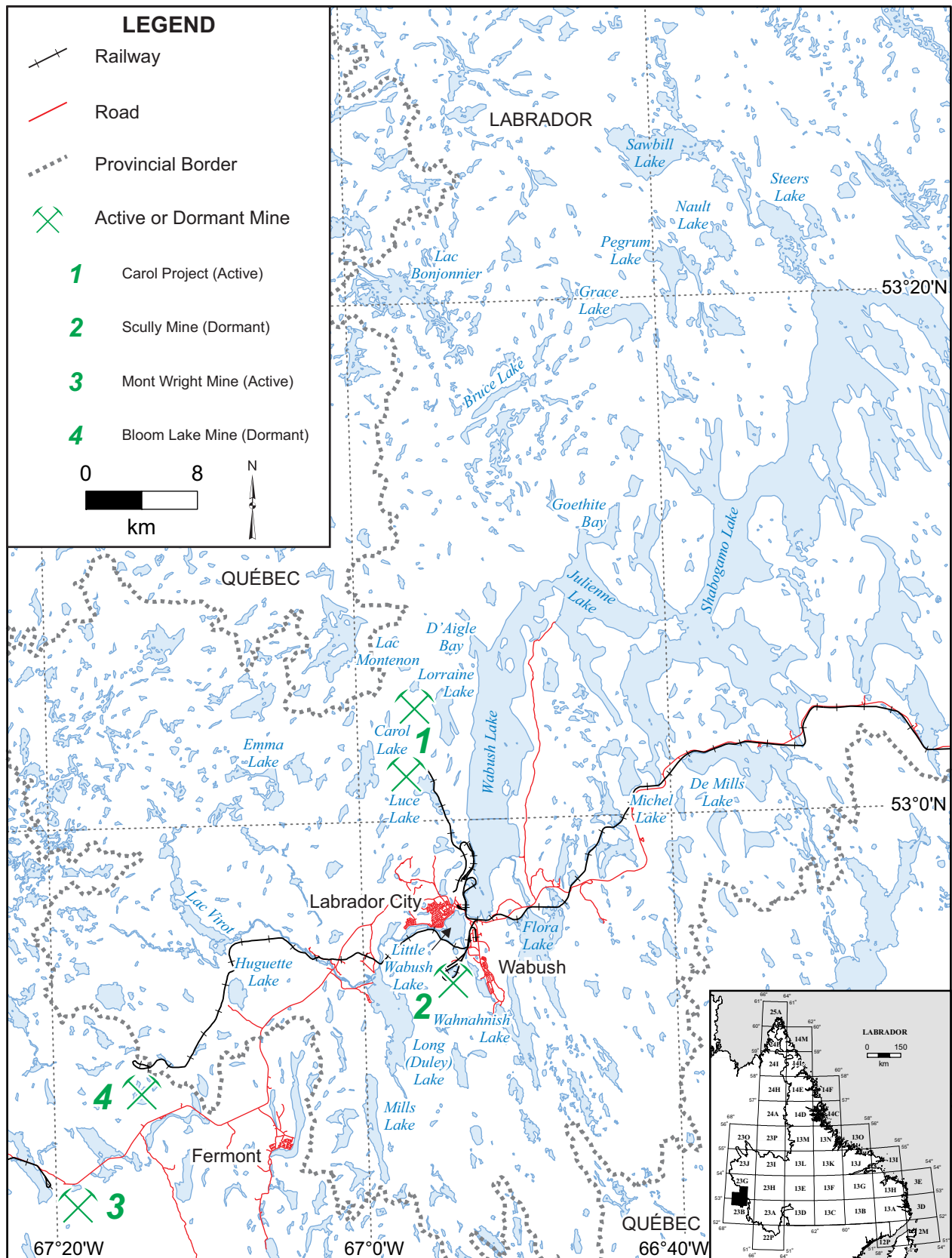


Figure 2. Simplified topographic map of the study area, showing location of the main geographical features.



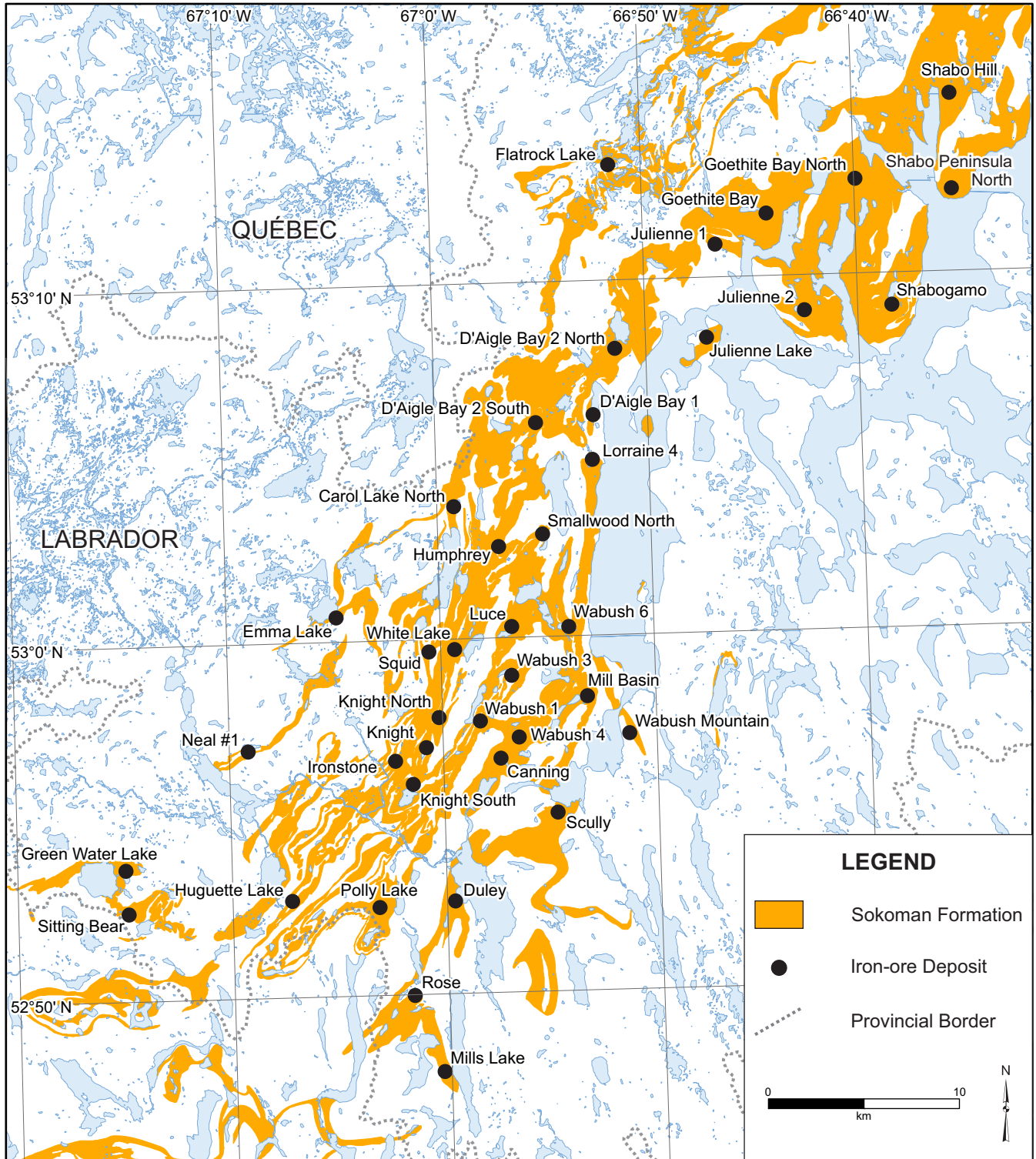


Figure 3. Location of the major iron-ore occurrences in the study area.



**Table 1.** Main iron-ore deposits and occurrences in the study area discussed, in detail, in this publication

<b>Deposit Name</b>	<b>No.</b>	<b>Status</b>	<b>Structural Basin</b>	<b>NTS Area</b>	<b>UTM Zone</b>	<b>Northing (NAD 27)</b>	<b>Easting (NAD 27)</b>
Canning	1	Prospect	Carol	23B/15	19	5867803	637400
Carol Lake North	2	Prospect	Carol	23G/02	19	5880930	634914
D'Aigle Bay 1	3	Showing	Carol	23G/02	19	5885761	642191
D'Aigle Bay 2 North	4	Prospect	Carol	23G/02	19	5889203	643341
D'Aigle Bay 2 South	5	Prospect	Carol	23G/02	19	5885323	639216
Duley	6	Prospect	Wabush	23B/15	19	5860313	635012
Emma Lake	7	Showing	n/a	23G/03	19	5875103	628766
Flatrock Lake	8	Showing	n/a	23G/02	19	5898808	642953
Goethite Bay	9	Prospect	Carol	23G/02	19	5896291	651250
Goethite Bay North	10	Showing	Carol	23G/02	19	5898086	655898
Green Water Lake	11	Showing	n/a	23B/14	19	5861869	617795
Huguette Lake	12	Showing	Carol	23B/14	19	5860307	626505
Humphrey	13	Producer	Carol	23G/02	19	5878834	637280
Ironstone	14	Showing	Carol	23B/14	19	5867603	631895
Julienne 1	15	Prospect	Carol	23G/02	19	5894668	648571
Julienne 2	16	Prospect	Wabush	23G/02	19	5891224	653250
Julienne Lake	17	Developed Prospect	Wabush	23G/02	19	5889776	648142
Knight	18	Prospect	Carol	23B/14	19	5868315	633501
Knight North	19	Showing	Carol	23B/15	19	5869906	634155
Knight South	20	Prospect	Carol	23B/14	19	5866416	632802
Lorraine 4	21	Prospect	Carol	23G/02	19	5883410	642180
Luce	22	Producer	Carol	23G/02	19	5874676	637970
Mill Basin	23	Prospect	Carol	23B/15	19	5871055	641925
Mills Lake	24	Developed Prospect	Mills Lake	23B/14	19	5851399	634485
Neal #1	25	Showing	n/a	23B/14	19	5868104	624167
Polly Lake	26	Developed Prospect	Carol	23B/14	19	5859963	631068
Rose	27	Developed Prospect	Wabush	23B/14	19	5855360	632907
Scully	28	Producer	Wabush	23B/15	19	5864970	640380
Shabo Hill	29	Showing	Carol	23G/07	19	5902599	660827
Shabo Peninsula North	30	Showing	Wabush	23G/02	19	5897615	660955
Shabogamo	31	Prospect	Wabush	23G/02	19	5891514	657826
Sitting Bear	32	Showing	n/a	23B/14	19	5859592	617940
Smallwood North	33	Prospect	Carol	23G/02	19	5879492	639555
Squid	34	Showing	Carol	23B/14, 23B/15	19	5873331	633627
Wabush 1	35	Prospect	Carol	23B/15	19	5869718	636305
Wabush 3	36	Developed Prospect	Carol	23B/15	19	5872119	637949
Wabush 4	37	Prospect	Carol	23B/15	19	5868890	638330
Wabush 6	38	Developed Prospect	Carol	23G/02, 23B/15	19	5874670	640919
Wabush Mountain	39	Showing	Wabush	23B/15	19	5869120	644130
White Lake	40	Prospect	Carol	23B/15, 23G/02	19	5873457	634974

because it was remote and essentially uncharted. In 1929, high-grade (>55% Fe) iron ore was first discovered in the Knob Lake area near the Québec–Labrador border, in the vicinity of present day Schefferville, by W.F. James and J.E. Gill, working for the New Québec Company. These discoveries sparked new interest in the region, and exploration by Labrador Mining and Exploration (LM&E) in the 1930s and 1940s identified significant resources of high-grade direct-shipment ore (DSO). In total, a resource of over 400 million

tonnes of high-grade DSO was identified, and production began in Schefferville in 1954.

The area, later to become Labrador City and Wabush, was visited by James and Gill in 1933, who compiled the first topographic and geologic maps of the region. Their expedition focussed on the gold potential of the region, and although they recorded the occurrence of iron-bearing formations, they did not consider that the grade was sufficient for commercial

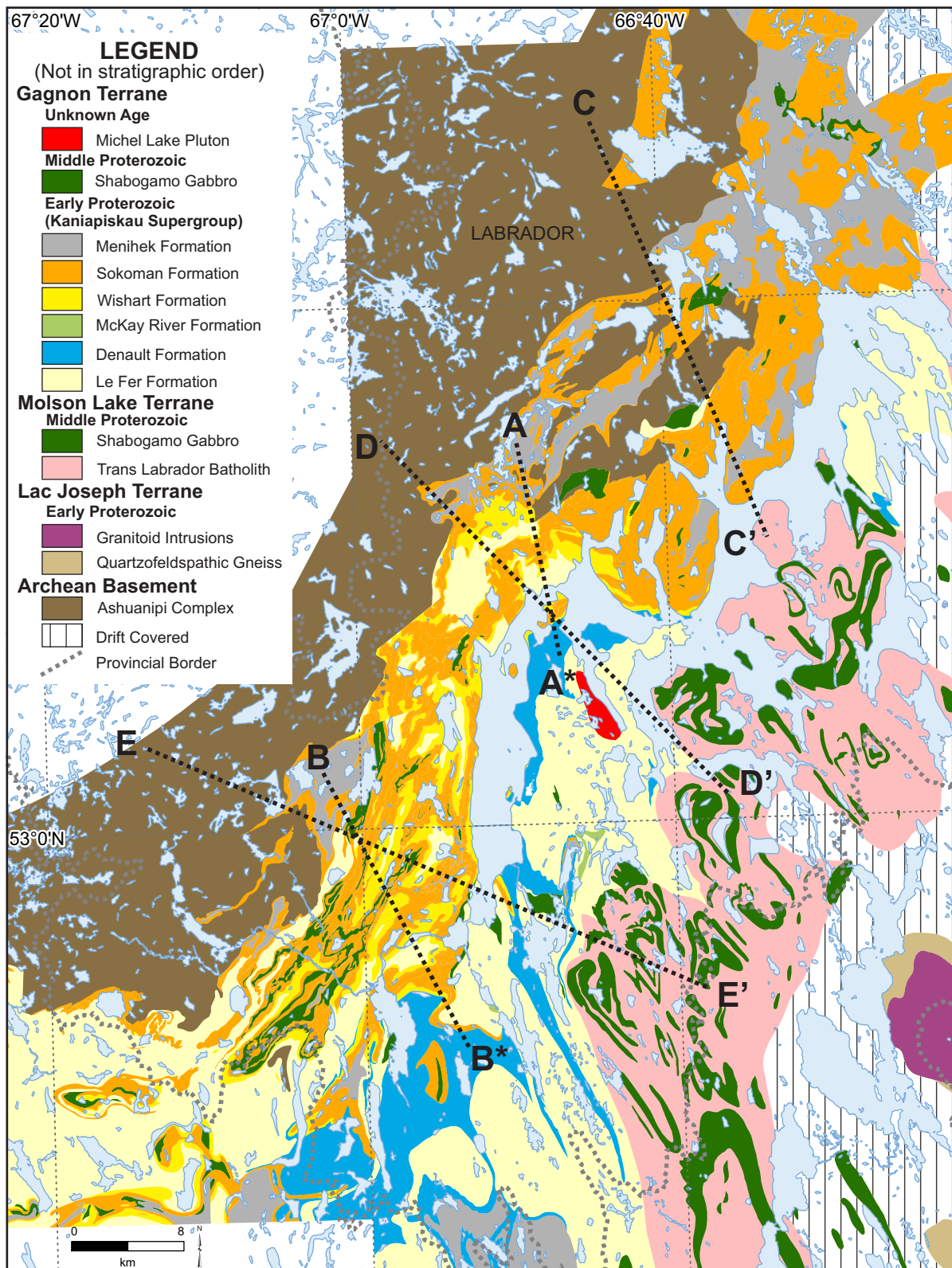


**Figure 4.** Lithological map, showing the location of schematic restored cross-sections through the continental margin prior to Grenvillian deformation (A-A\*, B-B\*; Figure 10) and structural cross-sections (C-C', D-D', E-E'; Figure 13). Geological map adapted from unpublished company data (IOC and Alderon) and published maps of the study area (Rivers 1985a, b; Rivers and Massey, 1985; van Gool, 1992).



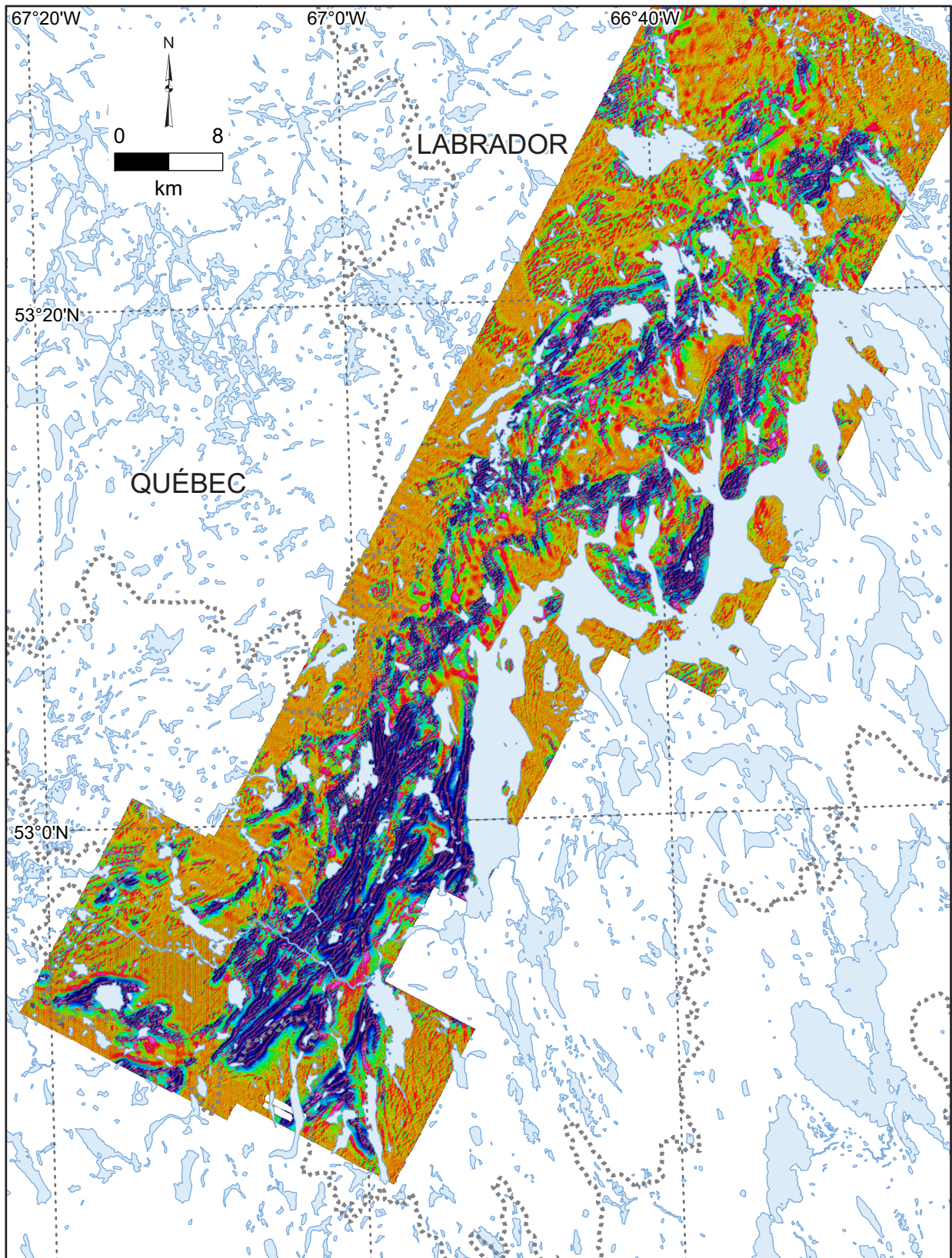


**Figure 5.** Regional aeromagnetic map of the study area (2<sup>nd</sup> vertical derivative colour-shade image, shaded from the northwest). Adapted from Cotnoir *et al.* (2002).

exploitation (Gill and James, 1933; Gill *et al.*, 1937). In 1936, LM&E were granted a mining concession in southwestern Labrador, covering an area of ~23 000 square miles. This included the areas mapped by James and Gill in 1933, and covered all the deposits currently outlined in the Labrador City and Wabush areas. Although LM&E carried out shoreline traverses in 1936, this concession received little detailed exploration until 1949, when a recent graduate of the University of Toronto, H.E. “Buzz” Neal led a seven-man geological field crew that assessed the potential of the region for economic iron deposits. This work mapped an area of about 125 square miles and recognized ten zones of economic interest (Neal, 1950a). Neal (*op. cit.*) suggested that the friable iron formation could be readily concentrated to form iron-ore concentrate (Neal, 1998), but this view was not shared by all in LM&E. Notably, the president of M.A Hanna, Mr. George Humphrey, stated that “this is for our grandchildren” when shown a sample of the iron formation in August 1949 (Geren and McCulloch, 1990). Despite these reservations, a 240-pound bulk sample was collected for testwork, which confirmed that the ore could produce a concentrate having low impurities (Neal, 1950b).

In November 1949, IOC was chartered to develop the Schefferville deposits, and the new company retained the mining rights to all the land west and north of a line demarcated by Julianne, Wabush and Duley lakes. Further exploration in the early- to mid-1950s confirmed the presence of large iron-ore deposits west of Wabush Lake, and in 1959, IOC announced plans to develop its Carol Project. This project, which included a number of occurrences north of Labrador City (Figure 6), also comprised the construction of a concentrator, and a pellet plant (Plate 1), a new town (Labrador City), a railway spur connecting the mine to the Québec North Shore and Labrador (QNS&L) main line, and a hydroelectric plant at Twin Falls (Geren and McCulloch, 1990). By 1962, construction on all these elements was completed, and the Wabush 5 deposit (subsequently termed the Smallwood Mine) was selected to be the first deposit mined, coming into production on May 30th, 1962 (MacDonald, 1963). The Smallwood Mine was operational from 1962 to 1984, and it was joined by the nearby Humphrey Main Pit (also known as the Carol East deposit), which entered production in 1964. As of 2018, there were five operating pits in IOC’s Carol Project; Humphrey Main/West/Sherwood (Plate 2), Humphrey South, Luce (Plate 3), Lorraine South and Moss Pit (Wabush 3), with one existing pit to be reactivated (Spooks) and environmental assessment registration documents submitted for a new pit at Smallwood North (Iron Ore Company of Canada, 2018; Figure 6). The Carol Project contains significant remaining reserves and resources, with 1410 million tonnes of proven and probable reserves (at 38% Fe) and an additional 2486 million tonnes of measured and indicated resources (Iron Ore Company of Canada, 2015; Table 2).

Following an aeromagnetic survey of the Wabush Lake area flown by IOC in 1951, three large magnetic anomalies, later shown to represent iron-ore deposits, were identified to the east of Wabush Lake, outside the concession area retained by IOC. The mineral rights for these areas, later shown to contain the Julianne Lake, Wabush Mountain and Scully deposits, were given to the Newfoundland and Labrador Corporation (NALCO), who leased the concession to Canadian Javelin Limited in 1953. Fieldwork from 1954 to 1956, including mapping, drilling and additional geophysical surveys, confirmed the presence of large iron-ore deposits (Knowles, 1955; Gastil, 1956). The largest of these deposits was the Scully deposit, located between Little Wabush Lake and Long Lake (Figures 2 and 3), and this deposit was subleased in 1957 by the Wabush Iron Company (formed by a number of steel companies in Canada, the United States and Europe). Production from this deposit, which came to be known as the Scully Mine (Plate 4), began in 1965 and continued until the mine was idled in 2014. In 2018, Tacora Resources Inc. announced plans to restart operations at the Scully Mine in 2019, and released new NI 43-101 compliant proven and probable reserves of 444 million tonnes at 35% Fe (Ginac *et al.*, 2018).

Exploration in the southern Labrador Trough in Québec began in the late 1940s, and in 1952 the Oliver Mining Division, part of United States Steel Corporation, began exploration over an area stretching 150 km southwest of the Québec–Labrador border (Gross, 1968). This work delineated a number of iron-ore occurrences, and the Québec Cartier Mining (QCM) company was incorporated in 1957 to develop the Lac Jeannine deposit. A new town was constructed at Gagnon, close to the Lac Jeannine deposit, and a railway was constructed from Port Cartier on the Québec North Shore. The Lac Jeannine Mine commissioned in 1961, was active until the resource was exhausted in 1977. A second mine was located ~75 km north of Lac Jeannine at Fire Lake, which operated from 1973 to 1984. In 1970, QCM began construction of a third mine at Mont Wright, approximately 35 km southwest of Labrador City (Figure 2). The Mont Wright deposit is located along strike from the deposits in the study area, and the mine has been active from 1974 through to the present day. In order to provide living quarters to the workers at Mont Wright, the community of Fermont was constructed close to the Québec–Labrador border (Figure 2).

Outside of the mining leases, exploration for, and assessment of, iron-ore occurrences in southwestern Labrador were sporadic and intermittent. Much of this work was carried out by IOC and LM&E, and included aeromagnetic surveys, ground prospecting and diamond drilling. A total of 1405 drillholes were completed during reconnaissance exploration from the 1950s to the 1980s (Hulstein and Lee, 2001). However, many of these were only designed to test



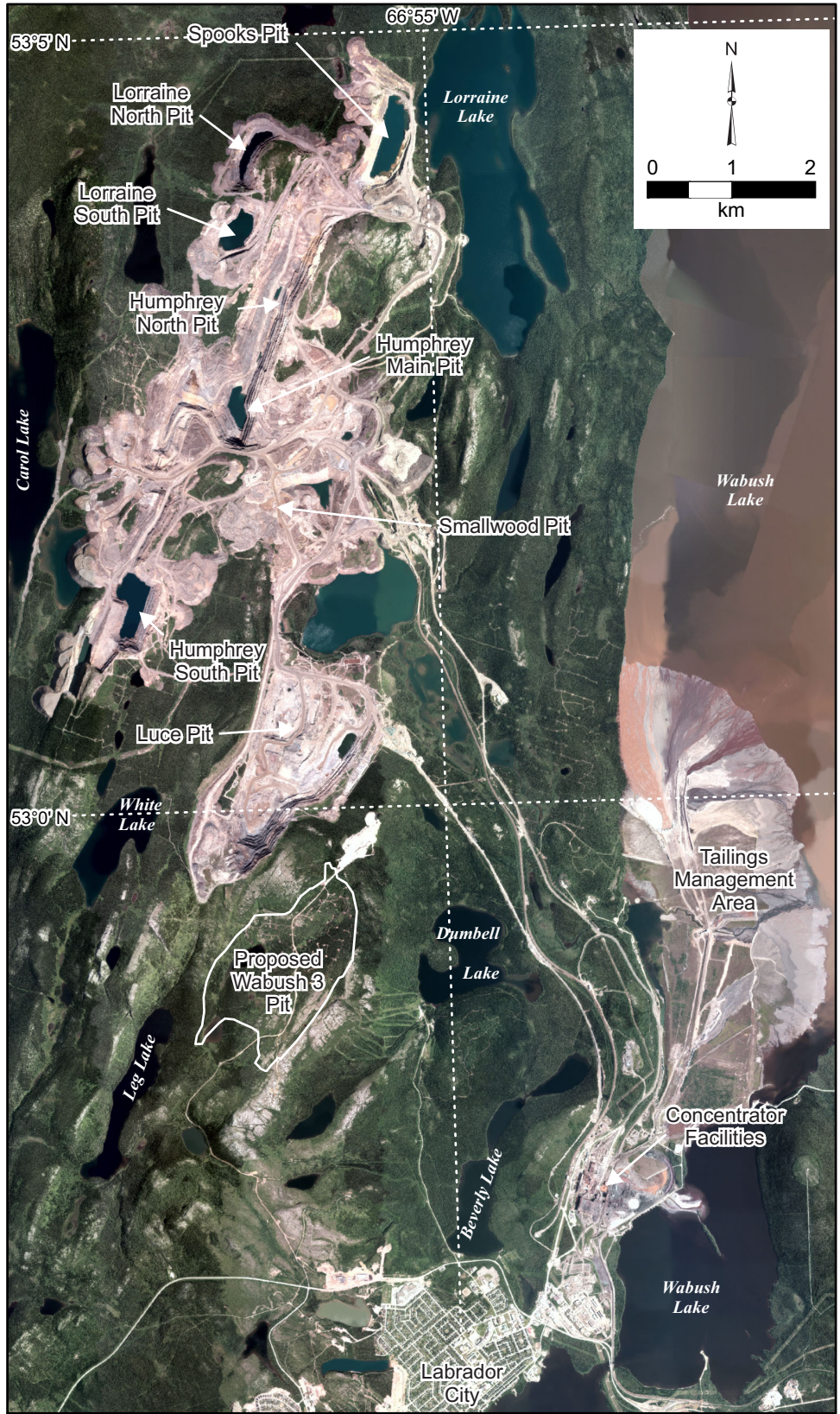


**Figure 6.** Aerial photograph showing the location of current, past and future mining activity in the Carol Project area (image courtesy of IOC).



**Plate 1.** IOC concentrator and pellet plant, Carol Project.



**Plate 2.** Humphrey Main pit, Carol Project.

bedrock geology in areas of poor exposure and the precise location and/or rocks encountered in these drillholes are often missing or poorly documented. In 2000, IOC initiated a Resource Assessment Program (RAP) to define additional iron-ore reserves outside of their mining lease (Cotnoir *et al.*, 2002). The initial stage of the RAP included compilation of historical data, geophysical surveys (regional aeromagnetic and ground-gravity surveys), geological mapping and structural analysis, and prospecting and drilling on a number of prospects (Cotnoir *et al.*, 2002). Following this initial evaluation, IOC carried out detailed exploration on a number

of occurrences, with 112 diamond-drill holes being completed from 2001 to 2012.

In 2006, Altius Resources Inc. staked a number of claims in the south of the study area, close to Mills Lake (Figures 2 and 3). The economic potential of this area was previously evaluated during the RAP by IOC, but was considered a low priority (Cotnoir *et al.*, 2002). Subsequent work by Altius from 2006 to 2008, and Alderon Iron Ore Corporation from 2010 to 2012, identified a number of iron-ore deposits on the property (Rose Central, Rose North and Mills Lake deposits),

**Table 2.** Major active and dormant mines and developed prospects in the study area, including mineral reserves and resources

Project	Deposit	Status	Reserves						Resources							
			Proven		Probable		Proven and Probable		Measured		Indicated		Inferred		Measured and Indicated	
			Mt	%	Mt	%	Mt	%	Mt	%	Mt	%	Mt	%	Mt	%
Carol Project <sup>1</sup>	Luce	Active	350	37	212	37	562	37	38	37	62	37	37	36	100	37
	Humphrey Main	Active	248	39	253	38	501	38	65	41	317	39	191	37	382	39
	Humphrey South	Active	205	39	89	38	294	39	65	40	70	40	125	38	135	40
	Lorraine South	Active	33	38	2	36	35	38								
	Spooks	Dormant	15	43	3	44	18	43	18	39	73	43	19	41	91	42
	Wabush 3 (Moss Pit)	Active							419	38	325	38	66	38	744	38
	Wabush 6	Prospect							156	37	878	37	268	35	1034	37
Wabush Mines <sup>2</sup>	Scully	Dormant	145	35	299	35	444	35	214	35	521	34	237	34	735	35
Kamistiatusset (Kami) Project <sup>3,4</sup>	Rose Central	Prospect	211	29	43	28	254	29	250	29	295	29	161	29	544	29
	Rose North	Prospect	182	29	82	29	264	29	236	30	313	31	287	30	549	30
	Mills Lake	Prospect							51	31	131	30	75	29	181	30
Julienne Lake <sup>5</sup>	Julienne Lake	Prospect							66	35	801	34	299	34	867	34
Total			1389	35	983	36	2372	35	1578	35	3784	35	1765	34	5362	35

<sup>1</sup>Mineral Resources exclude Mineral Reserves (Iron Ore Company of Canada, 2014)

<sup>2</sup>Mineral Resources include Mineral Reserves (Ginac *et al.*, 2018)

<sup>3</sup>Mineral Resources include Mineral Reserves (Grandillo *et al.*, 2018)

<sup>4</sup>Mineral Resources include Mineral Reserves (Grandillo *et al.*, 2012)

<sup>5</sup>Coates *et al.*, 2010





**Plate 3.** View of the Luce pit from observation deck.



**Plate 4.** Aerial view of Wabush Mines concentrator, with Scully Mine in background.

which are grouped together as the Kamistiasusset (Kami) iron-ore property (Lyons *et al.*, 2013). The Kami property has a total proven and probable mineral reserve of 518 Mt at 29% Fe (Lyons *et al.*, 2013; Grandillo *et al.*, 2018; Table 2).

In 2010, the Government of Newfoundland and Labrador conducted a drilling and trenching program, as well as a preliminary metallurgical study, on the Julienne Lake deposit (categorized as Exempt Mineral Land since 1975). The results of the study were released in October 2012, with a measured and indicated resource of 867 Mt at 33.7% Fe (Coates *et al.*,

2012; Table 2). Other companies carried out exploration in the study area from 2007 to 2013, including Rio Tinto Canada (formerly Kennecott Exploration Canada), Ridgemont Iron Ore Corporation and Century Iron Mines. This work included prospecting, geological mapping, diamond-drilling and geophysical surveys.

## REGIONAL GEOLOGY

The Labrador Trough extends for more than 1100 km from the northwest corner of Ungava Bay south to Lac Plétipi (Figure 1; Neal, 2000; Clark and Wares, 2005). It is composed of sedimentary and volcanic rocks collectively known as the Kaniapiskau Supergroup (Zajac, 1974; Wardle and Bailey, 1981; Le Gallais and Lavoie, 1982; Clark and Wares, 2005), which were deposited on the eastern margin of the Archean Superior Craton during the Paleoproterozoic (2.17 to 1.87 Ga; Rohon *et al.*, 1993; Findlay *et al.*, 1995; Machado *et al.*, 1997). The geology of the Labrador Trough records a long history of rifting and passive margin sedimentation, described in detail by a number of authors (*e.g.*, Dimroth *et al.*, 1970; Zajac, 1974; Wardle *et al.*, 1990; Wares and Goutier, 1990; Wardle and van Kranendonk, 1996; Clark and Wares, 2005). These authors focussed on the stratigraphy of relatively undeformed and unmetamorphosed Kaniapiskau Supergroup sediments to the north of the study area, and the following description is based on their work. As shown by Rivers (1983a), and detailed below, the stratigraphic units defined by these studies to the north are correlative with metasediments in the current study area.

The Kaniapiskau Supergroup is divided into three sedimentary and volcanic cycles (Figure 7; Clark and Wares, 2005).

Cycle 1 (the lower cycle) is composed of immature sandstones and siltstones associated with rifting of the Superior Craton. The immature sandstones and siltstones of the Seaward Group were deposited in fluvial systems, during rifting, on the eastern margin of the Superior Craton at least 2.17 billion years ago (Rohon *et al.*, 1993), and are overlain by passive margin sedimentary and volcanic rocks. In western Labrador, the Seaward Group is conformably overlain by the Le Fer Formation of the Swampy Bay Group (Wardle and Bailey, 1981). The Le Fer Formation was assigned to the Swampy Bay Group by Clark and Wares (2005), and is composed of a sequence of marine shales and siltstones. It has a gradational upper contact with the Denault Formation dolomite, with lensoidal interbedding locally observed (Evans, 1978). The Denault Formation is grouped with the Dolly and Fleming formations in the Attikamagen Group

(Clark and Wares, 2005). The Attikamagen Group initially formed as a dolomitic reef and subsequently deformed into a series of basins and ridges. The shale and siltstone of the Dolly Formation formed in the basins, and the distinctive Fleming Formation chert breccias formed due to the erosion of exposed and silicified Denault Formation carbonates and evaporates (Wardle and Bailey, 1981).

Cycle 2 is a transgressive sequence of sedimentary rocks that are grouped together as the Ferriman Group (Clark and Wares; 2005). The group includes the shelf-type rocks of the Wishart and Sokoman formations at the base, and deeper water turbidites of the Menihék Formation at the top (Wardle and Bailey, 1981; Clark and Wares, 2005). Some authors have suggested that the boundary between Cycle 1 and Cycle 2 may represent a major hiatus in sedimentation of >175 Ma (Clark and Wares, 2005). However, mapping in the Schefferville area indicates that the contact between the Attikamagen and Ferriman groups is locally conformable, with local interbedding between the Wishart Formation at the base of Cycle 2 and the underlying Denault and Fleming formations of Cycle 1 (Harrison, 1952; Baragar, 1967; Zajac, 1974; Clark *et al.*, 2006). This suggests that the Cycle 1 and Cycle 2 sedimentary rocks represent almost continuous sedimentation from >2142 to <1880 Ma, and the apparent hiatus in sedimentation may be related to the paucity of available geochronological data.

The Wishart Formation is composed mainly of orthoquartzites, siltstones and shales deposited in a high-energy shelf environment. It is overlain by the Sokoman Formation, a 30- to 350-m-thick sequence of cherty, iron-rich sedimentary rocks that hosts all the known iron-ore deposits in the Labrador Trough. Stratigraphic and sedimentological studies of the Sokoman Formation in the Schefferville area show that it was deposited in a shallow, to moderately deep, shelf environment (Zajac, 1974; Pufahl *et al.*, 2014), with significant lateral and vertical facies variations that represent changes in basin architecture and relative sea level. It has been traditionally subdivided into three units, the Upper, Middle, and Lower iron formations, which, in turn, are subdivided into a number of distinct subunits (Zajac, 1974; Klein and Fink, 1976; Wardle, 1979). The Lower Iron Formation is predominantly an iron oxide-poor carbonate-silicate-facies (Plate 5). This grades upward into the Middle Iron Formation, dominated by an oxide facies and abundant hematite and/or magnetite (commonly >50%) and sugar-textured quartz (Plates 6 and 7). The Upper Iron Formation is another iron oxide-poor, carbonate-silicate-facies.

A distinct dark-green to black ferruginous shale (Plate 8) at the base of the Sokoman Formation is sometimes separated into a discrete formation termed the Ruth Formation (*e.g.*,

Age	Super-group	Group	Formation	Cycle
Paleoproterozoic	Kaniapiskau		Tamarack River	3
		Ferriman	Menihék	2
			Sokoman	
			Nimish	
			Wishart	
		Attikamagen	Fleming	1
			Dolly	
			Denault	
		Swampy Bay	Le Fer	
		Seaward	Sawyer Lake	
Snelgrove Lake				
Discovery Lake				
Archean	Ashuanipi Metamorphic Complex			

**Figure 7.** Simplified stratigraphy of the Kaniapiskau Supergroup and the underlying Archean basement in the Schefferville Zone.





**Plate 5.** Silicate Carbonate Iron Formation (SCIF) facies at the base of the Sokoman Formation, showing characteristic orange weathering of Fe-silicates.



**Plate 7.** Lower Red Cherty (LRC) facies of the Middle Iron Formation of the Sokoman Formation.

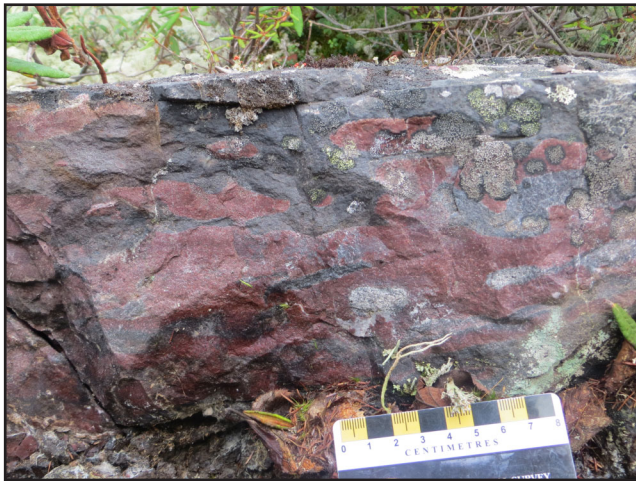


**Plate 6.** Outcrop of the Upper Red Cherty (URC) facies of the Middle Iron Formation of the Sokoman Formation in the central Labrador Trough.

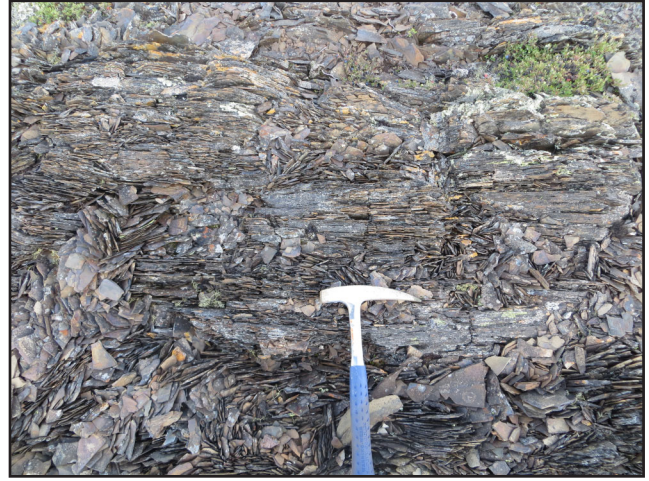


**Plate 8.** Fissile and carbon-rich shales of the Ruth Formation at the base of the Sokoman Formation in the central Labrador Trough.

Pufahl *et al.*, 2014). However, the Ruth Formation is chemically, genetically and mineralogically related to the Sokoman Formation, and Zajac (1974) proposed that it be considered a unit of the Sokoman Formation rather than a distinct formation. The Sokoman Formation is also locally interbedded with a sequence of mafic to intermediate volcanic and volcanoclastic rocks of the Nimish Formation (Evans, 1978). A syenite cobble from a polymictic conglomerate in the Nimish Formation yielded a U–Pb age of  $1877.8 \pm 1.3$  Ma, and interpreted as an approximate age for the coeval Sokoman Formation (Findlay *et al.*, 1995). The Sokoman Formation is overlain by deep-water turbidites (shales and siltstones) of the Menihek Formation.

In places, Cycle 2 is unconformably overlain by the Tamarack River Formation arkosic sandstones and siltstones (Cycle 3), which are interpreted as a synorogenic molasse.

#### LITHOTECTONIC ZONES AND METAMORPHIC TERRANES IN WESTERN LABRADOR

In western Labrador, the rocks of the Labrador Trough are divided by the Grenville Front (Figure 8), which marks the northern limit of deformation associated with the Grenvillian Orogeny in the latest Mesoproterozoic to earliest Neoproterozoic (Rivers, 1983a; Rivers *et al.*, 1993). North of the Grenville Front, the rocks are subdivided into a series of lithotectonic zones, each with internally similar lithological as-

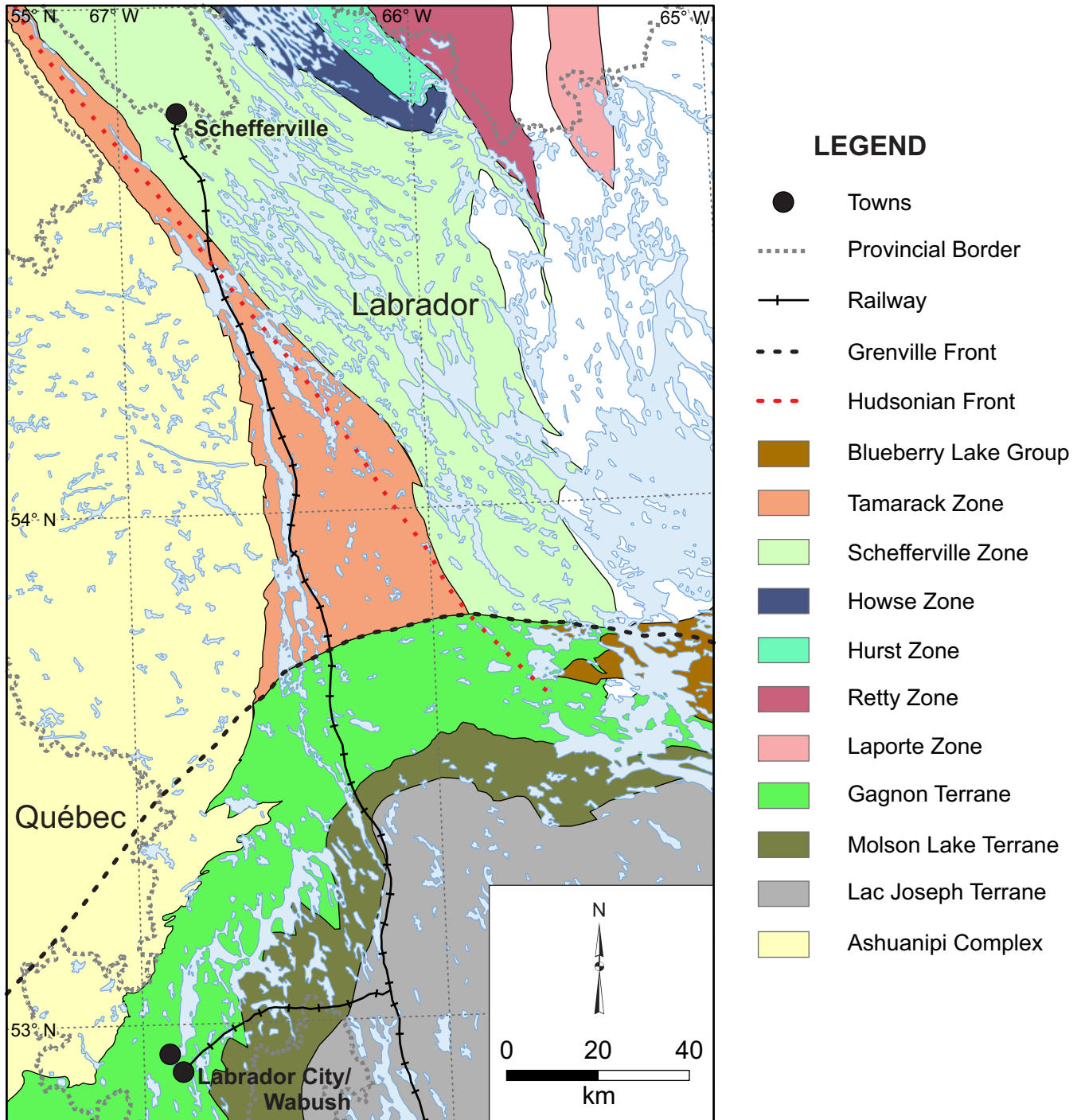


**Figure 8.** Location of major lithotectonic zones in the Labrador Trough and limits of deformation associated with the Hudsonian and Grenville orogenies. Compiled from Wardle and Bailey (1981); Clark and Wares (2005) and van Gool et al. (2008).

semblages and structural styles that are separated by thrust faults or erosional unconformities (Wardle and van Kranendonk, 1996; Clark and Wares, 2005). In western Labrador, the Tamarack and Schefferville zones form the western and southern portion of the Labrador Trough, with other lithotectonic zones (Howse, Hurst, Retty and Laporte) restricted to

the eastern margin of the trough, in an area north of latitude 54°30'N (Figure 8).

The Tamarack Zone is composed of autochthonous sediments occurring on the western margin of the Labrador Trough, which unconformably overlie the Archean Superior



Provence, including the granulite to upper-amphibolite-facies rocks of the Ashuanipi Complex in western Labrador (Percival, 1987; van Nostrand and Bradford, 2014). The Tamarack Zone includes rocks of the Wishart, Sokoman and Menihék formations of Cycle 2, as well as the Tamarack River Formation of Cycle 3 (Figure 9). The rocks of the Tamarack Zone generally lie west of the Hudsonian Front and were largely undeformed during the New Québec Orogen (with only minor folding and slaty cleavage development in the Menihék Formation (Harrison *et al.*, 1972).

The Schefferville Zone is parautochthonous to allochthonous and is composed of Cycle 1 and Cycle 2 sediments (Figure 9). These sediments, and associated volcanic rocks, were deformed during the New Québec Orogen, which records the oblique convergence and collision of the Archean Superior Craton to the west and an Archean core zone to the east at 1.82 to 1.77 Ga (Wardle *et al.*, 1990, 2002). The Schefferville Zone can be further subdivided into two subzones, with distinct stratigraphic and structural characteristics (Harrison *et al.*, 1972; Conliffe, 2015; Figure 9).

South of the Grenville Front, the rocks of southwestern Labrador form three metamorphic terranes; the Lac Joseph, Molson Lake and Gagnon terranes (Figure 8; van Gool, 1992;

Rivers *et al.*, 1993; Connelly *et al.*, 1995). The Paleoproterozoic rocks of the Lac Joseph Terrane were metamorphosed to upper amphibolite- to granulite-facies during the Labradorian Orogeny (~1670 to 1620 Ma), and were subsequently emplaced over the Molson Lake Terrane late in the Grenvillian Orogeny (Connelly, 1991). The Molson Lake Terrane is dominated by granitoid gneisses of the Trans-Labrador Batholith (~1650 Ma) that are intruded by the Mesoproterozoic Shabogamo Gabbro (Connelly, 1991; Connelly *et al.*, 1995). The gneisses of the Molson Lake Terrane were originally mapped as metamorphosed equivalents of the Le Fer Formation shales (*e.g.*, Rivers, 1985a, b; Rivers and Massey, 1985), and this is reflected in much of the published company data from this region. However, more detailed mapping and U–Pb geochronology reclassified these rocks as the southwest extension of the Trans-Labrador Batholith (Connelly, 1991; van Gool, 1992; Connelly and Heaman, 1993). The Molson Lake Terrane was subsequently deformed and metamorphosed during the Grenvillian Orogeny at ~1000 Ma (Connelly and Heaman, 1993; Connelly *et al.*, 1995; Rivers *et al.*, 2002), and it structurally overlies the Gagnon Terrane to the northwest. The Gagnon Terrain is host to all of the iron-ore deposits of southern Labrador, and its stratigraphic, structural and metamorphic characteristics are discussed further in the following *Geology of the Gagnon Terrane Section*.

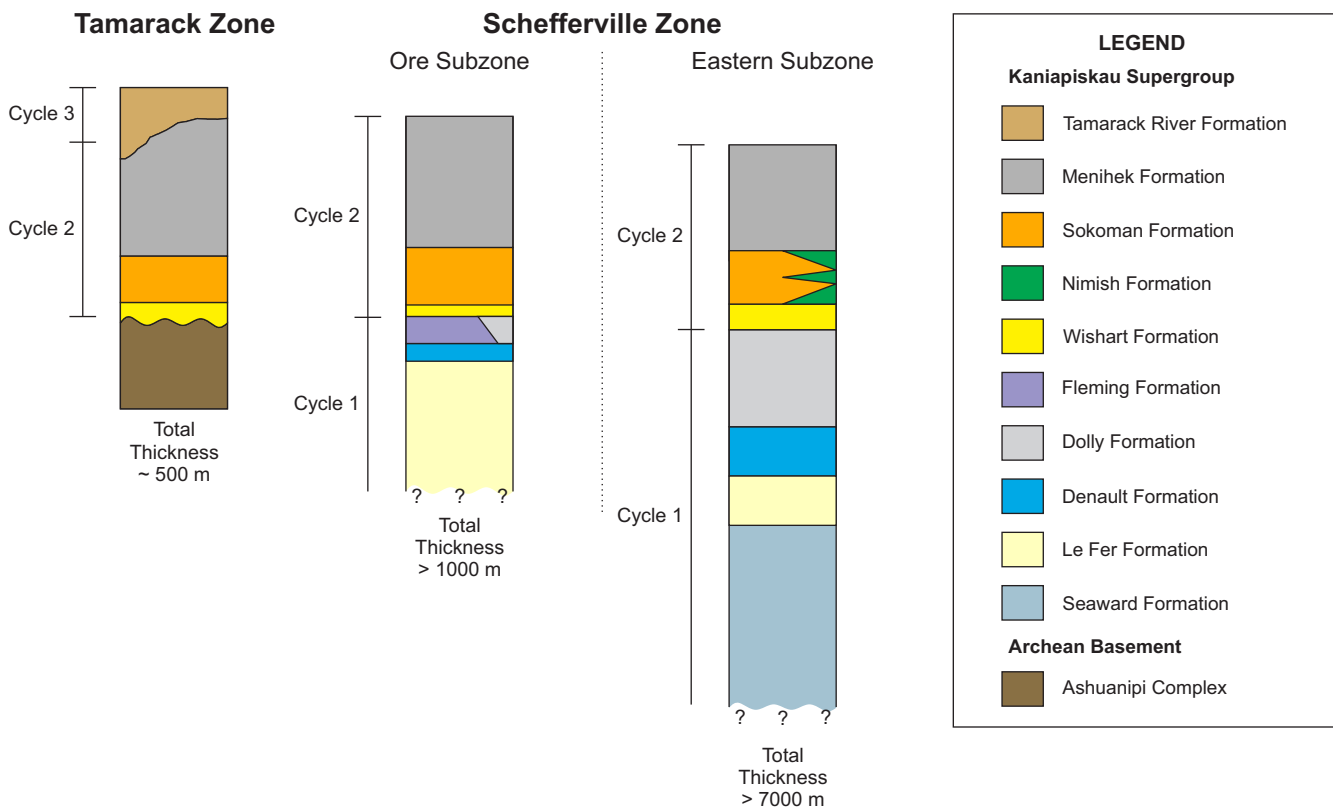


**Figure 9.** Schematic stratigraphy of the Kaniapiskau Supergroup in the Tamarack and Schefferville zones in the central Labrador Trough.

# GEOLOGY OF THE GAGNON TERRANE

## STRATIGRAPHY

The metasedimentary rocks of the Gagnon Terrane represent the continuation of the Kaniapiskau Supergroup south of the Grenville Front. This section consists of a brief description of the main rock types (in ascending order from oldest to youngest), excluding the Sokoman Formation, which is described in detail in the *Sokoman Formation* Section. This is followed by a short discussion on the nature of the sedimentary basin prior to deformation, and on the difficulties in distinguishing between various quartzofeldspathic units in the field.

The similarities between the rocks of the Wabush Lake area and those of the Kaniapiskau Supergroup in the Scheferville area were recognized by Neal (1950a). However, the high degree of metamorphism south of the Grenville Front complicated stratigraphic interpretations and the rocks were given separate stratigraphic names, with those to the south commonly referred to as the Gagnon Group (Dimroth *et al.*, 1970; Muwais, 1974). Further mapping demonstrated that these units are continuous across the Grenville Front, and Rivers (1980d) proposed that this dual nomenclature be abandoned, and that the formational names of the Kaniapiskau Supergroup be adopted across the Grenville Front and throughout the Labrador Trough. The correlation between the formations recognized in the Gagnon Group and those of the Kaniapiskau Supergroup are shown in Table 3. Although only the formation names defined in the Kaniapiskau Supergroup are used throughout the remainder of this document, the reader is cautioned that all pre-1980 publications, and some recent company assessment reports, refer to the former nomenclature.

### Ashuanipi Complex

The Ashuanipi Complex is a granulite-grade sub-province of the Archean Superior Province that forms the basement rocks in the study area. It is primarily composed of mafic, intermediate and felsic, migmatitic orthogneiss and paragneiss and has been described in detail by James (1997). South of the Grenville Front, the Ashuanipi Complex has been variably retrogressed and reworked by Grenvillian metamorphism and deformation (van Gool, 1992; van Gool *et al.*, 2008).

### Le Fer (Attikamagen) Formation

The Le Fer Formation is the oldest metasedimentary unit in the Kaniapiskau Supergroup rec-

ognized in the study area. It is referred to the Attikamagen Formation by Rivers (1980d, 1983a, b), van Gool (1992) and van Gool *et al.* (2008), and has been named the Katsao Formation in a number of company reports (*e.g.*, Lyons *et al.*, 2013; Steele, 2013). However, as it represents the metamorphic equivalents of the Le Fer Formation shales, siltstones and greywackes that are present north of the Grenville Front, it is herein referred to as the Le Fer Formation to preserve the stratigraphic continuity.

The Le Fer Formation consists of white to light-brown, banded, medium- to coarse-grained quartzofeldspathic schists and gneisses (van Gool, 1992). Its mineralogy is predominantly quartz–plagioclase–biotite ± K-feldspar ± garnet and aluminous layers composed of quartz–plagioclase–muscovite ± staurolite ± kyanite (Rivers, 1983b; van Gool *et al.*, 2008). The eastern portion of the Le Fer Formation was deposited in a deep-water turbiditic environment and has stratigraphic thicknesses up to 300 m. It is commonly interbedded with thin units of dolomitic marble, calc-silicates, and metavolcanic amphibolites (possible equivalents of the Denault and McKay River formations). The Le Fer Formation thins to the west, where it represents clastic slope deposits in shallow to moderate water depths (van Gool, 1992). On the western edge

**Table 3.** Stratigraphic correlations between the formations of the Gagnon Group (as defined by Clarke, 1965) and those of the Kaniapiskau Supergroup in the central Labrador Trough (adapted from Rivers, 1980d)

Former Nomenclature (pre-1980) Gagnon Group	Current Nomenclature Kaniapiskaue Supergroup
<i>Middle Proterozoic</i> Shabogamo Gabbro	<i>Middle Proterozoic</i> Shabogamo Intrusive Suite
<i>Lower Proterozoic</i> Nault Formation Wabush Formation Huguette Formation <sup>1</sup> Wapussakatoo (or Carol) Formation Felix Formation <sup>2</sup> Nault Metavolcanics Duley Formation Katsao Formation	<i>Lower Proterozoic</i> Menihek Formation Sokoman Formation Ruth Formation Wishart Formation Dolly Formation McKay Formation <sup>3</sup> Denault Formation Le Fer Formation <sup>4</sup>
<i>Archean</i> Ashuanipi Complex	<i>Archean</i> Ashuanipi Complex <sup>5</sup>

<sup>1</sup>Discontinuous unit at base of Sokoman Formation (Dimroth *et al.*, 1970), not included in Gagnon Group by most authors and can be considered a basal unit of the Sokoman Formation

<sup>2</sup>Discontinuous unit only recognized south of the study area by Jackson (1976), not included in Gagnon Group by most authors

<sup>3</sup>Stratigraphic position varies, may correlate in part with the Nimish Formation (Noel, 1992)

<sup>4</sup>Commonly referred to as Attikamagen Formation

<sup>5</sup>Commonly referred to as Ashuanipi Metamorphic Complex

of the basin, the Le Fer Formation tapers out completely, leaving the upper stratigraphy resting conformably on the basement rocks of the Ashuanipi Complex (Figure 10).

### Denault Formation

The Denault Formation occurs to the east and south of Wabush Lake, where it forms a narrow strip conformably overlying the Le Fer Formation (Figure 4). The Denault Formation consists of coarse-grained, banded to massive, dolomitic marble (dolomite–calcite ± quartz), having minor calc-silicate phases (tremolite, diopside, talc), and rare fluorite- and phlogopite-rich horizons (van Gool *et al.*, 2008). In the study area it is extensively recrystallized and is devoid of any original sedimentary textures. However, in proximity to the Grenville Front, the Denault Formation is locally stromatolitic (Brown *et al.*, 1992), and van Gool (1992) interpreted the Denault Formation dolomite as a stromatolitic reef on the edge of a continental shelf separating a platformal environment to the west from deep-water basins to the east. van Gool (1992) indicated that the Denault Formation is in direct contact with the Sokoman Formation in the east of the study area.

East of Wabush Lake, the Denault Formation has been subdivided into three units; a lower silicate-rich unit transitioning into the underlying Le Fer Formation, a middle low-

silica unit (<5% SiO<sub>2</sub>), and an upper silica-rich unit having minor quartzite layers (Campbell and Simpson, 1987). The low silica unit has been mined for dolomite by IOC in a number of locations east of Wabush Lake since 1986, with the Leila Wynne dolomite mine having been active from 1989 to 2005, and the Plateau dolomite mine active since 2009. The dolomite is used as a flux in the smelting process for the production of iron-ore pellets.

### Dolly Formation

The Dolly Formation is located stratigraphically above the Denault Formation in the Schefferville Zone, but has not been reported in the study area. However, Jackson (1976) described metasediments similar to the Le Fer Formation stratigraphically above the Denault Formation to the south of the study area, which he called the Félix Formation and which may represent a metamorphosed equivalent of the Dolly Formation (Rivers, 1980d).

### McKay River Formation

The McKay River formation is an informal name that has been applied to a wide variety of meta-volcanic and meta-tuffaceous rocks that occupy different stratigraphic positions throughout the Kaniapiskau Supergroup. These rocks com-

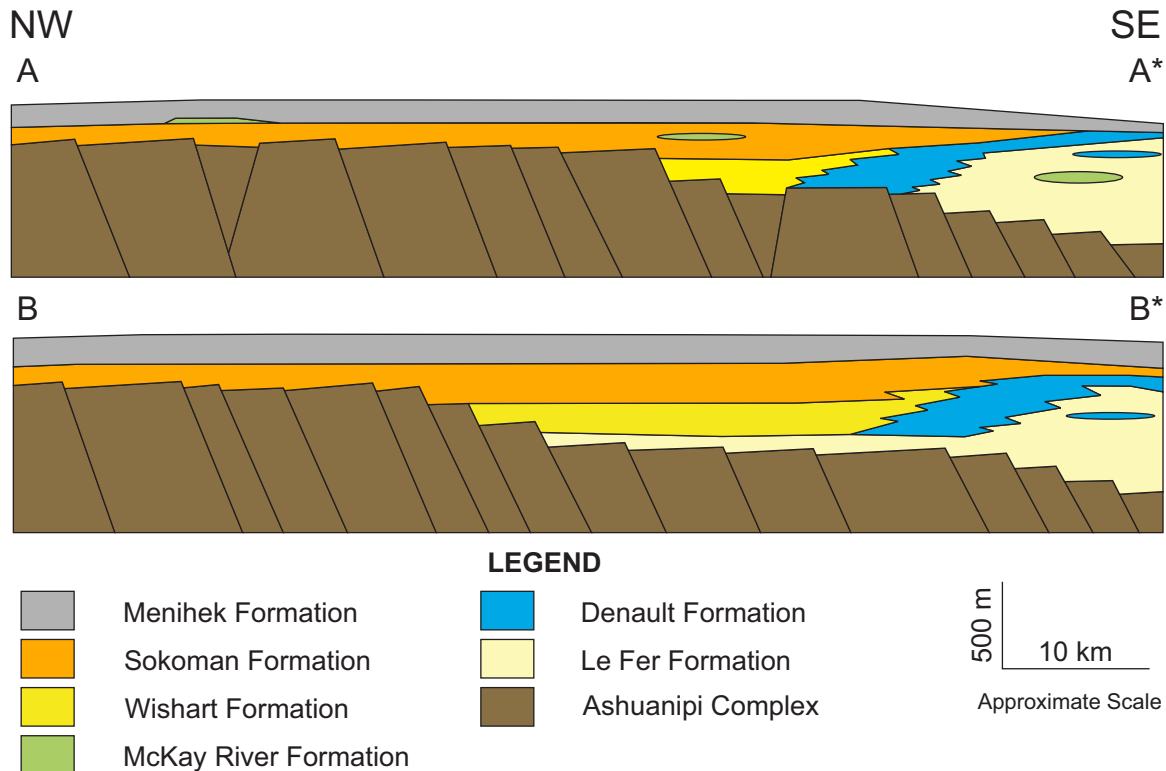


**Figure 10.** Schematic restored cross-sections through the continental margin in the study area prior to Grenvillian deformation (from van Gool, 1992). Location of cross-sections shown in Figure 4.

monly occur to the north of the study area, where they are subdivided into two allochthonous sequences of mafic and ultramafic volcanic rocks (McKay River and Rose Bay formations; Noel, 1992) and a series of fine-grained chlorite–actinolite schists associated with the Sokoman Formation (possible equivalents of the Nimish Formation; Noel, 1992). In the study area, the McKay River formation refers to thin (generally less than 20 m thick) lenses derived from mafic volcanoclastic sediments. The lenses occur either as amphibolites within the Le Fer Formation in the east of the area, or as chlorite–actinolite schists within the Sokoman Formation and at the base of the Menihek Formation to the west (van Gool, 1992).

### **Wishart Formation**

The Wishart Formation forms a distinctive marker horizon in the study area. Where present, it conformably overlies the Denault Formation or the Le Fer Formation. It shows considerable lateral variations in thickness, with a maximum thickness of ~200 m south of Lorraine Lake (van Gool, 1992). The Wishart Formation is not present to the north of Goethite Bay (Figures 2 and 4), and is absent in drillholes both to the west and southeast of the study area, where the Sokoman Formation directly overlies the Archean basement and the Denault Formation, respectively (Lyons *et al.*, 2013; Steele, 2013).

The lower part of the Wishart Formation consists of fine- to medium-grained pelitic schists, composed of quartz–muscovite–sericite ± garnet ± staurolite ± kyanite (van Gool, 1992). Above this, the Wishart Formation occurs as white, medium- to coarse-grained quartzite, with quartz >> carbonate ± amphibole ± muscovite ± garnet ± hematite. This quartzite is generally massive with no sedimentary structures preserved, and forms a series of prominent ridges to the north and west of Labrador City. When weathered, the quartzite is extremely friable and has a sugary texture (Meyer and Dean, 1987). A number of high-purity silica occurrences occur in the study area (Meyer and Dean, 1987), and high-quality silica (98–99%) was mined from 1999 to 2009 at Roy’s Knob, located approximately 0.5 km southeast of the Luce deposit.

The upper contact of the Wishart Formation with overlying units is variable across the study area. In the Carol Lake area, the upper part of the Wishart Formation has been described as a distinct unit having a gradational contact with the overlying Sokoman Formation (Muwais, 1974). The upper part of the Wishart Formation is composed of alternating carbonate (± grunerite) and quartz-rich bands, and lesser layers of muscovite- and biotite-rich schists. Elsewhere, this carbonate-rich upper unit is absent, resulting in the massive quartzites of the Wishart Formation having a sharp contact with the Ruth or Sokoman formations.

### **Ruth Formation**

In the central Labrador Trough, the ferruginous shales of the Ruth Formation overlie the Wishart Formation, and are often included as a subunit of the Sokoman Formation (Zajac, 1974). Although the Ruth Formation has not been formally traced across the Grenville Front (Rivers, 1980d), early mapping identified a thin (<30 m thick), discontinuous unit at the base of the Sokoman Formation, which was referred to as the Huguette formation (Gastil and Knowles, 1960; Jackson, 1963; Dimroth *et al.*, 1970). This unit is described as a quartz–mica ± feldspar schist, and was considered to be the metamorphosed equivalent of the Ruth Formation shales (Dimroth *et al.*, 1970; Rivers, 1980d). A distinctive Fe-silicate-rich lithology with common garnet porphyroblasts (possibly correlative with the Ruth Formation), is also recorded at the base of the Sokoman Formation in a number of deposits to the east and south of Wabush Lake; *e.g.*, Julienne Lake (Conliffe, 2013); Scully deposit (O’Leary, 1973; Farquharson and Thalenhorst, 2006), and Rose and Mills Lake deposits on the Kami property (Lyons *et al.*, 2013), and is discussed in the *Wabush Basin* Section.

### **Menihek Formation**

The Menihek Formation consists of a 15- to 75-m-thick sequence of semipelitic to pelitic schist and gneiss, and forms the top of the Kaniapiskau Supergroup. In the north and west of the study area, it is fine grained, well foliated, dark-grey to black, and consists of quartz–muscovite–biotite–chlorite ± garnet ± plagioclase (van Gool, 1992). To the southwest, the metamorphic grade increases, and the Menihek Formation occurs as a medium-grained, porphyroblastic unit having a mineralogy similar to the Le Fer Formation, making differentiating between the two difficult in the field (Rivers, 1983b; van Gool, 1992). The Menihek Formation is commonly graphitic, with layers of massive- to semi-massive graphite (± sulphides). A number of graphite prospects are hosted in the Menihek Formation in the study area, and the Lac Knife graphite deposit is located approximately 30 km south of Fermont (proven and probable reserves of 7.86 Mt at 15.13% graphitic carbon).

### **Shabogamo Gabbro**

The Shabogamo Gabbro is composed predominantly of medium- to coarse-grained olivine gabbro, minor norite and anorthositic gabbro, and rare ultramafic cumulate rocks (Gower *et al.*, 1990). In the Gagnon Terrane, the Shabogamo Gabbro occurs as sills within the metasediments having undergone greenschist- to upper amphibolite-facies metamorphism (Indares and Rivers, 1995). In the Molson Lake Terrane, the abundance of gabbro increases, commonly occurring as small plutons and dykes that have reached epidote-



facies metamorphism (Indares and Rivers, 1995). Connelly and Heaman (1993) reported a U–Pb age of 1459 ± 23/–22 from the Shabogamo Gabbro in the Molson Lake Terrane, which is interpreted to represent the intrusion age of the gabbro sills in the Gagnon Terrane.

Similarities between the Shabogamo and Michel gabbros (in eastern Labrador) were noted by Gower *et al.* (1990), who suggested they represent a broadly contemporaneous magmatic event having a strike length of more than 750 km. Geochronological evidence (Connelly and Heaman, 1993) supports this contention, and geochemical and isotopic data suggests comparable parental sources within the subcontinental lithospheric mantle (Emslie *et al.*, 1997).

### **Michel Lake Pluton**

The Michel Lake Pluton is the largest example of a number of foliated tonalitic intrusions that occur within the Le Fer Formation. The intrusions display a gneissic banding and consist mainly of plagioclase–quartz–biotite ± muscovite. Although the age of the intrusions is unknown, they have been affected by the same deformation and metamorphism as the surrounding metasediments, and therefore must have been intruded after deposition of the Kaniapiskau Supergroup, but before Grenvillian deformation (van Gool, 1992).

### **Restoration of the Sedimentary Basin**

Rivers (1983a) and van Gool (1992) developed schematic palinspastic reconstructions of the sedimentary basin in the study area, which indicate that the sedimentary sequence was deposited on a subsiding continental margin on the eastern edge of the Superior Province, similar to models developed from elsewhere in the Labrador Trough (Wardle and Bailey, 1981). Despite the extensive deformation of the sediments after deposition, van Gool (1992) suggested that the rapid lateral changes in stratigraphic thickness were related to original lateral variations, likely due to basement topography at the time of deposition. van Gool (1992) conceived two schematic cross-sections through the basement (Figure 10) that displayed the spatial relationship between the sedimentary units. In the northeast, close to the margin with the Superior Province, a thin veneer of Sokoman and Menihek formations sediments (minor Wishart Formation) were deposited onto the Archean basement. This is similar to the stratigraphy represented in the Tamarack Zone to the north. The lower stratigraphic units appear to the south and east of the study area, indicating that the basin deepens to the southeast. He suggested that this marked a significant break in the stratigraphy, with the sediments of the Le Fer Formation to the east representing continental slope deposits.

### **Distinguishing between Metamorphosed Rock Units**

The Le Fer Formation, Menihek Formation, and Ashuanipi Complex gneisses and granitoid gneisses of the Molson Lake Terrane are all quartzofeldspathic rocks, making distinguishing between the different rock units difficult in the field, particularly when the rocks have been exposed to high-grade metamorphism. This has led to difficulties in interpreting the geology and accounts for significant differences between various published and unpublished geological maps of the study area (*see* Rivers, 1980a; Connelly, 1991).

Rivers (1980a, b, c; 1985a, b) and Rivers and Massey (1985) indicated that the Le Fer Formation rocks are dominant in the east of the study area, in the region now recognized as the Molson Lake Terrane. Although Connelly (1991) showed that these rocks are significantly younger than the Kaniapiskau Supergroup metasediments and classified them as part of the Trans-Labrador Batholith (~1650 Ma), no updated maps have been published, and most industry-derived publications show this area as being underlain by Le Fer Formation gneisses.

Differentiating between the Menihek and Le Fer formation gneisses and basement rocks of the Ashuanipi Complex is also difficult, as they all appear as gneisses or pelitic schists (van Gool, 1992). The Menihek Formation is locally distinguished due to the presence of graphitic layers, or by determining its stratigraphic position above the Sokoman Formation. However, its stratigraphic position can often be difficult to determine, and in the north the graphite-poor schists of the Menihek Formation are very similar to phyllitic basement rocks in areas of high strain and lower metamorphic grades (van Gool, 1992). This led Klein (1966) to group the Menihek Formation (then called the Nault Formation) with the Ashuanipi Complex basement rocks.

As the Le Fer Formation directly overlies the Ashuanipi Complex, these rocks cannot be differentiated based on stratigraphic relations. van Gool (1992) provided a number of distinctive characteristics that can be used as criteria to determine the protolith of these rock units. The Ashuanipi Complex locally contains felsic and mafic interlayers and low-strain lenses of granulite-grade rocks or granitoids, and its mineralogy is composed of common K-feldspar, amphibole and epidote, whereas garnet, aluminosilicates and muscovite are only rarely recorded. In contrast, the Le Fer Formation has abundant muscovite and garnet in pelitic schists, but K-feldspar and amphiboles are uncommon.

### **STRUCTURAL GEOLOGY**

The Gagnon Terrane lies south of the Hudsonian Front (Figure 8; Wardle and Bailey, 1981) and, therefore, was not

affected by deformation associated with the New Québec Orogen. Although unequivocal evidence for deformation during the Labradorian Orogeny (~1670 to 1620 Ma) is absent, Brown (1991) reported that deformation of Gagnon Terrane metasediments ~100 km northeast of Labrador City predates emplacement of the Shabogamo Gabbro and therefore may be related to the Labradorian Orogen. Further evidence for pre-Grenvillian deformation is suggested by the presence of folded inclusion trails in garnets from the southeast of the study area (van Gool, 1992). However, for the most part, it is believed that the Kaniapiskau Supergroup sediments were essentially undeformed prior to the Grenvillian Orogeny (Figure 11A; van Gool *et al.*, 2008).

During the Grenvillian Orogeny, the Gagnon Terrane was extensively deformed as part of a foreland-directed fold-thrust belt (Rivers, 1983a; van Gool *et al.*, 2008). This deformation was associated with the emplacement of the Molson Lake Terrane as an orogenic wedge above the Gagnon Terrane along a ductile shear zone (Figure 11B), and subsequent basal accretion of the Kaniapiskau Supergroup sedimentary rocks into the thrust wedge (Figure 11C–E; van Gool, 1992; van Gool *et al.*, 2008). This basal accretion was, in part, controlled by the reactivation of Paleoproterozoic normal faults within the Archean basement rocks (van Gool *et al.*, 2008). van Gool (1992) and van Gool *et al.* (2008) identified two northwest-vergent thrust systems within the Gagnon Terrane. The upper thrust system is thin skinned and dominated by rocks of the Kaniapiskau Supergroup (Figure 11C, D). It consists of a number of ductile-deformed imbricated thrust sheets (~200 m to several kilometres thick; van Gool, 1992). The basal detachment of the upper thrust sheet lies close to the contact between the Kaniapiskau Supergroup and the underlying Archean basement rocks of the Ashuanipi Complex, with only thin slices of basement rocks incorporated into these thrust slices (Figure 11C–E). The development of the thick-skinned thrusting in the lower sheet postdates the emplacement of the upper thrust sheet, and formed along a basal detachment several kilometres deep in the Archean basement (Figure 11E). The lower thrust system predominantly affects Archean basement rocks, with weakly deformed, kilometre-thick thrust sheets separated by steeply dipping ductile shear zones (van Gool, 1992). These thrusts formed due to reactivation of normal faults in the basement under oblique convergence with the Molson Lake Terrane (van Gool *et al.*, 2008). This oblique collision is also responsible for the development of several kilometre-scale north-northwest-trending ductile shear zones, including the Flora Lake Shear Zone and the Julienne Lake Fault Zone (van Gool, 1992). Overall, this Grenvillian deformation resulted in significant crustal shortening. The amount of shortening accommodated by the upper thrust system may have been as much as 50 to 100 km (van Gool *et al.*, 2008).

All internal deformation of the thrust sheets is ductile, with three episodes of deformation and folding recognized (van Gool, 1992; van Gool *et al.*, 2008). The  $D_1$  structures include a pervasive southeast-dipping foliation ( $S_1$ ) and south-southeast-dipping lineation ( $L_1$ ) in the upper thrust system and shear zones in the lower thrust system (van Gool, 1992). The  $F_1$  folds are generally tight to isoclinal and have a west to southwest vergence (Cotnoir *et al.*, 2002). During progressive deformation and thrusting, the  $D_1$  structures were folded into northwest- to west-verging  $F_2$  folds (van Gool, 1992; Cotnoir *et al.*, 2002). The tight to isoclinal  $F_2$  folds are difficult to distinguish from  $F_1$  folds in the field without evidence of fold-interference patterns (Cotnoir *et al.*, 2002). van Gool *et al.* (2008) demonstrated that  $D_1$  and  $D_2$  structures represent progressive stages of deformation within the fold-thrust belt, with  $D_1$  structures forming during basal accretion at the base of the master thrust and  $D_2$  structures related to the displacement of the overriding wedge toward the foreland. The final phase of deformation associated with the Grenvillian Orogeny is represented by open, southeast-plunging, kilometre-scale  $F_3$  cross folds, which postdate all  $D_2$  structures. The  $F_3$  folds formed during gravitational collapse in a sinistral transpressive setting (van Gool *et al.*, 2008) and are common in the southeast of the study area.

## LITHOTECTONIC DOMAINS

van Gool (1992) and van Gool *et al.* (2008) subdivided the study area into five lithotectonic domains (Figure 12), each consisting of one or more thrust sheets. Geological cross-sections through these five domains are shown in Figure 13. From northwest to southeast these domains are:

- Domain I: Domain I straddles the northern limit of the Grenville Front and is composed predominantly of Archean basement rocks having a veneer of cover rocks (Sokoman and Menihek formations) in the north of the study area. These thrust sheets are cut by widely spaced Grenvillian shear zones but otherwise appear to be unaffected by Grenvillian deformation on an outcrop scale.
- Domain II: Thrust sheets in Domain II are 100 m to several hundreds of metres thick, are predominantly composed of rocks of the Menihek and Sokoman formations and have thin slivers of reworked basement rocks. These rocks are strongly deformed, have well-developed  $S_1$  fabrics, and common interference patterns are observed between  $F_1$  and  $F_2$  folds.
- Domain III: This wedge-shaped series of thrust sheets is only present in the northern part of the study area and are variably composed of intensely deformed basement rocks (previously mapped as Le Fer Formation), lenses of undeformed basement rocks and minor Menihek and

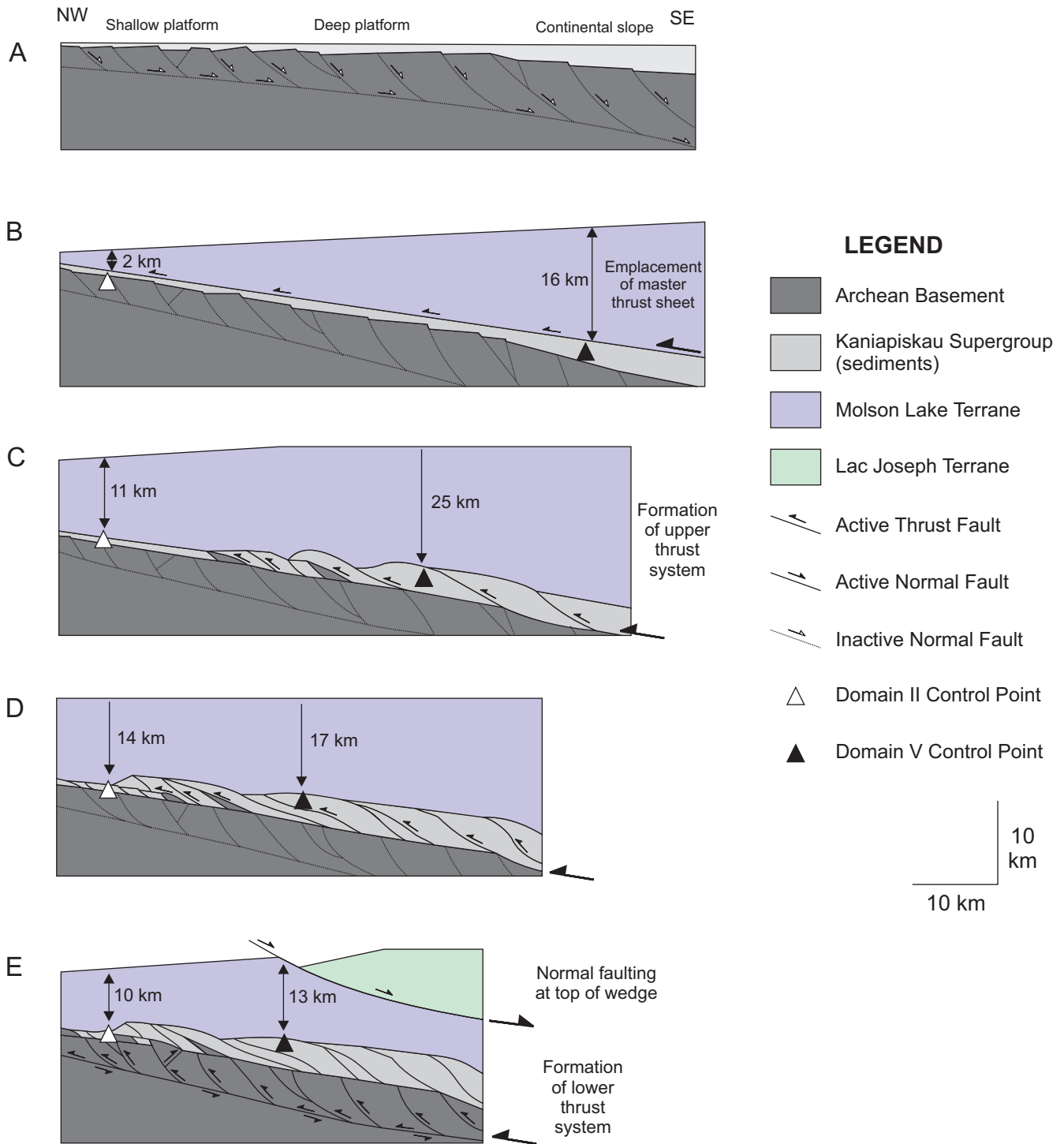


**Figure 11.** Schematic tectonic model for the development of the dual-level, fold-thrust belt in the Gagnon terrane, with open and filled triangles as control points. A) The extended Archean basement with inactive Paleoproterozoic normal faults and Knob Lake Group prior to the Grenvillian Orogeny; B) Emplacement of the Molson Lake terrane as a thrust wedge on top of the extended Paleoproterozoic continental margin; C and D) Progressive development of the thin-skinned, upper-level thrust stack; E) Formation of the lower, thick-skinned, level of the thrust stack, with local out-of-sequence thrusting in the upper system. Normal faulting at the top of the wedge occurred after formation of the lower thrust system. Adapted from van Gool et al. (2008); see text and van Gool et al. (op. cit.) for detailed discussion.

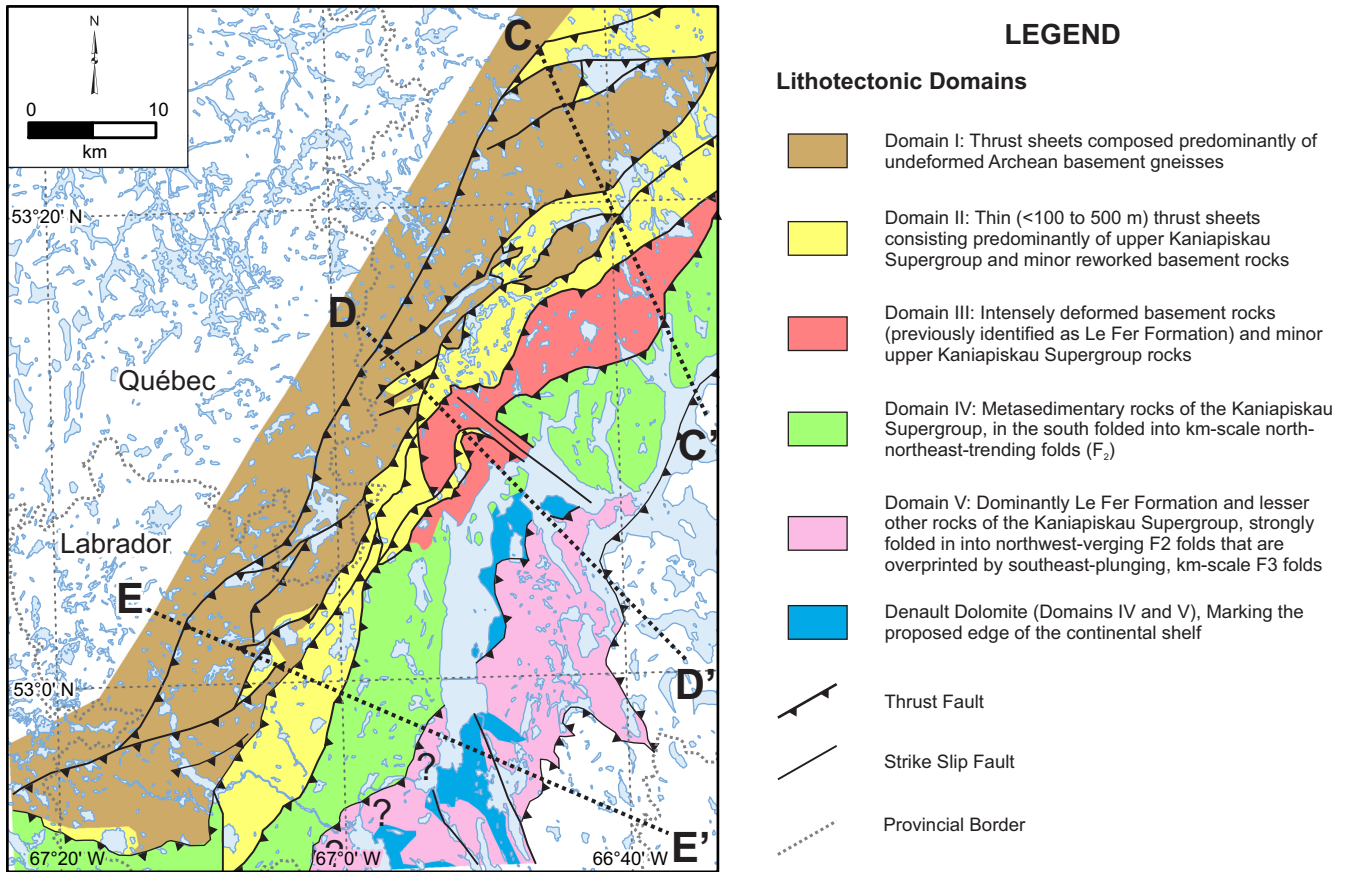


**Figure 12.** Lithotectonic domains in the study area, as defined by van Gool (1992) and van Gool et al. (2008). C-C', D-D', E-E' refer to cross-sections shown in Figure 13. Adapted from van Gool et al. (2008).

Sokoman formation cover rocks. Deformation is similar to Domain II, but an open  $F_3$  synform marks the most northerly evidence for  $D_3$  deformation.

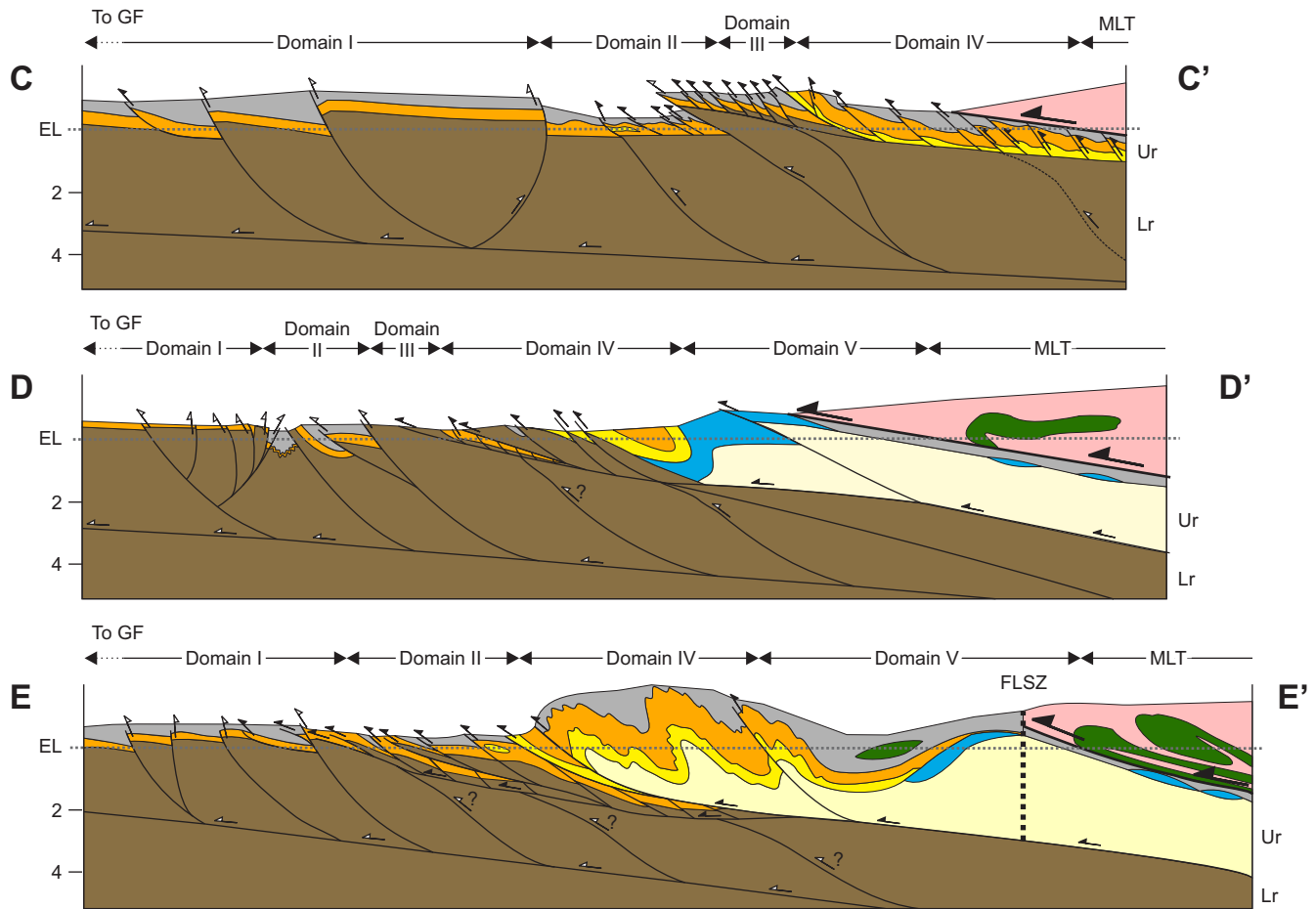
- Domain IV: Kaniapiskau Supergroup rocks dominate having minor amounts of reworked basement. In the south of Domain IV, the Kaniapiskau Supergroup is folded into northwest-vergent  $F_2$  folds overprinted by southeast-plunging  $F_3$  folds, and interference between  $F_1$  and  $F_2$  folds is important in developing economic thicknesses of iron formation (see *Grenvillian Deformation and Metamorphism Section*; Cotnoir et al., 2002). van Gool et al. (2008) indicated that the Denault Formation at the proposed edge of the former continental shelf marks the eastern margin of Domain IV.
- Domain V: East of Wabush Lake, Domain V is mainly composed of the deep-water sediments of the Le Fer Formation, and is intruded by gabbro of the Shabogamo Gabbro. These rocks retain little evidence of  $D_1$  deformation, and are characterized by northwest-verging  $F_2$  folds overprinted by southeast-plunging  $F_3$  folds. van Gool (1992) and van Gool et al. (2008) grouped the rocks

south of Wabush Lake (Duley Lake thrust sheet of van Gool, 1992) in Domain V. However, this thrust sheet contains an almost complete sequence of Kaniapiskau Supergroup metasediments, with similar deformation to the southern portion of Domain IV. In addition, regional aeromagnetic data (Figure 5) suggest that the area mapped as Domain V north of Labrador City represents a southern extension of the Lorraine Lake thrust sheet of van Gool (1992). Therefore, it is likely that rocks south of the Flora Lake Shear Zone belong to Domain IV, with  $D_3$  deformation becoming stronger to the south.

## REGIONAL METAMORPHISM

Regional-scale metamorphism in the Gagnon Terrane is associated with the terminal stages of the Grenvillian Orogeny (~1005 to 980 Ma; van Gool et al., 2008), where peak metamorphic grades ranged from lower-greenschist to upper-amphibolite facies (Rivers, 1983a, b; van Gool, 1992; van Gool et al., 2008). Regionally, the area exhibits an inverted metamorphic grade, with the highest P-T conditions in the structurally higher thrust sheets to the southeast (lithotectonic domains IV and V), and lower P-T rocks in the





### LEGEND

#### Gagnon Terrane

Mesoproterozoic

Shabogamo Gabbro

Paleoproterozoic (Kaniapiskau Supergroup)

Menihék Formation

Sokoman Formation

Wishart Formation

Denault Formation

Le Fer Formation

#### Archean Basement

Ashuanipi Complex

#### Molson Lake Terrane (MLT)

Mesoproterozoic

Shabogamo Gabbro

Trans Labrador Batholith

Thrust fault in upper thrust system (Gagnon Terrane)

Thrust fault in lower thrust system (Gagnon Terrane)

Master roof thrust at base of Molson Lake Terrane

Ductile Shear Zone

Scale 2 km

**Figure 13.** Geological cross-sections through the Gagnon terrane (see Figures 4 and 12 for locations). FLSZ, Flora Lake Shear Zone; GF, Grenville Front; MLT, Molson Lake terrane; EL, erosion level; Lr and Ur, lower and upper levels of the thrust belt. Adapted from van Gool et al. (2008).

structurally lower thrust sheets of lithotectonic domains I and II, close to the Grenville Front (van Gool, 1992; van Gool *et al.*, 2008).

Rivers (1983b) presented a petrographic study of pelitic and quartzofeldspathic rocks of the Le Fer and Menihék formations in which he identified six metamorphic zones, separated by north- to northeast-trending isograds (Figure 14). These zones are, in order of increasing metamorphic grade: Zone 1: chlorite–muscovite; Zone 2: chlorite–muscovite–biotite; Zone 3: muscovite–biotite–garnet; Zone 4: muscovite–staurolite–kyanite; Zone 5: muscovite–biotite–garnet–kyanite; and Zone 6: kyanite–biotite–garnet–leucosome (Rivers, 1983b; van Gool *et al.*, 2008). A detailed description of the petrology and metamorphic reactions of each zone is given in Rivers (1983b). van Gool (1992) carried out a geothermobarometric

study of garnet-bearing metapelites and calculated the peak metamorphic conditions for zones 3 to 6, where the estimated peak P-T conditions for these zones are shown in Figure 14. This work showed that depth of burial increased from ~18 km in Zone 3 to ~30 km in Zone 6, and a corresponding increase in temperature of ~300°C (van Gool *et al.*, 2008).

### SOKOMAN FORMATION

The Sokoman Formation (Wabush Formation) conformably overlies the Wishart Formation quartzites. In areas where the Wishart Formation is absent, the Sokoman Formation unconformably overlies the Denault Formation or Ashuanipi Complex basement rocks. The actual thickness of the Sokoman Formation is difficult to determine due to complex folding and thrusting. The current thickness varies from >100

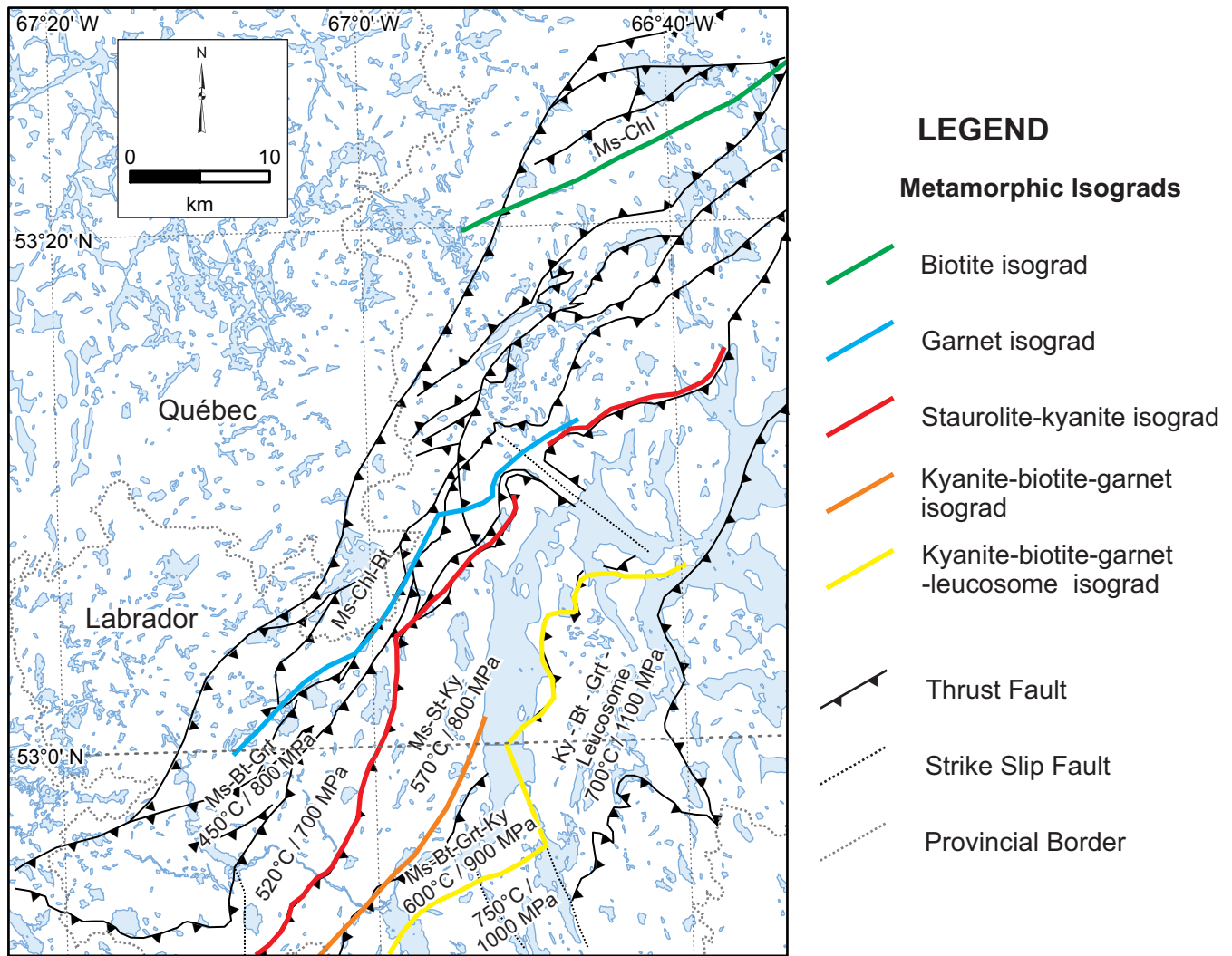


**Figure 14.** Map showing metamorphic zones and isograds in pelitic and semipelitic rocks in the Gagnon terrane (after Rivers, 1983b) with estimated P-T conditions from garnet and coexisting matrix minerals in quartz–garnet–biotite ± kyanite ± plagioclase ± muscovite ± leucosome assemblages (after van Gool, 1992). Adapted from van Gool *et al.* (2008). Bt = Biotite; Chl = Chlorite; Grt = Garnet; Ky = Kyanite; Ms = Muscovite; St = Staurolite.



m in the north and east of the study area (van Gool, 1992; Steele, 2013) to more than 250 m in the Carol Lake area (Muwais, 1974), and between 200 and 350 m in the Scully deposit, as well as in the Rose North and Rose Central deposits at the Kami property (Farquharson and Thalenhorst, 2006; Lyons *et al.*, 2013).

## IRON FORMATION FACIES AND MINERALOGY

The Sokoman Formation consists of three broadly defined facies: oxide-facies, silicate-facies and carbonate-facies. However, the iron formation is generally heterogeneous and there is commonly significant overlap between these facies, with bands of different compositions recorded at metre to micro-millimetre scales (Plates 9 and 10). The following is a short



**Plate 9.** *Folded iron formation, with alternating layers of magnetite and of Fe-silicates and quartz (from outcrop along Trans-Labrador Highway close to the Québec border).*



**Plate 10.** *Mixed oxide-carbonate-facies iron formation with alternating bands of magnetite and carbonate-rich iron formation (from Wabush 3 deposit, drillhole W3-11-101 @ 212 m).*

description of the mineralogy of the three main facies; a more detailed description of the mineralogy and petrology of the Sokoman Formation is given by Klein (1966, 1978).

## Oxide Facies

The oxide-facies consists of massive to banded iron formation, along with abundant quartz and iron oxides (Plates 11, 12 and 13), and lesser carbonate minerals (ankerite, Fe-dolomite or siderite) and iron silicates (grunerite, actinolite, cummingtonite, anthophyllite). Iron oxides consist of magnetite and hematite in variable proportions. Coarse-grained Mn-silicates (rhodonite) and Mn-carbonates (rhodochrosite) also occur in oxide-facies iron formation in some deposits. There is evidence for relict primary sedimentary structures, with circular structures identified in samples from the Carol Lake area, possibly representing oolites (Cotnoir *et al.*, 2002; Plate 14). Quartz and magnetite are generally fine to medium grained (rare coarse-grained magnetite), where grain size increases with metamorphic grade (Klein, 1973). Hematite occurs as medium- to coarse-grained specular hematite and martite (hematite partially to completely pseudomorphing magnetite) and imparts a distinct schistosity to quartz-



**Plate 11.** *Oxide-facies iron formation, with coarse-grained specularite and quartz filling vug (from boulder in Carol Project).*



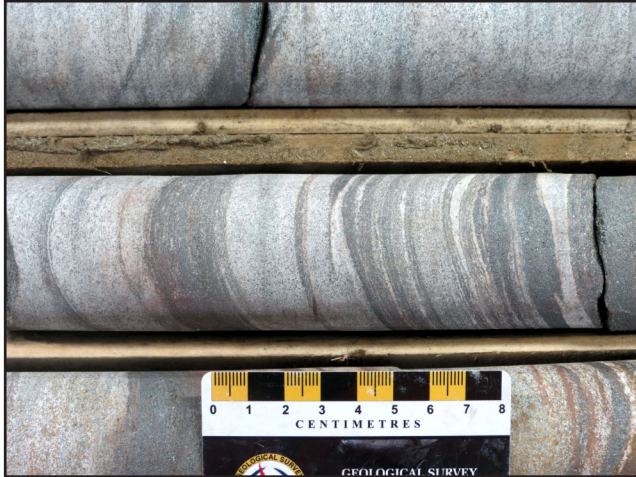


**Plate 12.** Moderately altered, hematite-rich iron formation, with bands of specular hematite and quartz (from Duley prospect, drillhole DU-10-03 @ 131.7 m).

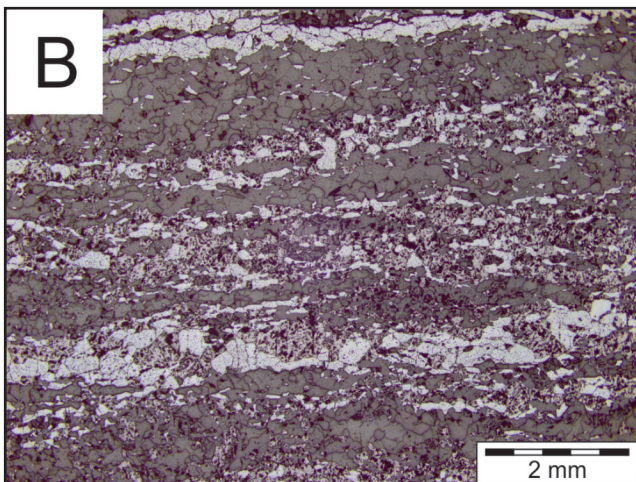
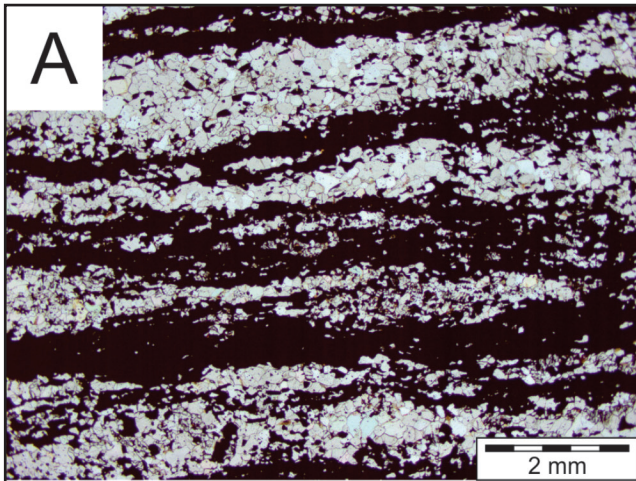


**Plate 13.** A) Photomicrograph of typical banded oxide-facies iron formation, with bands of fine-grained magnetite-hematite and quartz (from Polly Lake Prospect, plane-polarized light); B) Same view as A, in reflected light.

hematite-rich oxide-facies iron formation (Plate 15). The relative amount of magnetite and hematite in the oxide-facies is highly variable, which may reflect primary variations in the parent iron formation (due to changes in the depositional and diagenetic environment) or the effects of regional metamorphism (see *Grenvillian Deformation and Metamorphism* Section for discussion).

### Carbonate Facies

The carbonate-facies consists predominantly of quartz and carbonate (Klein, 1966) that form millimetre- to centimetre-scale bands (Plate 16). This unit commonly occurs in the northern part of the study area but is restricted to small en-

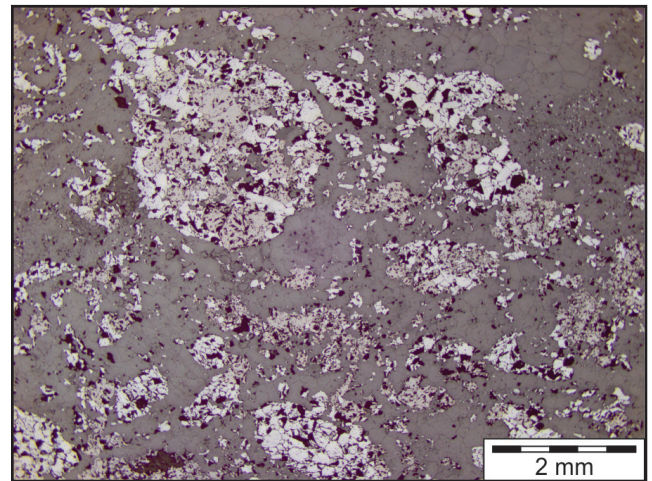


**Plate 14.** Photomicrograph of specular hematite and magnetite replacing possible ooliths in parent iron formation (from Humphrey deposit; drillhole HS-10-72 @ 218 m, reflected light).

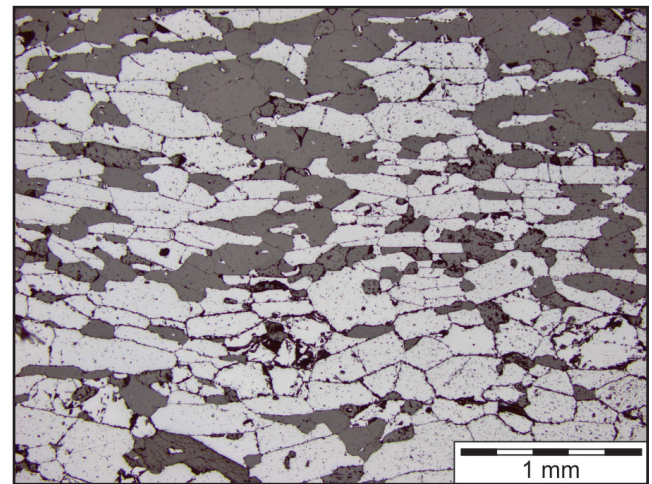


**Plate 15.** Photomicrograph of specular hematite and quartz, with elongate specular hematite imparting schistosity to sample (from Duley prospect; drillhole DU-10-03 @ 131.7 m, reflected light).



claves in the south due to the increased metamorphic grade (see *Grenvillian Deformation and Metamorphism* Section). Quartz is fine to medium grained (Plate 17) and generally granular (may be cherty in north). The carbonate minerals are white to cream, and appear red-brown on weathered surfaces and range in composition from ankerite to Fe-dolomite to siderite. In places, minor magnetite and grunerite are recorded.

### Silicate Facies

The silicate-facies iron formation consists of banded schists, and quartz-rich and Fe-silicate-rich bands, with magnetite, carbonate, biotite, rhodonite ± garnet (Plates 18 and

19). Grunerite is the most common Fe-silicate recorded, with actinolite abundant in some locations (Klein, 1966; Muwais, 1974). Grunerite is fine to medium grained, beige to light brown in hand sample (Plate 18) and brown in thin section, and occurs as columnar, bladed and acicular crystals.



**Plate 16.** Carbonate-facies, with alternating bands of siderite–dolomite and quartz (from D’Aigle Bay 2 North prospect; drillhole DB-10-14 @ 165.9 m).

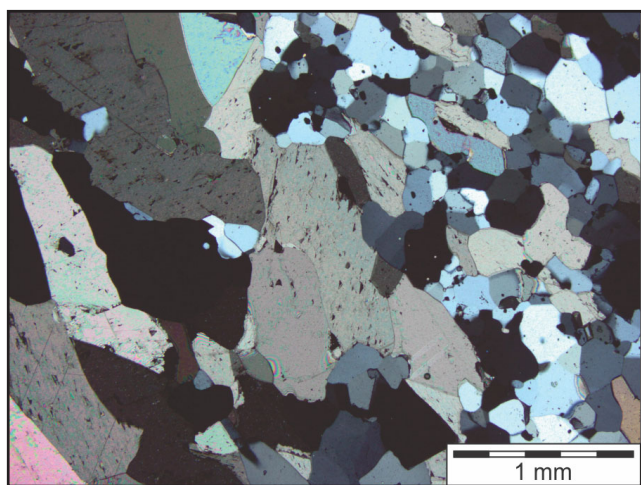


**Plate 17.** Photomicrograph of carbonate-facies iron formation with bands of coarse-grained carbonate and medium-grained quartz (from Knight prospect; drillhole KN-06-A @ 204.7 m, cross-polarized light).

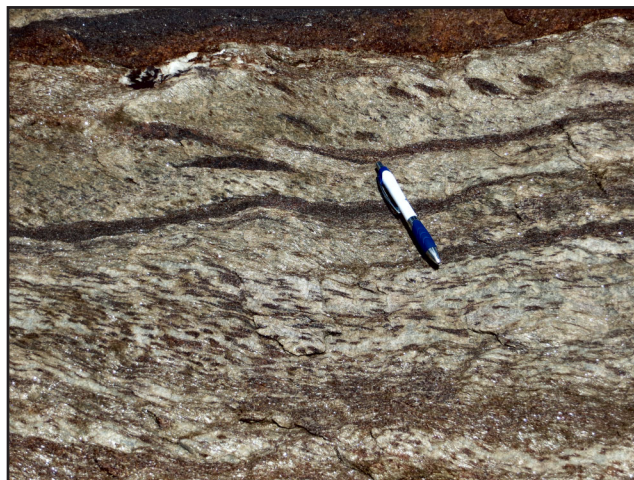


**Plate 18.** Silicate-facies iron formation, with abundant brown-weathering grunerite (from Carol Lake area).



**Plate 19.** Silicate-facies iron formation with discontinuous bands of quartz (mantled by biotite) and Fe-silicates (actinolite, grunerite).



Actinolite forms light- to dark-green acicular subhedral to euhedral crystals (Plate 19). Hornblende has also been recorded in some Fe-silicate-facies units (Cotnoir *et al.*, 2002). The Fe-silicate minerals commonly align parallel to the bedding plane or form clusters and rosettes of acicular crystals (Muwais, 1974). Orthopyroxene (enstatite, ferrosillite) and clinopyroxene (diopside, aegirine–augite) also occur in association with quartz–garnet schists in some locations, and large (up to 10 cm) orthopyroxene porphyroblasts recorded in the south. These pyroxenes make up a relatively larger component of the silicate-facies iron formation farther south in Québec (Mount Reed–Gagnon area; Klein, 1978). The carbonate (calcite, Fe-dolomite, ankerite, siderite) and magnetite content in the silicate-facies rocks is highly variable, with intermediate silicate–carbonate and oxide–silicate-facies common.

### STRATIGRAPHY

The stratigraphy of the Sokoman Formation has been described in detail for the Carol Lake area (Muwais, 1974), Scully deposit (O’Leary, 1973), and the Rose deposit on the Kami property (Lyons *et al.*, 2013). Outside of these areas, the stratigraphy is less well understood because of the overlap between the facies, variable degrees of alteration and metamorphism, complex folding and faulting, and the lack of detailed geological data. It is likely that there are significant variations in the stratigraphy of the iron formations across the study area, where studies in the Schefferville area clearly show that there are rapid facies changes both, across and along strike, due to changes in the basement topography and depositional environments (Zajac, 1974).

Despite these limitations, broad stratigraphic similarities have led to the identification of two large, parallel, north-northeast-trending basins; the Carol Lake Basin to the west and the Wabush Basin to the east. A third smaller basin, the Mills Lake Basin, has been identified to the southeast (Figure 15). The following section includes a detailed discussion of the stratigraphy of the Sokoman Formation in these three basins, focusing mainly on the three areas with the most intense exploration (the Carol Lake area, the

Scully and Rose deposit areas, and the Mills Lake deposit). The stratigraphy of the Sokoman Formation in areas where it cannot be correlated with either of these basins, or for which there is insufficient data to determine their stratigraphy, will also be discussed briefly. For a detailed description of the stratigraphy of individual deposits and showings, see Part B.

### Carol Lake Basin

The Carol Lake Basin extends from the Polly Lake deposit in the south to the Shabo Hill showing in the north, and includes all the major iron-ore occurrences of the Carol Lake area (Figure 15). Muwais (1974) described the stratigraphy

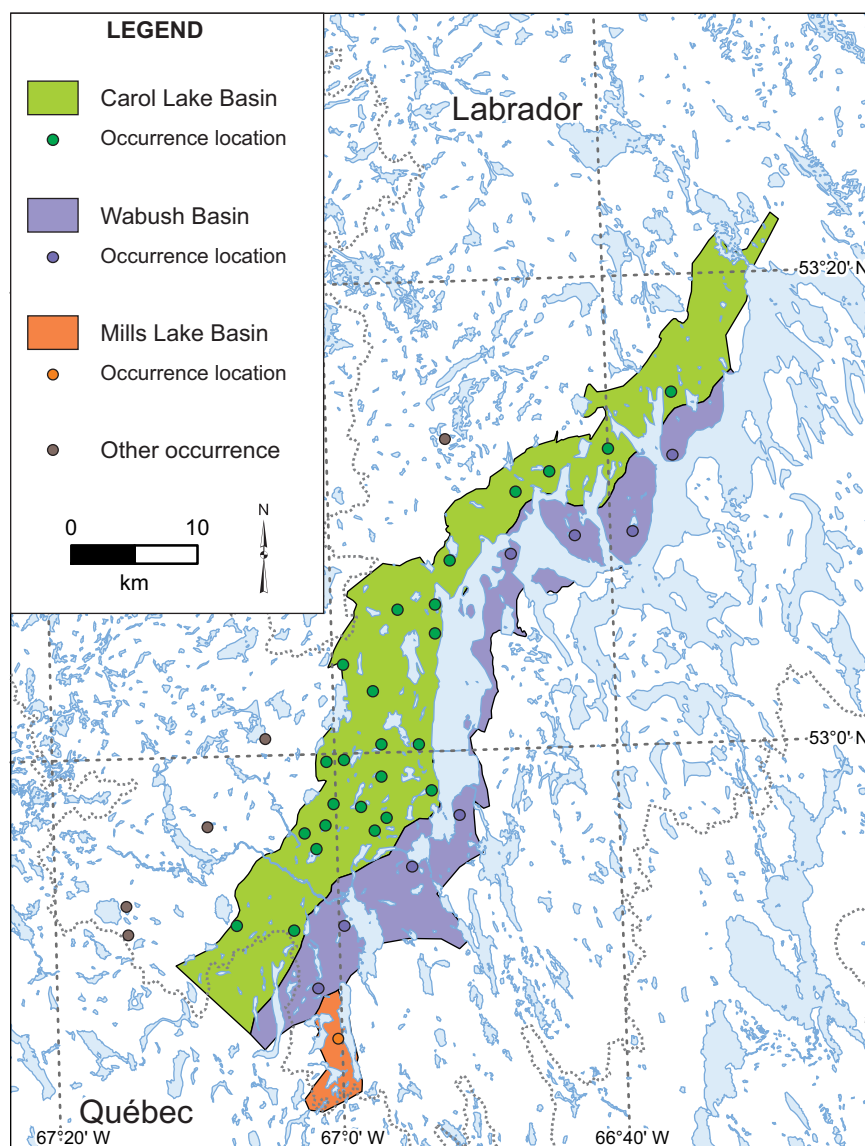


**Figure 15.** Location of the Carol Lake, Wabush and Mills Lake basins described in the text. Refer to Figure 3 for locations of individual iron-ore occurrences mentioned in the text.

of the Sokoman Formation in the Carol Lake area, based on detailed lithological analyses of the Humphrey, and Luce deposits. He subdivided the Sokoman Formation iron formation into three units, each of which was further subdivided into a number of subunits (Figure 16). The units are referred to as the Lower Iron Formation (LIF), Middle Iron Formation (MIF) and Upper Iron Formation (UIF), and may represent metamorphosed equivalents of the units of the same names described from the Schefferville area.

The LIF consist primarily of carbonate-facies iron formation, with lesser mixed carbonate–silicate, and oxide facies. In the Carol Lake area, it ranges in thickness from 45 to 75 m and has been subdivided into three subunits (Muwais, 1974). The lower and upper subunits (LIF 1 and LIF 3) are similar and consist of banded, coarse- to medium-grained

quartz–carbonate with grunerite, and accessory magnetite, chlorite, garnet, pyrite and biotite. The LIF 2 subunit is fine to medium grained and contains a number of thin bands of oxide-facies iron formation separated by zones of mixed carbonate–silicate-facies iron formation.

The MIF ranges in thickness from 45 to 110 m, and consists predominantly of oxide-facies iron formation. Muwais (1974) subdivided the MIF into four subunits (Figure 16), based on variations in the ratios of magnetite and specular hematite, as well as changes in the total iron content. The lowest subunit in the MIF (MIF 1) consists of banded quartz–magnetite–hematite or quartz–hematite–magnetite, with bands of coarse-grained quartz–carbonate–magnetite common towards the base of the subunit and in a brecciated or conglomeratic band in the middle of the subunit. This is overlain by subunit MIF 2, consisting of alternating bands of quartz and foliated specular hematite with little or no magnetite present. The MIF 3 is similar to MIF 2 but has lower iron content. The uppermost subunit (MIF 4) is relatively thin and characterized by higher magnetite content than the underlying subunits.

The UIF is predominantly carbonate- and silicate-facies iron formation, and rare oxide-facies bands. It is 45 to 75 m thick, and subdivided by Muwais (1974) into three subunits (Figure 16). The lowest subunit (UIF 1) is thin and discontinuous, and composed of quartz–carbonate and minor grunerite. Subunit UIF 2 consists of quartz–carbonate–magnetite or quartz–magnetite–carbonate and minor hematite. The uppermost subunit in the Sokoman Formation, UIF 3, consists of quartz, carbonate and Fe-silicates, where the amount of Fe-silicates increases toward the top of the subunit. The Fe-silicates are grunerite and actinolite (actinolite restricted to the upper part of the subunit) and overall UIF 3 has a banded, gneissic texture.

This division of the Sokoman Formation into three main units (LIF, MIF and UIF) has also been recognized outside the main mine area where there has been a significant amount of recent exploration drilling (e.g., Wabush 3, Wabush 6, Polly Lake deposits). The Sokoman Formation in the Wabush 6 deposit, located east of the Luce deposit, can clearly also be subdivided into the LIF, MIF and UIF (Marshall, 2012), despite localized, significant, deformation. In the Wabush 3 deposit, directly south of the Luce deposit, the iron formation consists of a lower quartz–carbonate ± grunerite unit (LIF), a middle quartz–hematite–magnetite unit (MIF) and an upper quartz–carbonate ± grunerite unit (UIF) (Pond, 2013). The oxide-bearing MIF can be further subdivided into a high-magnetite lower subunit (similar to MIF 1), and an upper subunit consisting of specular hematite > magnetite (similar to MIF 2). Similarly, recent drilling at the Polly Lake deposit, located ~13 km southeast of the

Menihek Formation			
Sokoman Formation	Upper Iron Formation (UIF)	UIF 3 Qtz - Gru - Act - Cb Qtz - Cb - Gru Qtz - Cb (Gru)	45-75 m
		UIF 2 Qtz - Mag - Cb Qtz - Cb - Mag	
		UIF 1 Qtz - Cb (Gru)	
	Middle Iron Formation (MIF)	MIF 4 Qtz - Hem - Mag Qtz - Mag - Hem	45-110 m
		MIF 3 Lean Qtz - Hem	
		MIF 2 Qtz - Hem	
		MIF 1 Qtz - Hem - Mag Qtz - Mag - Hem Qtz - Mag (Cb)	
	Lower Iron Formation (LIF)	LIF 3 Qtz - Cb (Gru)	45-75 m
		LIF 2 Qtz - Cb - Mag Qtz - Mag - Cb Qtz - Hem - Mag	
		LIF 1 Qtz - Cb (Gru)	
	Wishart Formation		

**Figure 16.** Stratigraphic column for the Sokoman Formation in the Carol Lake area (after Muwais, 1974).



Wabush 3 deposit has recognized the full sequence of UIF, MIF and LIF (Bineli Betsi, 2012).

North of the Carol Lake area, the stratigraphy of the Carol Lake Basin (with distinctive carbonate- and silicate-facies units above and below the oxide-rich MIF) appears to continue along strike to the Julienne 1, Goethite Bay, Goethite Bay North and Shabo Hill occurrences. However, these correlations remain speculative due to the low density of drilling, intense local alteration and lack of understanding of the structural complexity of some occurrences (see Part B for detailed discussion of stratigraphy at each occurrence).

### Wabush Basin

The Wabush Basin is located directly to the east of the Carol Lake Basin, and extends from the Rose Central and Rose North deposits in the south, to the Shabo Peninsula North showing located north of Shabogamo Lake. Although these occurrences have been variably overprinted by late-stage alteration (see *Late-stage Alteration* Section), the stratigraphy in the Wabush Basin has been shown to be markedly different from that described from the Carol Lake Basin, with a silicate unit at the base of the iron formation, called the Basal Silicate Iron Formation (BSIF). This may correlate with the Ruth Formation in the central Labrador Trough (see *Ruth Formation* Section). It ranges in thickness up to 30 m and, where fresh, consists of quartz–amphibole ± biotite ± chlorite ± garnet (Plates 20 and 21), with rare pyrite recorded in some locations. This unit is directly overlain by oxide-facies iron formation (in contrast to carbonate- and silicate-facies of the LIF in the Carol Lake Basin). In the Scully and Rose deposits, the stratigraphy has been described, in



**Plate 20.** Garnet-bearing BSIF from the base of the Sokoman Formation in the Duley prospect (drillhole DU-10-03 @ 147 m).

detail, by a number of authors (O’Leary, 1973; Farquharson and Thalenhorst, 2006; Lyons *et al.*, 2013; Figure 17) and is summarized here.

### Scully Deposit

The Sokoman Formation at the Scully deposit has been strongly affected by late-stage alteration (see *Late-stage Alteration* Section), and has been subdivided into three main oxide-bearing units (Lower, Middle and Upper members) and two marker units that can be traced throughout the mine area (BSIF and Unit 41; Figure A17). The lower marker unit, the BSIF, is ~25 m thick and consists primarily of quartz and grunerite, and minor chlorite, biotite and garnet (garnet increases in abundance toward the base of this unit). The grunerite is commonly strongly altered to goethite.

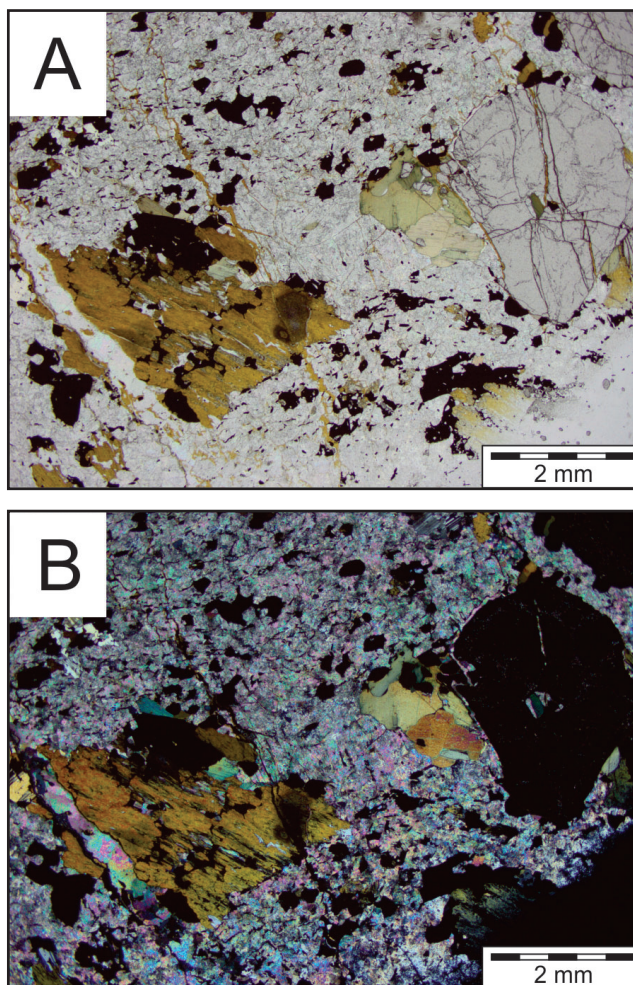


**Plate 21.** A) Photomicrograph of BSIF from the base of the Sokoman Formation, with a quartz-carbonate matrix and large brown grunerite, green chlorite and transparent garnet crystals (from Duley prospect; drillhole DU-10-03 @ 147 m, plane-polarized light); B) Same view as A, in cross-polarized light.



## Rose Central Zone

## Scully Deposit

Rose North Zone		Rose Central Zone		Scully Deposit	
Menihiek Formation		Sokoman Formation		Sokoman Formation	
Upper carbonate and silicate facies iron formation (+ minor oxide facies)	Upper carbonate and silicate facies iron formation (+ minor oxide facies)	Upper carbonate and silicate facies iron formation (+ minor oxide facies)	Upper carbonate and silicate facies iron formation (+ minor oxide facies)	Unit 21: Massive to thinly banded, Goe-rich unit with minor Hem and Mag (waste)	Upper Member
<b>RN3:</b> Weakly altered, banded Mag-rich oxide facies with minor Hem. Fe-silicate and Fe-carbonate content increase upwards	<b>RC3:</b> Banded Mag-rich oxide facies with minor Hem. Fe-silicate and Fe-carbonate content increase upwards	<b>RC3:</b> Banded Mag-rich oxide facies with minor Hem. Fe-silicate and Fe-carbonate content increase upwards	<b>RC3:</b> Banded Mag-rich oxide facies with minor Hem. Fe-silicate and Fe-carbonate content increase upwards	Unit 22: Banded, semi-friable to competent, oxidized Qtz - Hem - Goe unit (ore)	~135 m
Thin carbonate-silicate facies	Thin carbonate-silicate facies	Thin carbonate-silicate facies	Thin carbonate-silicate facies	Unit 23: Massive to thinly banded, Goe-rich unit with minor Hem and mag (waste)	Middle Member
<b>RN2:</b> Interlayered Qtz-Mag and Qtz-Hem units with moderate alteration and secondary Mn-oxides (psilomelane and pyrolucite)	<b>RC2:</b> Interlayered Mag-rich and Hem-rich oxide facies with minor Fe-carbonates and Mn-carbonates (rhodochrosite)	<b>RC2:</b> Interlayered Mag-rich and Hem-rich oxide facies with minor Fe-carbonates and Mn-carbonates (rhodochrosite)	<b>RC2:</b> Interlayered Mag-rich and Hem-rich oxide facies with minor Fe-carbonates and Mn-carbonates (rhodochrosite)	Unit 31: Thinly banded, friable to semi-friable Hem-rich unit (ore)	~120 m
Thin carbonate-silicate facies	Thin carbonate-silicate facies	Thin carbonate-silicate facies	Thin carbonate-silicate facies	Unit 32: Thin siliceous Qtz-rich band with minor Hem (waste)	~10 m
<b>RN1:</b> Banded Qtz-Hem. Moderately to strongly altered with coarse Hem crystals and rhodonite oxidized to psilomelane and pyrolucite	<b>RC1:</b> Fresh, banded Qtz-Hem with minor Mag, Gru, Fe-carbonates and Mn-silicates (rhodonite)	<b>RC1:</b> Fresh, banded Qtz-Hem with minor Mag, Gru, Fe-carbonates and Mn-silicates (rhodonite)	<b>RC1:</b> Fresh, banded Qtz-Hem with minor Mag, Gru, Fe-carbonates and Mn-silicates (rhodonite)	Unit 33: Massive, friable, Hem-rich unit with low Mn (ore)	Lower Member
Altered Basal Silicate Iron Formation (BSIF)	Basal Silicate Iron Formation (BSIF)	Basal Silicate Iron Formation (BSIF)	Basal Silicate Iron Formation (BSIF)	Unit 34: Banded oxidized iron formation with abundant Goe and Mn-bands (waste and ore)	~50 to 80 m
Ruth?	Ruth?	Ruth?	Ruth?	Unit 41: Massive, white quartzite unit with secondary Goe and Mn-oxides (waste)	~25 m
Wishart Formation		Wishart Formation		Unit 51: Massive, black, friable Qtz-Hem-Mag unit with high Mn content (ore)	~10 m
Wishart Formation		Wishart Formation		Unit 52: Competent, maroon, thickly banded Qtz - Goe - Hem unit (waste)	~50 to 80 m
Wishart Formation		Wishart Formation		Unit 53: Banded, friable to semi-competent Qtz - Hem - Mn oxide unit (ore)	~50 to 80 m
Wishart Formation		Wishart Formation		Basal Silicate Iron Formation (BSIF) with rare garnet pseudomorphs (waste)	~25 m
Wishart Formation		Wishart Formation		Wishart Formation	~25 m

**Figure 17.** Stratigraphic column for the Sokoman Formation in the Scully deposit (Wabush Mines) and Rose deposit. Compiled from unpublished company data and lithological descriptions in O'Leary (1973); Farquharson and Thalenhorst (2006) and Lyons et al. (2013).

The BSIF grades upward into the Lower Member with a gradual increase in the proportion of iron oxides and a decrease in grunerite. The Lower Member is ~50 to 80 m thick and has been mined as ore. It is subdivided into three units (Units 51 to 53; Figure 17; Farquharson and Thalenhorst, 2006). Unit 53 is banded, friable to semi-competent, and comprises quartz–hematite ± magnetite, and has a relatively high Mn content (2.7 wt. % Mn in concentrate, increasing close to the contact with Unit 52; O’Leary, 1973; Farquharson and Thalenhorst, 2006). The Mn commonly occurs as fine-grained psilomelane and pyrolusite. Unit 52 is thick banded and competent, and has a distinct maroon colour. It consists predominantly of quartz, goethite and some martite, and is considered a waste unit. Unit 51 is a thin, friable, oxide-rich unit (quartz–hematite–magnetite–Mn-oxides) with up to 9 wt. % Mn (O’Leary, 1973).

The Lower Member is overlain by a distinct quartzite horizon (Unit 41), which is the main marker unit in the Sokoman Formation. It is a waste unit, and consists mainly of friable to semi-massive quartzite having numerous vugs and veins filled with goethite, Mn-oxides and specular hematite. Occurring conformably above this, the Middle Member has the highest iron content and the lowest Mn-content in the Scully deposit, and therefore is the best quality ore (Farquharson and Thalenhorst, 2006). It is approximately 120 m thick and is divided into four units (Units 31 to 34; Figure 17). Unit 34 is thin to thick banded and is generally oxidized with a high proportion of goethite and occasional Mn-rich bands. It is typically classified as a waste unit, but in some areas it has a high enough iron-oxide content to be considered ore. Unit 33 is massive and friable, and is composed of quartz and hematite, with numerous cm-scale oblong pits and vugs. Unit 32 is a thin horizon of waste rock with a high proportion of quartz and lesser magnetite and hematite. The uppermost unit in the Middle Member, Unit 31, is friable to semi-friable, thinly banded and rich in hematite.

The Upper Member is ~135 m thick and has a much lower iron-oxide content than the Lower and Middle members. It is generally a waste unit, but reaches ore grade in some areas. O’Leary (1973) suggested that the Upper Member represented carbonate-facies iron formation with minor oxide-facies bands, with carbonate replaced by goethite during late-stage alteration. Therefore, the Upper Member is very similar to the UIF in the Carol Lake area. The Upper Member has three units, Units 21 to 23. Unit 23 is thinly banded and rich in goethite, with minor magnetite and hematite (specular hematite and martite). Unit 22 is a banded, semi-friable to competent unit with quartz–goethite–hematite–magnetite and is ore grade in places. Unit 21 is similar to Unit 23, with high goethite content and only minor iron oxides.

### **Rose Deposit**

The Rose deposit is subdivided into three main zones, Rose North, Rose Central and South Rose/Elfie Lake zones, which represent different components of a series of gently plunging north-northeast–south-southwest upright to slightly overturned anticlines and synclines (Lyons *et al.*, 2013). Although the thickness of individual units, and the degrees of alteration, vary across these zones, Lyons *et al.* (2013) recognized three main oxide units separated by thin (<10 m), discontinuous silicate and carbonate units with low Fe-oxides, as well as an overlying carbonate–silicate unit and a thin BSIF unit at the base of the iron formation (Figure 17). Exploration at the Rose deposit has focussed on the Rose North and Rose Central zones, as these have the thickest sequence of oxide facies iron formation, and the following discussion is based on the stratigraphy in these zones.

The BSIF in the Rose Central zone is predominantly composed of Fe-silicates (grunerite > actinolite) and quartz, with minor Fe-carbonates, garnet, magnetite and hematite. In the Rose North zone, this unit is commonly altered, with Fe-silicates replaced by goethite. In the Rose Central zone, the lower oxide unit, termed RC-1, is banded, hematite-rich with magnetite and restricted to the margins of the facies or as occasional crystalline clusters replacing hematite. The Fe-silicates and Fe-carbonates are rare, whereas crystalline rhodonite is locally common. The equivalent oxide-facies in the Rose North zone (RN-1) is very similar in appearance when fresh. However, in the Rose North zone, RN-1 is commonly altered and friable, gangue quartz partially leached, specular hematite recrystallized to coarser grained subhedral to euhedral hematite, Fe-silicates and Fe-carbonates replaced by Fe-hydroxides (*e.g.*, goethite), and rhodonite oxidized to psilomelane, and rare pyrolusite.

The middle oxide unit (RC-2 in Rose Central zone) consists of interlayered hematite- and magnetite-rich oxide-facies iron formation, with magnetite-rich rocks more common. The main gangue minerals are quartz, Fe-carbonates and Fe-silicates, and rhodochrosite is locally common. In the Rose North zone, the RN-2 oxide unit is moderately altered, with an increase in the hematite content and rhodochrosite commonly oxidized to psilomelane and pyrolusite.

The RC-3 and RN-3 are the upper oxide units in the Rose Central and Rose North zones, respectively. These units are both similar with fine-grained magnetite >> hematite within a fine-grained Fe-silicate gangue. There is a relatively much lower degree of secondary alteration in RN-3 compared to RN-2 and RN-1. Mn-bearing minerals are rare and the proportion of Fe-silicate and Fe-carbonate minerals increase to-

ward the top of this unit. The upper oxide units have a gradational diachronous upper contact with the upper non-oxide iron formation.

**Other Occurrences**

Although the stratigraphy of the Sokoman Formation north of the Scully deposit is less well understood, some broad correlations are made. The Julienne Lake deposit consists of a thick sequence of oxide-facies iron formation having minor lean quartzite and Mn-rich units, which are separated from the underlying Wishart Formation by a thin (<20 m) BSIF unit, similar to that described in the Scully and Rose deposits (Conliffe, 2013). In addition, exploration drilling from deposits farther to the north, including the Julienne 2, Shabo Peninsula South and Shabo Peninsula North occurrences, have shown a similar stratigraphy, with oxide-facies iron formation separated from the underlying Wishart Formation quartzite by a thin silicate-facies that may correlate to the Ruth Formation.

**Mills Lake Basin**

A third structural basin, southeast of the Wabush Basin, has been suggested by Lyons *et al.* (2013) based on the stratigraphy of the Mills Lake deposit. Lyons *et al.* (2013) suggested that the Mills Lake Basin may also include the Mont-Wright deposit and several smaller iron deposits west of Fermont.

Much of the information on the stratigraphy on these deposits comes from the Mills Lake deposit, where exploration drilling has identified significant stratigraphic differences compared to the Carol Lake and Wabush basins (Lyons *et al.*, 2013). The base of the Sokoman Formation is defined by a thin (<20 m) BSIF, which is similar to that recorded at the nearby Rose deposit, and may correlate with the Ruth Formation in the central Labrador Trough (Lyons *et al.*, 2013). This is overlain by carbonate-facies iron formation with minor disseminated magnetite, above which is the main oxide-facies iron formation. This oxide-facies iron formation is 30–130 m thick in the Mills Lake deposit, thinning to < 25 m in the Mart Lake area. It is subdivided into three stratigraphic units (Lyons *et al.*, 2013); a lower magnetite-dominated unit, a middle unit with abundant hematite and layers of rhodonite and Mn-rich Aeg (Plates 22 and 23), and an upper magnetite-rich unit. Overlying the main oxide-facies unit is 20 to 50 m of carbonate-facies iron formation, a diffuse and a thin (<25 m) hematite-rich oxide-facies, and >50 m of carbonate-facies iron formation at the top of the Sokoman Formation. Zones of silicate-facies iron formation are reported within the carbonate-facies iron formation, which are thought to represent metamorphic reactions during decarbonation (Lyons *et al.*, 2013).



**Plate 22.** Mixed silicate and oxide (hematite) facies iron formation, with pink rhodochrosite (from Mills Lake deposit, drillhole K-10-95 @ 76.3 m).

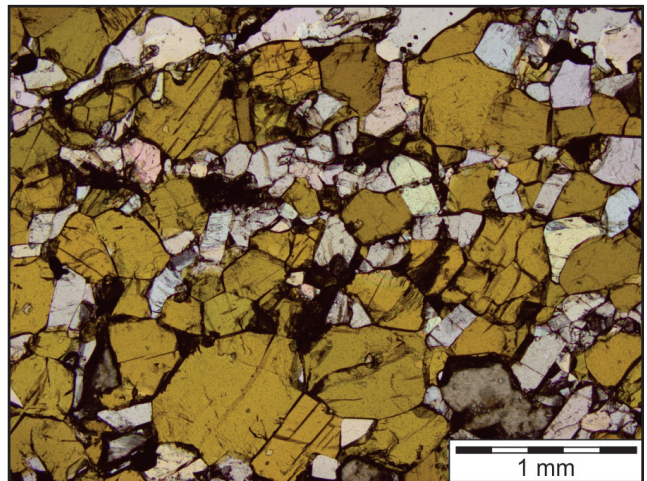


**Plate 23.** Photomicrograph of silicate-facies iron formation, with brown manganoean aegirine and pink to transparent rhodochrosite (from Mills Lake deposit; drillhole K-10-95 @ 76.3 m, plane-polarized light).

**Other Occurrences**

On the western margin of the Gagnon Terrane (Lithotectonic Domains I and II of van Gool *et al.*, 2008), the Sokoman Formation occurs as multiple, repeating thrust sheets inter-layered with the Menihék Formation and the Archean basement rocks. The absence of a full stratigraphic section makes correlations with the stratigraphy elsewhere in the study area difficult. However, recent drilling in the Emma Lake, Lac Virot and Sudbury Lake areas have confirmed the presence of oxide-, silicate- and carbonate-facies iron formation (Goldner *et al.*, 2013; Steele, 2013).



## GRENVILLIAN DEFORMATION AND METAMORPHISM

Deformation and metamorphism of the Sokoman Formation during the Grenvillian Orogeny were the main factors in the development of economic iron-ore deposits in the study area. Cotnoir *et al.* (2002) presented the results of a regional analysis of the geology and structure, with specific focus on the effects of deformation on the location of economic concentrations of iron ore. Although there may have been some primary control on the thickness of iron formation (due to thicker accumulations of iron-rich sediments in topographic depressions controlled by basement structures), the presence of economically mineable thicknesses of oxide-facies iron formation is mainly due to fold repetition and/or viscous flow of hematite-rich oxide-facies iron formation into fold hinges during  $D_1$  and  $D_2$  deformation. In the Humphrey orebody, the complex interference of  $F_1$  and  $F_2$  folds has resulted in a 6-fold thickening of the oxide facies, while interpreted drill sections across the Luce deposit have shown more than ten  $F_1$  fold repetitions. The more viscous flow of hematite vs. magnetite during high temperature and pressure deformation may also be important in developing thick accumulations of oxide-facies iron formation in fold hinges, although the effects of this viscous flow is considered secondary to fold repetition (Cotnoir *et al.*, 2002). The authors considered that  $D_3$  deformation was not important in the development of localized concentrations of iron ore, although the dome and basin structures associated with km-scale  $F_3$  folds may be important in the distribution of some deposits.

The effects of Grenvillian metamorphism on the Sokoman Formation also had important implications for the metallurgy of iron ores, and the metamorphic reactions in the iron formation are described, in detail, by Klein (1973, 1978). The unmetamorphosed MIF from the Schefferville area initially consisted mainly of chert, magnetite and hematite, and upon increased metamorphic conditions, the chert and iron oxides were recrystallized (accompanied by a marked increase in grain size) and formed the oxide-facies iron formation (Klein, 1973). Despite this pervasive recrystallization, original sedimentary layering and relict sedimentary features (*e.g.*, oolites, Plate 14) are commonly preserved. The presence of coexisting magnetite and hematite with no evidence of replacement textures in some deposits (Plate 24) led Klein (1966, 1973, 1978) to argue that oxygen was generally immobile and  $fO_2$  was narrowly buffered during metamorphism, and the ratio of hematite to magnetite in the oxide-facies iron formation reflected the original mineralogy of the parent iron formation (Muwais, 1974). The presence of martite after magnetite in some samples (Plate 25) was attributed either to minor movement of oxygen during regional metamorphism (Klein, 1973), or to low-temper-

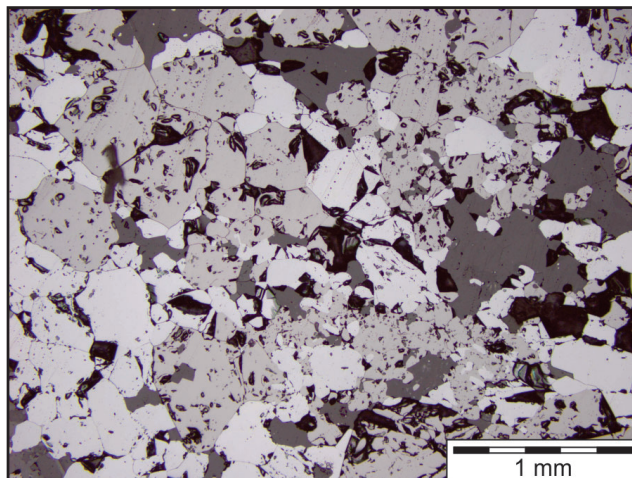


**Plate 24.** Photomicrograph of co-existing euhedral to subhedral hematite and magnetite (from Humphrey deposit; drill-hole HS-10-72 @ 218 m, reflected light).

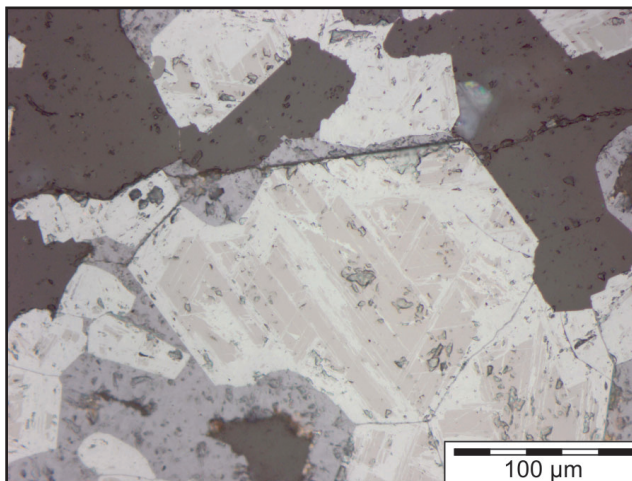


**Plate 25.** Photomicrograph of hematite replacing an euhedral grain of magnetite (forming martite and kenomagnetite), with secondary goethite infilling space around the grain (from Julienne 2 prospect; drillhole J2-10-08 @ 153.2 m, reflected light).

ature meteoric fluid infiltration (Cotnoir *et al.*, 2002). However, Kaul *et al.* (2012) showed that iron ores from the Luce deposit displayed evidence for both martitization and mushketovitization (transformation of hematite to kenomagnetite under reducing conditions), which was attributed to regional metamorphism as well as later low-temperature fluid alteration. They also documented kenomagnetite replacing carbonates, indicating that at least some of the oxides in the Sokoman Formation formed due to processes other than simple recrystallization of oxides in the unmetamorphosed precursor iron formation.

Some unmetamorphosed iron formations in the Schefferville area have relatively high Mn values (up to 1.7% MnO; Conliffe 2016a), mainly occurring as Mn-rich siderite and ankerite (Zajac, 1974), whilst Mn-oxides, such as pyrolusite and manganite, are common in weathered and altered iron formation. During metamorphism, these Mn-rich horizons are transformed into rhodochrosite-rich layers, and at progressively higher metamorphic grades the rhodochrosite is transformed into rhodonite (commonly associated with Mn-garnets and Mn-clinopyroxenes, Klein, 1973).

The original unmetamorphosed carbonate-facies iron formation in the Schefferville area consists of chert-carbonate layers (dominantly siderite) and minor Fe-silicates and magnetite, and is most abundant near the base and top of the Sokoman Formation (Zajac, 1974). At lower grades of metamorphism, if the chemical potential of CO<sub>2</sub> remains locally high, the original mineralogy is generally retained and only recrystallization and increased grain size is observed (Klein, 1973). However, at higher metamorphic grades, and if the chemical potential of CO<sub>2</sub> is relatively low, the carbonate minerals react with silica to produce Fe-silicates (Klein, 1973). These Fe-silicates include amphiboles such as grunerite and actinolite (in the presence of H<sub>2</sub>O) and various clinopyroxenes and orthopyroxenes in the absence of H<sub>2</sub>O (Klein, 1973, 1978). However, these reactions require CO<sub>2</sub> to be mobile within the iron formation. The highly variable nature of the metamorphosed iron formation, with carbonate-facies iron formation sometimes present at high metamorphic grades, indicates metamorphism intermittently occurred in closed systems (Klein, 1978). Despite these local variations, the breakdown of carbonate and quartz to Fe-silicate minerals with increasing metamorphic grade accounts for the distribution of carbonate-facies iron formation across the study area. Quartz-carbonate-rich units are common in the upper and lower part of the iron formation in the northeast of the study area, amphibole-rich units common in the south and pyroxenes common farther south in Québec (Mount Reed-Gagnon area; Klein, 1978).

In the Schefferville area, silicate-facies iron formation is composed of various Fe-silicate minerals (minnesotaite, greenalite, stilpnomelane, crocidolite) mixed with carbonate, quartz, and iron-oxide minerals (Zajac, 1974). With metamorphism, reactions take place between silicate minerals and between silicate and carbonate minerals to form amphibole (grunerite and actinolite) assemblages in the presence of H<sub>2</sub>O and pyroxene-rich assemblages with progressive dehydration and decarbonatization (Klein, 1973, 1978). These assemblages are often identical to the high-grade metamorphic assemblages produced through metamorphism of carbonate-facies iron formation, making distinguishing the original sedimentary mineralogy difficult.

## LATE-STAGE ALTERATION

Moderate to intense secondary alteration has been recorded in some deposits, often occurring at depths of >300 m (Farquharson and Thalenhorst, 2006; Grandillo *et al.*, 2012; Conliffe, 2013). The distribution of these altered zones is important in determining the economic viability of iron-ore occurrences because the presence of significant alteration minerals (*e.g.*, goethite) can greatly affect metallurgy. Secondary alteration is most pervasive in the Scully, Julienne Lake, Julienne 1, Julienne 2, Canning and Wabush Mountain occurrences, as well as in the northwest limb of the Rose deposit and the eastern portion of the White Lake prospect (*see* Part B for detailed description of individual deposits). However, minor alteration zones have been recorded in other occurrences, particularly those associated with fault zones. Although this late-stage alteration is most often reported from the Sokoman Formation, other occurrences of deeply weathered rocks have been reported from elsewhere in the study area. These include the strongly leached Wishart Formation quartzites in a quarry along the Trans-Labrador Highway between Labrador City and Fermont (Meyer and Dean, 1987), and the altered Menihék and Wishart formations in the Rose deposit (Grandillo *et al.*, 2012).

The intensity of this secondary alteration partially depends on the original mineralogy of the iron formations. Oxide facies are generally more friable than the unaltered metaconites, with magnetite partially to completely oxidizing to secondary martite having common goethite rims (Plates 25–27), and in more strongly altered zones, the iron oxides are almost completely transformed to goethite (Plate 28). Silicate and carbonate facies are difficult to recognize due to the

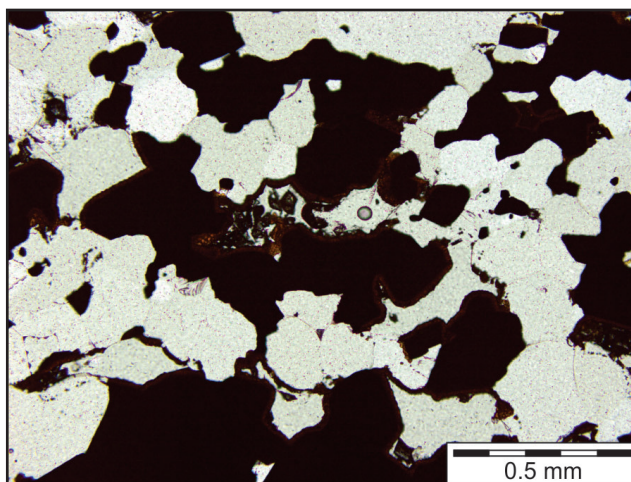


**Plate 26.** Photomicrograph of moderately altered oxide-facies iron formation, and hematite grains mantled by brown goethite (from Julienne 2 prospect; drillhole J2-10-08 @ 153.2, plane-polarized light).



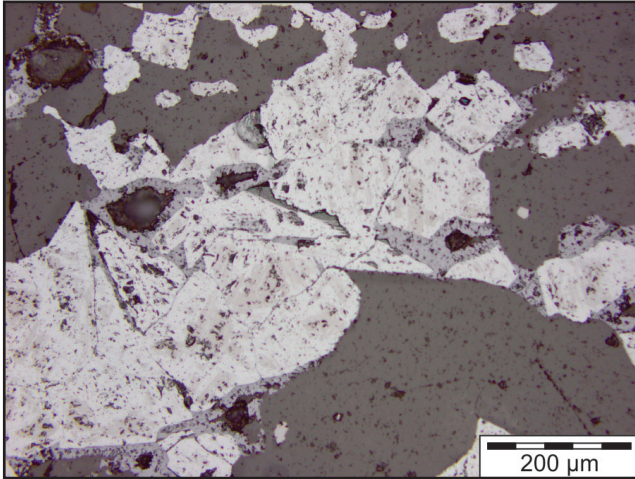


**Plate 27.** Photomicrograph of moderately altered oxide-facies iron formation, and magnetite partially replaced by hematite and mantled by secondary goethite (from Julienne 2 prospect; drillhole J2-10-08 @ 153.2 m, reflected light).

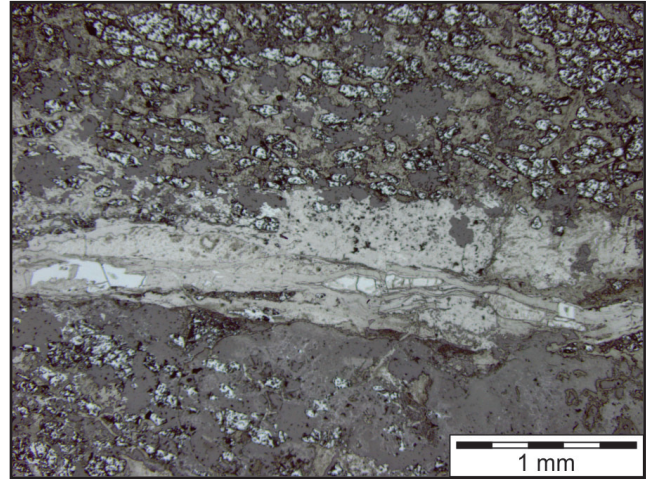


**Plate 29.** Photomicrograph of strongly altered oxide-facies iron formation, with vein of remobilized Mn-oxides (from Julienne Lake deposit, reflected light).

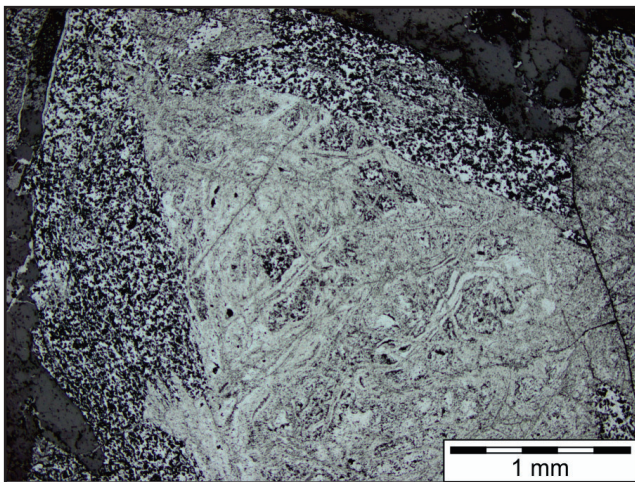


**Plate 28.** Photomicrograph of strongly altered oxide-facies iron formation, with magnetite and hematite completely replaced by secondary goethite (from Julienne Lake deposit; drillhole JL-10-17B @ 2.5 m, reflected light).

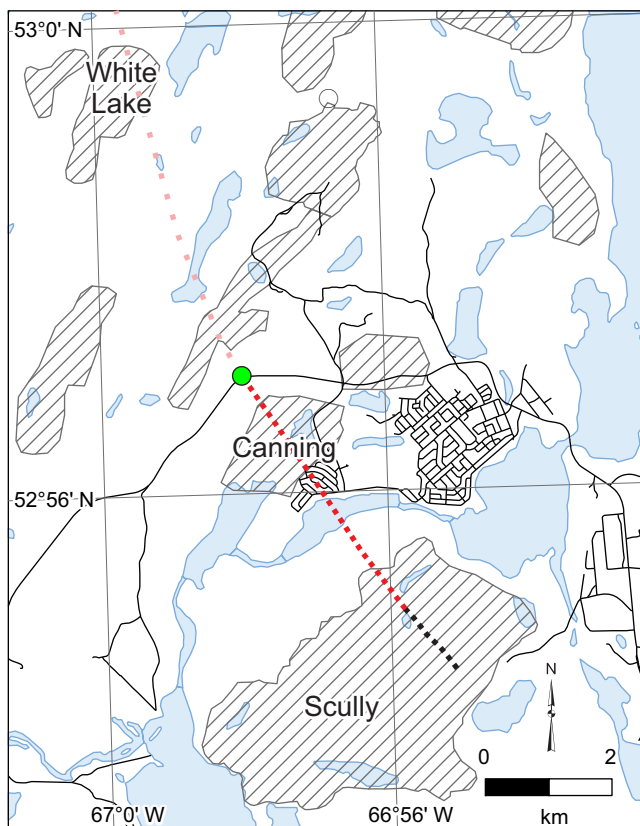
strong leaching and alteration, but are characterized by destruction of Fe-silicates, leaching of carbonate and the abundance of goethite (likely after carbonate; Klein, 1966; Muwais, 1974). This goethite locally displays a colloform texture, infilling secondary porosity, or occurs mixed with other Fe-oxides as fine-grained yellow limonite. This alteration is also associated with the secondary precipitation of Mn-oxides (psilomelane, pyrolusite, manganite) in discreet veins or layers (Plate 29), due to the destruction of Mn-silicates and carbonates.

The relationship between late-stage alteration and fault zones is evident in a number of deposits. The Scully deposit is cut by a number of northwest–southeast-trending reverse faults, the most prominent of which offsets the basement rocks by ~75 m (O’Leary *et al.*, 1972). If this fault is extrapolated to the northwest (Figure 18), it intersects the strongly altered Canning prospect, as well as the altered Wishart Formation quartzite, in a quarry close to the Trans-Labrador Highway. It may even continue through the White Lake prospect, where strongly altered zones appear to be associated with late faulting on the eastern side of a syncline (Duvergier, 2012). Grandillo *et al.* (2012) also stated that weathering at the Rose deposit is controlled by younger northwest-trending extensional faults. These northwest-trending fault zones are similar in orientation to the nearby Flora Lake shear zone, a major kilometre-scale strike-slip fault zone (van Gool, 1992) that reflects oblique convergence during the Grenvillian Orogeny and may have provided a conduit for late-stage fluids.






The presence of a similar northwest-trending fault having a throw of >200 m has been suggested at the Julienne Lake deposit (Conliffe, 2013), which is located directly south of another major strike–slip shear zone, the Julienne Lake Fault Zone (van Gool, 1992). A similar pattern of alteration is seen in the deposits directly north of this shear zone (Julienne 1 and Julienne 2 occurrences). This suggests that the Julienne Lake Fault Zone may have also served as a conduit for late-stage fluid flow associated with the alteration of the Sokoman Formation in these deposits.

Despite the obvious importance of, and implications thereof, this secondary alteration for metallurgy in individual





### LEGEND

- |   |                           |   |                |
|---|---------------------------|---|----------------|
|  | Iron-ore Deposit          |  | Fault defined  |
|  | Altered Wishart Formation |  | Fault assumed  |
|   |                           |  | Fault inferred |

**Figure 18.** Map showing alignment of zones of strong secondary alteration in the Sokoman Formation in the Scully deposit, Canning prospect and eastern part of the White Lake prospect. Also shown is the location of the strongly altered Wishart Formation quartzite in a quarry north of the Trans-Labrador Highway. Broken black line indicates location of major northwest–southeast-trending reverse fault in the Scully deposit, broken red line indicates likely extension of this fault to the northwest through the Canning prospect and broken pink line indicates possible continuation of this fault to the eastern portion of the White Lake prospect

deposits has not been studied in any detail. Some authors have compared it to the supergene alteration associated with the high-grade martite–goethite ores of the Schefferville area, and have assumed it is related to deep weathering during the Cretaceous (e.g., Connelly *et al.*, 1996; Coates *et al.*, 2012; Grandillo *et al.*, 2012). However, the alteration of metaconites is not associated with any supergene enrichment and there is no persuasive evidence that the iron formation was exposed during the Cretaceous. The close association between altered iron formation and late-stage brittle faults indicates that these faults may have been reac-

tivated during tectonic movement after ductile deformation and metamorphism (Cotnoir *et al.*, 2002). Any late-stage fluid movement responsible for secondary alteration of the iron formation, including circulation of formational waters and/or downward percolation of groundwater, would have focussed along these structures.

## GEOCHEMISTRY

### SAMPLING AND METHODOLOGY

In total, 108 samples were analyzed, representing 20 individual iron-ore occurrences. Samples were collected from outcrops, drillcore and sample pulps during fieldwork conducted from 2012 to 2104. Outcrop samples were cleaned of any obvious external weathering before analysis. The samples were subdivided based on the structural basin the deposit is located in (Carol Lake, Wabush and Mills Lake basins; *see Stratigraphy* Section), the sample lithology (oxide-facies iron formation or BSIF), and the degree of alteration (weak *vs.* moderate to strong alteration, determined by visual inspection). Fifty-three samples of oxide-facies iron formation were collected from 14 separate occurrences in the Carol Lake Basin, of which 33 were classified as having weak alteration and 20 having moderate to strong alteration. A total of 47 samples were analyzed from 6 occurrences in the Wabush Basin, 40 oxide-facies iron formation (15 weakly altered, 25 moderately to strongly altered) and 7 samples of BSIF (3 weakly altered, 4 moderately to strongly altered). Seven samples of weakly altered oxide-facies iron formation and a single sample of weakly altered BSIF were analyzed from the Mills Lake deposit in the Mills Lake Basin. Complete sample descriptions are available in Appendix A, and detailed geochemical analysis of samples from each basin are summarized in Table 4, with full results in Appendix B.

All analyses were carried out at the GSNL geochemistry laboratory in St. John's using the analytical methods described in Finch *et al.* (2018). Samples were milled using ceramic and tungsten carbide mills, and due to possible contaminations from the tungsten carbide mill, W and Co values are not reported for samples collected during 2013, 2014 and 2015. Major elements are reported in weight percent (wt. %), and trace elements are reported in parts per million (ppm). A negative number indicates the concentration of the specific element in the sample was below the detection limit (e.g., -0.01 indicates the measured value was below the detection limit of 0.01). Detection limits are listed for each element in the .csv files. The code -99 indicates the sample was not analyzed for that element. Major-element compositions (plus Cr, Zr and Ba) were analyzed using ICP-OES methods, following lithium tetraborate and metaborate fusion. The REE and selected trace elements were determined by ICP-MS analysis following an identical sample digestion procedure, whereas other trace el-

**Table 4.** Summary statistics for major-element, trace-element, and REE concentrations of oxide-facies iron formation and Basal Silicate Iron Formation in the Labrador City/Wabush area

Lithology Basin Alteration n	Oxide Carol Basin Weak 33				Oxide Carol Basin Moderate/Strong 20				Oxide Wabush Basin Weak 15				Oxide Wabush Basin Moderate/Strong 25			
	Av	StDev	Max	Min	Av	StDev	Max	Min	Av	StDev	Max	Min	Av	StDev	Max	Min
<b>SiO<sub>2</sub> (wt. %)</b>	35.0	8.7	62.9	17.5	44.8	13.9	70.5	16.3	38.8	9.3	54.4	22.9	42.3	14.9	71.2	10.1
<b>Al<sub>2</sub>O<sub>3</sub></b>	0.15	0.11	0.67	0.05	0.10	0.05	0.27	0.04	0.18	0.13	0.57	0.06	0.15	0.10	0.57	0.06
<b>Fe<sub>2</sub>O<sub>3</sub></b>	54.4	8.6	66.5	34.1	52.8	12.9	72.0	26.6	49.6	9.3	70.8	39.0	52.2	12.3	72.7	17.6
<b>Fe</b>	38.1	6.0	46.5	23.8	36.9	9.0	50.3	18.6	34.6	6.5	49.5	27.3	36.5	8.6	50.8	12.3
<b>MgO</b>	1.9	1.4	7.1	0.2	0.1	0.3	1.1	0.0	1.8	0.8	3.2	0.4	0.1	0.1	0.4	dl
<b>CaO</b>	2.7	1.8	9.0	0.3	0.2	0.2	0.7	dl	2.3	1.6	6.1	0.1	0.0	0.0	0.2	dl
<b>Na<sub>2</sub>O</b>	0.04	0.03	0.13	dl	0.04	0.02	0.10	dl	0.08	0.08	0.31	dl	0.03	0.02	0.08	dl
<b>K<sub>2</sub>O</b>	0.05	0.04	0.20	0.01	0.04	0.02	0.07	dl	0.09	0.06	0.18	0.01	0.10	0.14	0.59	dl
<b>TiO<sub>2</sub></b>	0.01	0.01	0.05	0.00	0.01	0.01	0.03	dl	0.02	0.01	0.04	0.00	0.01	0.01	0.04	0.00
<b>MnO</b>	0.7	0.6	3.1	0.1	0.8	2.2	10.0	0.1	2.5	1.8	7.4	0.7	3.3	5.4	20.0	0.0
<b>P<sub>2</sub>O<sub>5</sub></b>	0.04	0.03	0.12	0.00	0.02	0.01	0.06	0.00	0.03	0.02	0.08	0.01	0.03	0.03	0.10	dl
<b>LOI</b>	4.9	4.8	24.7	GOI	1.0	0.9	3.6	GOI	4.3	2.6	9.6	GOI	1.4	1.2	4.8	GOI
<b>Total</b>	99.8	0.8	101.0	98.2	99.7	1.0	101.0	98.1	99.3	0.7	100.6	98.1	99.6	1.0	100.9	96.5
<b>Rb (ppm)</b>	2	1	6	dl	2	1	3	dl	5	5	17	dl	4	3	10	dl
<b>Sr</b>	8	6	27	dl	5	10	37	dl	16	14	54	2	24	49	222	dl
<b>Ba</b>	17	31	163	dl	6	5	20	1	199	460	1712	4	214	472	1861	3
<b>V</b>	21	13	46	1	18	10	48	dl	17	9	38	3	17	10	43	3
<b>Cr</b>	4	4	18	dl	3	1	7	dl	4	2	6	dl	4	3	10	dl
<b>Ni</b>	28	5	38	19	27	6	44	19	27	7	42	12	23	8	52	9
<b>Cu</b>	4	2	10	3	4	2	9	2	6	3	11	2	5	4	19	1
<b>Zn</b>	23	7	39	11	21	6	34	13	21	6	30	10	22	13	73	6
<b>Y</b>	6	2	11	2	5	3	15	1	9	4	16	4	9	9	41	1
<b>Zr</b>	17	4	30	9	18	6	32	7	22	6	41	15	19	13	68	6
<b>Nb</b>	2	1	5	dl	3	1	7	dl	4	2	11	2	4	3	11	dl
<b>Ge</b>	14	5	28	9	15	4	24	11	14	3	21	9	16	4	26	4
<b>La (ppm)</b>	3.5	2.3	11.6	0.9	4.5	7.1	33.1	1.1	9.2	7.2	31.1	2.8	9.4	10.7	39.1	0.7
<b>Ce</b>	5.6	3.9	17.0	1.1	5.7	8.2	39.1	1.3	16.0	10.7	47.8	5.6	13.2	15.1	58.9	1.8
<b>Pr</b>	0.6	0.4	2.0	0.2	0.6	0.9	4.4	0.1	1.6	1.2	5.3	0.6	1.5	1.5	5.3	0.2
<b>Nd</b>	2.6	1.6	8.1	0.5	2.7	3.6	17.6	0.8	6.4	4.9	21.3	2.5	6.0	5.6	20.3	0.6
<b>Sm</b>	0.5	0.3	1.3	0.1	0.4	0.5	2.3	0.1	1.2	0.8	3.1	0.4	1.1	0.9	3.3	0.1
<b>Eu</b>	0.2	0.1	0.5	dl	0.2	0.1	0.7	dl	0.4	0.3	1.1	0.2	0.4	0.3	1.3	dl
<b>Gd</b>	0.7	0.4	1.6	0.2	0.6	0.5	2.6	0.2	1.4	0.8	3.3	0.6	1.3	1.2	5.0	0.1
<b>Tb</b>	0.2	0.0	0.2	dl	0.2	0.1	0.3	dl	0.2	0.1	0.5	dl	0.2	0.2	0.7	dl
<b>Dy</b>	0.7	0.3	1.5	0.2	0.7	0.4	2.1	0.2	1.3	0.7	2.6	0.5	1.3	1.0	4.6	dl
<b>Ho</b>	0.2	0.1	0.3	dl	0.2	0.2	0.6	dl	0.3	0.2	0.6	0.1	0.3	0.2	1.1	dl
<b>Er</b>	0.5	0.2	1.0	0.2	0.5	0.3	1.4	0.1	0.9	0.5	1.8	0.3	0.9	0.7	3.3	0.3
<b>Tm</b>	0.1	0.0	0.2	dl	0.1	0.0	0.2	dl	0.1	0.1	0.3	dl	0.1	0.1	0.4	dl
<b>Yb</b>	0.5	0.2	1.1	0.1	0.4	0.2	0.9	0.1	0.7	0.4	1.5	0.3	0.7	0.6	2.6	0.2
<b>Lu</b>	0.09	0.03	0.18	dl	0.09	0.03	0.14	dl	0.12	0.06	0.23	dl	0.13	0.07	0.31	dl
<b>Σ REE</b>	15.5	9.3	45.7	4.2	16.2	21.8	105.4	5.3	39.7	27.4	119.8	15.0	36.2	36.1	141.4	3.5
<b>Eu/Eu*</b>	1.4	0.4	2.3	0.8	1.4	0.4	2.2	0.7	1.4	0.2	1.7	1.2	1.5	0.3	2.1	1.0
<b>Ce/Ce*</b>	0.9	0.3	1.7	0.4	0.8	0.2	1.3	0.5	1.0	0.2	1.3	0.8	0.9	0.3	1.8	0.3
<b>Pr/Yb (sn)</b>	0.4	0.2	0.8	0.2	0.5	0.3	1.5	0.1	0.6	0.2	1.3	0.4	0.7	0.6	3.0	0.1
<b>Y/Ho</b>	37.1	5.6	46.9	25.1	36.6	11.0	58.5	23.8	31.8	4.4	43.0	24.4	30.8	7.3	46.6	14.3

elements (As, Be, Cu, Li, Mn, Ni, Pb, Rb, Sc, Ti, Zn, V, Co) were analyzed by ICP-MS after total acid digestion.

Volatiles are represented as LOI (loss-on-ignition) at 1000°C, which represents the breakdown of all minerals and release of all volatiles. A value of -1.00 indicates gain-on-ignition. The mass percent of Fe in each sample was calcu-

lated from the total Fe<sub>2</sub>O<sub>3</sub> values, using the conversion factor of 100 wt. % Fe<sub>2</sub>O<sub>4</sub> to 69.95 wt. % Fe.

Analytical duplicates were inserted at a frequency of one in 20, with the duplicate selected at random. In addition, a selection of reference standards was analyzed, also at a frequency of one in 20. For ICP-OES-FUS (major element) and

**Table 4. Continued** (Summary statistics for major-element, trace-element, and REE concentrations of oxide-facies iron formation and Basal Silicate Iron Formation in the Labrador City/Wabush area)

Lithology Basin Alteration n	Oxide Mills Lake Weak 7				Basal Wabush Basin Weak 3				Basal Wabush Basin Moderate/Strong 4				Basal Mills Lake Weak 1
	Av	StDev	Max	Min	Av	StDev	Max	Min	Av	StDev	Max	Min	
SiO <sub>2</sub> (wt. %)	39.0	10.0	51.3	25.6	37.9	8.5	44.3	28.2	31.6	17.1	46.0	6.9	43.0
Al <sub>2</sub> O <sub>3</sub>	0.28	0.25	0.71	0.07	1.00	0.39	1.40	0.61	1.39	0.57	2.12	0.92	2.64
Fe <sub>2</sub> O <sub>3</sub>	47.7	7.6	62.5	37.9	44.4	2.5	46.8	41.9	57.6	11.2	73.6	48.1	37.9
Fe	33.3	5.3	43.7	26.5	31.0	1.7	32.7	29.3	40.3	7.9	51.4	33.6	26.5
MgO	3.5	2.1	7.6	1.1	4.5	0.4	4.8	4.1	0.1	0.0	0.1	0.0	4.6
CaO	1.6	0.7	2.5	0.7	4.4	4.1	8.8	0.7	0.1	0.1	0.2	0.0	3.5
Na <sub>2</sub> O	0.65	1.00	2.57	0.03	0.05	0.05	0.10	0.02	0.03	0.01	0.04	dl	0.45
K <sub>2</sub> O	0.14	0.13	0.39	0.01	0.10	0.05	0.15	0.06	0.03	0.02	0.05	0.01	0.45
TiO <sub>2</sub>	0.02	0.01	0.04	0.00	0.14	0.10	0.21	0.03	0.19	0.07	0.28	0.12	0.83
MnO	4.3	6.4	17.2	0.3	2.5	0.3	2.8	2.1	0.7	1.0	2.2	0.1	2.2
P <sub>2</sub> O <sub>5</sub>	0.06	0.05	0.14	dl	0.14	0.08	0.23	0.06	0.23	0.19	0.50	0.09	0.18
LOI	2.4	2.0	5.9	GOI	6.6	6.7	11.3	GOI	7.6	3.9	13.2	4.6	2.9
<b>Total</b>	<b>99.2</b>	<b>0.7</b>	<b>100.4</b>	<b>98.5</b>	<b>99.5</b>	<b>1.0</b>	<b>100.7</b>	<b>98.7</b>	<b>99.5</b>	<b>0.6</b>	<b>100.1</b>	<b>98.7</b>	<b>98.7</b>
<b>Rb (ppm)</b>	8	8	19	dl	6	3	9	dl	5	4	11	2	11
<b>Sr</b>	33	36	109	8	43	39	83	6	12	4	16	dl	59
<b>Ba</b>	813	1911	5142	13	248	409	720	8	43	29	77	7	77
<b>V</b>	16	11	27	1	44	19	63	25	78	49	145	39	126
<b>Cr</b>	2	1	3	dl	9	2	11	6	9	5	17	5	17
<b>Ni</b>	31	7	42	22	31	2	33	30	42	11	57	33	32
<b>Cu</b>	5	1	6	3	10	6	14	3	18	21	49	4	27
<b>Zn</b>	21	7	32	13	39	17	58	29	48	13	65	35	62
<b>Y</b>	12	11	34	3	13	8	23	7	13	10	27	5	15
<b>Zr</b>	24	9	37	13	41	25	62	14	44	13	60	28	64
<b>Nb</b>	4	2	7	dl	9	5	12	3	10	3	12	6	12
<b>Ge</b>	14	2	17	11	17	4	21	13	14	3	18	12	11
<b>La (ppm)</b>	12.5	11.2	30.7	1.8	14.8	11.4	28.0	7.6	15.0	10.4	24.6	3.0	17.9
<b>Ce</b>	16.2	12.3	33.1	3.3	27.3	20.5	50.9	13.5	32.0	22.7	59.9	5.8	32.8
<b>Pr</b>	1.9	1.6	4.3	0.4	3.3	2.4	6.1	1.6	3.5	2.3	6.0	1.0	3.9
<b>Nd</b>	7.6	6.1	17.3	1.6	13.9	10.7	26.1	6.3	14.7	10.0	26.1	4.0	15.6
<b>Sm</b>	1.3	1.0	2.9	0.3	2.8	2.1	5.3	1.6	2.9	1.9	4.9	1.0	3.2
<b>Eu</b>	0.5	0.4	1.1	0.1	0.8	0.5	1.3	0.4	0.9	0.5	1.4	0.3	1.1
<b>Gd</b>	1.6	1.4	4.1	0.4	2.5	1.8	4.5	1.4	2.8	1.8	4.5	0.8	2.9
<b>Tb</b>	0.3	0.2	0.7	dl	0.3	0.2	0.5	0.2	0.4	0.2	0.6	0.2	0.5
<b>Dy</b>	1.6	1.6	4.6	0.4	1.8	1.1	3.1	1.1	2.0	1.2	3.7	0.8	2.5
<b>Ho</b>	0.4	0.4	1.1	0.1	0.4	0.2	0.6	0.2	0.4	0.3	0.8	0.2	0.5
<b>Er</b>	1.1	1.1	3.3	0.3	1.0	0.6	1.6	0.6	1.1	0.8	2.2	0.4	1.5
<b>Tm</b>	0.2	0.2	0.4	dl	0.1	0.1	0.2	0.1	0.2	0.1	0.4	0.1	0.2
<b>Yb</b>	0.9	0.8	2.5	0.2	0.7	0.3	1.1	0.4	0.9	0.6	1.7	0.4	1.3
<b>Lu</b>	0.16	0.12	0.32	dl	0.12	0.05	0.16	0.07	0.14	0.11	0.30	0.07	0.26
<b>Σ REE</b>	<b>45.9</b>	<b>37.9</b>	<b>106.1</b>	<b>8.7</b>	<b>69.7</b>	<b>51.7</b>	<b>129.2</b>	<b>36.2</b>	<b>76.7</b>	<b>50.8</b>	<b>131.3</b>	<b>17.8</b>	<b>84.0</b>
<b>Eu/Eu*</b>	1.5	0.2	1.9	1.3	1.5	0.4	1.9	1.2	1.5	0.1	1.6	1.4	1.6
<b>Ce/Ce*</b>	0.8	0.1	1.0	0.6	0.9	0.0	0.9	0.9	1.0	0.2	1.2	0.8	0.9
<b>Pr/Yb (sn)</b>	0.7	0.2	1.0	0.5	1.4	0.6	1.8	0.7	1.4	1.1	3.2	0.8	0.9
<b>Y/Ho</b>	34.3	3.9	29.5	29.7	35.0	5.9	39.4	28.3	33.6	3.4	37.4	29.8	27.3

ICP-MS-FUS (trace element) standards were supplied by the Canadian Certified Reference Materials Project (SCH-1) and the United States Geological Survey (AGV-1, W-2). Two standards were used for ICP-OES-FUS (trace elements) analysis, supplied by the Canadian Certified Reference Materials Project (SY-4, WGB-1). The raw, unprocessed data from duplicates and standards is included in the appendices, and can be used by the reader to assess accuracy and precision.

## MAJOR-ELEMENT GEOCHEMISTRY

### Carol Lake Basin

The Fe<sub>2</sub>O<sub>3</sub> and SiO<sub>2</sub> are the dominant major elements in oxide-facies samples from the Carol Lake Basin, with Fe<sub>2</sub>O<sub>3</sub> + SiO<sub>2</sub> concentrations averaging 89.5 ± 7.7 wt. % in weakly altered samples, and 97.6 ± 3.3 wt. % in moderately to



strongly altered samples. Total Fe contents range from  $38.1 \pm 6$  wt. % in weakly altered samples to  $36.9 \pm 9$  wt. % in samples with moderate to strong alteration. The MnO values are generally low ( $<1$  wt. %, Figure 19), with a single strongly altered sample having 10 wt. % MnO. The MgO and CaO concentrations are highly variable in weakly altered samples, ranging from 0.2 to 7.1 wt. % MgO and 0.3 to 9.0 wt. % CaO. However, moderately to strongly altered samples all have low MgO and CaO concentrations (generally  $<1$  wt. % MgO + CaO, Figure A19). All other major-element concentrations are less than 0.2 wt. %, with no significant variations due to late-stage alteration.

### **Wabush Basin**

Oxide-facies iron formation from deposits in the Wabush Basin consist predominantly of  $\text{Fe}_2\text{O}_3$  and  $\text{SiO}_2$  (Figure 19), with weakly altered samples having  $49.6 \pm 9.3$  wt. %  $\text{Fe}_2\text{O}_3$  ( $34.6 \pm 6.5$  wt. % Fe) and  $38.8 \pm 9.3$  wt. %  $\text{SiO}_2$ , and moderately to strongly altered samples having  $52.2 \pm 12.3$  wt. %  $\text{Fe}_2\text{O}_3$  ( $36.5 \pm 8.6$  wt. % Fe) and  $42.3 \pm 14.9$  wt. %  $\text{SiO}_2$ . The MnO concentration of weakly altered oxide facies in the Wabush Basin range from 0.7 to 7.4 wt. %, and are generally higher than weakly altered samples from deposits in the Carol Lake Basin. Moderately to strongly altered samples have a wide range of MnO concentrations (Figure 19), with some samples strongly depleted in MnO ( $<0.5$  wt. %) and others strongly enriched (up to 20 wt. % MnO). The MgO and CaO concentrations have the same pattern as samples from the Carol Lake Basin (Figure 19), decreasing from  $1.8 \pm 0.8$  wt. % MgO and  $2.3 \pm 1.6$  wt. % CaO in weakly altered samples to  $<0.4$  wt. % MgO and  $<0.2$  wt. % CaO in moderately to strongly altered samples. All other major-element concentrations are low ( $<0.6$  wt. %).

The BSIF samples have  $\text{Fe}_2\text{O}_3$  concentrations of  $44.4 \pm 2.5$  wt. % in weakly altered samples and  $57.6 \pm 11.2$  wt. % in moderately to strongly altered samples. The MnO, MgO and CaO concentrations are higher in weakly altered samples compared to strongly altered samples (Figure 20). The  $\text{Al}_2\text{O}_3$ ,  $\text{TiO}_2$  and  $\text{P}_2\text{O}_5$  concentrations of all samples are higher than those recorded in oxide-facies iron formations from the same deposits (Figure 20).

### **Mills Lake Basin**

All oxide samples from the Mills Lake Basin display only weak late-stage alteration. These samples have  $47.7 \pm 7.6$  wt. %  $\text{Fe}_2\text{O}_3$  (equivalent to  $33.3 \pm 5.3$  wt. % Fe) and  $39.0 \pm 10.0$  wt. %  $\text{SiO}_2$  (Figure 19). The MgO + CaO concentrations are  $5.1 \pm 2.1$  wt. %, and MnO concentrations are highly variable from 0.3 to 17.2 wt. %. In addition, two samples have high  $\text{Na}_2\text{O}$  concentrations (1.5 and 2.6 wt. % NaO), whereas all other major-element concentrations are low ( $<0.71$  wt. %).

A single, weakly altered, BSIF sample was also analyzed from the Mills Lake Basin. It has similar  $\text{Fe}_2\text{O}_3$ ,  $\text{SiO}_2$ , MgO, CaO, MnO and  $\text{P}_2\text{O}_5$  concentrations as BSIF samples from the Wabush Basin (Figure 20), but has higher concentrations of  $\text{Al}_2\text{O}_3$  (2.64 wt. %) and  $\text{TiO}_2$  (0.83 wt. %).

## **TRACE-ELEMENT GEOCHEMISTRY**

The trace-element concentrations for all samples are generally low and less than  $<50$  ppm for individual elements. Rare samples have high Sr and V concentration ( $>100$  ppm), whereas Ba concentrations are highly variably but commonly greater than 10 ppm. The average trace-element concentration of oxide-facies iron formation and BSIF is shown in Figure 21. In addition, the average trace-element concentration of oxide-facies iron formation samples has been normalized to the average Sokoman Formation taconite in the central Labrador Trough (data from Conliffe, 2016a, 2017) to determine relative concentrations of selected trace elements (Figure 21).

### **Carol Lake Basin**

Oxide-facies iron formation from deposits in the Carol Lake Basin have variable large ion lithophile element (LILE) concentrations, with Sr concentrations enriched relative to the average taconite, and Sr concentrations relatively depleted (Figure 21A). The Cr concentration is slightly enriched, but all other transition metal concentrations are similar to the average taconite. Yttrium concentrations are slightly depleted, whereas all other high-field-strength-element (HFSE) concentrations are similar to the average taconite compositions (Figure 21B).

### **Wabush Basin**

Oxide-facies iron formation samples from the Wabush Basin are characterized by higher LILE concentrations than samples from the Carol Lake Basin. The Ba concentrations are highly variable, ranging from 3 to 1712 ppm in weakly altered samples, and 4 to 1861 ppm in moderately to strongly altered samples, but, in general, show strong relative enrichment compared to average taconites (Figure 21). Transition metals show a similar pattern to samples from the Carol Lake Basin, with minor enrichment in Cr and no enrichment or depletion in other elements. The HFSE elements are slightly enriched compared to the average taconite.

The trace-element concentration of BSIF is generally higher than the oxide-facies iron formations (Figure 21), with highly variable LILE concentrations, and the transition metals and HFSE showing similar distributions as the oxide-facies iron formation.

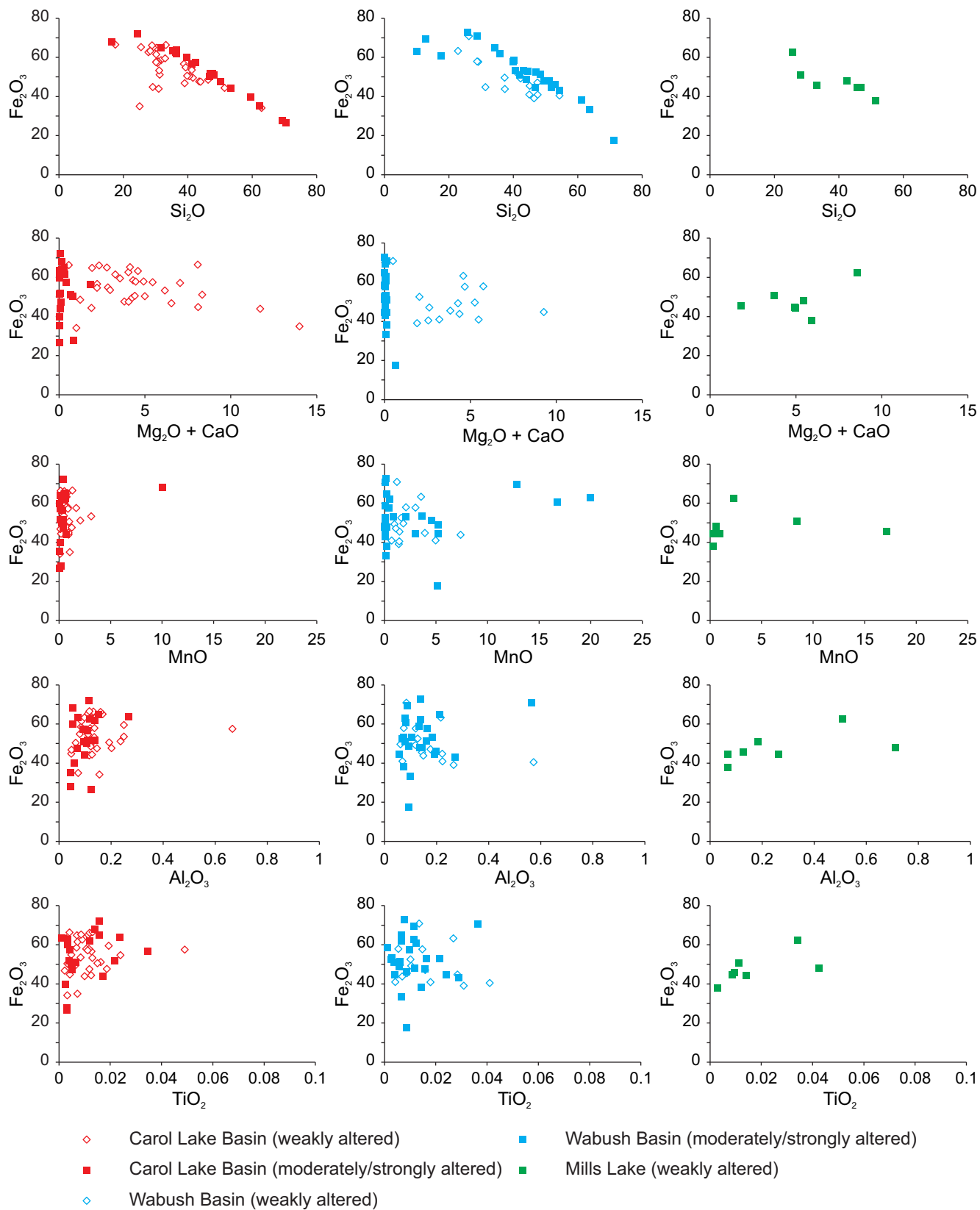


**Figure 19.** Bivariate plots of  $Fe_2O_3$  vs. select major elements for samples of oxide-facies iron formation in the Carol Lake, Wabush and Mills Lake basins.

### Mills Lake Basin

Oxide-facies iron formation samples from the Mills Lake Basin have highly variable LILE concentrations (*e.g.*, Ba from 13 to 5142 ppm), but, in general, are relatively enriched in LILE compared to the average taconite (Figure 21). The

transition metals show no relative enrichment or depletion, and HFSE elements are all relatively enriched when compared to the average taconite. The single BSIF sample from the Mills Lake Basin has similar trace-element concentration to weakly altered BSIF samples from the Wabush Basin.

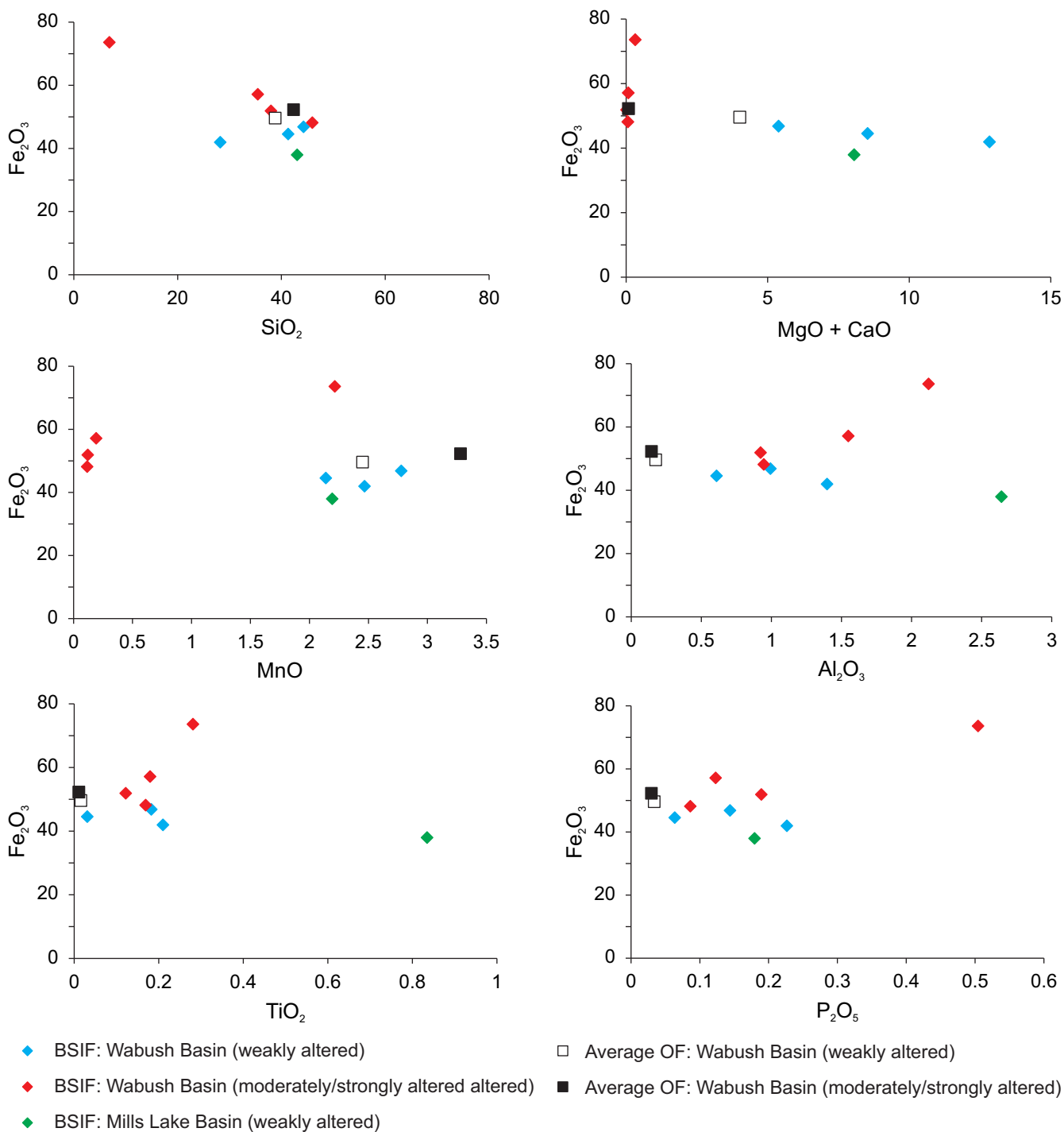
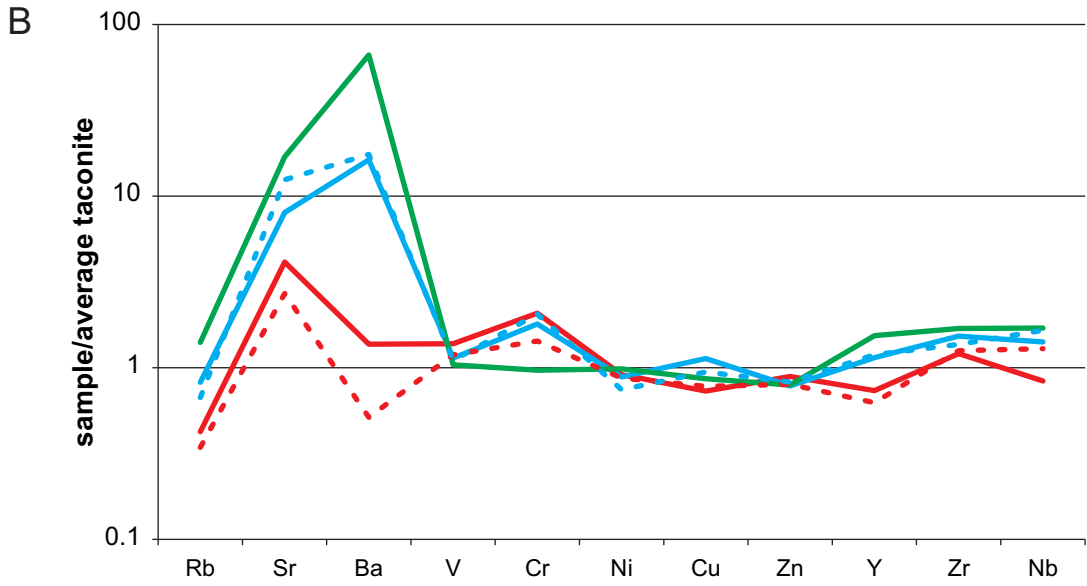
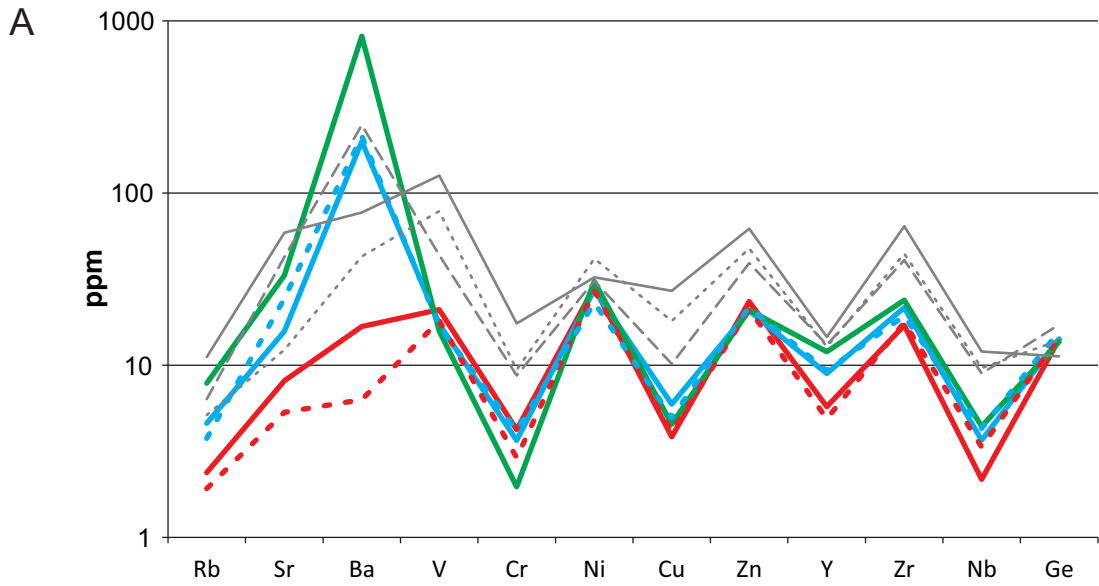


**Figure 20.** Bivariate plots of  $Fe_2O_3$  vs. select major elements for samples of BSIF in the Wabush and Mills Lake basins. Also included are the average values of oxide-facies iron formation samples from the same basins.





**Oxide-facies Iron Formation**

**Basal Silicate Iron Formation**

- Carol Lake Basin (weakly altered)
- - - Carol Lake Basin (moderately/strongly altered)
- Wabush Basin (weakly altered)
- - - Wabush Basin (moderately/strongly altered)
- Mills Lake Basin (weakly altered)

**Figure 21.** A) Trace-element composition of oxide-facies iron formation and BSIF from the Carol Lake, Wabush and Mills Lake basins; B) Trace-element composition of oxide-facies iron formation from the Carol Lake, Wabush and Mills Lake basins normalized against the average value of taconite from the Schefferville area (data from Conliffe, 2016a).

## RARE-EARTH-ELEMENT (REE) GEOCHEMISTRY

The REE concentrations of all samples are summarized in Table 4. The REE data have been normalized to the average value of post-Archean Australian shale (PAAS) from McLennan (1989), and are hereby referred to as REE<sub>(SN)</sub>. The REE<sub>(SN)</sub> profiles for weakly altered oxide-facies iron formations are shown in Figure 22. The ratios of light REE

(LREE) to heavy REE (HREE) were calculated by comparing Pr<sub>(SN)</sub> to Yb<sub>(SN)</sub>, and the Y/Ho ratio was also calculated using the raw data. The Ce<sub>(SN)</sub> anomalies were determined by comparing Ce/Ce\* ( $Ce_{(SN)}/(0.5Pr_{(SN)} + 0.5La_{(SN)})$ ) and Pr/Pr\* ( $Pr_{(SN)}/(0.5Ce_{(SN)} + 0.5Nd_{(SN)})$ ) using the method described by Bau and Dulski (1996), which differentiates between true Ce<sub>(SN)</sub> anomalies and the apparent Ce anomalies created by anomalous La concentrations. The Eu anomalies

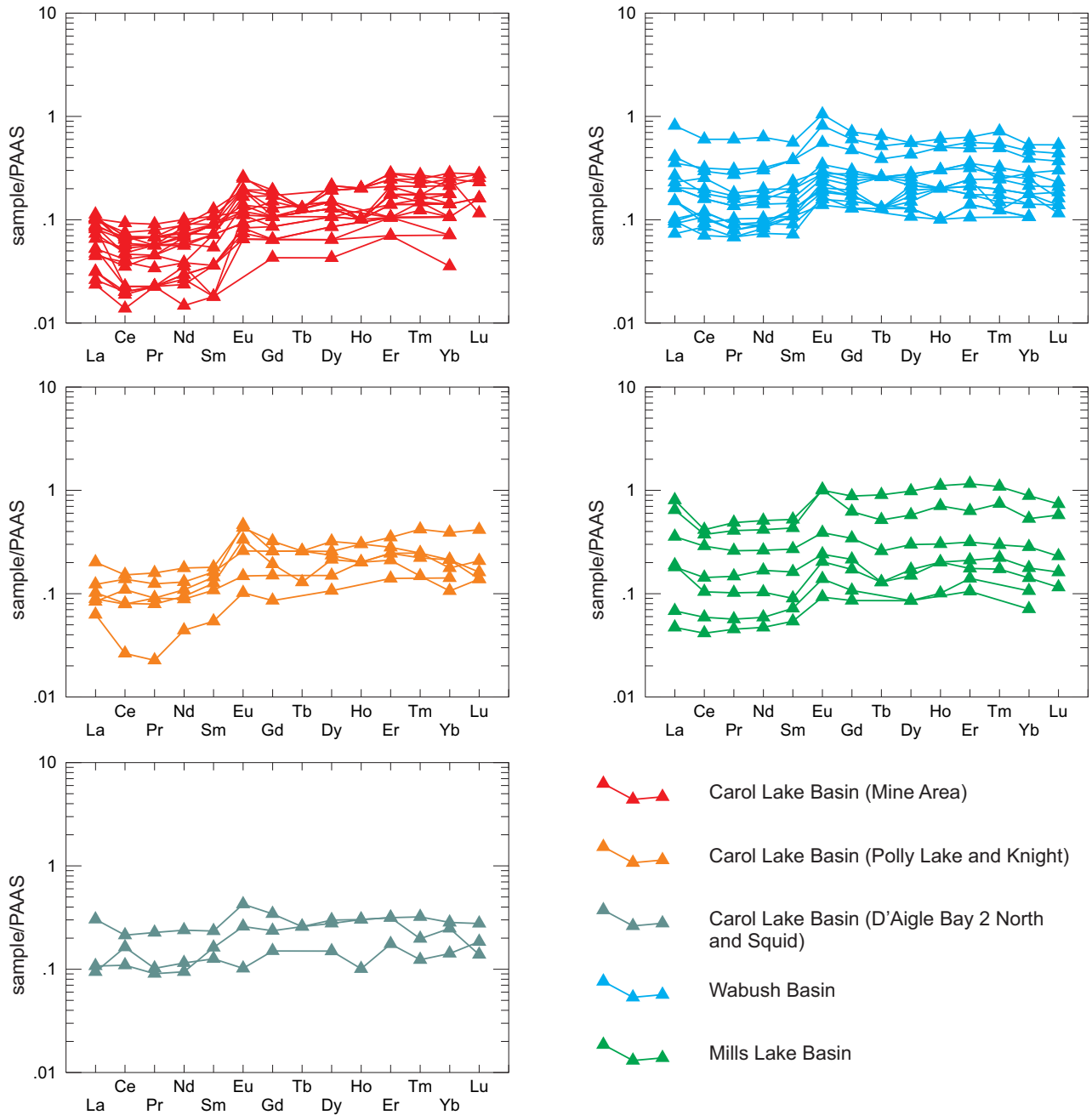


**Figure 22.** The REE distribution patterns normalized to Post-Archean average Australian Shale (PAAS) for weakly altered oxide-facies iron formation in the Carol Lake, Wabush and Mills Lake basins. Samples from the Carol Lake Basin separate into deposits from the mine area of the Carol Project, samples from south of the mine area (Polly Lake and Knight prospects) and samples from north and west of the mine area (D'Aigle Bay 2 North prospect and Squid showing). See text for details.

$(Eu/Eu^* = Eu_{SN}/(0.5Sm_{SN} + 0.5GdPAAS_{SN}))$  were also calculated for all samples.

### Carol Lake Basin

Based on their REE signatures, weakly altered oxide-facies iron formation samples from the Carol Lake Basin have been divided into three distinct groups (Figures 22 and 23). Most of the samples, representing samples from deposits close to the IOC mine area (Figure 6), are characterized by HREE enrichment ( $Pr/Yb_{(SN)} = 0.33 \pm 0.12$ ; Figures 22 and 23), relatively high Y/Ho ratios ( $38.6 \pm 5.6$ ; Figure 23) and low total REE concentrations ( $\sum REE$ ) of 4.2 to 19.9 ppm. Samples from the D'Aigle Bay 2 North prospect (north of the mine area) and Squid showing (west of the mine area) have higher  $\sum REE$

concentrations (22.7 to 45.7 ppm), and generally have higher  $Pr/Yb_{(SN)}$  ratios ( $0.65 \pm 0.31$ ) and lower Y/Ho ratios ( $32.2 \pm 6.1$ ). Samples from south of the mine (Knight and Polly Lake deposits) have intermediate characteristics, with  $\sum REE$  of  $22.6 \pm 8.9$  ppm,  $Pr/Yb_{(SN)}$  of  $0.50 \pm 0.21$  and Y/Ho of  $35.7 \pm 4.3$ . Only a few samples show positive or negative Ce anomalies, with most samples displaying no anomalies or positive La anomalies (Figure 23), and no distinction between the groups described above. The Eu anomalies vary from strongly positive, to weakly negative, with most samples having positive Eu anomalies (average  $1.42 \pm 0.37$ , Figure 24).

Moderately to strongly altered oxide-facies iron formation samples have highly variable REE profiles, with  $Pr/Yb_{(SN)}$  ratios ranging from 0.10 to 1.52 and Y/Ho ratios from

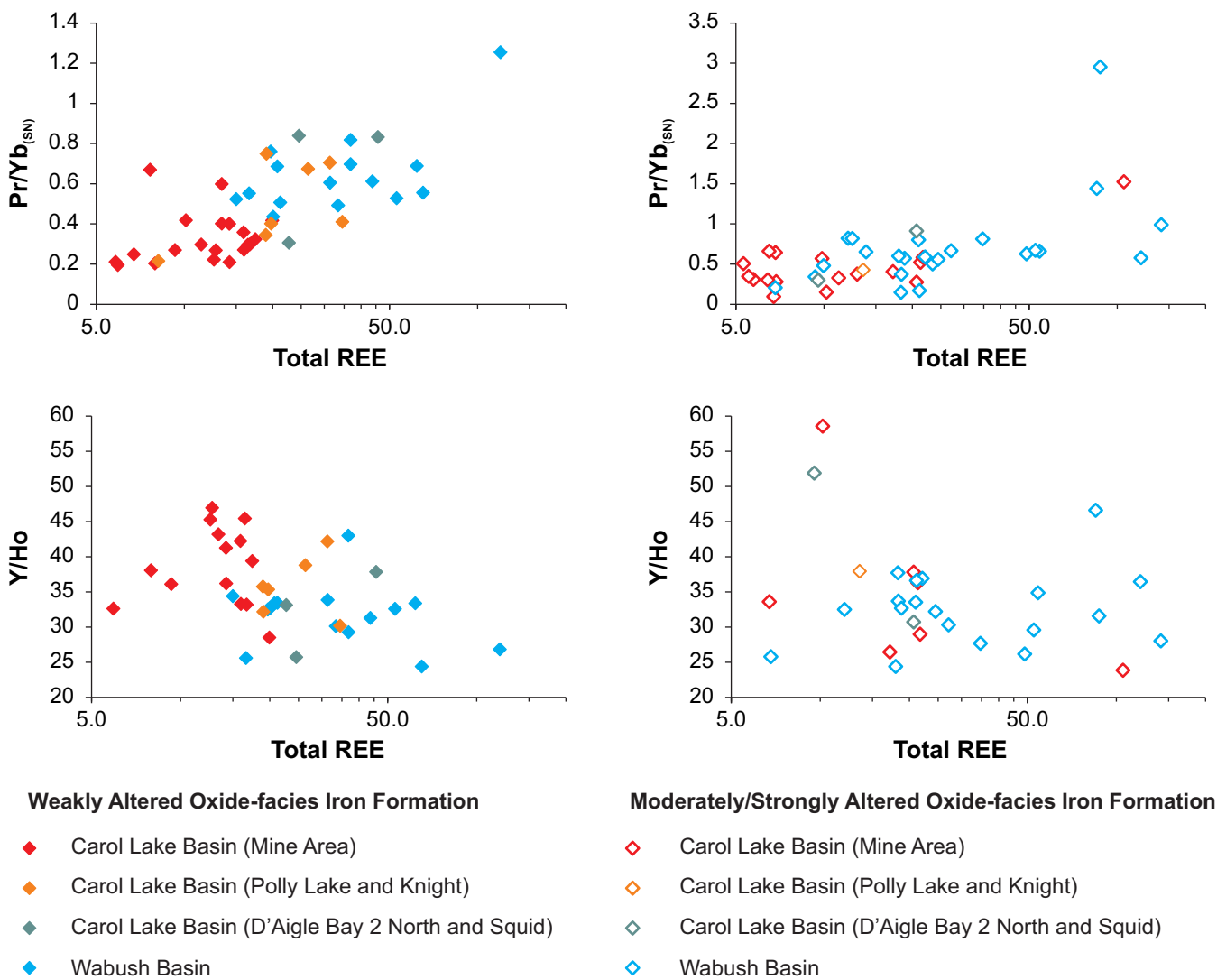


**Figure 23.** Bivariate plots of  $Pr/Yb_{(SN)}$  and Y/Ho against total REE ( $\sum REE$ ) concentration of oxide-facies iron formation in the Carol Lake and Wabush basins. Samples from the Carol Lake Basin separate into deposits from the mine area of the Carol Project, samples from south of the mine area (Polly Lake and Knight prospects) and samples from north and west of the mine area (D'Aigle Bay 2 North prospect and Squid showing). See text for details.



23.83 to 58.55 (Figure 23). The  $\Sigma$ REE concentration ranges from 5.3 to 105.4 ppm, with all but one sample having <22 ppm  $\Sigma$ REE. Some samples display strong negative Ce anomalies (Figure A24) and Eu anomalies are generally positive (Figure 24).

### Wabush Basin

The PAAS-normalized REE profiles of weakly altered oxide-facies iron formation samples from the Wabush Basin are generally less HREE enriched than samples from the Carol Lake Basin (Figures 22 and 23), with  $Pr/Yb_{(SN)}$  ranging from 0.43 to 1.25 (average  $0.65 \pm 0.2$ ). With the exception of one sample, the Y/Ho ratio ranges from 24.4 to 34.4. These samples range from having no Ce anomaly to having slightly positive Ce anomalies (Figure 24), and most samples have

positive Eu anomalies (Figure 24). Moderately to strongly altered iron-formation samples have variable LREE to HREE ratios ( $Pr/Yb_{(SN)}$  of 0.15 to 2.95), and common, strong negative Ce and positive Eu anomalies (Figure 24).

Weakly altered BSIF samples have negligible Ce anomalies and positive Eu anomalies, and two of the three samples analyzed are LREE enriched. Moderately to strongly altered BSIF have similar Ce and Eu anomalies, but highly variable LREE to HREE ratios ( $Pr/Yb_{(SN)}$  of 0.78 to 3.17).

### Mills Lake Basin

Oxide-facies iron formation samples from the Mills Lake Basin (weakly altered) have flat to weakly HREE-enriched PAAS-normalized REE profiles (Figure A22), with  $Pr/Yb_{(SN)}$  of

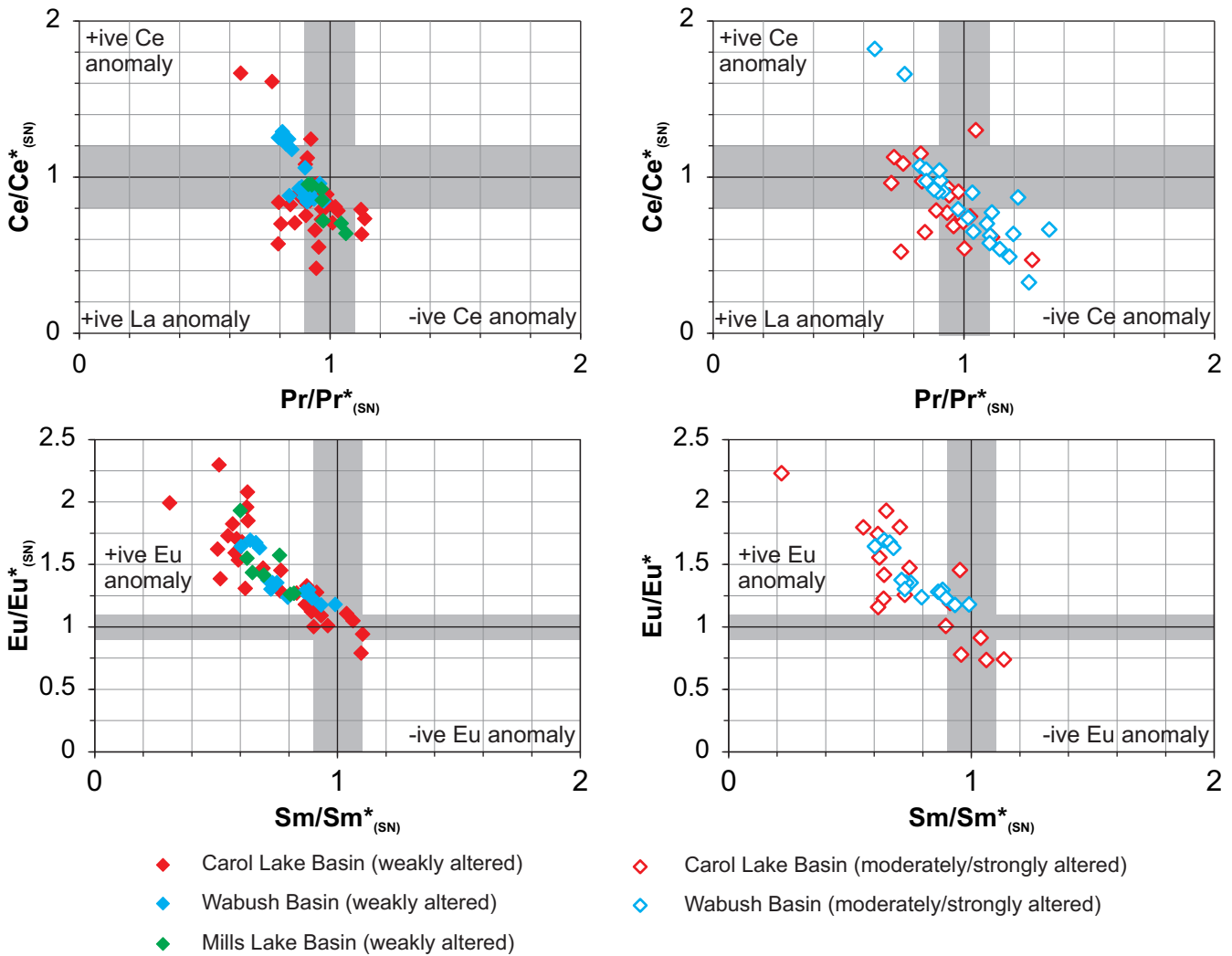


**Figure 24.** Bivariate plots of  $Ce/Ce^*_{(SN)}$  vs.  $Pr/Pr^*_{(SN)}$  (showing true Ce anomalies) and  $Eu/Eu^*_{(SN)}$  vs.  $Sm/Sm^*_{(SN)}$  (showing true Eu anomalies) from oxide-facies iron formation in the Carol Lake, Wabush and Mills Lake basins. Grey areas indicate no significant anomalies. See text for details.

$0.69 \pm 0.19$ . They do not display any true positive or negative Ce anomalies, but do display strongly positive Eu anomalies ( $1.49 \pm 0.23$ ). The single BSIF sample has a flat REE profile, no Ce anomaly and a strong positive Eu anomaly (1.64).

## DISCUSSION

### Depositional Environment of Oxide-facies Iron Formation

The geochemistry of iron formations, in particular the REE + Y composition, can provide insights into ocean chemistry and the depositional environment (Ewers and Morris, 1981; Bau and Dulski, 1996; Bolhar *et al.*, 2004; Pecoits *et al.*, 2009; Planavsky *et al.*, 2010; Mloszewska *et al.*, 2012; Haugaard *et al.*, 2013; Wang *et al.*, 2014). The effects of metamorphism on the distribution of REE + Y is thought to be insignificant (Bau and Dulski, 1996; Viehmann *et al.*, 2015), however, late-stage alteration, including supergene processes, commonly affect the REE + Y content of iron formations (Gutzmer *et al.*, 2008). Therefore, only the geochemical data from the least altered oxide-facies iron formation samples are used in the following discussion on the depositional environment of the Sokoman Formation iron formation in the study area.

All samples are characterized by low  $\text{Al}_2\text{O}_3$  (generally  $<0.5$  wt. %) and  $\text{TiO}_2$  ( $<0.05$  wt. %) concentrations (Figure A19), as well as low concentrations of the HFSE, which are considered immobile in ocean water, but which are enriched in clastic detritus (*e.g.*, Zr, Nb; Mloszewska *et al.*, 2012; Haugaard *et al.*, 2013). This indicates these samples represent pure chemically precipitated sediments, and are considered proxies for the chemical composition of the Paleoproterozoic Ocean during deposition (Bau, 1993; Pecoits *et al.*, 2009; Mloszewska *et al.*, 2012; Haugaard *et al.*, 2013). The major- and trace-element composition of samples from the Carol Lake and Wabush basins are generally similar (Figures 19 and 21), with the exception of MnO and LILE (particularly Ba), which are relatively enriched in samples from the Wabush Basin. The Mn concentration is considered representative of the redox condition of the ocean, which was stratified during the Paleoproterozoic, with an oxic upper layer and deeper anoxic water, separated by a chemical boundary known as the redoxcline (Figure 25; Planavsky *et al.*, 2010). The higher Mn concentration in samples from the Wabush Basin may indicate deposition at or below this redoxcline, as Mn-oxides are dissolved in seawater below the redoxcline. The increase in Ba in these samples may also indicate deposition below the redoxcline, as Ba is preferentially absorbed by Fe–Mn-oxides (Dymond *et al.*, 1992) and would have been transported below the redoxcline, where it was subsequently dissolved in the anoxic waters and the liberated Ba enriched the iron formation.

Numerous studies have shown that REE–Y concentrations in iron formations reflect the ocean chemistry during precipitation (Bau and Dulski, 1996; Bolhar *et al.*, 2004; Pecoits *et al.*, 2009; Planavsky *et al.*, 2010; Mloszewska *et al.*, 2012; Haugaard *et al.*, 2013; Wang *et al.*, 2014). In modern redox-stratified basins, which have a strong redoxcline separating the upper oxic and lower anoxic layers, LREEs are generally depleted in the upper oxic layer due to the preferential removal of LREE vs. HREE onto Fe–Mn oxyhydroxides. Also, the ratio of LREE to HREE increases with depth as you pass across the redoxcline due to the reductive dissolution of these Fe–Mn-rich particles (Planavsky *et al.*, 2010). In contrast, Y/Ho ratios decrease as you pass below the redoxcline, as Ho is relatively enriched compared to Y in Fe–Mn-rich particles (Planavsky *et al.*, 2010). Late Paleoproterozoic (1.9 to 1.8 Ga) oceans are believed to have been redox-stratified (Figure 25; Planavsky *et al.*, 2010), and therefore the PAAS-normalized REE patterns are likely to reflect the depth of deposition (Figure 25).

The  $\text{Pr}/\text{Yb}_{(\text{SN})}$  ratio of oxide-facies iron formation samples from the Wabush Basin ( $0.65 \pm 0.2$ ) are generally higher than those from the mine area in the Carol Lake Basin ( $0.33 \pm 0.12$ ), with a corresponding decrease in the Y/Ho ratio ( $31.8 \pm 4.4$  in the Wabush Basin vs.  $38.7 \pm 5.6$  in the mine area of the Carol Lake Basin). This suggests that the samples from the Wabush Basin were deposited in deeper water farther from the continental margin and below the redoxcline (Figure 25), which is consistent with the elevated Mn and Ba in these samples. However, the higher  $\text{Pr}/\text{Yb}_{(\text{SN})}$  and lower Y/Ho ratios of samples from outside the mine area in the Carol Lake Basin indicate that there is at least some lateral variation in water depth and/or depth to the redoxcline, and more research is warranted to determine how these geochemical signatures related to the ocean chemistry and depositional environment.

The geochemistry of oxide-facies iron formation samples from the Mills Lake Basin is broadly similar to those from the Wabush Basin, with relatively high Mn (up to 17.2 wt. %) and Ba (up to 5142 ppm), and similar  $\text{Pr}/\text{Yb}_{(\text{SN})}$  and Y/Ho ratios (Table 4), consistent with deposition in a deep-ocean basin below the redoxcline. High  $\text{Na}_2\text{O}$  values in some samples are likely due to the presence of riebeckite in the protolith, which was subsequently metamorphosed into Mn-rich aegirine. Riebeckite (and its asbestos form crocobilite) has also been reported from unmetamorphosed iron formation in the central Labrador Trough (Zajac, 1974). Zajac (*op. cit.*) argued that the riebeckite formed during diagenesis due to high Na content of the precursor sediments, rather than due to later hydrothermal alteration. If so, the unusual geochemistry of these samples reflects unusual ocean chemistry and/or major hydrothermal input into the basin.

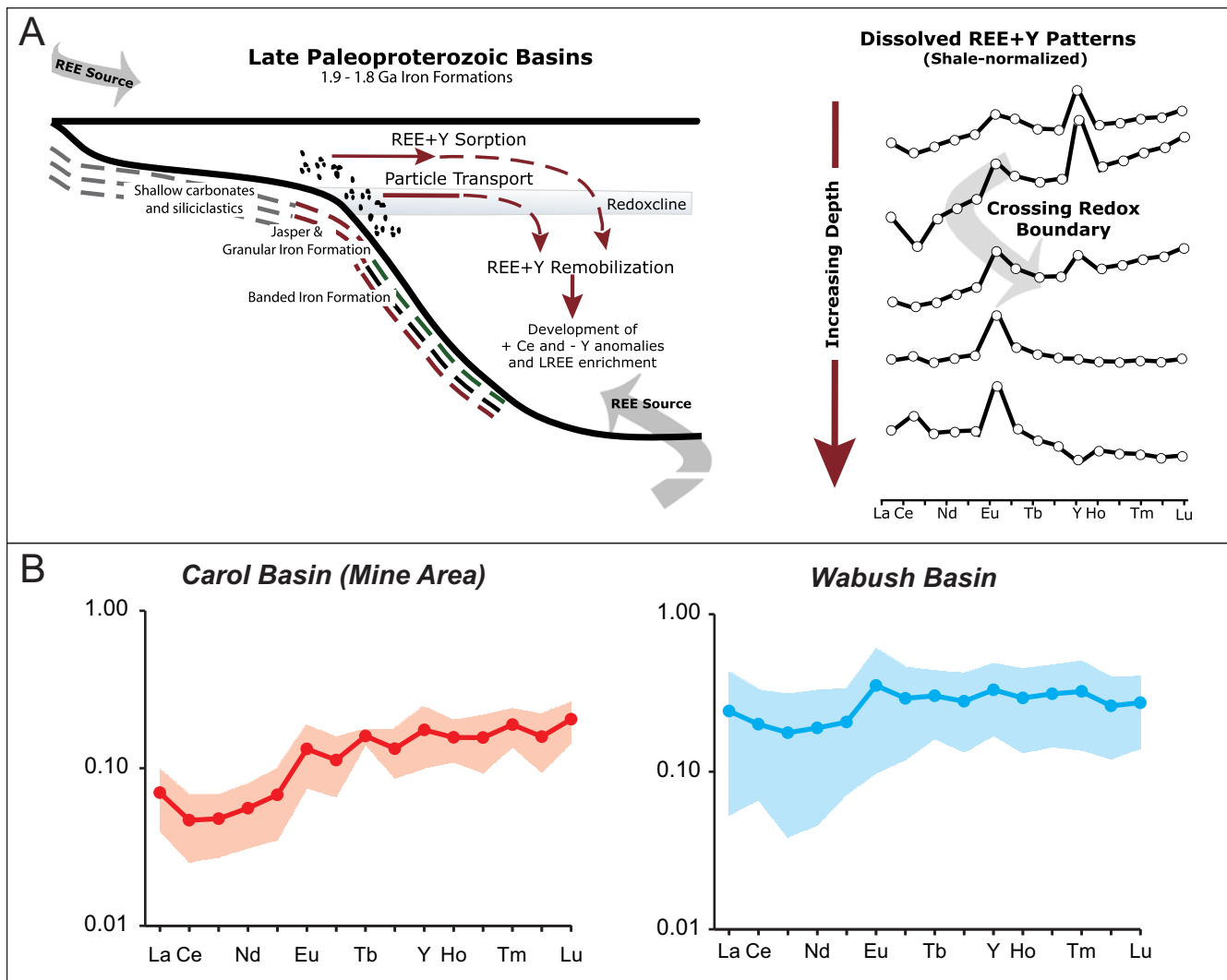


**Figure 25.** A) Model of ocean redox structure in the late Paleoproterozoic based on REE analyses from iron formations (adapted from Planavsky et al., 2010). The model shows a mechanism for the transport of metal and Ce oxides from oxic-shallow seawater across the redoxcline, with dissolution of Mn-oxides in anoxic waters lowering Y/Ho ratios and increasing LREE to HREE ratios (see schematic REE profiles); B) Average REE distribution patterns normalized to post-Archean average Australian Shale (PAAS) for weakly altered oxide-facies iron formation in the Carol Lake (mine area) and Wabush basins, showing increased LREE to HREE ratios in the Wabush Basin related to deposition in deeper water below the redoxcline.

### Depositional Environment of the Basal Silicate Iron Formation

Samples of BSIF from the Wabush and Mills Lake basins have much higher  $\text{Al}_2\text{O}_3$  (up to 2.64 wt. %),  $\text{TiO}_2$  (up to 0.83 wt. %) and  $\text{P}_2\text{O}_5$  (up to 0.5 wt. %) than the oxide-facies iron formation (Figure 20). This indicates a higher detrital content in these samples, as  $\text{Al}_2\text{O}_3$  and  $\text{TiO}_2$  are unlikely to have precipitated directly from seawater and are commonly interpreted to be immobile during late-stage alteration and metamorphism (Ewers and Morris, 1981; Horstmann and Hålbich, 1995). The low  $\text{K}_2\text{O}$  content of samples from the Wabush Basin (<0.15 wt. %) indicates that stilpnomelane,

which is considered a key indicator of volcanogenic provenance (Horstmann and Hålbich, 1995; Pickard, 2002), was not a major component of the protolith, and therefore volcanoclastic input into the basin was limited. The BSIF sample from the Mills Lake Basin has higher average  $\text{K}_2\text{O}$  content of 0.45 wt. %, and therefore there may have been a higher degree of volcanic input into this basin.

The BSIF samples are deposited as chemical muds during the transition from clastic sedimentation (Wishart Formation) to the deposition of the overlying iron formation. Similarities in stratigraphic position, detrital input and geochemical characteristics (high  $\text{Al}_2\text{O}_3$  and  $\text{TiO}_2$ ) between the



BSIF and the Ruth Formation support correlations between these two units. Pufahl *et al.* (2014) suggested that the Ruth Formation on the western margin of the Labrador Trough was deposited in shallow lagoons during a lowstand system tract. However, the Ruth Formation is not restricted to nearshore environments, and has been recorded in deeper water, outer-shelf or slope environments in the eastern margin of the Labrador Trough (Wardle, 1979; Lachance, 2015; Conliffe, 2017), which are considered equivalent to BSIF in the Wabush and Mills Lake basins.

### Late-stage Alteration

Late-stage alteration in all oxide-facies iron formation and BSIF samples is characterized by a strong depletion in MgO and CaO (Figures 19 and 20). This depletion corresponds to the removal of carbonates and iron silicates, with the resultant mineralogy consisting predominantly of quartz and iron oxides. Similar strong depletion of MgO and CaO is recorded in supergene Fe deposits (Gutzmer *et al.*, 2008). However, late-stage alteration is not associated with a similar depletion of SiO<sub>2</sub> or increase in total Fe content as has been reported from supergene Fe deposits (Gross, 1968; Conliffe, 2016b), indicating that the fluids responsible for this alteration were not able to leach quartz. This may be due to the chemical conditions of the fluids (fO<sub>2</sub>, pH) or to the implications of the larger grain size of the quartz grains in the metamorphosed iron formation, which would have impeded dissolution.

The MnO concentrations are highly variable and most samples are strongly depleted in MnO, whereas others are strongly enriched (up to 20 wt. % MnO). The Mn is highly mobile during weathering and the distribution of Mn results from the destruction of Mn-silicates and carbonates in the iron formation followed by secondary precipitation of Mn-oxides (psilomelane, pyrolusite, manganite) in discreet veins or layers. Manganese is commonly associated with redistribution of other highly mobile elements (*e.g.*, Ba), which are also enriched in some samples. This redistribution of Mn is most notable in samples from the Wabush Basin because of the higher initial Mn concentration of the unaltered iron formation, and has important implications for processing of ore from some deposits.

Other trace-element concentrations of altered samples are similar to the weakly altered equivalents (Figure 20), indicating that these elements have not been remobilized during alteration. In contrast, the REE profiles of altered samples are highly variable (Figure 23), with some samples displaying strong enrichment in LREEs (Pr/Yb<sub>(SN)</sub> up to 3.0) and others displaying enrichment in HREEs (Pr/Yb<sub>(SN)</sub> < 0.1). This is related to the behaviour of REE during alteration, with mobilization of HREE in a low-temperature environment and

LREE becoming enriched in the weathering residue (Nesbitt, 1979; Babechuk *et al.*, 2014). Similar REE distribution is recorded from supergene Fe deposits (Gutzmer *et al.*, 2008) as well as the enriched Fe deposits in the Schefferville area (Conliffe, 2016b).

## SUMMARY AND CONCLUSIONS

Southwestern Labrador is host to numerous iron-ore occurrences, which were first discovered in the 1940s and have been mined since the 1960s. These occurrences occur in the Paleoproterozoic Sokoman Formation iron formation, which can be traced throughout the Labrador Trough over a strike length of 1100 km. The sedimentary and volcanic rocks of the Labrador Trough are, collectively, known as the Kaniapiskau Supergroup, and record a long history of rifting and passive margin sedimentation on the margin of the Superior Continent, from 2.17 to 1.87 Ga. In southwestern Labrador, the rocks of the Kaniapiskau Supergroup extend into the younger Grenville Province. During the Grenville Orogeny, they were extensively deformed as part of a foreland directed fold–thrust belt. Previous work has shown that this deformation resulted in the formation of a series of thrust sheets, with three episodes of deformation and folding recognized in the study area (van Gool, 1992; van Gool *et al.*, 2008). Economically mineable thicknesses of oxide-facies iron formation are related to fold repetition and/or viscous flow into fold hinges during D<sub>1</sub> and D<sub>2</sub> deformation (Cotnoir *et al.*, 2002). Metamorphism during the Grenville Orogeny also had important implications for the metallurgy of iron ores, with the chert and iron oxides having been recrystallized (accompanied by a marked increase in grain size), resulting in the formation of a class of deposits known in the Labrador Trough as metataconites.

The Sokoman Formation consists of three broadly defined end-member facies: oxide-facies, silicate-facies and carbonate-facies. Oxide-facies iron formation, which is the main economic unit, consists of variable proportions of magnetite and hematite, quartz, and lesser carbonate and iron silicate minerals. The stratigraphy of the Sokoman Formation varies across the study area, and based on these variations, the area has been subdivided into two parallel, north-northeast-trending belts; the Carol Lake Basin to the west and the Wabush Basin to the east, and a small third basin (Mills Lake Basin) in the southeast of the study area. The Sokoman Formation in the Carol Lake Basin consists of a Lower Iron Formation (LIF) dominated by a carbonate-facies iron formation, a Middle Iron Formation (MIF) consisting predominantly of oxide-facies iron formation, and an Upper Iron Formation (UIF) with carbonate- and silicate-facies iron formation, and rare oxide-facies bands. In the Wabush Basin, the Sokoman Formation has a distinctive BSIF at the base, which may correlate to the Ruth Formation shales in the Schefferville area.

This is overlain by a thick sequence of oxide-facies iron formation, with the carbonate-facies LIF being absent. The upper part of the Sokoman Formation within the Wabush Basin, where recorded, consists mainly of carbonate-facies iron formation and minor oxide- and silicate-facies iron formation. In the Mills Lake Basin, the stratigraphy consists of a lower BSIF overlain by a carbonate-facies iron formation, the main oxide-facies iron formation and an upper zone of carbonate-facies iron formation having a thin (<25 m) oxide-facies layer.

When determining the economic viability of deposits, moderate to intense secondary alteration and leaching have important implications as the presence of significant alteration minerals (*e.g.*, goethite) can greatly affect metallurgy. Alteration has been recorded in some deposits to depths of >300 m. In the oxide-facies iron formation, this alteration results in magnetite being partially to completely oxidized to secondary martite and common goethite. The altered oxide-facies iron formation is highly friable. The close spatial association between altered iron formation and late-stage brittle faults suggests that these faults may have been reactivated during tectonic movement, after ductile deformation and metamorphism (Cotnoir *et al.*, 2002). Further, any late-stage fluid movement responsible for secondary alteration of the iron formation, including circulation of formational waters and/or downward percolation of groundwater, would have focused along these structures.

New geochemical data, when combined with stratigraphic interpretations, support the identification of separate depositional basins, possibly representing separate depositional centres that have been juxtaposed during later defor-

mation and crustal shortening. The least altered samples from the Wabush and Mills Lake basins generally have elevated Mn and Ba, lower Y/Ho ratios, and are enriched in LREE compared to samples from the Carol Lake Basin. All samples have low Al and Ti, indicating that detrital input was minimal to these basins, and that the geochemistry of the iron formation reflects the ocean chemistry during deposition. Hence, the distinct geochemical signature of samples from the Wabush and Mills Lake basins is interpreted to represent deposition in relatively deeper water compared to the Carol Lake Basin, below the redoxcline in a stratified ocean (with an oxic upper layer and reduced lower layer). However, more detailed geochemical analyses (including microanalysis of individual mineral phases) is warranted to determine how these geochemical signatures relate to the ocean chemistry and depositional environment.

The effects of late-stage alteration include strong depletion of Mg and Ca, corresponding to the removal of carbonates and iron silicates, and remobilization of Mn into discrete layers and veins. The remobilization of Mn has implications for the processing of these deposits, as Mn is deleterious to steel making. Similar late-stage alteration of Sokoman Formation rocks is observed in the Schefferville area, where it is associated with the leaching of Si and residual enrichment of the residual iron formation during the genesis of high-grade (>55% Fe) DSO deposits (Gross, 1968; Conliffe, 2015, 2016b). However, late-stage alteration in the study is not associated with any Si depletion or Fe enrichment, which may be due to the chemistry of the fluids or the larger quartz grain size in the metamorphosed iron formation that would impede dissolution.

## PART B

### INTRODUCTION

Part B summarizes the geological setting and history of exploration of 40 named iron-ore occurrences in southwestern Labrador (NTS map areas 23B/14, 15, 23G/02, 03 and part of 07). The descriptions are based on assessment reports (available *via* the Government of Newfoundland and Labrador GeoFiles Collection), company reports (available on the SEDAR system at [www.sedar.com](http://www.sedar.com)) and information gathered during fieldwork by the author in 2012, 2013 and 2014.

Southwestern Labrador is host to numerous iron-ore occurrences, first discovered in the 1940s, that have been mined since the 1960s. Today, mining forms the backbone of the economy of western Labrador, and the iron-ore deposits in the region account for more than half of the gross value of mineral shipments for Newfoundland and Labrador (2016 GNL statistics website: [https://www.geosurv.gov.nl.ca/minesen/mineral\\_shipments/](https://www.geosurv.gov.nl.ca/minesen/mineral_shipments/)).

All the occurrences hosted by the Paleoproterozoic Sokoman Formation iron formation, are part of a sequence of sedimentary and volcanic rocks of the Labrador Trough, collectively known as the Kaniapiskau Supergroup, which record a long history of rifting and passive margin sedimentation from 2.17 to 1.87 Ga. In southwestern Labrador, the rocks of the Kaniapiskau Supergroup extend into the younger Grenville Province, and during the Grenville Orogeny (*ca.* 1.0 Ga) they were extensively metamorphosed and deformed. This metamorphism was responsible for the formation of metataconite deposits, where iron formation rich in Fe-oxides (hematite and magnetite) was recrystallized to medium- to coarse-grained magnetite, specular hematite and quartz, which are easily beneficiated into iron concentrates (approximately 65% Fe) ideal for pellet production. Deformation during the Grenville Orogeny was also important in the development of structurally influenced mineable thicknesses of oxide-facies iron formation.

The regional geological setting, stratigraphy of the Kaniapiskau Supergroup metasedimentary rocks in the study area, stratigraphy of the Sokoman Formation and the effects of Grenvillian deformation and metamorphism are described, in detail, in Part A. This report also includes whole-rock geochemical data (Appendices A to F) from select iron-ore occurrences.

### NOTES ON THE STRUCTURE OF PART B

Part B provides a brief summary of the geological setting and exploration history of 40 named occurrences in the study area. Each description is designed as a stand-alone record including references, geological maps and other images, where appropriate. The location of each occurrence is shown in Figures 26 and 27, with the number referring to a number prescribed to each occurrence alphabetically (Table 1).

Each occurrence has been given a location, based on the approximate centre of the occurrence, or location of a representative mineralized drillhole. Where appropriate, any alternate name for the occurrence is provided, as well as an appropriate reference to the occurrence in the Mineral Occurrence Data System (MODS). The current status of the occurrence is provided, which represents an indicator of the amount of work done on the occurrence, and hence, the amount of information that exists about it. The occurrences in this report are classified into five major designations based on the criteria outlined in the MODS. These criteria are as follows:

- *Producer* – A mineral deposit from which ore is being extracted for commercial gain or benefit. Does not include deposits from which the only material extracted has been for test purposes.
- *Developed Prospect* – A mineral deposit on which, in the opinion of the author, enough development work has been done to provide data for the making of a reasonable estimate of the amounts of one or more commodities present, even though the data themselves may not be available.
- *Past Producer (Dormant)* – A mineral deposit from which production is no longer obtained, but there are additional reserves or demonstrated resources. Does not include those mineral deposits on which work was stopped after extracting a bulk sample for milling and other tests, even though the sample may have been large.
- *Prospect* – A mineral deposit upon which, in the opinion of the author, enough development work has been done to provide data for the making of a reasonable estimate of the spacial extent of the deposit, but not enough to estimate the amount of any commodity present.



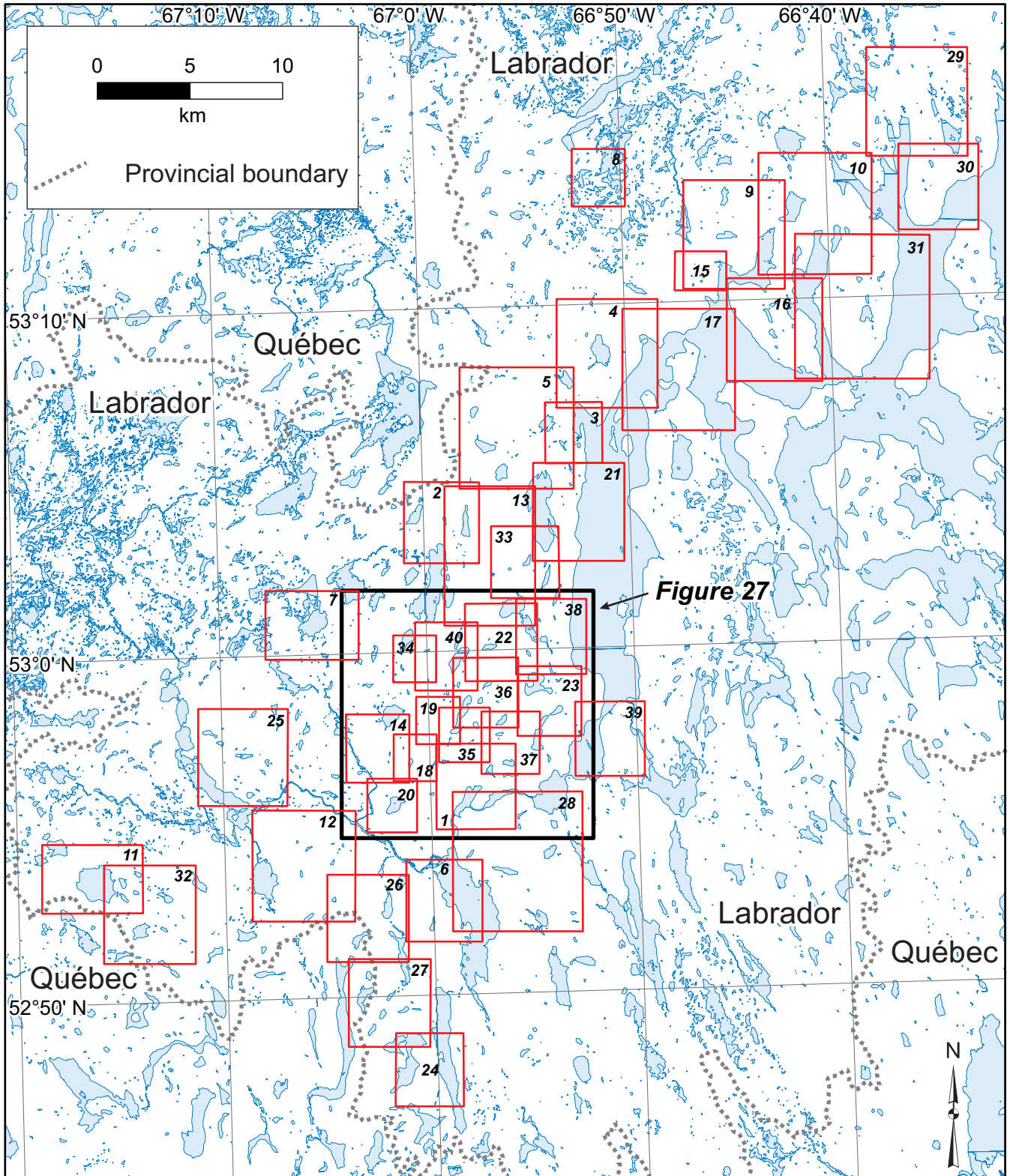


**Figure 26.** Overview map showing location of individual showings, prospects and deposits discussed in detail. Number refers to deposit number listed in Table 1. For detailed location of showing, prospects and deposits in the area indicated by the black box outline, see Figure 27.

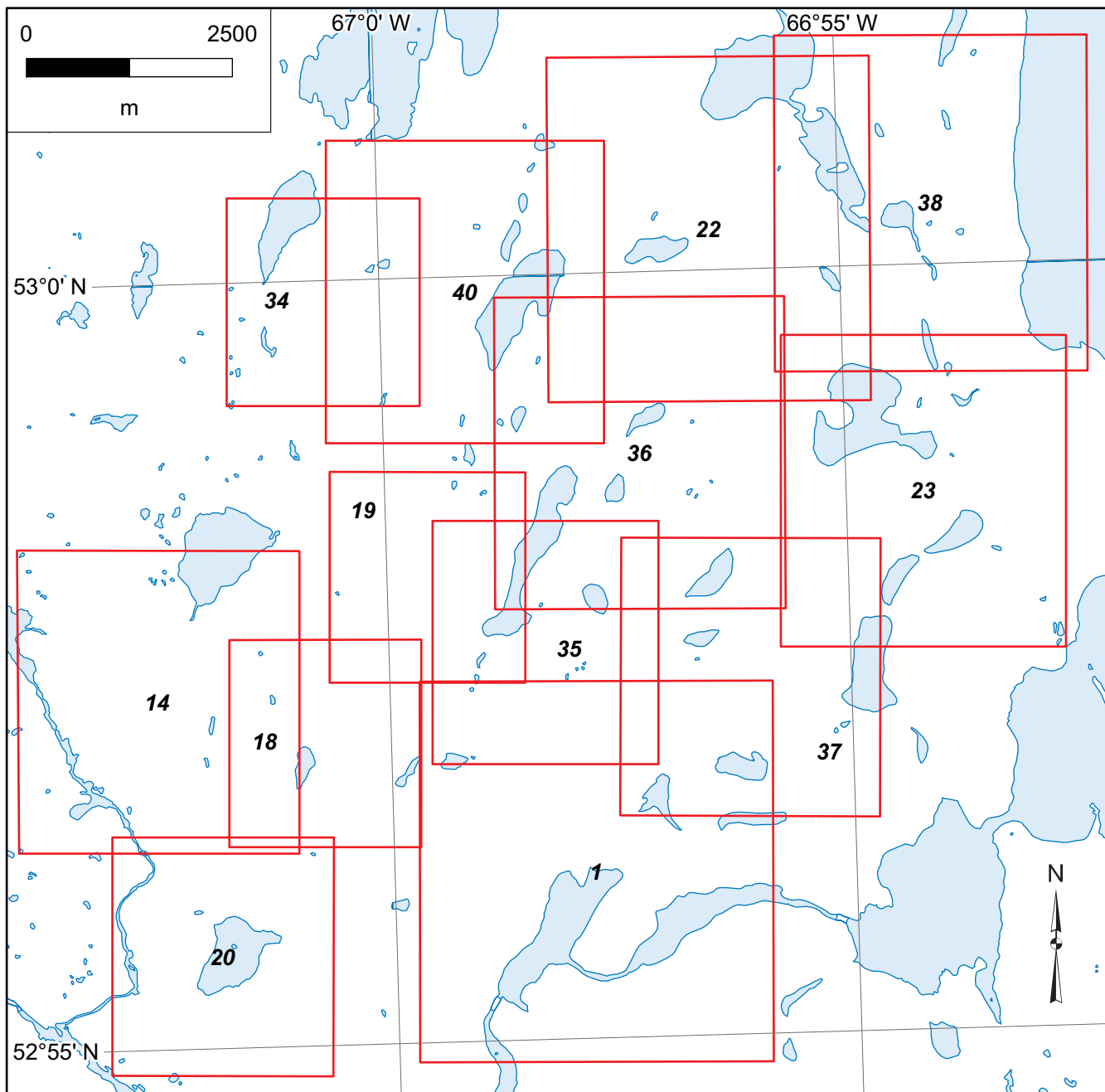


**Figure 27.** Map showing location of individual showings, prospects and deposits. Numbers refer to deposits in Table 1.

- *Showing* – A mineral deposit upon which some development work may have been done, but the extent of such work was not adequate, in the opinion of the author, to provide enough data to estimate its spacial dimensions.

The description of each occurrence includes information on the location of, and access to, the occurrence, as well as brief summaries of the geology and stratigraphy, mineralization, structure and geophysical signature of the occurrence.

The history of exploration summarizes the exploration and development history of the occurrence, based on information available in assessment reports and company documents available on SEDAR.

## PROSPECT/DEPOSIT DESCRIPTIONS

### 1. CANNING

**Alternate Name:** Canning Lake, Canning No. 1, New Townsite

**MODS Showing(s):** 023B/15/Mn003

**Status:** Prospect

**Structural Basin:** Carol

**UTM Zone:** 19

**NTS Area:** 23B/15

**Northing (NAD27):** 5867803

**Easting (NAD27):** 637400

**Latitude:** 52.9442

**Longitude:** -66.9552

**Object Located:** Drillhole CA-10-02

#### Description of Occurrence

The Canning prospect is located 3.5 km southeast of Labrador City. The prospect extends for over 3600 m, from southeast of Canning Lake to north of the Trans-Labrador Highway (TLH; Figure 28), and likely represents the southern extension of the Wabush 4 prospect. Access is by a series of gravel roads.

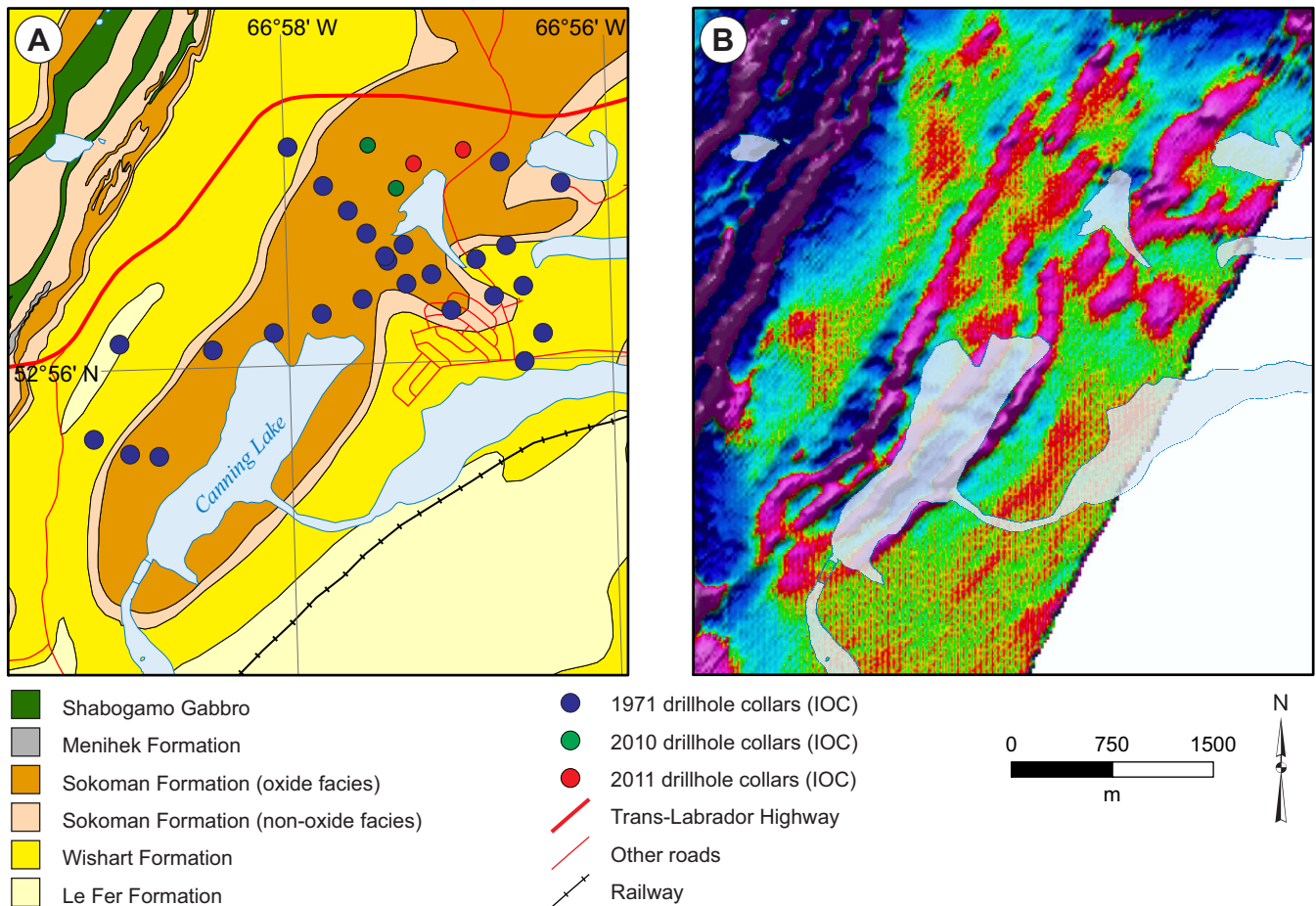


**Figure 28.** A) Geological map of the Canning prospect (adapted from Cotnoir et al., 2002), showing location of drillholes from 1971, 2010 and 2011 exploration programs (Muwais and Broemling, 1971; Carter, 2011a; Marshall, 2012a); B) Airborne magnetics (second vertical derivative) illustrates the extent of iron formation (data from Cotnoir et al., 2002).



## Geology and Stratigraphy

Outcrop in the Canning Lake area is sparse, but geophysical data show that it is a southern extension of the Wabush 4 prospect (Cotnoir *et al.*, 2002). The Sokoman Formation is stratigraphically underlain by the Wishart and Le Fer formations (Figure 28). Diamond drilling in the Canning Lake area has shown that appreciable thicknesses of iron formation are present (up to 300 m in drillhole CA-10-02). The iron formation is commonly altered, and no detailed stratigraphic information is available. However, at the Wabush 4 prospect, along strike to the north, the dominant lithology is the MIF and LIF, with only irregular in-folded sections of UIF (Darch *et al.*, 2003a).

## Mineralization

The Sokoman Formation at the Canning prospect is dominantly composed of quartz–hematite schist (Plate 30A). The iron formation is commonly friable and alteration is strong to moderate throughout, with abundant secondary goethite and leaching of carbonates and Fe-silicates (Plate 30B). This alteration is likely related to late-stage (post-metamorphic) fluid flow, secondary leaching and/or deep weathering along major faults, and is similar to alteration seen in the nearby Scully deposit. Manganese contents are generally low (<0.2% Mn), but some intervals have Mn contents of up to 5.92% Mn over 4 m (Carter, 2011a; Marshall, 2012a).

Carter (2011a) and Marshall (2012a) reported on some metallurgical testwork on drillcore samples from the Canning Lake prospect (SAG Power index (SPI) and iron recovery testing (TT)). These data show that the ore is soft (low SPI), with low to moderate iron recovery.

The best assay results are from drillholes CA-10-01 (32.1% Fe over 126.8 m at 9 m depth) and CA-11-04 (31.7 % Fe over 81 m at 12 m depth).

## Structure

The Canning prospect is located in a northeast–southwest-trending, northwest-verging syncline, which is plunging to the southwest in the northern part of the prospect, and to the northeast in the southern portion of the deposit (Cotnoir *et al.*, 2002). A northeast-trending normal fault cuts through the centre of the deposit (Muwais and Broemling, 1971), which may represent the northeastern extension of the major normal fault recorded in the Scully deposit.

## Geophysics

Regional airborne magnetic surveys (Cotnoir *et al.*, 2002) show that the Canning prospect has a lower magnetic response than other iron-ore showings and prospects along strike (*e.g.*, Wabush 4 prospect). This is likely due to the strong alteration of

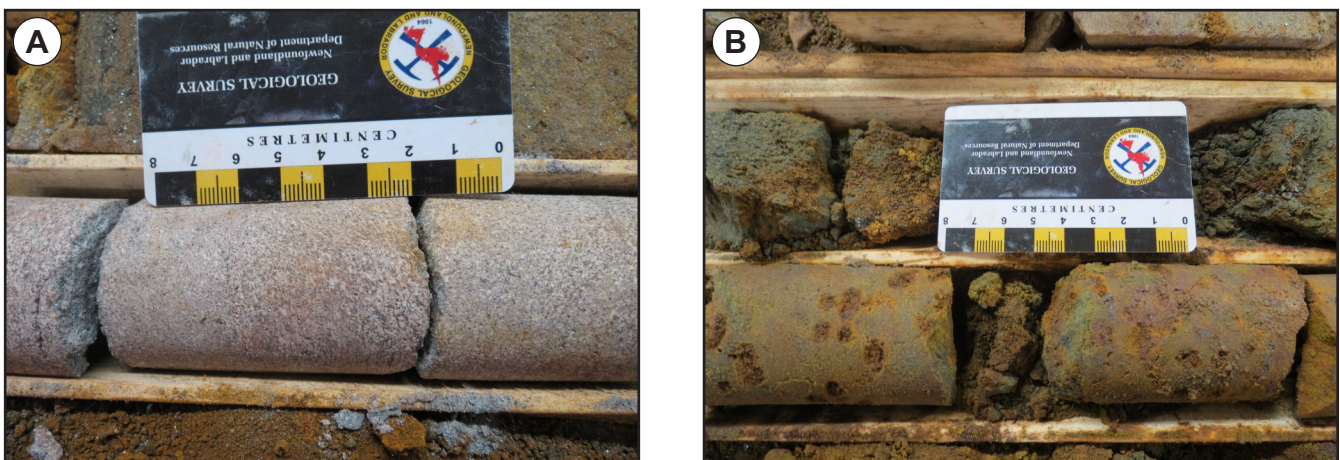


**Plate 30.** A) Typical lean quartz–specularite schist with moderate hematite alteration (drillhole CA-10-02 @ 241.8 m); B) Strongly altered quartz–specularite schist, with secondary goethite replacing carbonates (drillhole CA-10-02 @ 227 m).

the iron formation, and associated oxidation of magnetite to hematite. No gravity data are available from the Canning Lake area, but Hulstein and Lee (2001) indicated that unpublished gravity data show that the deposit is flat-lying and shallow.

### **Resource and/or Reserves**

No NI 43-101 compliant mineral resource or reserve estimate available.

Non 43-101 compliant historical estimates based on limited data range from 35 to 750 Mt grading 27% Fe (Hulstein and Lee, 2001).

### **History of Exploration**

- 1949: Geological mapping (Neal, 1950a)
- 1953: Geological mapping and prospecting (Crouse, 1954)
- 1959: Geological mapping and magnetic survey (Nincheri, 1959)
- 1971: Geological mapping and prospecting, diamond drilling (30 drillholes, 651.66 m, Muwais and Broemling, 1971)
- 1972: Aeromagnetic survey (unpublished IOC report)
- 1979: Ground magnetometer survey (Price, 1979a)
- 1982: Airborne geophysical surveys (EM, magnetics, radiometrics, Johnson, 1982)
- 2000: Data compilation, structural synthesis (Hulstein and Lee, 2001)
- 2001: Data compilation, geological mapping and prospecting, regional airborne magnetic surveys, structural/ stratigraphic interpretation (Cotnoir *et al.*, 2002)
- 2010: Diamond drilling (2 drillholes, 435.8 m, Carter, 2011a)
- 2011: Diamond drilling (2 drillholes, 522 m, Marshall, 2012a)

## 2. CAROL LAKE NORTH

**Alternate Name:** Lac Montenon, Carol Lake North 1, Carol Lake North 2

**MODS Showing(s):** 023G/02/Mn005, 023G/02/Mn006

**Status:** Prospect

**Structural Basin:** Carol

**UTM Zone:** 19

**NTS Area:** 23G/02

**Northing (NAD27):** 5880930

**Easting (NAD27):** 634914

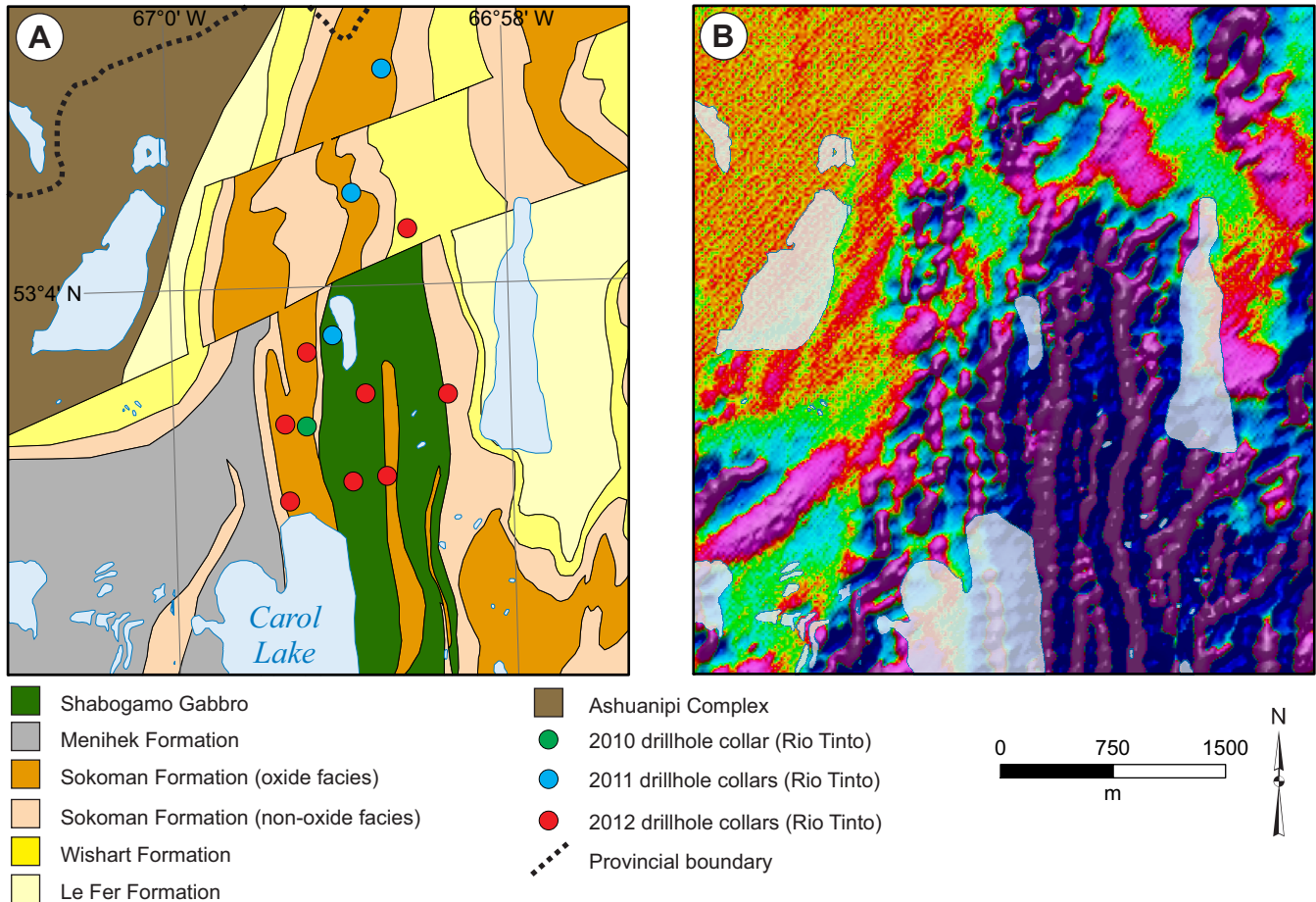
**Latitude:** 53.0628

**Longitude:** -66.9867

**Object Located:** Drillhole 12LB0043

### Description of Occurrence

The Carol Lake North prospect is located to the north of Carol Lake (Figure 29), west of IOC's Carol Lake mining operation and approximately 14 km northwest of Labrador City. There are no roads in the area, and access is *via* helicopter.





## ***Geology and Stratigraphy***

The geology to the north of Carol Lake comprises Kaniapiskau Supergroup metasedimentary rocks, which are intruded by Shabogamo Gabbro sills and cut by east–northeast-trending normal faults, that offset the stratigraphy and subdivide the property into three structural packages (Figure 29).

Geological mapping indicates that Le Fer Formation schists and Wishart Formation quartzites are located at the base of the stratigraphic sequence, and are overlain by Sokoman Formation iron formation. Shabogamo Gabbro sills intrude the Sokoman Formation, particularly in the southern portion of the property where they form topographic highs of resistant material. Menihek Formation shales occur at the top of the sequence, and have been mapped to the west of Carol Lake (Figure 29). Diamond drilling in the central portion of the property intersected thick sequences of graphitic schist (Menihek Formation), which is not shown on geological maps due to lack of outcrop control.

The stratigraphy of the Sokoman Formation is poorly understood due to the lack of distinctive marker horizons and the structural complexity, with individual units pinching and swelling over short distances (Goldner *et al.*, 2013). Diamond drilling has recorded significant thicknesses of iron formation, particularly in the south of the property (up to 150 m thick). Oxide-, carbonate- and silicate iron formation have all been recorded, with carbonate- and silicate-facies iron formations commonly displaying alteration with abundant secondary goethite.

## ***Mineralization***

The thickest sequences of oxide-facies iron formation have been recorded from the southern portion of the property, with only thin (<20 m) intervals of magnetite-rich oxide-facies iron formation recorded from the centre and northern portions of the property. Oxide-facies iron formation at the southern portion of the property consists of magnetite- and hematite-rich iron formation, with abundant secondary goethite in places. This alteration is likely related to late-stage (post-metamorphic) fluid flow, secondary leaching and/or deep weathering along major faults.

Goldner *et al.* (2013) reported on metallurgical testwork from drillcore samples from the prospect. Heavy Liquid Separation (HLS) and Davis Tube Recovery (DTR) both indicated that a moderate- to high-grade, low contaminant concentrate can be achieved, but iron weight recoveries were generally low. Bond Work Index results show that the ore is relatively soft. However, this data is only preliminary, and may not be representative of the prospect as a whole.

Assay data from diamond-drill holes show significant thicknesses of oxide-facies iron formation in the southern portion of the property, with highlights including 33.7% Fe over 72.86 m at 1.28 m depth (drillhole 12LB0043), 32.7% Fe over 65.42 m at 5.18 m depth (drillhole 12LB0039) and 30.8% Fe over 97.07 m at 1.78 m depth (drillhole 12LB0047).

## ***Structure***

A structural interpretation of the Carol Lake North prospect by Goldner *et al.* (2013) suggests the Sokoman Formation has been intensely folded, forming a series of north–south-trending, east-dipping folds that plunge to the south. However, this interpretation was hampered by the lack of recognizable marker horizons and an abundance of micro- and macro-folding observed in drillcore. Additionally, it is difficult to recognize repeated layers and folding patterns, or to decipher their scale, in the Carol Lake North drillcore (Goldner *et al.*, 2013).

Prominent east–northeast-trending normal faults are located north of Carol Lake, which are evident on geological maps and in airborne magnetic data (Figure 29). Numerous thrust faults have also been intercepted during diamond drilling.

## ***Geophysics***

Regional airborne magnetic surveys show that the southern portion of the Carol Lake North prospect is characterized by a strong magnetic response (Figure 29; Cotnoir *et al.*, 2002), which is coincident with the thickest intervals of iron formation encountered during diamond drilling. The central part of the prospect has a lower magnetic response, corresponding to the thick sequences of graphitic schist (Menihek Formation) and only minor iron formation encountered during diamond drilling, whereas

the northern portion of the prospect has a moderate magnetic response interpreted to be related to the relatively thin (<20 m) intervals of magnetite-rich iron formation encountered during drilling.

Ground gravity surveys have identified a significant gravity anomaly to the northeast of Carol Lake (Goldner and Sauve, 2012), which corresponds to thick sequences of iron formation and Shabogamo Gabbro sills.

#### **Resource and/or Reserves**

No NI 43-101 compliant mineral resource or reserve estimate available.

#### **History of Exploration**

- 1949: Geological mapping (Neal, 1950a)
- 1953: Prospecting and mapping (Almond, 1953)
- 1958: Diamond drilling (1 drillhole, 17.4 m, Eade, 1958)
- 1959: Ground gravity and magnetometer survey (Grimaldi, 1959a)
- 1978: Ground magnetometer survey (Stubbins, 1978a)
- 1979: Diamond drilling (1 drillhole, 16 m, Grant, 1979a)
- 1982: Diamond drilling (1 drillhole, 44.5 m, Simpson and Bird, 1982), airborne geophysical surveys (EM, magnetics, radiometrics, Johnson, 1982)
- 2001: Regional airborne magnetic surveys (Cotnoir *et al.*, 2002)
- 2008: Prospecting, ground gravity survey (Downing and Mitchell, 2009a)
- 2009: Geological mapping and prospecting (Downing, 2010)
- 2010: Diamond drilling (1 drillhole, 150.3 m, Hovis and Goldner, 2011a)
- 2011: Diamond drilling (3 drillholes, 787 m) and ground gravity survey (Goldner and Sauve, 2012)
- 2012: Diamond drilling (8 drillholes, 2154.9 m) and metallurgical testwork (Goldner *et al.*, 2013), airborne gravity gradiometer survey (Suave *et al.*, 2012)

### 3. D'AIGLE BAY 1

**Alternate Name:** D'Aigle Bay (IOCC) Property

**MODS Showing(s):** n/a

**Status:** Showing

**Structural Basin:** Carol

**UTM Zone:** 19

**NTS Area:** 23G/02

**Northing (NAD27):** 5885761

**Easting (NAD27):** 642191

**Latitude:** 53.1044

**Longitude:** -66.8760

**Object Located:** Drillhole DB-06-09

#### Description of Occurrence

The D'Aigle Bay 1 showing is located on the southern shore of D'Aigle Bay (Figure 30), a small bay on the western shore of Wabush Lake approximately 18 km north of Labrador City. There is no road access to the area, and access is by boat from Wabush Lake, helicopter or by foot or ATV from the IOC mine area.

#### Geology and Stratigraphy

The bedrock geology of the D'Aigle Bay 1 area consists of the Sokoman and Wishart formations (Figure 30). The Le Fer Formation outcrops on the northern shore of D'Aigle Bay, below the Wishart Formation, and a large sill of Shabogamo Gabbro intrudes the lower part of the Sokoman Formation to the west of the showing (Figure 30).

Information on the stratigraphy of the Sokoman Formation in the area is based on a single drillhole (Clark, 2006), which intersected the Sokoman Formation from 17 to 141 m. Carbonate-facies iron formation with minor oxide-facies (hematite-rich) was recorded from 17 to 73 m, which was interpreted as UIF. This was underlain by 55 m of oxide-facies iron formation (MIF). The lower 11 m of the Sokoman Formation was logged as carbonate-facies LIF. The drillhole finished in quartzite of the Wishart Formation.

#### Mineralization

The oxide-facies iron formation (MIF) encountered in diamond drilling (Clark, 2006) and in outcrop on the shores of D'Aigle Bay (Darch *et al.*, 2003b; Darch, 2004) is hematite-rich, and is classified as quartz-specularite schist. In places, the iron formation is moderately to strongly altered, with friable and sandy sections. Manganese contents of oxide-facies iron formation are generally low (<0.5% Mn), but assay data show that Mn values are higher at the top of the MIF (1.5% Mn over 15 m, Clark, 2006).

There is no published metallurgical testwork available from the D'Aigle Bay 1 showing.

Assay results from drillhole DB-06-09 show that the oxide-facies Sokoman Formation averages 35.1% Fe over 55 m (from 73 to 128 m).

#### Structure

The D'Aigle Bay 1 showing is interpreted to occur within the core of an open synformal fold dipping shallowly to the east (10 to 30°), which plunges to the south-southeast (Darch, 2004).

#### Geophysics

The D'Aigle Bay 1 showing has a subdued magnetic response compared to the Sokoman Formation directly to the northwest (Figure 30), which is likely due to the low magnetite content of the oxide-facies iron formation. Darch *et al.* (2003b) reported on gravity surveys across the showing, which identified a number of areas of anomalous high gravity readings.



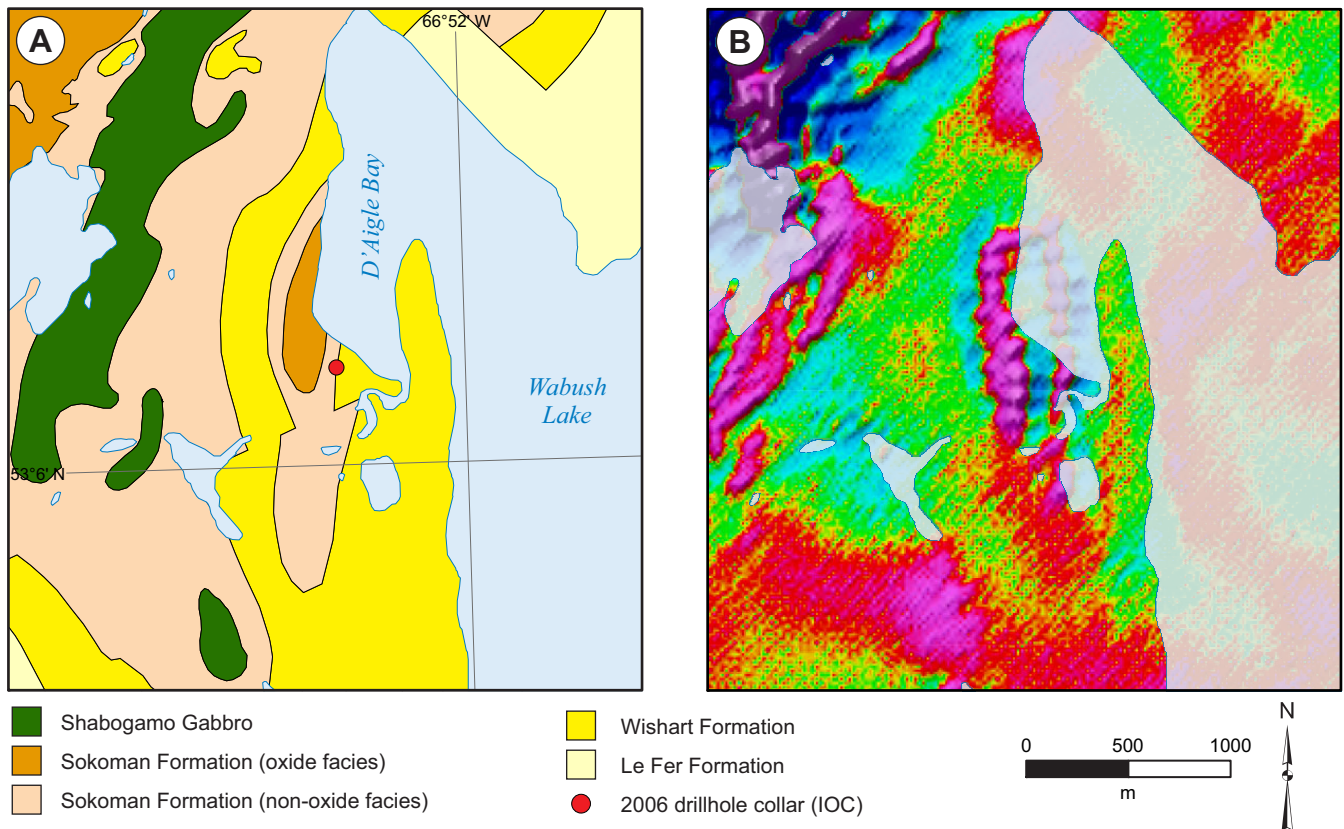


**Figure 30.** A) Geological map of the D'Aigle Bay area (adapted from Cotnoir et al., 2002), showing location of drillhole from 2006 drilling program (Clark, 2006); B) Airborne magnetics (second vertical derivative) showing extent of iron formation (data from Cotnoir et al., 2002).

### Resource and/or Reserves

No NI 43-101 compliant mineral resource or reserve estimate available.

Hulstein and Lee (2001) reported on a combined estimate (non 43-101 compliant) of 280 million tons grading 33% Fe for the D'Aigle Bay 1 showing and D'Aigle Bay 2 North and 2 South prospects based on limited data.

### History of Exploration

- 1950: Geological mapping (Neal, 1951)
- 1953: Geological mapping and prospecting (Almond, 1953)
- 1957: Geological mapping and prospecting (Crouse, 1957)
- 1958: Geological mapping, sampling, dip needle, 52 diamond-drill holes, 732 m (see Hulstein and Lee, 2001)
- 1972: Aeromagnetic survey (unpublished IOC report)
- 1982: Airborne geophysical surveys (radiometrics) (Johnson, 1982)
- 2000: Data compilation, structural synthesis (Hulstein and Lee, 2001)
- 2001: Data compilation, geological mapping and prospecting, regional airborne magnetic surveys, structural/stratigraphic interpretation (Cotnoir et al., 2002)
- 2003: Geological mapping and prospecting, ground gravity survey (Darch et al., 2003b)
- 2004: Geological mapping and prospecting (Darch, 2004)
- 2006: Diamond drilling (1 drillhole, 171.5 m, Clark, 2006)
- 2011: Airborne gravity gradiometer, electromagnetic and magnetic geophysical surveys (Wallace, 2012a)

#### 4. D'AIGLE BAY 2 NORTH

**Alternate Name:** D'Aigle Bay (LIORC) Property, Bondurant Lake

**MODS Showing(s):** 023G/02/Fe017

**Status:** Prospect

**Structural Basin:** Carol

**UTM Zone:** 19

**NTS Area:** 23G/02

**Northing (NAD27):** 5889203

**Easting (NAD27):** 643341

**Latitude:** 53.1349

**Longitude:** -66.8571

**Object Located:** Drillhole DB-10-14

#### Description of Occurrence

The D'Aigle Bay 2 North prospect refers to a large exposure of iron formation that outcrops for ~4 km (strike length) to the north and southwest of Bondurant Lake (Figure 31), approximately 22 km north of Labrador City. It is located along strike from the D'Aigle Bay 2 South prospect (*see below*), but they are separated by a dextral fault that offsets the stratigraphy (*see Structure*). Access is by helicopter.

#### Geology and Stratigraphy

The Sokoman Formation outcrops to the southwest and north of Bondurant Lake, and it is clearly imaged by the airborne magnetic data (Figure 31C). However, exposure elsewhere on the property is poor, which combined with structural complexities has resulted in a number of differing interpretations of the bedrock geology. Rivers and Massey (1985) indicated that the bedrock geology to the northwest and southeast of Bondurant Lake was predominantly quartzofeldspathic schists of the Le Fer Formation, and minor Wishart Formation quartzite (Figure 31A). van Gool (1992) reinterpreted the quartzofeldspathic gneisses as basement rocks of the Archean Ashuanipi Complex, which are separated from cover rocks of the Sokoman and Wishart formations by thrust faults. In contrast, geological mapping by IOC (Darch *et al.*, 2003b) interpreted the rocks to the east of Bondurant Lake as Sokoman Formation (Figure 31B), although this is not consistent with the aeromagnetic data (Figure 31C). In 2010, two diamond-drill holes were drilled to the east of Bondurant Lake (Figure 31; Carter, 2011b). These showed interbedded quartz–feldspar–biotite schists (Le Fer Formation?) and quartzite with minor muscovite (Wishart Formation?), consistent with the mapping of Rivers and Massey (1985).

Outcrops of the Sokoman Formation are dominantly oxide-facies and carbonate-facies (van Gool, 1992; Darch *et al.*, 2003b), interpreted as representing the MIF and LIF, respectively. In 2011, diamond drilling to the south of Bondurant Lake encountered the Sokoman Formation from 15 to 166 m depth. The drillhole collared in Wishart Formation quartzite, and the sequence, is likely folded with interbedded carbonate-facies LIF and oxide-facies MIF and minor silicate-facies iron formation. The base of the Sokoman Formation is marked by a conformable contact with a thin unit of Wishart Formation quartzite, followed by quartz–sericite–muscovite schist (possible Le Fer Formation).

#### Mineralization

The oxide-facies Sokoman Formation consists of banded iron formation, oxide- and chert-rich bands and lesser carbonate and silicate bands (Plate 31A). In general, magnetite > hematite (Plate 31B), but sections of quartz–hematite schist are common throughout (Carter, 2011). In outcrop, the oxide-facies iron formation is commonly friable and weathered, where the carbonate minerals have leached out (Darch *et al.*, 2003b), but at depth, the iron formation is generally fresh and unaltered. Assay data show that the Mn content of oxide-facies iron formation ranges from 0.2 to 2.4% Mn (Carter, 2011b).

Six composite samples from the 2010 drilling program were sent for metallurgical testwork (SAG Power index (SPI) and iron recovery testing (TT)) (Carter, 2011b). These data show that the oxide-facies iron formation is moderately hard and has low to moderate iron recoveries.

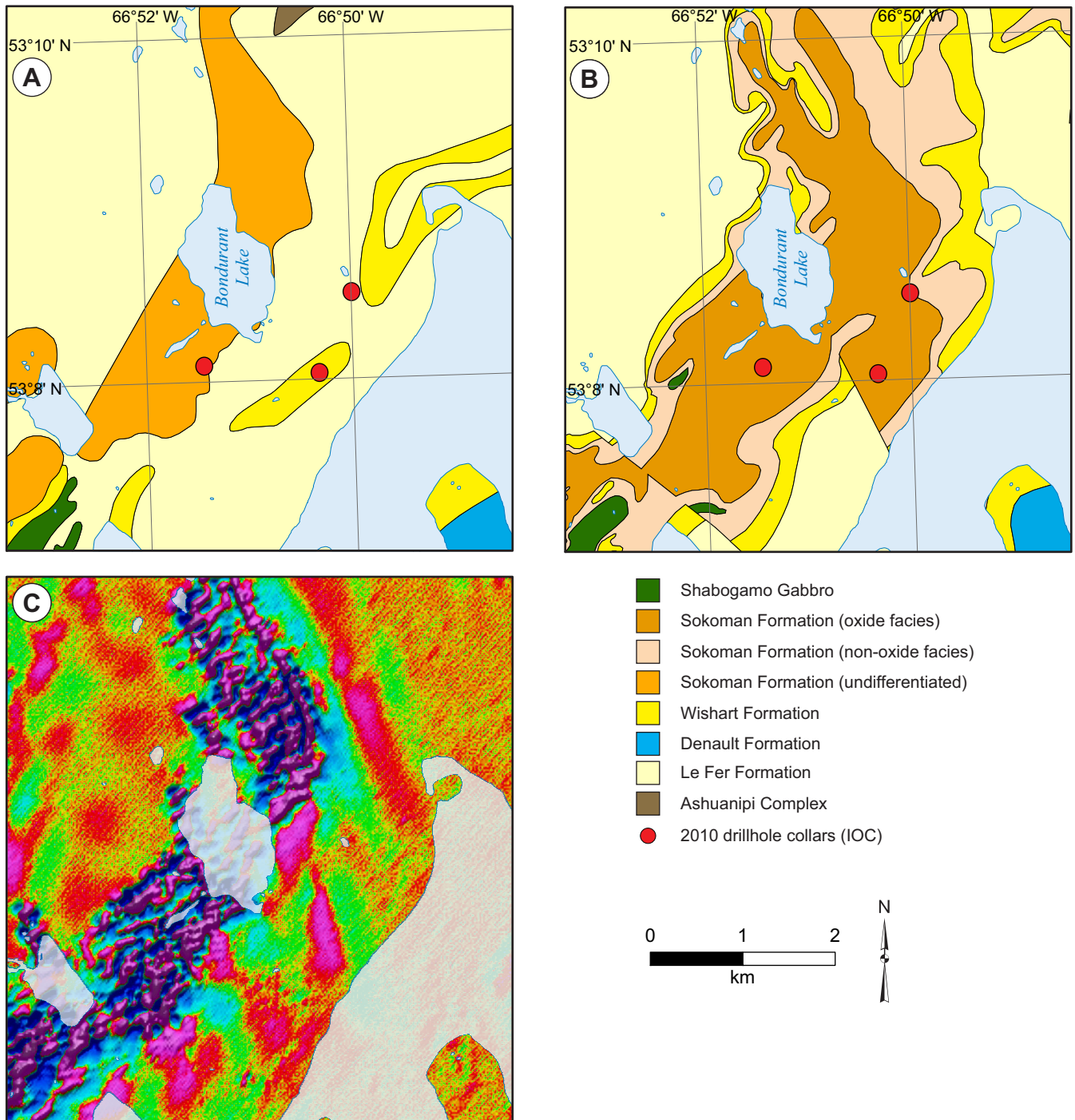


**Figure 31.** Geological maps and aeromagnetic data from the D'Aigle Bay 2 North prospect in the Bondurant Lake area, showing location of drillhole from 2010 drilling program (Carter, 2011b). A) Geological map of Rivers and Massey (1985); B) Geological map based on IOC mapping (adapted from Cotnoir et al., 2002); C) Airborne magnetics (second vertical derivative) in the Bondurant Lake area, showing extent of iron formation (data from Cotnoir et al., 2002).



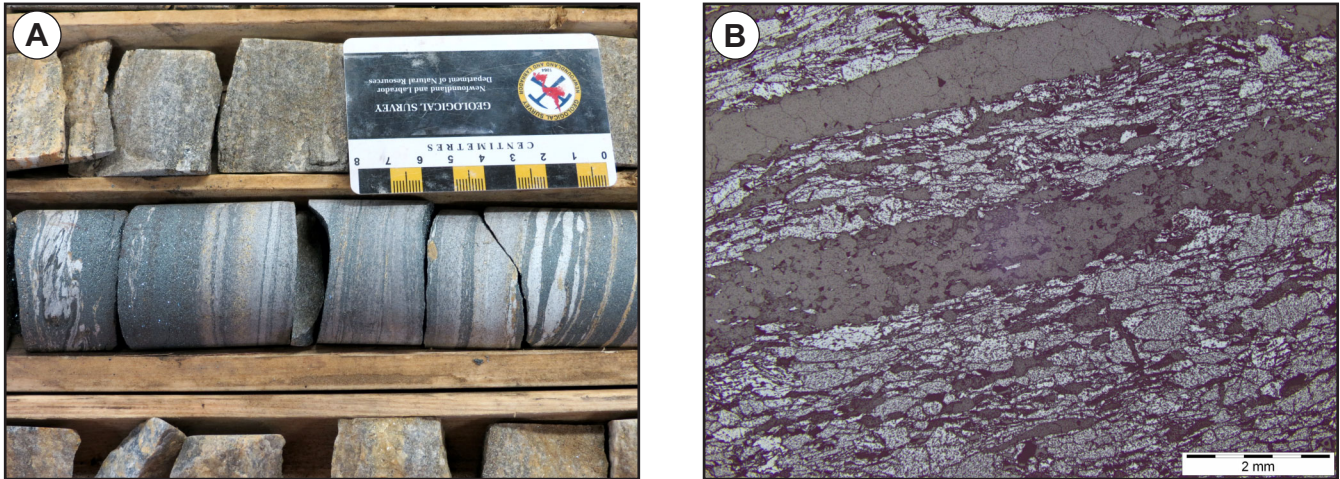


**Plate 31.** A) Banded oxide-facies iron formation with dark-grey magnetite-rich layers, white–light-grey chert-rich layers and lesser yellow carbonate-rich layers (drillhole DB-10-14 @ 162.9 m); B) Photomicrograph of banded, magnetite-rich ore with magnetite (minor hematite) and quartz-rich bands (drillhole DB-10-14 @ 163.1 m, reflected light).

Assay data from the 2010 drilling program show that the iron formation is relatively low grade (generally <30% Fe), with the best mineralized section observed in drillhole DB-10-14 from 117 to 132 m (31.1% Fe over 15 m).

### **Structure**

van Gool (1992) showed that the structural history in the area north of Bondurant Lake is complex, with multiple thrust sheets and, at least, three generations of folding. He suggested that thrusting during the Grenville orogeny was responsible for the formation of a duplex complex, with interleaved sections of the Sokoman Formation and gneiss of the Ashuanipi Complex. Geological mapping combined with geophysical data show that the Sokoman Formation occupies a series of open synformal dominated folds that dip shallowly to the east (10 to 30°) and plunge shallowly to the south (Darch *et al.*, 2003b).

Two generations of faulting have been recognized. The earliest faults recognized in the D’Aigle Bay area are northwest–southeast-trending faults with a dextral offset, which divide the area into a number of tectonic blocks, separating the D’Aigle Bay 2 North and South prospects (Darch *et al.*, 2003b). A second set of faults trend northeast–southwest and have been observed to truncate the earlier northwest–southeast fault set (Darch *et al.*, 2003b). The northwest–southeast fault set mark the northern and southern boundaries of the D’Aigle Bay 2 North and South prospects, and are interpreted to be thrust faults associated with the Grenville orogeny (Darch *et al.*, 2003b).

### **Geophysics**

Regional aeromagnetic data show that the D’Aigle Bay 2 North prospect has a strong magnetic response, with a width of >1 km and a strike length of more than 4 km extending to the southwest and north of Bondurant Lake (Figure 31C; Cotnoir *et al.*, 2002). The relatively strong magnetic response is due to the high magnetite content of the oxide-facies iron formation. Darch *et al.* (2003b) reported that reconnaissance-style gravity surveys indicate a broad, low-amplitude gravity anomaly to the south of Bondurant Lake, interpreted as representing a 100- to 150-m-thick sequence of oxide-facies iron formation.

### **Resource and/or Reserves**

No NI 43-101 compliant mineral resource or reserve estimate available.

Hulstein and Lee (2001) reported on a combined estimate (non 43-101 compliant) of 280 million tons grading 33% Fe for the D’Aigle Bay 1 showing and D’Aigle Bay 2 North and 2 South prospects based on limited data.



## History of Exploration

- 1950: Geological mapping (Neal, 1951)
- 1953: Geological mapping and prospecting (Almond, 1953)
- 1958: mapping, sampling, dip needle, 52 diamond-drill holes, 732 m, (*see* Hulstein and Lee, 2001)
- 1972: Aeromagnetic survey (unpublished IOC report)
- 1979: Ground magnetometer survey, prospecting (Price, 1979b)
- 1982: Airborne geophysical surveys (radiometrics, Johnson, 1982)
- 2000: Data compilation, structural synthesis (Hulstein and Lee, 2001)
- 2001: Data compilation, geological mapping and prospecting, regional airborne magnetic surveys, structural/stratigraphic interpretation (Cotnoir *et al.*, 2002)
- 2003: Geological mapping and prospecting, ground gravity survey (Darch *et al.*, 2003b)
- 2004: Geological mapping and prospecting (Darch, 2004)
- 2010: Diamond drilling (3 drillholes, 491 m, Carter, 2011b)
- 2011: Airborne gravity gradiometer, electromagnetic and magnetic geophysical surveys (Wallace, 2012a)
- 2012: Airborne gravity gradiometer survey (Suave *et al.*, 2012)

## 5. D'AIGLE BAY 2 SOUTH

**Alternate Name:** D'Aigle Bay (LIORC) Property, Tuffy Zone, Tuffy Lake

**MODS Showing(s):** 023G/02/Fe021

**Status:** Prospect

**Structural Basin:** Carol

**UTM Zone:** 19

**NTS Area:** 23G/02

**Northing (NAD27):** 5885323

**Easting (NAD27):** 639216

**Latitude:** 53.1011

**Longitude:** -66.9207

**Object Located:** Drillhole DB-05-05

### Description of Occurrence

The D'Aigle Bay 2 South prospect refers to a large area of oxide-facies iron formation located between Lost Lake and Tuffy Lake (Figure 32), to the west of Wabush Lake and approximately 18 km north of Labrador City. It forms part of a linear band of iron formation that continues to the north of Lost Lake and south of Tuffy Lake for a strike length of more than 6 km. There is no road access to the area, and access is by boat, helicopter or on foot or ATV from the IOC mine area.

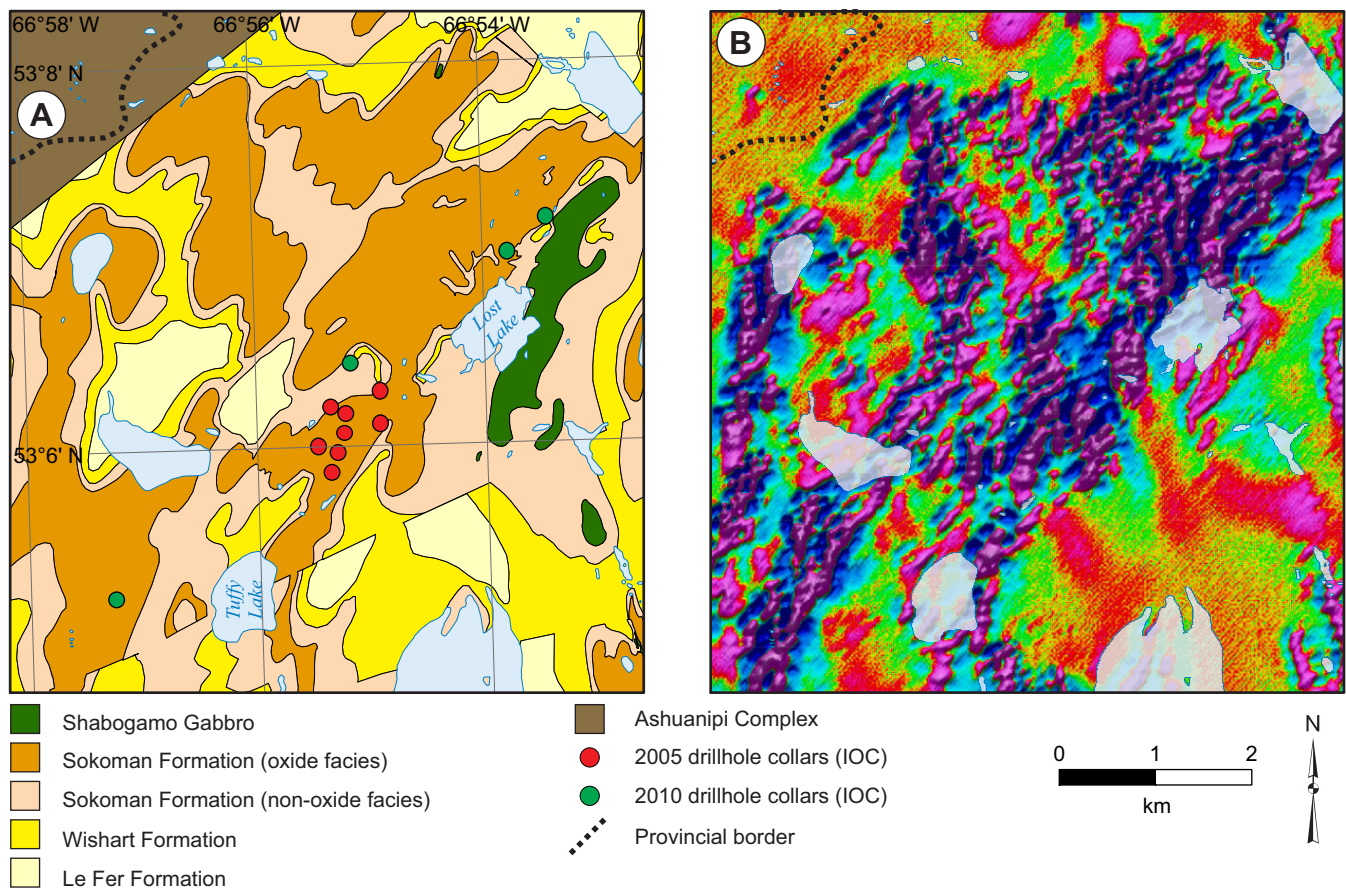


**Figure 32.** A) Geological map of the D'Aigle Bay 2 South prospect (adapted from Cotnoir et al., 2002), showing location of drillholes from 2005 and 2010 exploration programs (Darch, 2005a; Carter, 2011b); B) Airborne magnetics (second vertical derivative) showing extent of iron formation (data from Cotnoir et al., 2002).

## ***Geology and Stratigraphy***

Outcrop at the D'Aigle Bay 2 South prospect is sporadic, but where observed the bedrock geology is dominated by oxide-facies MIF (magnetite and hematite-rich) and carbonate-facies LIF. East of Lost Lake, the LIF is intruded by a Shabogamo Formation gabbro sill (Figure 32), and the Sokoman Formation is underlain by a thin quartzite unit (Wishart Formation) and quartzofeldspathic schists (Le Fer Formation; Rivers and Massey, 1985, and Darch, 2004). To the west, the Sokoman Formation is thrust over the Archean Ashuanipi Complex (van Gool, 1992).

Diamond drilling on the D'Aigle Bay 2 South prospect indicates that the Sokoman Formation consists of alternating intervals of oxide-facies iron formation (magnetite > hematite) and carbonate-facies iron formation, with lesser bands of silicate-facies iron formation (Darch, 2005a). Although the structural complexity of the area is poorly understood, these relationships were interpreted by Darch (2005a) as representing thick sequences of LIF having oxide bands. Drilling results from the north of Lost Lake and south of Tuffy Lake (Carter, 2011b) indicate that the iron formations in these areas also consist of alternating oxide- and carbonate-facies iron formation.

## ***Mineralization***

Oxide-facies iron formation consists predominantly of quartz–magnetite–specularite schist, with magnetite concentrated in bands or as disseminations in lean iron formation (Darch, 2005a). Specular hematite occurs in bands or as coarse-grained segregations associated with quartz-rich areas (Darch, 2005a). Manganese contents are also relatively high (>1% Mn; Darch, 2005a). In outcrop, the oxide-facies iron formation is commonly friable and altered, with carbonate minerals leached out (Darch *et al.*, 2003b). Drilling at the south of the prospect intersected significant thicknesses of altered iron formation to depths of >95 m, with abundant goethite and leaching of carbonate and iron silicate minerals.

Darch (2005a) reported on RMI (rod mill index) determination, minus 200 mesh weight fraction and iron weight recovery values from drillcore samples, which indicate that oxide-facies iron formation is relatively hard (high RMI values) and iron recoveries are low to moderate. Carter (2011b) reported on SAG Power index (SPI) and iron recovery testing (TT) results from 14 composite drillcore samples, with similar results to Darch (2005a).

Although much of the iron formation is low-grade (<30% Fe) and oxide-poor, significant mineralized intervals were recorded in a number of drillholes (Darch, 2005a). Drillhole DB-05-01 from the northern part of the prospect intersected 34.8% Fe over 74 m at 106 m depth (with 1.96% Mn). Higher grades are also associated with strongly altered iron formation from the southern part of the prospect, including 41.2% Fe over 26.7 m at the top of drillhole DB-05-06 and 39.5% Fe over 40.5 m at the top of drillhole DB-05-08.

## ***Structure***

Geological mapping combined with geophysical data show that the Sokoman Formation occupies a series of open synformal dominated folds, which dip shallowly to the east (10 to 30°) and plunge shallowly to the south (Darch *et al.*, 2003b).

Two generations of faulting have been recognized. The earliest faults recognized in the D'Aigle Bay area are northwest–southeast-trending faults with a dextral offset, which divide the area into a number of tectonic blocks, separating the D'Aigle Bay 2 North and South prospects (Darch *et al.*, 2003b). A second set of faults trend northeast–southwest and have been observed to truncate the earlier northwest–southeast fault set (Darch *et al.*, 2003b). The northwest–southeast fault set, mark the northern and southern boundaries of the D'Aigle Bay 2 North and South prospects, and are interpreted to be thrust faults associated with the Grenville orogeny (Darch *et al.*, 2003b).

## ***Geophysics***

Regional aeromagnetic data show that the D'Aigle Bay 2 South prospect is coincident with a broad magnetic anomaly (Figure 32; Cotnoir *et al.*, 2002), which is due to the high magnetite content of much of the iron formation. Darch *et al.* (2003b) reported that reconnaissance style gravity surveys indicate a broad, low-amplitude gravity anomaly over the D'Aigle Bay 2 South prospect, which was interpreted as representing a 100- to 150-m-thick sequence of oxide-facies iron formation.



### **Resource and/or Reserves**

No NI 43-101 compliant mineral resource or reserve estimate available.

Hulstein and Lee (2001) reported on a combined estimate of 280 million tons grading 33% Fe for the D'Aigle Bay 1 showing and D'Aigle Bay 2 North and 2 South prospects based on limited data.

### **History of Exploration**

- 1950: Geological mapping (Neal, 1951)
- 1953: Geological mapping and prospecting (Almond, 1953)
- 1957: Geological mapping and prospecting (Crouse, 1957)
- 1958: mapping, sampling, dip needle, 52 diamond-drill holes, 732 m, (*see* Hulstein and Lee, 2001)
- 1972: Aeromagnetic survey (unpublished IOC report)
- 1979: Ground magnetometer survey, prospecting (Price, 1979b)
- 1982: Airborne geophysical surveys (radiometrics, Johnson, 1982)
- 1985: Magnetic surveys and geological mapping (Simpson *et al.*, 1985)
- 2000: Data compilation, structural synthesis (Hulstein and Lee, 2001)
- 2001: Data compilation, geological mapping and prospecting, regional airborne magnetic surveys, structural/stratigraphic interpretation (Cotnoir *et al.*, 2002)
- 2003: Geological mapping and prospecting, ground gravity survey (Darch *et al.*, 2003b)
- 2004: Geological mapping and prospecting (Darch, 2004)
- 2005: Diamond drilling at D'Aigle Bay 2 South (8 drillholes, 1128 m, Darch, 2005a)
- 2010: Diamond drilling at D'Aigle Bay 2 South (1 drillhole, 189 m), as well as north of Lost Lake (2 drillholes, 298 m) and west of Tuffy Lake (1 drillhole, 144 m, Carter, 2011b)
- 2011: Airborne gravity gradiometer, electromagnetic and magnetic geophysical surveys (Wallace, 2012a)
- 2012: Airborne gravity gradiometer survey (Suave *et al.*, 2012)

## 6. DULEY

**Alternate Name:** Duley No. 2, Long Lake

**MODS Showing(s):** 023B/15/Fe008

**Status:** Prospect

**Structural Basin:** Wabush

**UTM Zone:** 19

**NTS Area:** 23B/15

**Northing (NAD27):** 5860313

**Easting (NAD27):** 635012

**Latitude:** 52.8775

**Longitude:** -66.9939

**Object Located:** Drillhole DU-10-02

### Description of Occurrence

The Duley prospect is located on the western shore of Long Lake (also known as Duley Lake), approximately 5 km south of Labrador City. The prospect extends for more than 2 km south of Long Lake (Figure 33), and is located along strike from the Scully deposit to the north and the Rose deposit to the south. Access is by a secondary road off the TLH (access to Duley Provincial Park and campsite), and by a series of gravel roads.

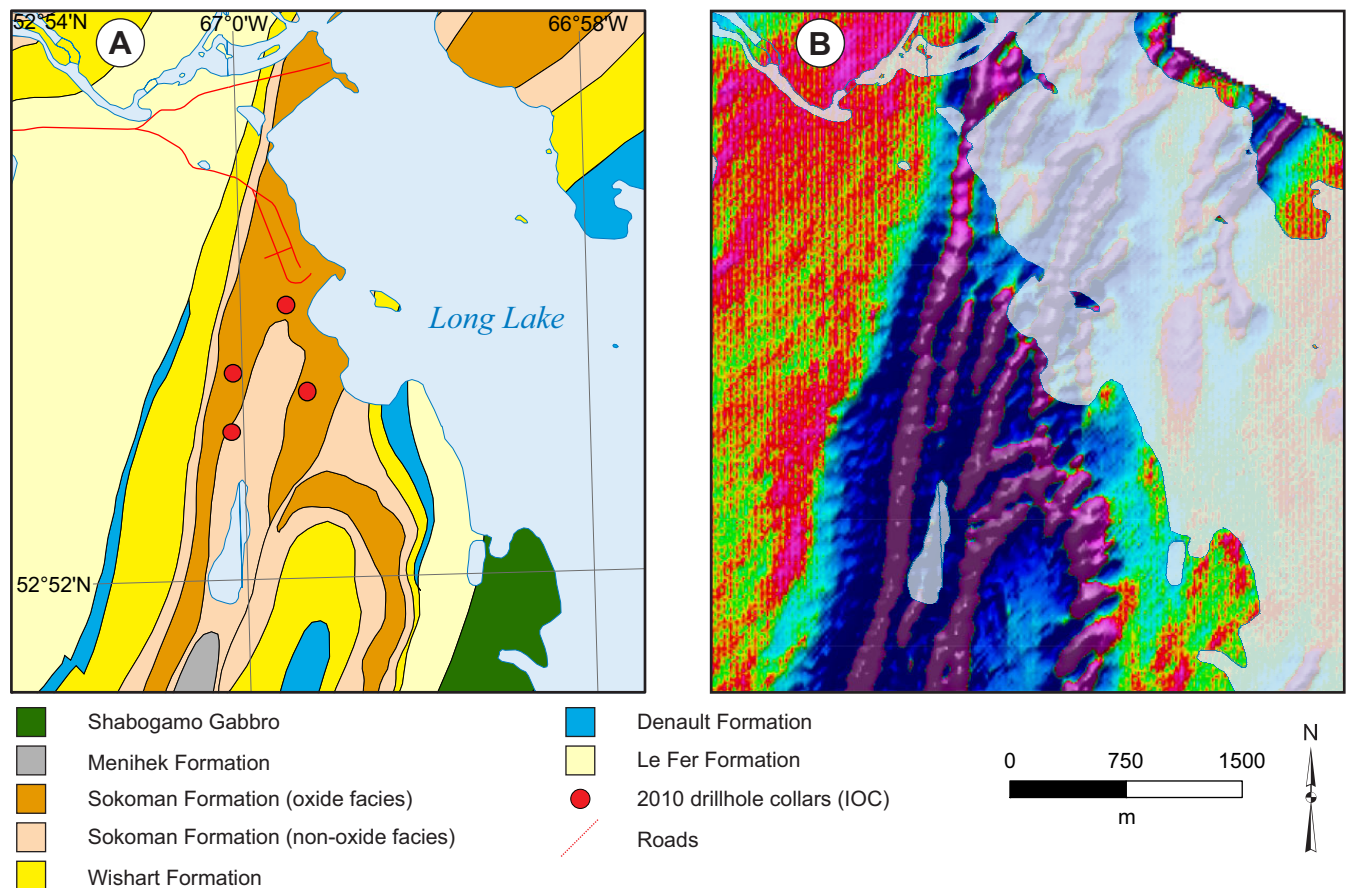


**Figure 33.** A) Geological map of the Duley prospect (adapted from Cotnoir et al., 2002), showing location of drillholes from 2010 exploration programs (Carter, 2011c); B) Airborne magnetics (second vertical derivative) showing extent of iron formation (data from Cotnoir et al., 2002).

## ***Geology and Stratigraphy***

The Duley prospect is hosted within a synclinal structure, which preserves a full sequence of the Kaniapiskau Supergroup (Figure 33). The Menihék Formation is located in the core of the syncline to the south of the Duley prospect, and overlies a thick sequence of Sokoman Formation iron formation. Wishart Formation quartzite outcrops on high ridges to the east and west of the iron formation, and is underlain by dolomites of the Denault Formation and schists of the Le Fer Formation. A number of thin (<10 m) gabbro sills intrude into the Sokoman Formation.

The stratigraphy of the Sokoman Formation was examined in detail in drillhole DU-10-03. There is good lateral continuity between the stratigraphy recorded in the Rose deposit along strike to the south of the Duley prospect. The drillhole collars in altered oxide-facies iron formation, which transitions into less-altered oxide-facies iron formation with high magnetite content (magnetite >> hematite) and numerous carbonate- and Fe-silicate-rich bands. This sequence correlates with RC3 at the Rose deposit. This is followed by interlayered magnetite-rich and hematite-rich oxide-facies iron formation (Plate 32A) from ~55 to 110 m (RC2 at Rose deposit). From 110 to 144.3 m, the oxide-facies iron formation occurs as a quartz–specularite schist (Plate 32B, C) with hematite >> magnetite and high Mn-content in places (up to 6.45 wt. % from 112 to 116 m; Carter, 2011c), which correlates to the lower RC1 member at the Rose Deposit. The base of the Sokoman Formation is marked by 3 m of silicate-facies iron formation with abundant garnet (Plate 32D, E), which is similar to the basal silicate iron formation recorded at both the Rose deposit and the Scully deposit.

## ***Mineralization***

The proportion of iron-oxides in oxide-facies iron formation at the Duley prospect is highly variable, with magnetite-rich and hematite-rich iron formation recorded throughout. The mineralization in drillhole DU-10-03 is similar to the central part of the Rose deposit, with an upper magnetite-rich unit, middle magnetite–hematite unit and lower hematite-rich unit. Although alteration is generally weak, moderate to strong alteration is recorded over the upper 10–20 m of the drillcore. Manganese content is generally high (average 1.43% Mn; Carter, 2011c).

Hulstein and Lee (2001) reported on metallurgical testwork carried out in 1958, which reported that the quartz–magnetite ore may be amenable to magnetic separation. In 2010, 24 composite drillcore samples were sent for SAG Power index (SPI) and iron recovery testing (TT), which showed that the oxide-facies iron formation is relatively hard (high SPI) and has moderate iron recovery values (Carter, 2011c).

Assay results from the Duley prospect have shown significant thicknesses of mineralized iron formation, with the highlights including 31.7% Fe over 150.2 m in drillhole DU-10-02 (92.3 to 250.5 m), 32.3% Fe over 51 m in drillhole DU-10-03 (68 to 119 m) and 33.4% Fe over 44 m in drillhole DU-10-04 (181 to 225 m).

## ***Structure***

Geological mapping indicates that the Duley prospect is located in a series of north–south-trending, west-verging synclines and anticlines (Cotnoir *et al.*, 2002). At least two generations of folding have been recorded, southeast-trending F<sub>1</sub> folds with shallow plunges and south- to southwest-trending F<sub>2</sub> folds that plunge to the south at 10–28° (Plate 32F), and structural thickening may have occurred (Cotnoir *et al.*, 2002).

## ***Geophysics***

Regional aeromagnetic surveys have shown that the Duley prospect is located in a prominent magnetic high (Figure 33, Cotnoir *et al.*, 2002), and lies within a magnetic anomaly that continues along strike for >12 km with the Scully deposit to the north and the Rose deposit to the south. Ground gravity surveys show that the Duley prospect coincides with a moderate gravity anomaly, consistent with the presence of buried masses of iron formation (Clark and Tshimbalanga, 2006).

## **Resource and/or Reserves**

No NI 43-101 compliant mineral resource or reserve estimate available.



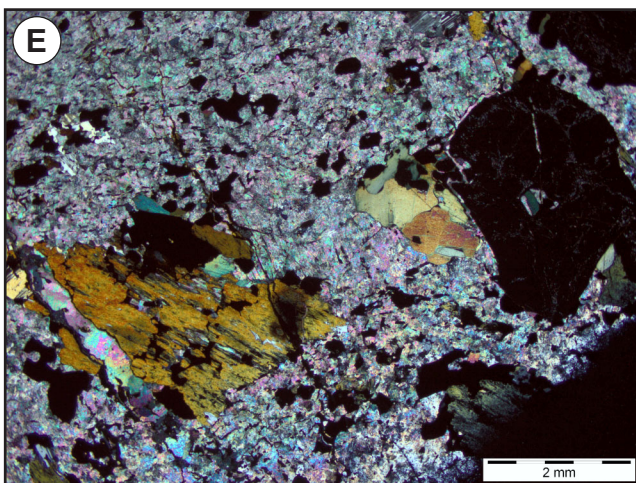
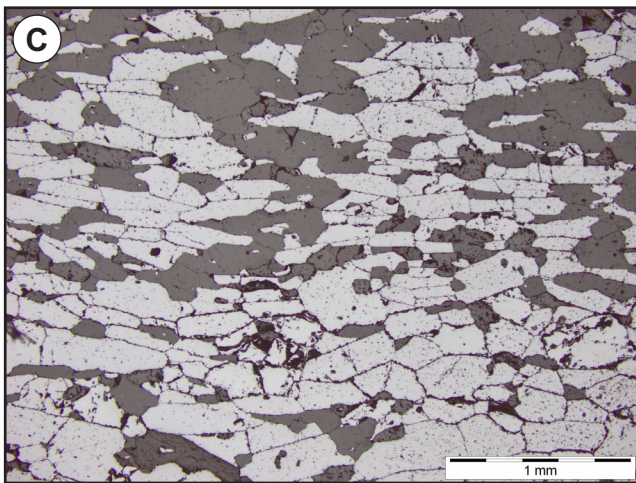
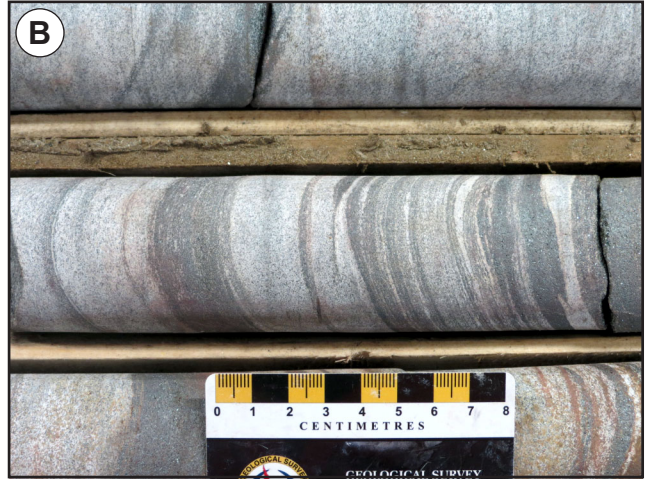


**Plate 32.** A) Interlayered magnetite-rich and hematite-rich oxide-facies iron formation, correlating with RC2 at the Rose deposit (drillhole DU-10-03 @ 84.5 m); B) Quartz-specularite schist correlating with RC1 at the Rose deposit (drillhole DU-10-03 @ 131.7 m); C) Photomicrograph of quartz-specularite schist (drillhole DU-10-03 @ 131.7 m, reflected light); D) Basal silicate iron formation with abundant garnet (drillhole DU-10-03 @ 146.9 m); E) Photomicrograph of garnet-bearing basal silicate iron formation (drillhole DU-10-03 @ 147 m, cross-polarized light); F) Probable  $F_2$  folding in the Sokoman Formation, located on the eastern limb of the syncline (view looking south).



Non 43-101 compliant historical estimates based on limited data range from 147.9 to 162 Mt grading 27% Fe (Hulstein and Lee, 2001).

### **History of Exploration**

- 1949: Geological mapping (Neal, 1950a)
- 1953: Geological mapping and prospecting (Crouse, 1954)
- 1957: Diamond drilling (29 drillholes, 1492 m) and geological mapping (Mathieson, 1957a)
- 1959: Geological mapping, magnetometer survey (Nicheri, 1959), ground gravity survey (described in Hulstein and Lee, 2001)
- 1972: Aeromagnetic survey (unpublished IOC report)
- 1978: Geochemical sampling and ground magnetometer survey (Stubbins, 1978b, c)
- 1980: Ground magnetometer survey on Long Lake (Grant, 1980a, b)
- 1982: Airborne geophysical surveys (radiometrics) (Johnson, 1982)
- 1985: Diamond drilling on Long Lake (2 drillholes, 74 m, Simpson *et al.*, 1985)
- 2000: Data compilation, structural synthesis (Hulstein and Lee, 2001)
- 2001: Data compilation, geological mapping and prospecting, ground gravity survey, regional airborne magnetic surveys, structural/stratigraphic interpretation (Cotnoir *et al.*, 2002)
- 2004: Geological mapping and prospecting (Darch, 2004)
- 2005: Ground gravity survey (Clark and Tshimbalanga, 2006)
- 2010: Diamond drilling (4 drillholes, 867 m, Carter, 2011c)

## 7. EMMA LAKE

**Alternate Name:** Emma Lake Southwest, Lac Virot Property

**MODS Showing(s):** 023G/03/Fe002

**Status:** Showing

**Structural Basin:** n/a

**UTM Zone:** 19

**NTS Area:** 23G/03

**Northing (NAD27):** 5875103

**Easting (NAD27):** 628766

**Latitude:** 53.0119

**Longitude:** -67.0808

**Object Located:** Drillhole LV-018

### Description of Occurrence

The Emma Lake showing is located south of Emma Lake (Figure 34), approximately 13.5 km northwest of Labrador City. Access to the showing is by helicopter, no roads or trails enter the area.

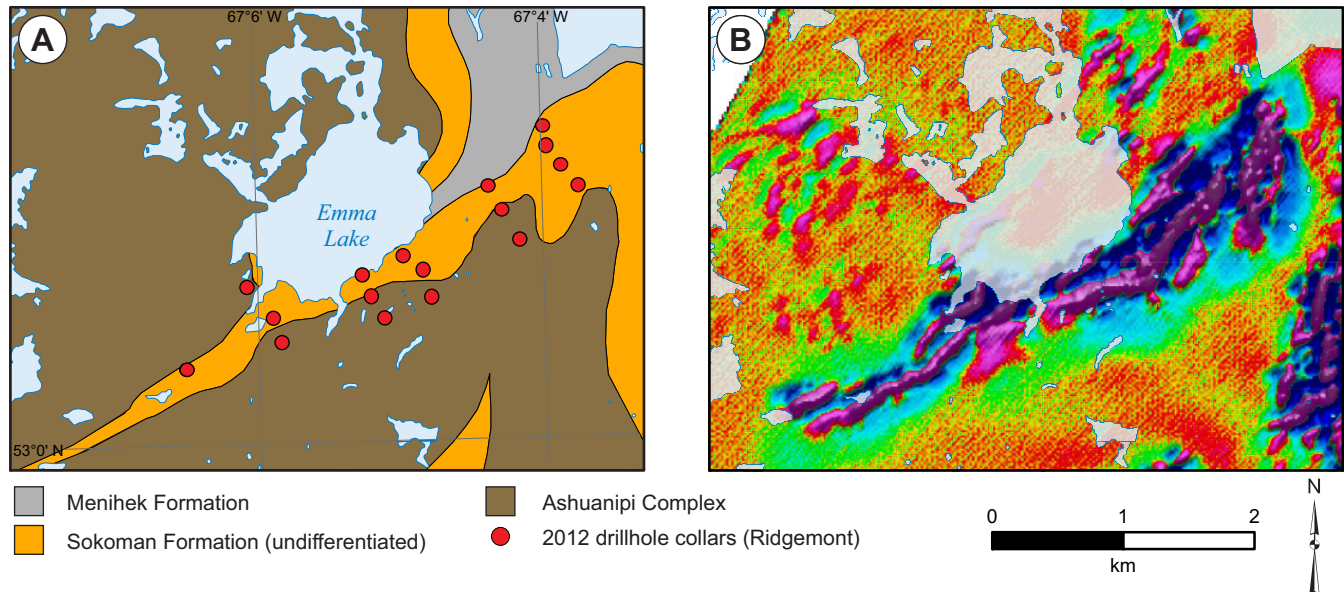


**Figure 34.** A) Geological map of the Emma Lake showing (adapted from Cotnoir et al., 2002), showing location of drillholes from 2012 exploration programs (Steele, 2013); B) Airborne magnetics (second vertical derivative) showing extent of iron formation (data from Cotnoir et al., 2002).

### Geology and Stratigraphy

The basement rocks of the Ashuanipi Complex are dominant in the area to the southwest of Emma Lake (Figure 34), with the proportion of cover rocks increasing to the northeast (Brown *et al.*, 1991). The basement rocks are predominantly composed of granulite-facies migmatite, gneiss and granitoid rocks. They are unconformably overlain by the Sokoman Formation iron formation, which is, in turn, overlain by schists of the Menihek Formation. No Wishart Formation quartzites are recorded in the Emma Lake area.

The Sokoman Formation was intercepted in 16 of the 18 drillholes in the Emma Lake area (Steele, 2013). It occurs either as thin (<20 m) thrust sheets interleaved with basement rocks or as thick sequences (>150 m) having sharp to gradational contacts with the overlying Menihek Formation and underlying basement rocks (Steele, 2013). The iron formation consists of carbon-

ate-, silicate- and oxide-facies iron formation in varying proportions. However, the stratigraphy of the iron formation is difficult to determine because of its structural complexity and probable repetition due to thrust stacking and folding.

### ***Mineralization***

Oxide-facies iron formation consists primarily of magnetite and quartz, and lesser coarse-grained specular hematite. Oxide-facies iron formation is commonly interbedded with silicate- and carbonate-facies iron formation. Intervals of ore-grade (>30% Fe) oxide-facies iron formation are generally <10 m thick, but thicker sequences up to 36 m have been recorded in some drillholes (e.g., LV-012, LV-024, LV-025, LV-028).

There is no published metallurgical testwork available from the Emma Lake showing.

The best assay results correspond to the thickest oxide-facies intervals in drillholes LV-012 (28.6% Fe over 27.7 m at 303.2 m depth), LV-024 (30.6% Fe over 35.9 m at 286 m depth), LV-025 (30.2% Fe over 21 m at 117 m depth) and LV-028 (31.4% Fe over 29.9 m at 146.9 m depth).

### ***Structure***

The structural geology of the Emma Lake area is complex and has been described in detail by Brown *et al.* (1991) and van Gool (1992). The basement and cover rocks form an imbricated stack of fold nappes, which repeat the stratigraphy several times. Two generations of thrusting have been recorded and consist of regular-sequence thrusts that developed under ductile conditions resulting in the thrusting of basement rocks over cover rocks, and out of sequence thrusts that occurred under brittle-ductile conditions and were responsible for the thrusting of cover rocks over the basement (Brown *et al.*, 1991; van Gool, 1992).

### ***Geophysics***

The Emma Lake showing coincides with a prominent aeromagnetic anomaly (Figure 34; Cotnoir *et al.*, 2002; Coates *et al.*, 2011). Ground gravity surveys have also recognized a large gravity anomaly south of Emma Lake (Steele, 2012).

### **Resource and/or Reserves**

No NI 43-101 compliant mineral resource or reserve estimate available.

### **History of Exploration**

- 1950: Geological mapping (Neal, 1951)
- 1953: Geological mapping (Jackson, 1954)
- 1957: Geological mapping and prospecting (Jury, 1957)
- 1979: Prospecting (Grant, 1979b)
- 1982: Airborne geophysical surveys (EM, magnetics, radiometrics, Johnson, 1982)
- 1985: Ground radiometric survey (Simpson *et al.*, 1985)
- 2001: Regional airborne magnetic surveys (Cotnoir *et al.*, 2002)
- 2011: Airborne magnetic, radiometric and VLF-EM survey, geological mapping and prospecting (Coates *et al.*, 2011)
- 2012: Airborne gravity gradiometer survey (Steele, 2012), diamond drilling (18 drillholes, 5978.7 m, Steele, 2013)



## 8. FLATROCK LAKE

**Alternate Name:** Bruce Lake  
**MODS Showing(s):** 023G/02/Fe026  
**Status:** Showing  
**Structural Basin:** n/a  
**UTM Zone:** 19  
**NTS Area:** 23G/02  
**Northing (NAD27):** 5898808  
**Easting (NAD27):** 642953  
**Latitude:** 53.2213  
**Longitude:** -66.8588  
**Object Located:** Drillhole 10LB0015

### Description of Occurrence

The Flatrock Lake showing is located to the south of Flatrock Lake (Figure 35), approximately 32 km north of Labrador City, and is accessible by helicopter or float plane.

### Geology and Stratigraphy

The geology of the Flatrock Lake/Bruce Lake area is predominantly a thin (<200 m) package of cover rocks that overlie Archean basement rocks of the Ashuanipi Complex (van Gool *et al.*, 2008). Geological mapping in the area has shown that the

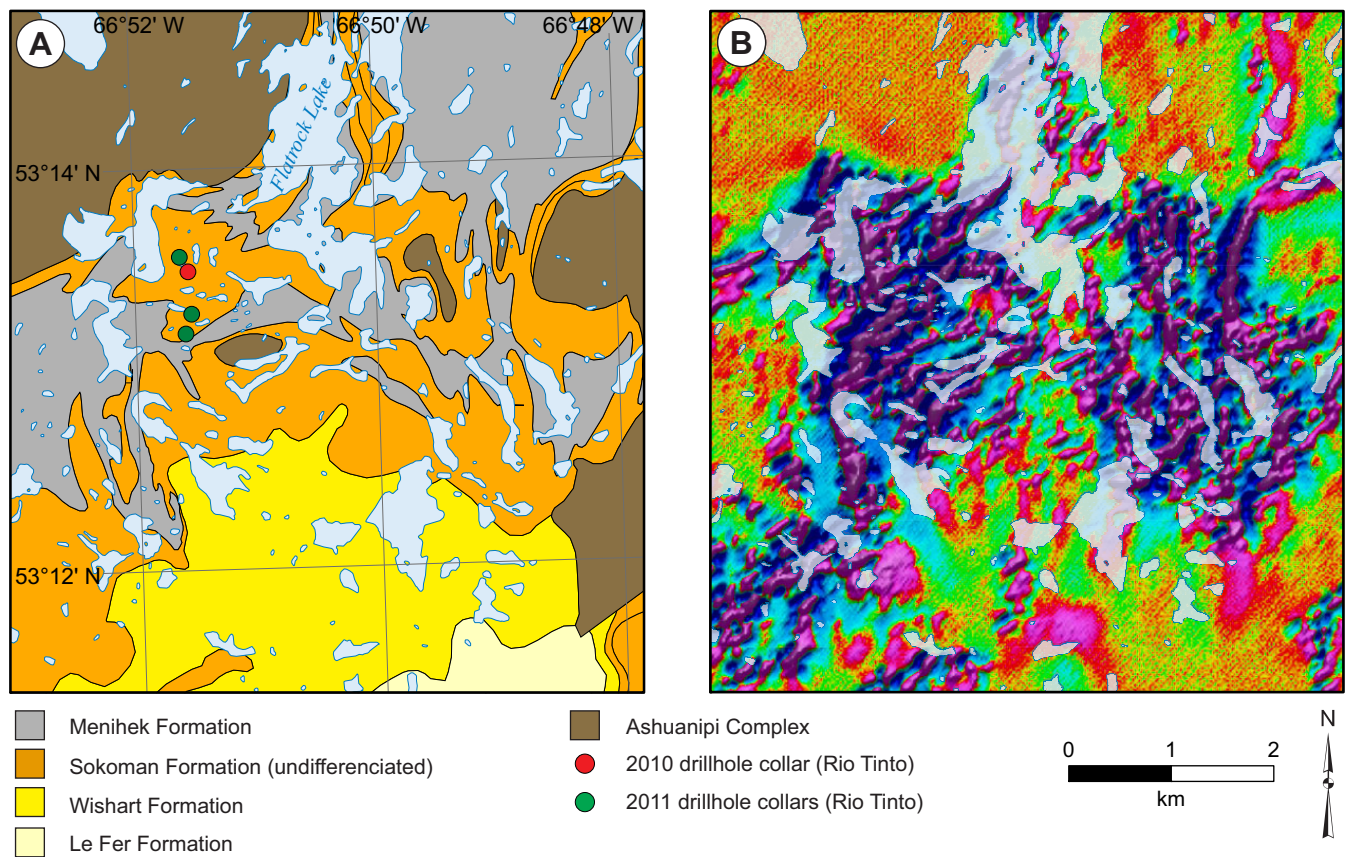


**Figure 35.** A) Geological map of the Flatrock Lake area (adapted from Cotnoir *et al.*, 2002), showing location of drillholes from 2010 and 2011 drilling programs (Hovis and Goldner, 2011b, 2012); B) Airborne magnetics (second vertical derivative) showing extent of iron formation (data from Cotnoir *et al.*, 2002).

cover rocks consist of Sokoman Formation (primarily of carbonate- and oxide-facies iron formation; van Gool *et al.*, 1987), which is stratigraphically overlain by fine-grained phyllite of the Menihek Formation.

Diamond drilling in the area south of Flatrock Lake targeted coincident gravity and magnetic anomalies (Hovis and Goldner, 2011b, 2012). Although all drillholes intercepted iron formation, the oxide-facies iron formation was shown to be relatively thin and anastomosing in nature (Hovis and Goldner, 2012), with maximum thicknesses of 25 m at 30.7% Fe (drillhole 10LB0013) and 22.4 m at 32.9% Fe (drillhole 10LB0015). The Sokoman Formation is structurally underlain by Menihek Formation graphitic schists indicating that the sequence was overturned, and oxide-facies iron formation occur close to the contact between the Sokoman and Menihek formations.

### ***Mineralization***

The Sokoman Formation is banded on a cm to m scale, and contacts between oxide- and carbonate-facies are generally gradational. The oxide-facies iron formation consists primarily of iron oxides (hematite, magnetite), quartz and carbonate and minor iron silicates and Mn carbonates. Magnetite and hematite generally make up 30–40% of the oxide facies, and when magnetite content is high, hematite content is generally low, and vice versa. The carbonate-facies iron formation consists predominantly of iron carbonates and quartz, with lesser magnetite, hematite, iron-silicates and garnet. Cm-scale siderite porphyroblasts are common in the carbonate bands.

There is no published metallurgical testwork available from the Flatrock Lake showing.

The best assay results are from drillhole 10LB0013 (30.7% Fe over 24 m at 25.5 m depth) and drillhole 10LB0015 (32.9% Fe over 22.5 m at 121 m depth).

### ***Structure***

The Flatrock Lake and Bruce Lake areas occur within the Flatrock Lake Thrust Sheet, and the structure of the area has been described in detail by van Gool (1992) and van Gool *et al.* (2008). The Flatrock Lake Thrust Sheet consists of a stack of thin thrust slices that repeat the stratigraphy (van Gool, 1992). These thrust slices interleave with thin sheets of basement rocks, and are strongly folded with common fold nappes. Diamond drilling indicates that the cover rocks are commonly overturned.

### ***Geophysics***

Regional airborne magnetic surveys (Cotnoir *et al.*, 2002) have shown a large magnetic anomaly to the south of Flatrock Lake (Figure 35), and geological mapping has shown that this anomaly coincides with abundant iron formation.

Ground gravity surveys have identified a significant gravity anomaly south of Flatrock Lake targeted by a number of diamond-drill holes (Hovis and Goldner, 2012). These drillholes failed to intercept significant oxide mineralization, and the reason for this gravity anomaly is unexplained.

### **Resource and/or Reserves**

No NI 43-101 compliant mineral resource or reserve estimate available.

### **History of Exploration**

- 1950: Geological mapping (Neal, 1951)
- 1956: Geological mapping and prospecting (Eckstrand, 1956)
- 1959: Geological mapping (Love, 1959)
- 1982: Airborne geophysical surveys (EM, magnetics, radiometrics, Johnson, 1982) ground geophysics, geological mapping and prospecting (Simpson and Bird, 1982)
- 2001: Regional airborne magnetic surveys (Cotnoir *et al.*, 2002)
- 2008: Geological mapping and prospecting, gravity surveys (Reynolds and Mitchell, 2008)

- 2009: Geological mapping and prospecting (Downing, 2010)
- 2010: Diamond drilling (3 drillholes, 415 m), geological mapping and prospecting, ground gravity survey (Hovis and Goldner, 2011b)
- 2011: Diamond drilling (1 drillhole, 357 m), geological mapping and prospecting, ground gravity survey (Hovis and Goldner, 2012), magnetic and electromagnetic airborne survey (Smith *et al.*, 2012)
- 2012: Airborne gravity gradiometer survey (Suave *et al.*, 2012)
- 2013: Mineralogical testwork (Sauve, 2014)



## 9. GOETHITE BAY

**Alternate Name:** Gregory River Northeast, Goethite Bay North, Goethite Bay

**MODS Showing(s):** 023G/02/Fe015, 023G/02/Fe016, 023G/02/Fe041

**Status:** Prospect

**Structural Basin:** Carol

**UTM Zone:** 19

**NTS Area:** 23G/02

**Northing (NAD27):** 5896291

**Easting (NAD27):** 651250

**Latitude:** 53.1943

**Longitude:** -66.7366

**Object Located:** Drillhole 12LB0055

### Description of Occurrence

The Goethite Bay prospect is located between Goethite Bay to the east and Gregory Lake to the west (Figure 36), approximately 30 km north of Labrador City. Access to the area is by helicopter, or by boat from Goethite Bay.

### Geology and Stratigraphy

The Goethite Bay area is dominated by the Sokoman Formation (Figure 36), which stratigraphically overlies quartzite of the Wishart Formation. Outcrops of Shabogamo Gabbro are located to the north and east of the prospect, and are believed to

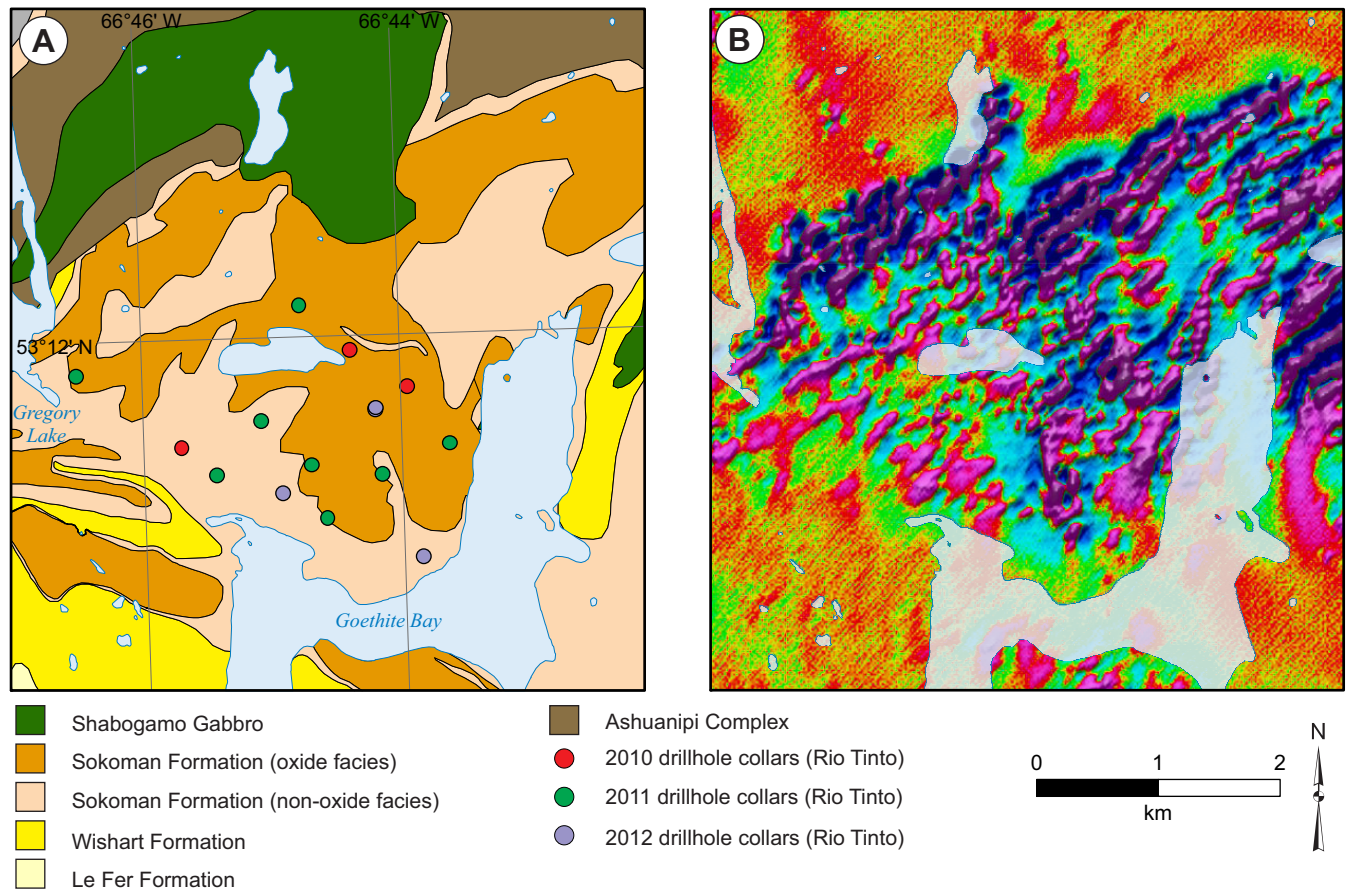


**Figure 36.** A) Geological map of the Goethite Bay area (adapted from Cotnoir et al., 2002), showing location of drillholes from 2010, 2011 and 2012 drilling programs (Hovis and Goldner, 2011b; 2012; Goldner et al., 2013); B) Airborne magnetics (second vertical derivative) showing extent of iron formation (data from Cotnoir et al., 2002).

have intruded the lower part of the Sokoman Formation and the Wishart Formation. The northern boundary of the prospect is marked by a thrust fault, which separates cover rocks of the Kaniapiskau Supergroup to the south from quartzofeldspathic gneisses to the north. The gneisses were originally mapped as part of the Le Fer Formation (Rivers and Massey, 1985), but were reinterpreted as representing basement rocks of the Ashuanipi Complex by van Gool (1992).

There has been extensive diamond drilling in the Goethite Bay area (17 drillholes, 3918 m; Hovis and Goldner, 2011b, 2012; Goldner *et al.*, 2013), and all drillholes have intersected Sokoman Formation iron formation. However, stratigraphic correlations between the drillholes are difficult due to moderate to strong alteration and structural complexity. All facies of the Sokoman Formation (oxide, silicate and carbonate) have been recognized, but the carbonate and silicate minerals are commonly altered and replaced with abundant secondary goethite. Within diamond-drill holes that intersect Wishart Formation quartzites, the lower 50–100 m of the iron formation is dominantly goethite-rich iron formation, and interpreted as strongly altered carbonate- and silicate-facies iron formation (LIF).

### ***Mineralization***

The oxide-facies iron formation is commonly strongly to moderately altered, with hematite >> magnetite and abundant secondary goethite. Weakly altered oxide-facies iron formation, intersected in drillhole 11LB0038 from the northern portion of the Goethite Bay prospect, occur as well-banded material having hematite- and magnetite-rich members. Manganese concentration is generally low (<0.2 % Mn), but occurrences of secondary pyrolusite associated with altered iron formation are associated with higher Mn concentrations in places (up to 1% Mn; Hovis and Goldner, 2011b, 2012; Goldner *et al.*, 2013).

Metallurgical test results from composite drillcore samples show that a moderate- to high-grade concentrate can be achieved by Heavy Liquid Separation and Davis Tube Recovery, but weight and iron recoveries were low (Goldner *et al.*, 2013). However, these data are only preliminary, and may not be representative of the entire prospect.

Assay data from diamond-drill holes show significant thicknesses of oxide-facies iron formation in some areas. Highlights include 31.9% Fe over 157.3 m at 56.3 m depth (drillhole 11LB0027); 32.76% Fe over 70.2 m at 11.1 m depth (drillhole 12LB0048); 30.0% Fe over 191 m at 56.9 m depth (drillhole 12LB0045), and 30.3% Fe over 71.1 m at 42.9 m depth (drillhole 12LB0055). However, these iron contents are due, in part, to enrichment in goethite in altered oxide-facies iron formation.

### ***Structure***

Structural interpretations of the Goethite Bay prospect are hampered because of its structural complexity, strong alteration encountered in many drillholes, and the lack of recognizable marker horizons. However, Goldner *et al.* (2013) reported abundant micro and macro folding in drillcore, suggesting that the Sokoman Formation was intensely folded. In addition, van Gool (1992) indicated that the Goethite Bay prospect was located in an imbricated thrust sheet, with multiple interleaved sequences of Sokoman and Wishart formations.

Late-stage alteration in the Goethite Bay area is likely associated with meteoric fluid flow along northwest-trending faults, with a similar orientation to the Julienne Lake Fault Zone, located ~5 km southeast of the Goethite Bay prospect.

### ***Geophysics***

The Goethite Bay area is characterized by a strong magnetic response on regional airborne magnetic surveys (Figure 36; Cotnoir *et al.*, 2002). This response corresponds to the presence of oxide-facies iron formation in outcrop and in diamond-drill holes. Areas with lower magnetic responses may correspond to non-oxide iron formation or altered-oxide iron formation where magnetite has been replaced by hematite.

Ground gravity surveys have identified a number of anomalies in the Goethite Bay area that have been tested by diamond drilling and were shown not to correspond with oxide-facies iron formation (Hovis and Goldner, 2011b, 2012).

### **Resource and/or Reserves**

No NI 43-101 compliant mineral resource or reserve estimate available.

## History of Exploration

- 1950: Geological mapping (Neal, 1951)
- 1952: Geological mapping and prospecting (Beemer, 1952)
- 1953: Geological mapping and prospecting (Almond, 1953)
- 1959: Gravity survey (Grimaldi, 1959b)
- 1960: Diamond drilling (4 drillholes, 117 m, Bruneau, 1960)
- 1979: Ground magnetometer survey and prospecting (Price, 1979c); prospecting (Grant, 1979c)
- 1982: Soil geochemistry (Simpson and Bird, 1982), airborne geophysical surveys (EM, magnetics, radiometrics, Johnson, 1982)
- 2001: Regional airborne magnetic surveys (Cotnoir *et al.*, 2002)
- 2008: Geological mapping and prospecting, gravity surveys (Reynolds and Mitchell, 2008)
- 2009: Geological mapping and prospecting (Downing, 2010)
- 2010: Diamond drilling (4 drillholes, 524 m), geological mapping and prospecting, ground gravity survey (Hovis and Goldner, 2011b)
- 2011: Diamond drilling (8 drillholes, 2276 m, Hovis and Goldner, 2012), magnetic and electromagnetic airborne survey (Smith *et al.*, 2012)
- 2012: Diamond drilling (5 drillholes, 1118 m), LiDAR survey, preliminary metallurgical testwork (Goldner *et al.*, 2013); Airborne gravity gradiometer survey (Sauve *et al.*, 2012)
- 2013: Mineralogical testwork (Sauve, 2014)

## 10. GOETHITE BAY NORTH

**Alternate Name:** Birch Hill

**MODS Showing(s):** n/a

**Status:** Showing

**Structural Basin:** Carol

**UTM Zone:** 19

**NTS Area:** 23G/02

**Northing (NAD27):** 5898086

**Easting (NAD27):** 655898

**Latitude:** 53.2106

**Longitude:** -66.6656

**Object Located:** Drillhole 10LB0011

### Description of Occurrence

The Goethite Bay North showing is located between Goethite Bay and Northwest Arm (Figure 37), to the north of Julienne Lake and approximately 35 km north-northeast of Labrador City. Access to the area is by helicopter, or by boat from Goethite Bay or Northwest Arm.

### Geology and Stratigraphy

The Goethite Bay North area is similar to the Goethite Bay area to the southwest, with common outcrops of carbonate- and oxide-facies Sokoman Formation iron formation in the vicinity of the occurrence, and outcrops of Shabogamo Gabbro located

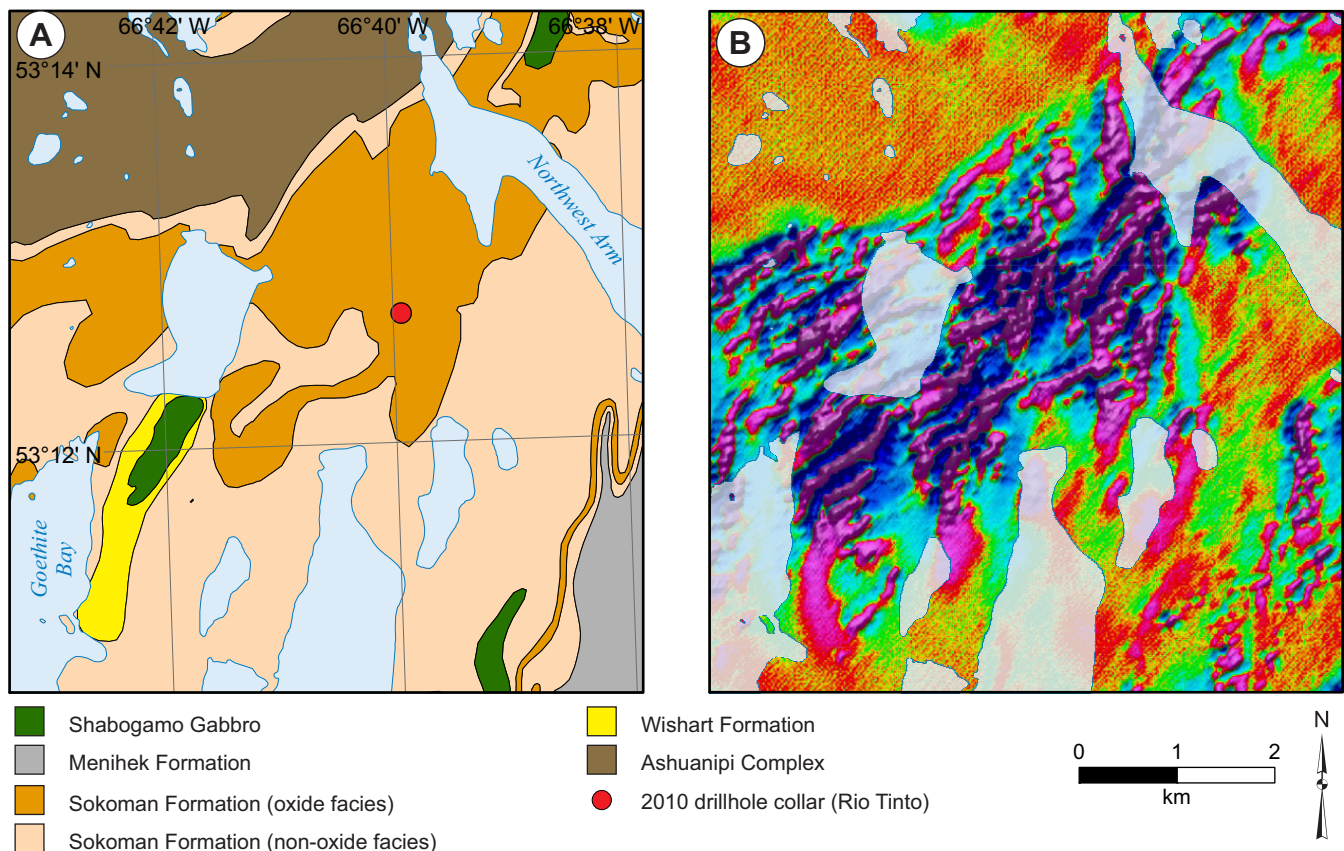


**Figure 37.** A) Geological map of the Goethite Bay North area (adapted from Cotnoir et al., 2002), showing location of drillhole 10LB0011 from 2010 drilling program (Hovis and Broadbent, 2010); B) Airborne magnetics (second vertical derivative) showing extent of iron formation (data from Cotnoir et al., 2002).



to the south of the main occurrence. The Sokoman Formation is stratigraphically underlain by the Wishart Formation, which outcrops on the western shores of Goethite Bay. The northern boundary of the showing is marked by a thrust fault separating rocks of the Kaniapiskau Supergroup from the underlying basement rocks of the Ashuanipi Complex.

The stratigraphy of the Sokoman Formation in the area is poorly understood, and information on the distribution of oxide-, silicate- and carbonate-facies iron formation is based on a single diamond-drillhole core (Hovis and Broadbent, 2010). From 11 to 96.33 m, the drillhole intersected mixed silicate- and oxide-facies iron formation, with oxide-facies iron formation dominant from 12.76 to 44.77 m and silicate-facies iron formation the dominant lithology in the rest of the interval. This may represent the UIF recorded in the Carol Lake area (Muwais, 1974). This is followed by oxide-facies iron formation to 163.56 m interpreted to represent the MIF. From 163.65 to 201 m (EOH) carbonate-facies iron formation predominates, which may represent the LIF of Muwais (1974). These interpretations assume that the sequence is not folded or repeated by thrusting.

### ***Mineralization***

The oxide-facies iron formation is generally lean, with <40% iron oxides (drillhole 10LB0011; Hovis and Broadbent, 2010). The upper sequence of oxide-facies iron is magnetite dominated, with only minor hematite, whereas the lower sequence has ~20% hematite and ~10% magnetite (Hovis and Broadbent, 2010).

There is no published metallurgical testwork available from the Goethite Bay North showing.

Iron grades are generally <30% Fe, with the best intersections from 18.5 to 28 m (28% Fe over 9.5 m) and from 122.5 to 160 m (27.5% Fe over 37.5 m) in drillhole 10LB0011.

### ***Structure***

Although there have not been any detailed structural studies at the Goethite Bay North showing itself, regional-scale mapping studies (van Gool, 1992) indicate that the area between Goethite Bay and Northwest Arm is located in the Goethite Bay thrust sheet, and likely has had a similar structural history as the nearby Goethite Bay prospect. However, the iron formation at the showing is generally unaltered, indicating that late-stage fluid infiltration along northwest-trending faults was not important in this area.

### ***Geophysics***

The area between Goethite Bay and Northwest Arm is characterized by a strong magnetic high on regional magnetic data (Figure 37), which corresponds to the mapped oxide-facies iron formation. Drillhole 10LB0011 targeted a gravity anomaly on the property, which was identified during fieldwork in 2008. However, no rocks thought to be capable of generating a gravity high were intersected in this drillcore (Hovis and Broadbent, 2010).

### **Resource and/or Reserves**

No NI 43-101 compliant mineral resource or reserve estimate available.

### **History of Exploration**

- 1950: Geological mapping (Neal, 1951)
- 1952: Geological mapping and prospecting (Beemer, 1952)
- 1953: Geological mapping and prospecting (Almond, 1953)
- 1956: Geological mapping and magnetometer survey (MacDermott, 1958)
- 1959: Gravity survey (Grimaldi, 1959b)
- 1982: Airborne geophysical surveys (EM, magnetics, radiometrics; Johnson, 1982)
- 2001: Regional airborne magnetic surveys (Cotnoir *et al.*, 2002)
- 2008: Geological mapping and prospecting, gravity surveys (Reynolds and Mitchell, 2008)
- 2009: Prospecting (Downing, 2009)
- 2010: Diamond drilling (1 drillhole, 201 m), prospecting (Hovis and Broadbent, 2010)
- 2011: Magnetic and electromagnetic airborne survey (Smith *et al.*, 2012)
- 2012: Airborne gravity gradiometer survey (Sauve *et al.*, 2012)

## 11. GREEN WATER LAKE

**Alternate Name:** Sudbury No. 1, Sudbury No. 2, Sudbury Lake West No. 2

**MODS Showing(s):** 023B/14/Fe003, 023B/14/Fe004, 023B/ 14/Fe017

**Status:** Showing

**Structural Basin:** n/a

**UTM Zone:** 19

**NTS Area:** 23B/14

**Northing (NAD27):** 5861869

**Easting (NAD27):** 617795

**Latitude:** 52.8954

**Longitude:** -67.2490

**Object Located:** Drillhole 12LB0052

### Description of Occurrence

The Green Water Lake showing is located along the shores of Green Water Lake (Figure 38), approximately 24 km west of Labrador City. There are no roads in the area, and access is *via* helicopter. The Green Water Lake showing encompasses outcrops of iron formation to the east of Green Water Lake (previously referred to as Sudbury No. 1) and to the northwest of Green Water Lake (previously referred to as Sudbury No. 2). Regional aeromagnetic studies indicate that all outcrops represent a continuous band of iron formation that continues along the northern shore of Green Water Lake (Figure 38).

### Geology and Stratigraphy

The Sokoman Formation iron formation occurs along the northern and eastern shores of Green Water Lake (Figure 38). The northern extent of the iron formation is thought to be in thrust contact with the Ashuanipi Complex, whereas there is a thin sequence of Wishart Formation mapped at the base of the Sokoman Formation to the east of Green Water Lake (Figure 38). Le Fer Formation schists occur to the south of Green Water Lake (Figure 38); potentially occurring in conformable contact with the overlying Sokoman Formation. However, given the relatively sparse outcrop and lack of drillhole data from below the iron formation, the presence of a thin sequence of Wishart Formation between the Sokoman and Le Fer formations cannot be discounted.

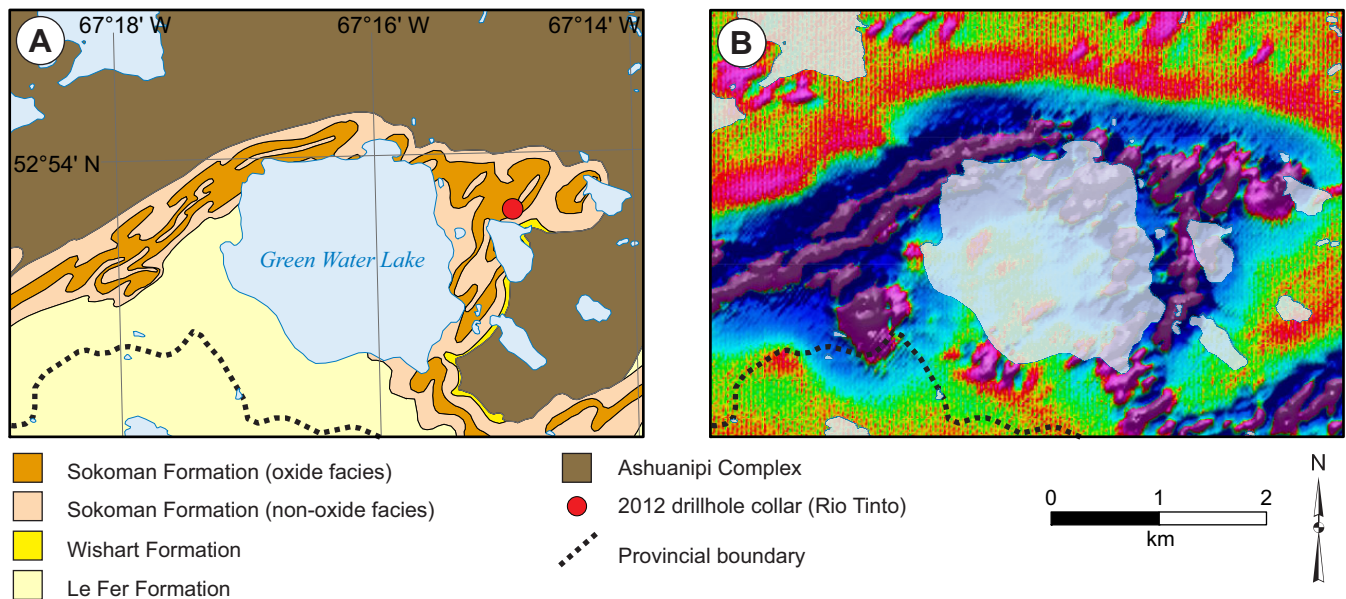


**Figure 38.** A) Geological map of the Green Water Lake showing (adapted from Cotnoir et al., 2002), showing location of drillhole from 2012 exploration program (Goldner et al., 2013); B) Airborne magnetics (second vertical derivative) showing extent of iron formation (data from Cotnoir et al., 2002).

Geological mapping and prospecting in the Green Water Lake area have identified oxide- and silicate-facies iron formation. Information on the stratigraphy of the Sokoman Formation in the area is restricted to data from a single diamond-drill hole located to the east of Green Water Lake (Goldner *et al.*, 2013). This drillhole intersected two intervals of iron formation separated by intervals of micaceous schist. The upper and lower part of the iron formation predominantly consists of silicate-facies iron formation, with minor carbonate-facies iron formation. Oxide-facies iron formation (up to 40 m thick) is concentrated near the middle of the iron formation.

### ***Mineralization***

Oxide-facies iron formation predominantly consists of quartz–carbonate–magnetite, with some thin quartz–hematite–martite units (Goldner *et al.*, 2013).

There is no published metallurgical testwork available from the Green Water Lake showing.

Assay results from drillhole 12LB0052 include 30.4% Fe over 18 m (from 97 m) and 27.9% Fe over 40.5 m (from 227.5 m).

### ***Structure***

The Green Water Lake showing is interpreted to be hosted within a syncline, with a northeast-trending overturned fold axis refolded about a later northwest-trending fold plane (Hulstein and Lee, 2001). No major faults have been recorded during geological mapping or diamond drilling (Hulstein and Lee, 2001).

### ***Geophysics***

Regional aeromagnetic surveys show that the Green Water Lake showing is located within a strong magnetic high, which continues for over 6 km along the eastern and northern shores of Green Water Lake (Cotnoir *et al.*, 2002; Figure 38). This magnetic high likely corresponds to magnetite-rich oxide-facies iron formation. Ground gravity surveys show that a moderate gravity high is located close to the eastern shore of Green Water Lake (Reynolds and Mitchell, 2008; Hovis and Goldner, 2011b).

### **Resource and/or Reserves**

No NI 43-101 compliant mineral resource or reserve estimate available.

Non 43-101 compliant historical estimates based on limited data of 1.85 Mt at 33% Fe and 8.3 Mt at 32% Fe were reported from the Sudbury No. 1 and Sudbury No. 2 occurrences by Hulstein and Lee (2001). However, the presence of iron formation between these two deposits indicates there is potential for greater tonnages at similar or better grades on the property (Hulstein and Lee, 2001).

### **History of Exploration**

- 1953: Geological mapping and prospecting (Jackson, 1954)
- 1972: Aeromagnetic survey (unpublished IOC report)
- 1979: Ground magnetometer survey and prospecting (Price, 1979d)
- 1982: Airborne geophysical surveys (EM, magnetics, radiometrics, Johnson, 1982), prospecting (Simpson and Bird, 1982)
- 1985: Diamond drilling (2 drillholes, 19.8 m, Simpson *et al.*, 1985)
- 2000: Data compilation, structural synthesis (Hulstein and Lee, 2001)
- 2001: Data compilation, regional airborne magnetic surveys, structural/stratigraphic interpretation (Cotnoir *et al.*, 2002)
- 2002: Geological mapping and prospecting (Darch and Clark, 2003)
- 2008: Geological mapping and prospecting, gravity surveys (Reynolds and Mitchell, 2008; Downing and Mitchell, 2009b)
- 2010: Geological mapping and prospecting, gravity surveys (Hovis and Goldner, 2011b, c)
- 2011: Magnetic and electromagnetic airborne survey (Smith *et al.*, 2012)
- 2012: Diamond drilling (1 drillhole, 367.9 m, Goldner *et al.*, 2013), airborne gravity gradiometer survey (Suave *et al.*, 2012)

## 12. HUGUETTE LAKE

**Alternate Name:** Huguette 1, Huguette Lake Southeast, Huguette Lake East, Huguette Lake Northeast

**MODS Showing(s):** 023B/14/Fe011; 023B/14/Fe012; 023B/ 14/Fe013

**Status:** Showing

**Structural Basin:** Carol

**UTM Zone:** 19

**NTS Area:** 23B/14

**Northing (NAD27):** 5860307

**Easting (NAD27):** 626505

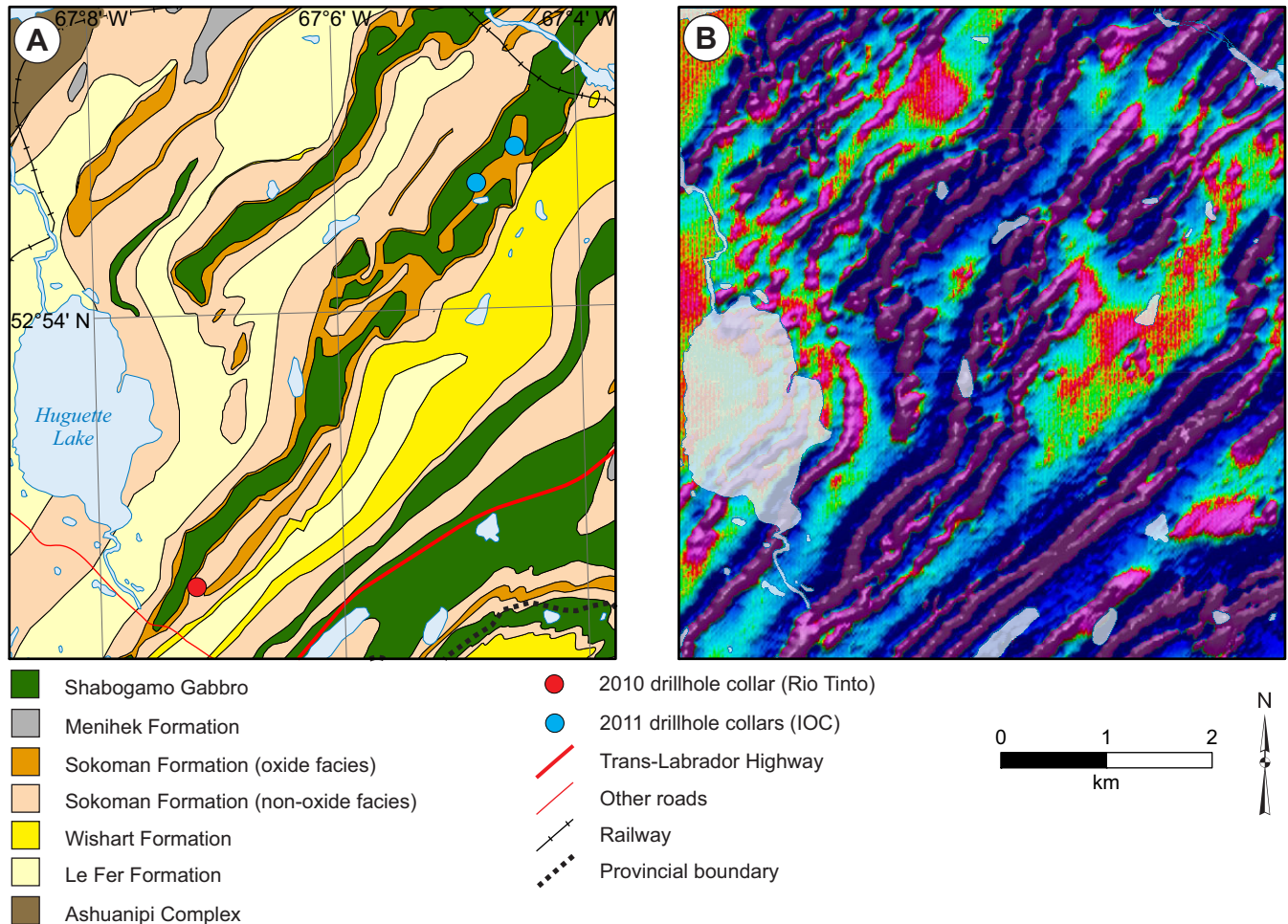
**Latitude:** 52.8774

**Longitude:** -67.1204

**Object Located:** Drillhole 10LB0017

### Description of Occurrence

The Huguette Lake showing refers to large area of Sokoman Formation iron formation that outcrops to the east of Huguette Lake and to the northwest of the TLH (Figure 39). It is located approximately 15 km southwest of Labrador City, and access is via the TLH and a minor road that crosses the southern boundary of the showing (Figure 39).





## ***Geology and Stratigraphy***

The Huguette Lake showing is composed of a series of anticlines and synclines cored by the Sokoman Formation iron formation, which is underlain by Wishart and Le Fer formations. The Sokoman Formation is intruded by sills of Shabogamo Gabbro.

Outcrop in the area is poor, and the Sokoman Formation occurs primarily as silicate-facies iron formation, possibly after metamorphism of carbonate-facies iron formation. Given the stratigraphic position of the silicate-facies iron formation immediately above Wishart Formation quartzites, it is interpreted as the LIF. However, drillhole HL-11-05 intersected 3 m of graphitic schist, which may represent Menihek Formation infolded with UIF. Although oxide facies of the MIF outcrops sporadically on the property, diamond drilling did not intercept significant thickness of this facies (Hovis and Goldner, 2011b; Wallace, 2012b).

## ***Mineralization***

Oxide minerals, predominantly magnetite, occur mainly in silicate-facies iron formation, where they form thin (0.2 to 2 cm) bands interbedded with acicular silicates and minor quartz.

There is no published metallurgical testwork available from the Huguette Lake showing.

Due to the presence of fibrous amphiboles in IOC drillholes, assay results were only returned from the single Rio Tinto drillhole (10LB0017). Highlights include 27.1% Fe over 12 m (from 12.4 to 24.4 m), but this includes iron in both oxide and silicate minerals, and total magnetite content does not exceed 12.4% (Hovis and Goldner, 2011b).

## ***Structure***

There is little information on the structural geology of the Huguette Lake property. Interpretations from regional geology mapping programs indicate that the Sokoman Formation is located in a series of northeast–southwest-trending, northwest-verging synclines, which plunge to the northeast.

## ***Geophysics***

Regional airborne magnetic surveys (Cotnoir *et al.*, 2002) show that the Huguette Lake showing is coincident with a strong linear magnetic anomaly, which is up to 1 km wide and has a strike length of >5 km (Figure 39). The strong magnetic signature is attributed to the presence of numerous thin (<10 cm) bands of magnetite in the silicate-facies iron formation. Ground gravity data are available in Hovis and Goldner (2011b), but no interpretation is presented.

## **Resource and/or Reserves**

No NI 43-101 compliant mineral resource or reserve estimate available.

## **History of Exploration**

- 1949: Geological mapping (Neal, 1950a)
- 1953: Geological mapping and prospecting (Jackson, 1954)
- 1957: Geological mapping and prospecting (Mathieson, 1957a)
- 1960: Geological mapping and prospecting, magnetic and gravity surveys (Love, 1961)
- 1972: Aeromagnetic survey (unpublished IOC report)
- 1979: Ground magnetometer survey (Price, 1979e)
- 1982: Airborne geophysical surveys (EM, magnetics, radiometrics, Johnson, 1982)
- 2000: Data compilation, structural synthesis (Hulstein and Lee, 2001)
- 2001: Regional airborne magnetic surveys, structural/ stratigraphic interpretation (Cotnoir *et al.*, 2002)
- 2009: Geological mapping and prospecting (Downing, 2010)
- 2010: Diamond drilling (1 drillhole, 150.3 m), ground gravity survey (Hovis and Goldner, 2011b)
- 2011: Diamond drilling (2 drillholes, 312.5 m), aerial photography survey (Wallace, 2012b)
- 2012: Airborne gravity gradiometer survey (Suave *et al.*, 2012)

### 13. HUMPHREY

**Alternate Name:** Humphrey Mine, Humphrey Main, Humphrey North, Humphrey South, Lorraine North, Lorraine South, Sherwood, Spooks, Carol East, Carol West, Wabush Signal, Lorraine No. 1, Lorraine No. 2, Lorraine No. 3

**MODS Showing(s):** 023G/02/Fe002, 023G/02/Fe003, 023G/02/Fe004,

**Status:** Producer

**Structural Basin:** Carol

**UTM Zone:** 19

**NTS Area:** 23G/02

**Northing (NAD27):** 5878834

**Easting (NAD27):** 637280

**Latitude:** 53.0433

**Longitude:** -66.9523

**Object Located:** Approximate centre of Humphrey Main pit

#### Description of Occurrence

The Humphrey deposit is located in IOC's Carol Lake Mine area, between Lorraine Lake in the northeast and Carol Lake in the southwest (Figure 40) and approximately 12 km north of Labrador City. Access to the deposit is *via* a series of mine roads that extend north from the IOC concentrator and pellet plant.

The deposit consists of a continuous band, or bands, of iron formation, which can be traced along strike for more than 7 km (Figure 41) and encompasses five active pits (Humphrey Main (Plate 33A), Humphrey North, Humphrey South, Lorraine South and Sherwood) and two dormant pits (Lorraine North and Spooks, Figure 40). These pits are herein grouped together based on similarities in stratigraphy, mineralization and structure across the deposit.

#### Geology and Stratigraphy

The geology of the Humphrey deposit consists of a folded sequence of Kaniapiskau Supergroup metasedimentary rocks (Figure 41). Le Fer Formation quartz-feldspar-biotite gneiss is located at the base of the sequence and is overlain by Wishart Formation quartzite. The Sokoman Formation occurs stratigraphically above the Wishart Formation, and Menihek Formation graphitic schist has been recorded in the core of synclines. Shabogamo Gabbro sills intrude the Sokoman Formation.

At the deposit, the stratigraphy of the Sokoman Formation has been described in detail by Muwais (1974), who subdivided the iron formation into three members: Lower Iron Formation (LIF), Middle Iron Formation (MIF) and Upper Iron Formation (UIF), each of which was further subdivided into a number of sub-members. The LIF is primarily composed of carbonate-facies iron formation, with lesser silicate and oxide facies. The MIF, predominantly composed of oxide-facies iron formation, has been subdivided into four sub-members based

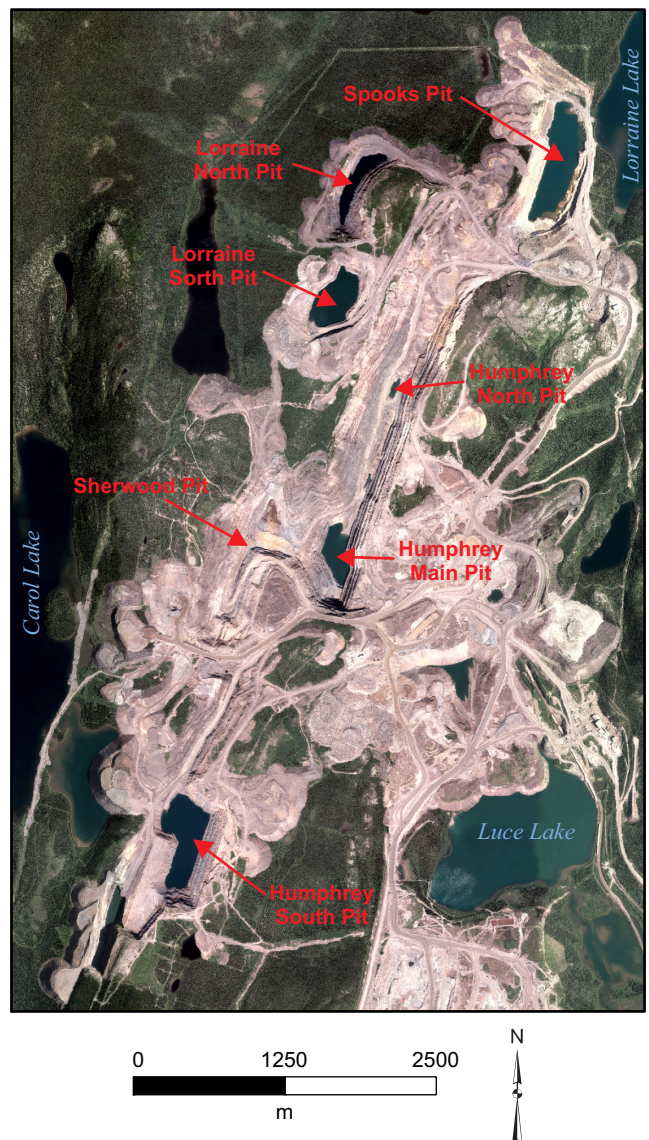


**Figure 40.** Aerial photograph of the Humphrey deposit, showing location of the active and dormant pits discussed in text (image courtesy of IOC).



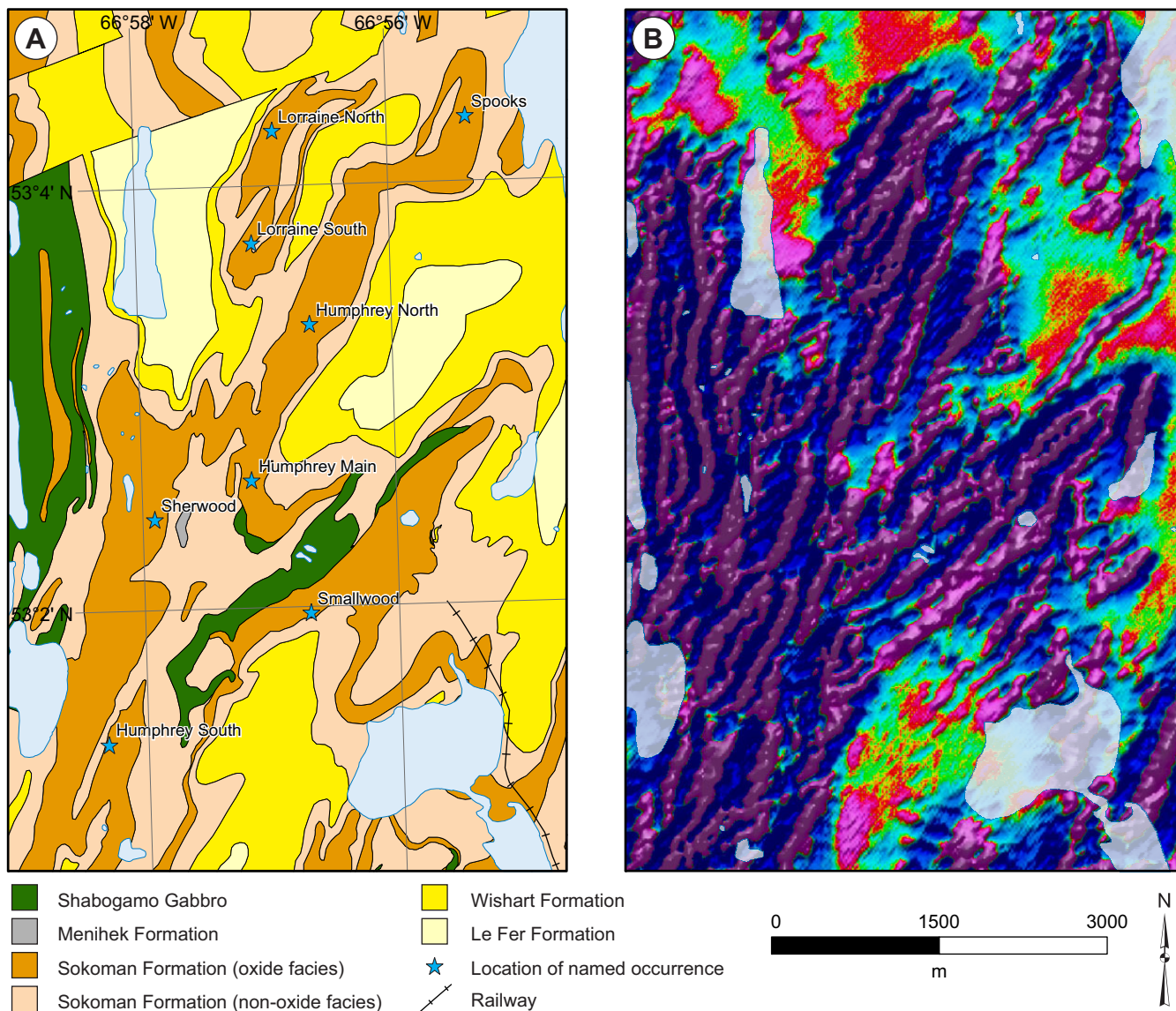


**Figure 41.** A) Geological map of the Humphrey deposit showing location of active and dormant pits discussed in text and of former Smallwood mine (adapted from Cotnoir et al., 2002); B) Airborne magnetics (second vertical derivative) showing extent of iron formation (data from Cotnoir et al., 2002).

on variations in the ratios of magnetite and hematite (Muwais, 1974). The UIF is predominantly composed of carbonate- and silicate-facies iron formation (Plate 33B), with rare oxide-facies bands.

### Mineralization

Oxide-facies iron formation consists of magnetite, hematite and gangue quartz, carbonates and minor Fe-silicates (anthophyllite). The proportion of magnetite and hematite is variable, with most samples containing magnetite and hematite in variable proportions (Plate 34). However, there is a general vertical zonation observed in the MIF. The lowest sub-member is magnetite rich (Plate 33C, D), and is overlain by two hematite-rich sub-members (Plate 33E, F; Muwais, 1974). A thin magnetite-rich sub-member is recorded at the top of the MIF (Muwais, 1974).

Although the oxide-facies iron formation is typically fresh to weakly altered, localized zones of strong alteration are recorded throughout the deposit (e.g., at the north end of the Sherwood Pit and at the southern end of the Humphrey South pit (Magy



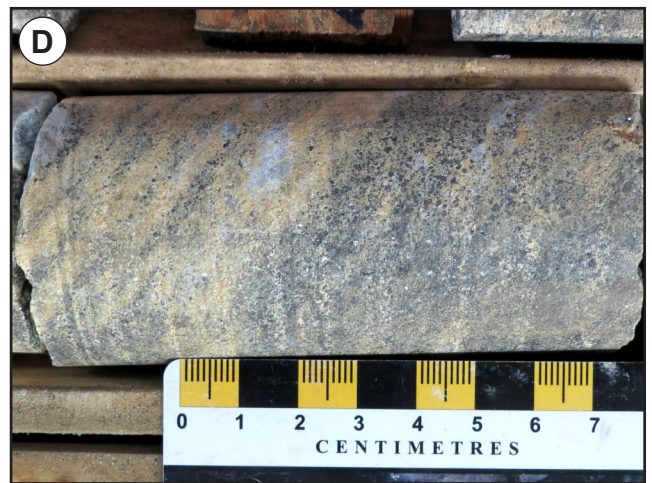
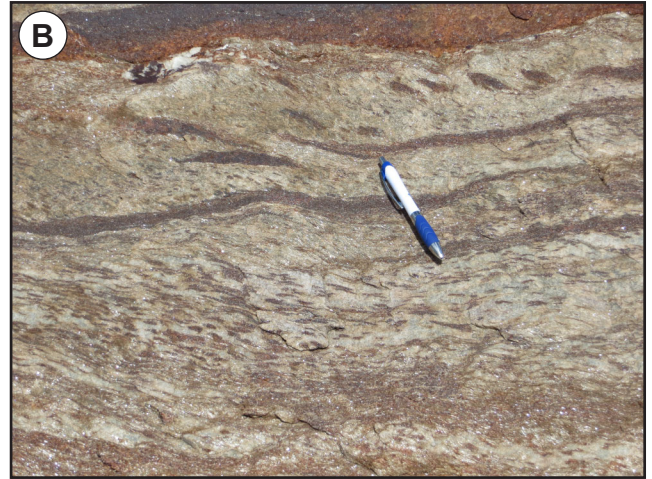


**Plate 33.** A) View of the Humphrey Main pit, looking north from observation point; B) Silicate-facies iron formation; C) Magnetite-rich oxide-facies iron formation with gangue carbonate and quartz (drillhole SW-10-69 @ 48.5 m); D) Oxide-facies iron formation, with medium- to coarse-grained magnetite and hematite and cream-coloured carbonate (drillhole SP-11-27 @ 77 m); E) Oxide-facies iron formation, with coarse-grained specular hematite and quartz-filling vug; F) Hematite-rich oxide-facies iron formation with gangue quartz (jasper) (drillhole HW-10-45 @ 13.3 m).



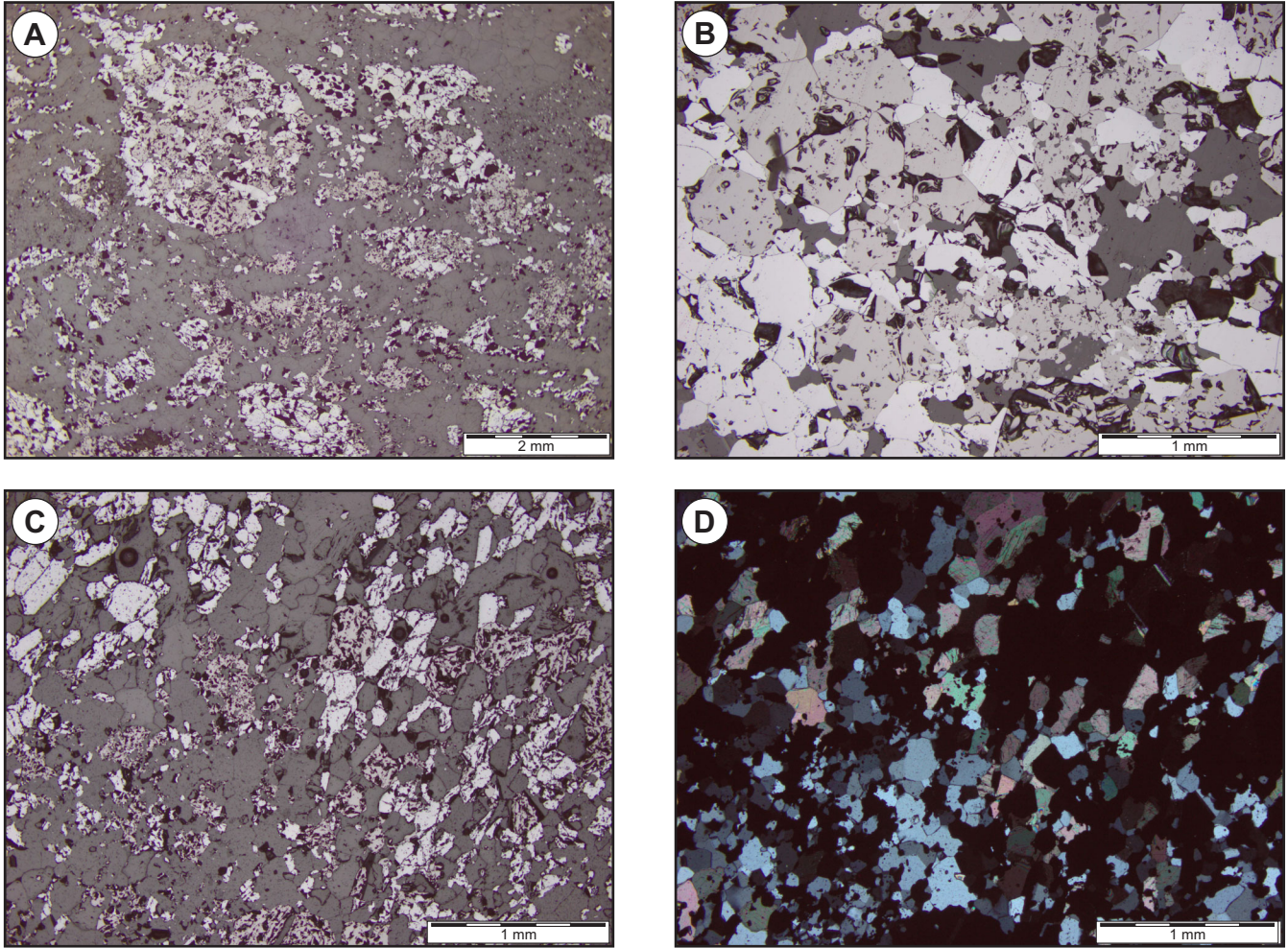


**Plate 34.** A) Photomicrograph of specular hematite and magnetite replacing possible oolites in parent iron formation (drillhole HS-10-72 @ 218 m, reflected light); B) Photomicrograph of co-existing euhedral to subhedral hematite and magnetite (drillhole HS-10-72 @ 218 m, reflected light); C) Oxide-facies iron formation, with disseminated magnetite (light grey) and hematite (pink grey) and gangue quartz (drillhole LO-10-04 @ 60.3 m); D) Same view as (C), in cross-polarized light.

Pit)). The alteration consists of abundant secondary goethite leaching carbonate and silica. Alteration is associated with broken ground (faulting) and is attributed to groundwater flow along permeable fault zones. Altered material was previously considered waste material, but recent work has shown that this material can be effectively processed at IOC's concentrator (Iron Ore Company of Canada, 2017, 2018).

Ore from the Humphrey deposit is processed at IOC's concentrator and pellet plant. The bulk ore characteristics, including RMI determination, minus 200 mesh weight fraction and iron weight recovery values, were documented by Cotnoir *et al.* (2002). Crushed ore is conveyed to the concentrator, where it is ground and upgraded to 65–67% Fe in the spiral, magnetite and hematite plants.

### **Structure**

The dominant structural trends in the Humphrey deposit are controlled by a series of northeast-trending  $F_2$  folds (Hulstein and Lee, 2001), which form overturned synclines with thin limbs and thickened fold hinges. These  $F_2$  folds re-fold earlier  $F_1$  folds, and the interference of  $F_1$  and  $F_2$  folds is responsible for repetition of the ore horizons resulting in significant structural thickening (Cotnoir *et al.*, 2002).

The presence of north–south-trending shear zones and normal faults is associated with alteration of the iron formation due to the ingress of groundwater along permeable structures. Such shear zones have been recorded at the north end of the Sherwood Pit and at the southern end of the Humphrey South pit (Magy Pit).

### **Geophysics**

The Humphrey deposit is associated with a strong magnetic anomaly (Figure 41) on regional aeromagnetic surveys (Cotnoir *et al.*, 2002), which is associated with the high magnetite content of the lower section of the MIF.

### **Resource and/or Reserves**

NI 43-101 compliant reserves, Iron Ore Company of Canada, 2014.

- Humphrey Main
  - Proven reserves: 248 Mt at 39% Fe
  - Probable reserves: 253 Mt at 38% Fe
- Humphrey South
  - Proven reserves: 205 Mt at 39% Fe
  - Probable reserves: 89 Mt at 38% Fe
- Lorraine South
  - Proven reserves: 33 Mt at 38% Fe
  - Probable reserves: 2 Mt at 36% Fe
- Spooks
  - Proven reserves: 15 Mt at 43% Fe
  - Probable reserves: 3 Mt at 44% Fe

NI 43-101 compliant resource, Iron Ore Company of Canada, 2014. Mineral resources exclude Mineral reserves.

- Humphrey Main
  - Measured resources: 65 Mt at 41% Fe
  - Indicated resources: 317 Mt at 39% Fe
  - Inferred resources: 191 Mt at 37% Fe
- Humphrey South
  - Measured resources: 65 Mt at 40% Fe
  - Indicated resources: 70 Mt at 40% Fe
  - Inferred resources: 125 Mt at 38% Fe
- Spooks
  - Measured resources: 18 Mt at 39% Fe
  - Indicated resources: 73 Mt at 43% Fe
  - Inferred resources: 19 Mt at 41% Fe

### **History of Exploration**

- 1949: Regional geological mapping, bulk sample (Neal, 1950a)
- 1950: Prospecting and metallurgical testwork (Neal, 1950b), geological mapping (Neal, 1951)
- 1956: Geological mapping, diamond drilling, bulk sample (Mathieson, 1957b)
- 1957: Geological mapping and sampling (Malchelosse, 1957)
- 1958 to 1964: Exploration activity, development of pilot plant and construction of mine facilities
- 1964: Production begins at Humphrey deposit (Humphrey Mine)
- 1972: Aeromagnetic survey (unpublished IOC report)
- 1974: Stratigraphic study of Humphrey deposit (Muwais, 1974)
- 2000: Structural synthesis (Hulstein and Lee, 2001)
- 2001: Regional airborne magnetic surveys, structural/ stratigraphic interpretation (Cotnoir *et al.*, 2002)



## 14. IRONSTONE

**Alternate Name:** Throne Lake, Ironstone River

**MODS Showing(s):** 023B/14/Fe018

**Status:** Showing

**Structural Basin:** Carol

**UTM Zone:** 19

**NTS Area:** 23B/14

**Northing (NAD27):** 5867603

**Easting (NAD27):** 631895

**Latitude:** 52.9438

**Longitude:** -67.0371

**Object Located:** Drillhole KN-10-15

### Description of Occurrence

The Ironstone showing refers to a narrow band of Sokoman Formation that stretches from Dispute Lake in the north to the Walsh River in the south (Figure 42). It is located approximately 8 km east of Labrador City. There are no roads on the property and access is *via* small trails or by helicopter.

### Geology and Stratigraphy

The Ironstone property geology is dominated by Sokoman Formation iron formation, which has been intruded by a series of Shabogamo Gabbro sills, occurring both above and below the MIF (Carter, 2011d). Le Fer Formation schists occur in probable

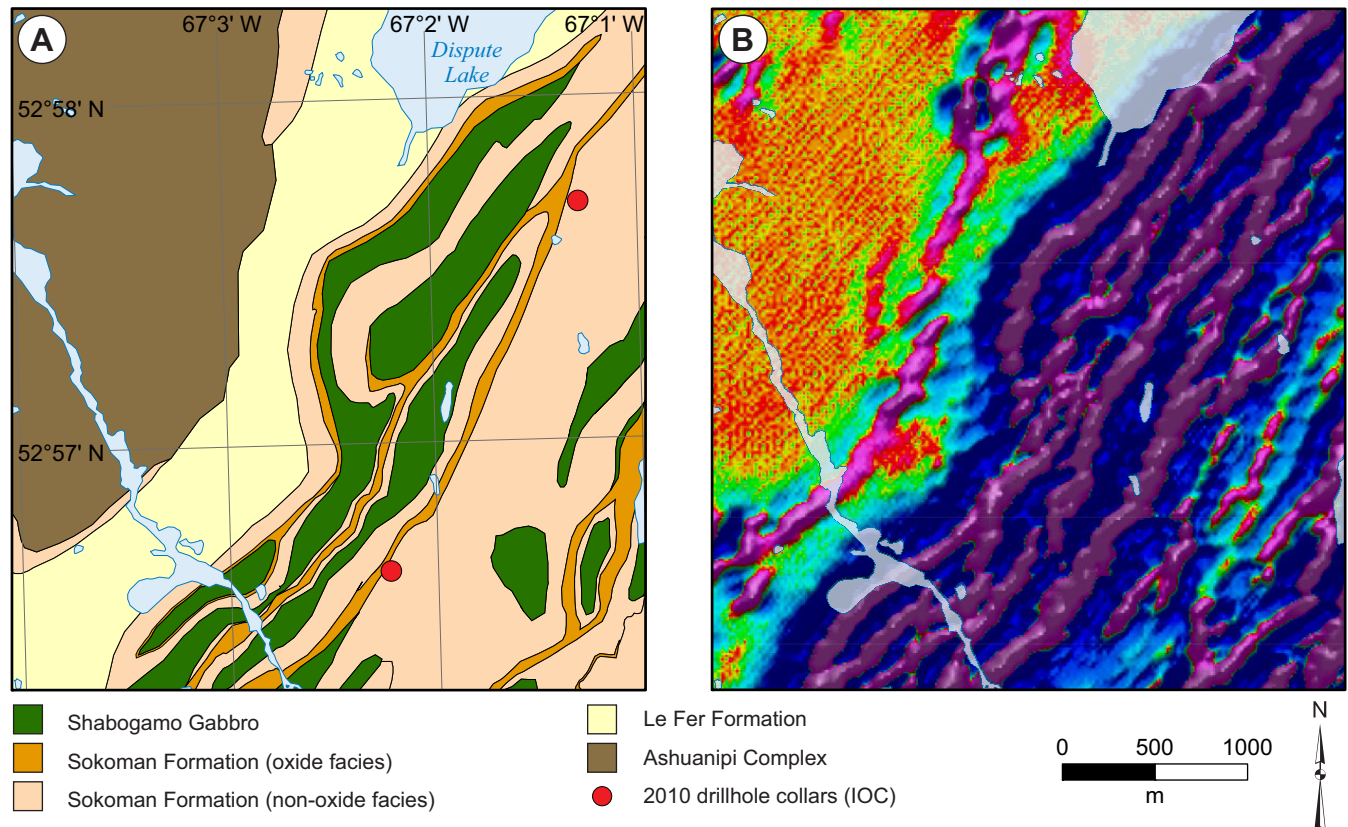


**Figure 42.** A) Geological map of the Ironstone showing (adapted from Cotnoir et al., 2002), showing location of drillholes from 2010 exploration program (Carter, 2011d); B) Airborne magnetics (second vertical derivative) showing extent of iron formation (data from Cotnoir et al., 2002).



conformable contact to the west with the overlying Sokoman Formation (Figure 42). However, due to the relatively sparse outcrop and lack of drillhole data from below the iron formation, the presence of a thin sequence of Wishart Formation between the Sokoman and Le Fer formations cannot be discounted.

Drillhole logs indicate that the Sokoman Formation is mainly composed of silicate-facies iron formation (possibly after metamorphism of carbonate-facies iron formation), with thin (generally <5 m) intervals of oxide-facies iron formation (Carter, 2011d). This is interpreted as the LIF, although this interpretation is only preliminary, given the lack of observed contacts with underling or overlying formations and the intense structural deformation. Significant thicknesses of oxide-facies (>5 m) were only recorded at the top of drillhole KN-10-15, and this may represent the base of the MIF (Carter, 2011d).

### ***Mineralization***

The oxide-facies iron formation consists predominantly of fine-grained magnetite and quartz, and minor iron silicates (Carter, 2011d). Assay data show Mn contents of <1%.

Two composite samples were chosen from the best intersections and sent for SAG Power index (SPI) and iron recovery testing (TT), which showed that the oxide-facies iron formation is relatively hard with moderate iron recoveries (Carter, 2011d).

Only eight samples were collected for assay from the 2010 drilling program, with the best results returned from the top of drillhole KN-10-15, with 9 m grading 36.5% Fe (from 8 to 17 m).

### ***Structure***

Structural deformation in the area is intense, with multiple generations of folding evident. Early northwest–southeast-orientated isoclinal folds (F<sub>1</sub>) have been refolded by a later event, resulting in broad open F<sub>2</sub> folds and the creation of dome and basin interference structures (Carter, 2011d).

### ***Geophysics***

Regional airborne magnetic surveys (Cotnoir *et al.*, 2002) show that the ironstone showing is coincident with a strong magnetic anomaly (Figure 42).

## **Resource and/or Reserves**

No NI 43-101 compliant mineral resource or reserve estimate available.

## **History of Exploration**

- 1949: Geological mapping (Neal, 1950a)
- 1953: Geological mapping (Crouse, 1954)
- 1960: Geological mapping and prospecting, magnetic and gravity surveys (Love, 1961)
- 1972: Aeromagnetic survey (unpublished IOC report)
- 1982: Airborne geophysical surveys (EM, magnetics, radiometrics, Johnson, 1982)
- 2000: Data compilation, structural synthesis (Hulstein and Lee, 2001)
- 2001: Data compilation, geological mapping and prospecting, ground gravity survey, regional airborne magnetic surveys, structural/stratigraphic interpretation (Cotnoir *et al.*, 2002)
- 2010: Diamond drilling (2 drillholes, 297 m, Carter, 2011d)
- 2011: Aerial photography program (Wallace and Leriche, 2012)

## 15. JULIENNE 1

**Alternate Name:** n/a

**MODS Showing(s):** 023G/02/Fe013

**Status:** Prospect

**Structural Basin:** Carol

**UTM Zone:** 19

**NTS Area:** 23G/02

**Northing (NAD27):** 5894668

**Easting (NAD27):** 648571

**Latitude:** 53.1825

**Longitude:** -66.7767

**Object Located:** Drillhole J2-06-05

### Description of Occurrence

The Julienne 1 property is located on the western shore of Goethite Bay (Figure 43), approximately 29 km north of Labrador City. Access is by boat from Julienne Lake, or by helicopter.

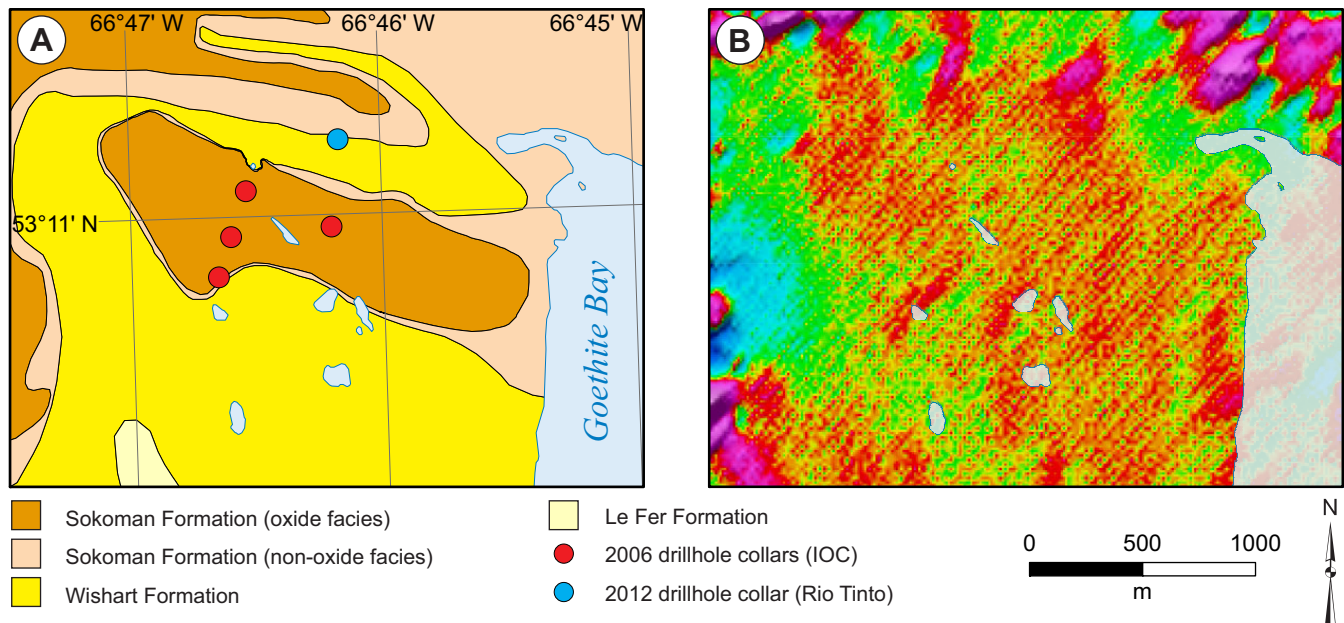


**Figure 43.** A) Geological map of the Julienne 1 prospect (adapted from Cotnoir et al., 2002) showing location of drillholes from 2006 and 2012 exploration programs (Clark, 2007a; Goldner et al., 2013); B) Airborne magnetics (second vertical derivative) (data from Cotnoir et al., 2002).

### Geology and Stratigraphy

The geology in the Julienne 1 area is composed of Sokoman Formation iron formation conformably underlain by quartzite of the Wishart Formation (Figure 43). Diamond drilling has shown appreciable thicknesses of iron formation (>109 m; Clark, 2007a). Due to strong alteration of the iron formation, stratigraphic interpretations are difficult, but Clark (2007a) indicates that a full sequence of Sokoman Formation (UIF, MIF and LIF) is preserved. The UIF and LIF are very similar in appearance and are differentiated based on their stratigraphic position above and below the MIF. They are predominantly composed of quartz-carbonate schist, and lesser specular hematite. Large, euhedral garnet crystals occur near to the contact with the underlying Wishart Formation (possible Ruth Formation, Plate 35A). The MIF consists of oxide-facies iron formation, with alternating bands of hematite and quartz (Plate 35B) and minor carbonate bands and carbonate spotting.



**Plate 35.** A) LIF close to the contact with Wishart Formation quartzite, with large euhedral garnets (drillhole J2-06-05 @ 117.3 m); B) Quartz–hematite oxide-facies iron formation (drillhole J2-06-05 @ 103.1 m).

### **Mineralization**

The oxide-facies iron formation is composed of friable quartz bands and hard hematite bands; magnetite content is very low (<0.5%). The iron formation is commonly friable and alteration is strong to moderate throughout, with goethite and limonite on fractures. Surface sampling has also noted common pyrolusite on fracture surfaces (Darch *et al.*, 2003b), but overall Mn contents are low (<0.6% Mn).

There is no published metallurgical testwork available from the Julienne 1 prospect.

Assay results from the 2006 drilling program returned significant thicknesses of mineralized iron formation (Clark, 2007a), with highlights including 41.3% Fe over 72 m in drillhole J2-06-06 (21 to 93 m), 41.1% Fe over 44 m in drillhole J2-06-05 (6 to 50 m) and 40% Fe over 39 m in drillhole J2-06-02 (18 to 57 m).

### **Structure**

The Julienne 1 prospect is located in an asymmetrical synclinal structure. Structural mapping indicates that the oxide-facies iron formation is located in the keel of a southeast-plunging (18°) and south-dipping (10 to 20°) overturned F<sub>1</sub> syncline intersected by an F<sub>2</sub> anticlinal axis (Darch *et al.*, 2003b). A north–northwest-trending (345°) fault having an approximate 80° dip has been recognized on aeromagnetic data, and coincides with a pronounced valley at the Julienne 1 prospect (Darch *et al.*, 2003b). The fault offsets the LIF and Wishart Formation, and may be related to the Julienne Lake Fault Zone, a north–northwest-trending ductile shear zone mapped by van Gool (1992) directly south of the Julienne 1 prospect. These faults would have provided a conduit for fluid flow responsible for the moderate to strong alteration of the iron formation.

### **Geophysics**

Due to the high hematite content and very low magnetite content of the oxide-facies iron formation, the Julienne 1 prospect is not characterized by a magnetic anomaly on the regional airborne magnetic survey (Figure 43; Cotnoir *et al.*, 2002). A very weak gravity response has been recorded over the Julienne 1 prospect (Darch *et al.*, 2003b).

### **Resource and/or Reserves**

No NI 43-101 compliant mineral resource or reserve estimate available.

Non 43-101 compliant historical estimates based on limited data of 90 Mt grading 33% Fe were reported by Hulstein and Lee (2001).



### History of Exploration

- 1950: Geological mapping (Neal, 1951)
- 1953: Geological mapping and prospecting (Almond, 1953), diamond drilling (9 drillholes, 201 m, Neal, 1953)
- 1972: Aeromagnetic survey (unpublished IOC report)
- 1982: Airborne geophysical surveys (radiometrics, Johnson, 1982)
- 1985: Diamond drilling (1 drillhole, 88 m, Simpson *et al.*, 1985)
- 2000: Data compilation, structural synthesis (Hulstein and Lee, 2001)
- 2001: Data compilation, geological mapping and prospecting, regional airborne magnetic surveys, ground gravity survey, structural/stratigraphic interpretation (Cotnoir *et al.*, 2002)
- 2003: Geological mapping and prospecting (Darch *et al.*, 2003b)
- 2006: Diamond drilling (4 drillholes, 456.5 m, Clark, 2007a)
- 2011: Airborne electromagnetic, magnetic, and gravity surveys (Wallace, 2012c)
- 2012: Diamond drilling north of Julienne 1 prospect (1 drillhole, 309 m, Goldner *et al.*, 2013)

## 16. JULIENNE 2

**Alternate Name:** Julienne #2

**MODS Showing(s):** 023G/02/Fe010

**Status:** Prospect

**Structural Basin:** Wabush

**UTM Zone:** 19

**NTS Area:** 23G/02

**Northing (NAD27):** 5891224

**Easting (NAD27):** 653250

**Latitude:** 53.1503

**Longitude:** -66.7083

**Object Located:** Drillhole J2-10-10

### Description of Occurrence

The Julienne 2 prospect is located on a peninsula in Julienne Lake, between Goethite Bay and Scott Bay (Figure 44). It is approximately 29 km north of Labrador City. Access is by boat from Julienne Lake, or by helicopter.

### Geology and Stratigraphy

Based on aeromagnetic data, the Julienne 2 prospect is interpreted to be a northerly extension of the Julienne Lake deposit (Cotnoir *et al.*, 2002), and the stratigraphy of the peninsula supports this correlation. Rocks of the Kaniapiskau Supergroup pre-

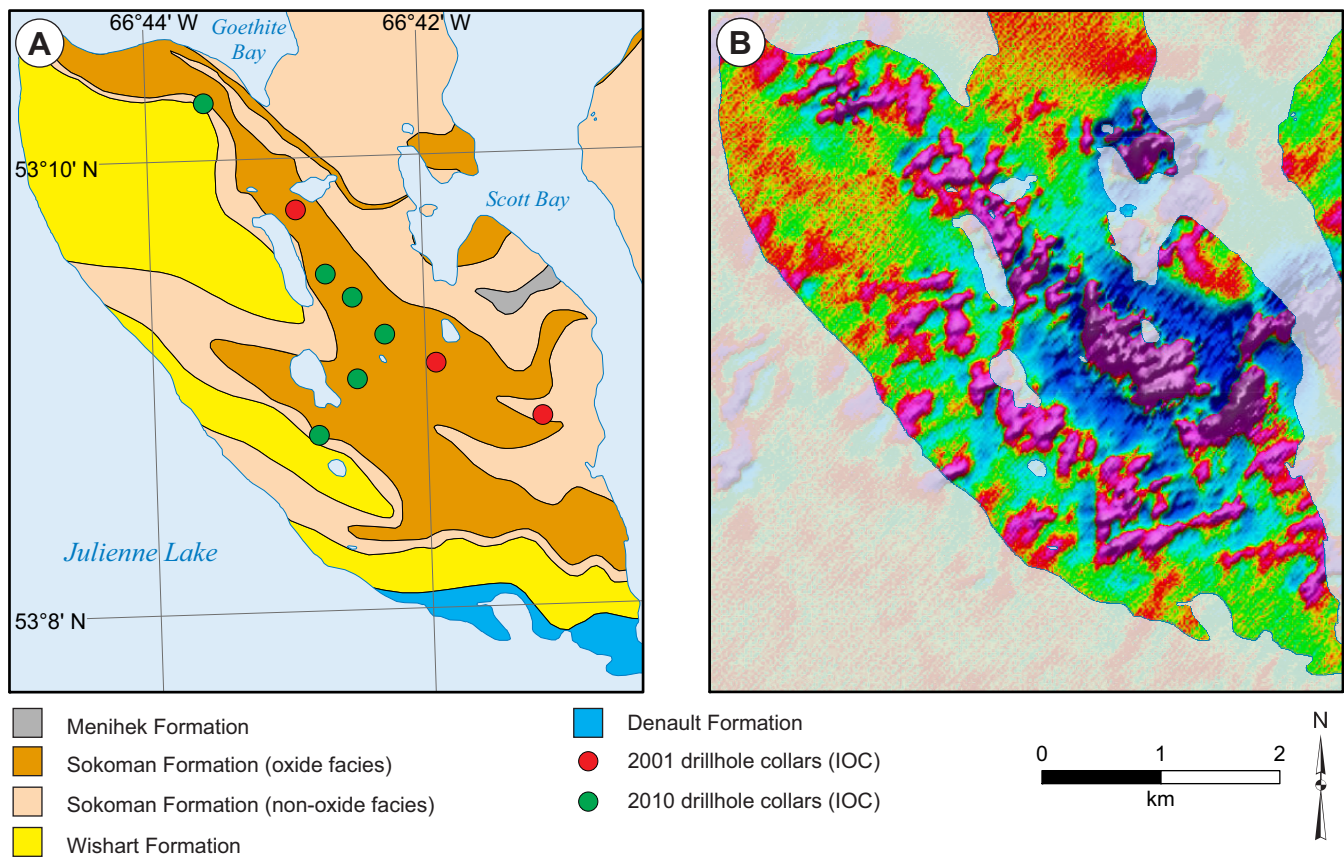


**Figure 44.** A) Geological map of the Julienne 2 prospect (adapted from Cotnoir *et al.*, 2002), showing location of drillholes from 2001 and 2010 exploration programs (Cotnoir *et al.*, 2002; Carter, 2011d); B) Airborne magnetics (second vertical derivative) showing extent of iron formation (data from Cotnoir *et al.*, 2002).

dominate the area (Figure 44), with Denault Formation dolomite (outcropping at the southern tip of the peninsula) overlain by Wishart Formation quartzite. The Wishart Formation is conformably overlain by the Sokoman Formation, which outcrops along the centre of the peninsula. Minor Menihek Formation schist has been reported from one drillhole along the eastern shore of the peninsula, but the formation does not outcrop (Darch *et al.*, 2003b). Diamond drilling has also recorded the presence of numerous Shabogamo Gabbro sills that intrude the Sokoman Formation.

The UIF is a banded carbonate-facies iron formation, where the carbonate minerals are altered and replaced by goethite (Darch *et al.*, 2003b). Oxide-facies iron formation of the MIF outcrop extensively on the northern half of the peninsula, and diamond drilling has intercepted up to 268 m of oxide-facies iron formation. The composition of the MIF is variable across the peninsula, with magnetite-rich iron formation common at the southeastern end of the peninsula, and hematite content increasing to the northwest (Plate 36) interpreted to be related to late-stage alteration of magnetite to martite. The LIF is composed of a thin unit of quartz and goethite-rich schist, and in drillhole J2-10-10, the base of the LIF is garnet-bearing and characterized by high Al<sub>2</sub>O<sub>3</sub> content (up to 3.2% Al<sub>2</sub>O<sub>3</sub>; Carter, 2011e). It has a transitional contact with the underlying Wishart Formation, and is similar to the Basal Silicate Member recognized in the Rose and Scully deposits.



**Plate 36.** Quartz–hematite oxide-facies iron formation (drillhole J2-10-08 @ 153.2 m).

### **Mineralization**

The oxide-facies iron formation is composed of quartz and variable proportions of magnetite and hematite, with hematite content increasing with increased alteration (due to transformation of magnetite to martite). The iron oxides are generally fine to medium grained, but very coarse-grained hematite has also been recorded (Carter, 2011e). The oxide-facies iron formation is friable and sandy in places, with multiple brecciated zones.

Alteration is moderate to strong in places and is characterized by the presence of goethite and limonite on fracture surfaces, increased hematite content, and leaching of carbonate and iron silicate minerals. The alteration is strongest in the most northerly drillhole (J2-10-13), and generally decreases to the southeast. Manganese-oxides, primarily pyrolusite, are locally common, with Mn contents ranging up to 11.7% over 3 m (drillhole J2-10-10 @ 87 m, Carter, 2011e).

Carter (2011e) reported on iron weight recovery and SAG Power Index (SPI) from 57 composite drillcore samples from the 2010 IOC drill program, with results indicating that iron weight recovery is similar to the range of IOC ore from the Humphrey deposit (Cotnoir *et al.*, 2002).

Assay results from the Julienne 2 prospect have shown significant thickness of oxide-facies iron formation, with highlights including 37.3% Fe over 268.5 m in drillhole J2-10-08 (4.5 to 273 m), 37.8% Fe over 191 m in drillhole J2-10-11 (9 to 200 m) and 33.7% Fe over 138.5 m in drillhole J2-10-10 (12 to 150.5 m).

### **Structure**

The Julienne 2 prospect is located in a complexly folded sequence, where the MIF horizon occurs within a series of tight northwest–southeast-trending F<sub>1</sub> synclinal folds that run along the centre of the peninsula. The UIF (and possible Menihek Formation) forms the core of a F<sub>1</sub> syncline at the northern part of the peninsula, whereas the LIF and Wishart Formation form the core of a F<sub>1</sub> anticline in the southern portion of the peninsula (Darch *et al.*, 2003). The F<sub>1</sub> folds plunge between 30 and 45° to the south-southeast, are northeast verging (30–50°) and are overturned (Darch *et al.*, 2003b). The F<sub>1</sub> folds were subsequently refolded around a broad F<sub>2</sub> anticlinal structure.



North-northeast-trending faults, similar to those recorded in the Julienne Lake deposit, are evident in the aeromagnetic data especially through the central portion of the Julienne 2 prospect (Darch *et al.*, 2003b). These faults likely provided conduits for late-stage fluid flow associated with alteration of the iron formation.

### ***Geophysics***

Regional aeromagnetic data (Cotnoir *et al.*, 2002) show that the southwestern part of the Julienne 2 prospect is associated with a significant magnetic high, interpreted to be related to the high magnetite content of MIF in that area (Figure 44). The magnetic signature decreases to the northwest, which is consistent with the decrease in magnetite content and stronger alteration. A gravity anomaly of 14 milligals has been delineated in the centre of the peninsula (Cotnoir *et al.*, 2002), which is coincident with the thickest intersections of oxide-facies iron formation.

### **Resource and/or Reserves**

No NI 43-101 compliant mineral resource or reserve estimate available.

Non 43-101 compliant historical estimates based on limited data of 306 Mt grading 32% Fe were reported by Hulstein and Lee (2001), whereas Cotnoir *et al.* (2002) suggested that the Julienne 2 prospect could host a geological resource exceeding 1000 Mt of iron ore.

### **History of Exploration**

- 1950: Geological mapping (Neal, 1951)
- 1952: Geological mapping and prospecting (Beemer, 1952)
- 1953: Geological mapping and prospecting (Almond, 1953)
- 1958: Diamond drilling (12 shallow drillholes, described in Hulstein and Lee, 2001)
- 1959: Ground gravity survey (Branch, 1959a)
- 1972: Aeromagnetic survey (unpublished IOC report)
- 1979 Ground magnetometer survey, prospecting (Grant, 1979d; Price, 1979f)
- 1982: Airborne geophysical surveys (radiometrics) (Johnson, 1982)
- 2000: Data compilation, structural synthesis (Hulstein and Lee, 2001)
- 2001: Data compilation, geological mapping and prospecting, diamond drilling (3 drillholes, 693 m), regional airborne magnetic surveys, ground gravity survey, structural/ stratigraphic interpretation (Cotnoir *et al.*, 2002)
- 2003: Geological mapping and prospecting (Darch *et al.*, 2003b)
- 2010: Diamond drilling (7 drillholes, 1146 m) (Carter, 2011e)
- 2011: Airborne electromagnetic, magnetic, and gravity surveys (Wallace, 2012c)

## 17. JULIENNE LAKE

**Alternate Name:** Boyko No. 1; Julien Ore Deposit

**MODS Showing(s):** 023G/02/Fe009

**Status:** Developed Prospect

**Structural Basin:** Wabush

**UTM Zone:** 19

**NTS Area:** 23G/02

**Northing (NAD27):** 5889776

**Easting (NAD27):** 648142

**Latitude:** 53.1368

**Longitude:** -66.7854

**Object Located:** Drillhole JL-10-06

### Description of Occurrence

The Julienne Lake deposit (and offshore extension) is located on the Julienne Lake peninsula between Wabush Lake to the west and Julienne Lake to the east (Figure 45). The deposit is approximately 23 km north of Labrador City, and access is by an unpaved road off the TLH (Route 500).

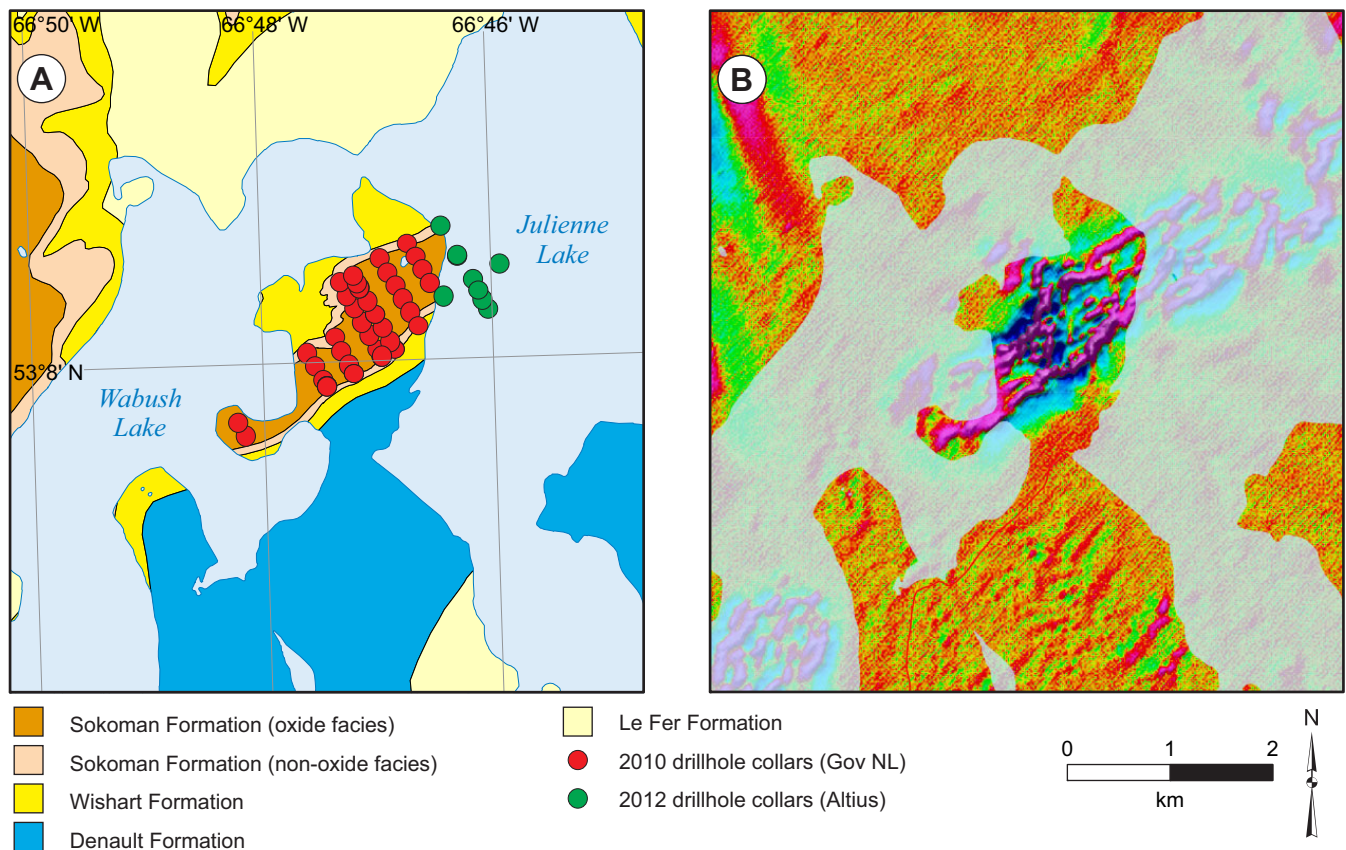


**Figure 45.** A) Geological map of the Julienne Lake deposit (adapted from Cotnoir et al., 2002), showing location of drillholes from 2010 and 2012 exploration programs (Coates et al., 2012; Seymour et al., 2012); B) Airborne magnetics (second vertical derivative) of Julienne Lake Peninsula, showing extent of iron formation and extension of the deposit into Julienne Lake (data from Cotnoir et al., 2002).

## ***Geology and Stratigraphy***

The Sokoman Formation outcrops extensively in the centre of the Julienne Lake peninsula (Figure 45), occurring in the shallowly exposed trenches and at the Pleistocene raised beach level (Plate 37A, B). Wishart Formation quartzite is located to the north and south of the peninsula, and is believed to either conformably underlie the Sokoman Formation, or lie in fault contact with the iron formation (Coates *et al.*, 2012; Conliffe, 2013).

The stratigraphy of the Sokoman Formation in the Julienne Lake Deposit is poorly understood because of its structural complexity, absence of recognizable marker horizons and late-stage alteration. Diamond drilling has recognized a thick (up to 575 m) sequence of oxide-facies iron formation (dominantly coarse-grained, friable quartz specularite schist; Plate 37C, D), interbedded with thin (generally less than 5 m) layers of lean white quartzite and Mn-rich oxide-facies iron formation (Plate 37E; Conliffe, 2013). The base of the Sokoman Formation is marked by strongly altered and brecciated iron formation and most of the primary textures and mineralogy have been destroyed. However, disseminated garnet is recorded in this member (Plate 37F) and Conliffe (2013) interpreted this as representing an altered equivalent of the Basal Silicate Member recognized in the Rose and Scully deposits.

## ***Mineralization***

The mineralogy of the oxide-facies iron formation is predominantly composed of medium- to coarse-grained specular hematite and quartz (with minor red granular hematite, goethite and limonite). Magnetite is generally rare, although several magnetite-rich horizons have been identified (Conliffe, 2013). These magnetite-rich horizons most likely represent remnant magnetite remaining after the transformation of magnetite to martite.

Alteration ranges from minor hematization to intense and pervasive alteration to hematite, goethite and limonite. Zones of intense alteration are distributed through the deposit, even at depths beyond 500 m. Alteration is strongest in brecciated zones or along foliations in banded quartz–specularite schist, and is interpreted to be related to late-stage (post-metamorphic) fluid flow, secondary leaching and/or deep weathering (Conliffe, 2013).

Manganese-rich oxide-iron formation is composed of disseminated specular hematite, quartz and pyrolusite and numerous pyrolusite-bearing veinlets, with Mn contents of up to 26.3% over 0.45 m (drillhole JL-10-27 @ 285.2 m; Coates *et al.*, 2012).

Coates *et al.* (2012) reported the results of metallurgical testwork on a bulk sample from drillholes JL-10-05 and JL-10-05A (total of 190 kg of core). This work demonstrated that it is possible to produce an iron-ore concentrate with an iron content of >66% Fe and a silica content of <5%, with ~75% Fe recovery and ~40% iron weight recovery. Bond Work Index results show that the ore is soft, and autogenous or semi-autogenous grinding was proposed as the preferred approach to milling the ore.

## ***Structure***

Based on variations in structural complexity, lithology, and alteration the deposit has been subdivided into southeastern and northwestern zones (Conliffe, 2013), separated by a north-northeast-trending vertical fault that can be identified on regional aeromagnetic data. The southeastern zone is interpreted as an overturned syncline having a maximum thickness of iron formation of 320 m. The northwestern zone is more structurally complex, and has complicated folding and thrust repetition responsible for thickening of the iron formation to >575 m. This zone is also characterized by more intense alteration and the presence of Mn-rich iron formation.

In all drillholes examined, the lower contact of the Sokoman Formation is strongly brecciated and commonly faulted, possibly representing a basal thrust (Conliffe, 2013). Coates *et al.* (2013) indicated that the southern margin of the deposit was marked by a high-angle fault.

## ***Geophysics***

Regional airborne magnetic surveys (Cotnoir *et al.*, 2002) and ground magnetometer surveys (Seymour *et al.*, 2011; Coates *et al.*, 2012) clearly outline the extent of the Julienne Lake deposit and show that the iron formation extends into Julienne Lake



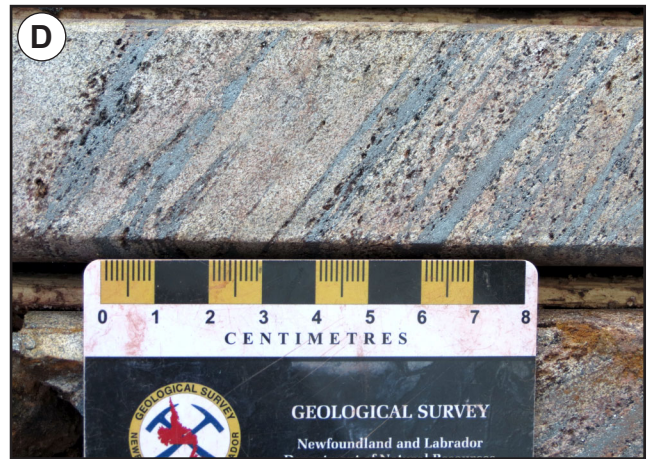
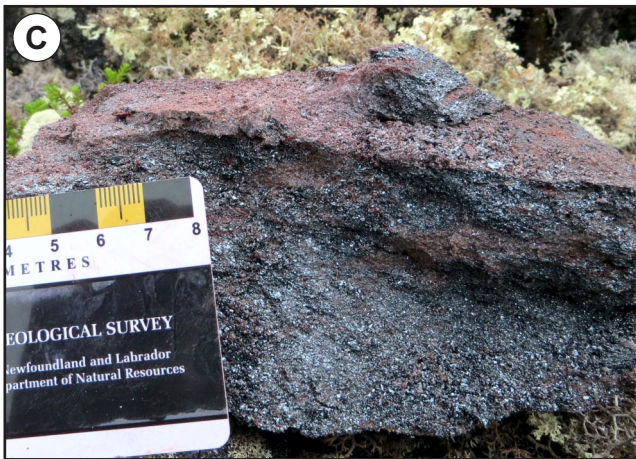


**Plate 37.** A) Aerial view of the Julienne Lake peninsula, looking south. Historic trench (T62-01) exposed on hilltop and Pleistocene-raised beach clearly visible; B) Historical trench (T62-01), with large boulder of folded oxide-facies iron formation; C) Massive, friable oxide-facies iron formation; D) Banded oxide-facies iron formation, with quartz-rich and hematite-rich layers (drillhole JL10-16 @ 53.6 m); E) Gently dipping bed of Mn-rich iron formation, from north end of Trench 10-01; F) Strongly altered Basal Silicate member, with large altered garnets (drillhole JL12-08 @ 85.6 m).

to the east and Wabush Lake to the west (Figure 45). Interpretation of the ground magnetometer survey shows that the magnetic response throughout the deposit is highly variable, and a magnetically elevated trend within the iron formation may represent a single magnetic member (Coates *et al.*, 2012).

### **Resource and/or Reserves**

NI 43-101 compliant resource (Coates *et al.*, 2012).

- Measured resources: 66 Mt at 34.7% iron, 0.38% Mn (cut-off grade = 15% Fe)
- Indicated resources: 801 Mt at 33.6% iron, 0.20% Mn (cut-off grade = 15% Fe)
- Inferred resources: 299 Mt at 34.1% iron, 0.12% Mn (cut-off grade = 15% Fe)

### **History of Exploration**

- 1953: Geological mapping and prospecting (Boyko, 1953)
- 1956: Geological mapping and prospecting, magnetic survey (Gastil, 1956)
- 1957: Diamond drilling (4 drillholes, 562 m, Pickand Matthews & Co., 1959a)
- 1958: Diamond drilling (5 drillholes, 479 m, Pickand Matthews & Co., 1959b)
- 1959: Geological mapping, mineralogical studies and magnetometer surveying (Knowles, 1960), and ore reserve calculation (Canadian Javelin Ltd., 1959)
- 1962: Trenching, test pits and metallurgical study (Knowles *et al.*, 1962)
- 1963: General geological study (Knowles, 1963), ground magnetometer survey (Knowles and Blakeman, 1963) and bulk sample (Knowles, 1967a)
- 1966: Bulk sample (Knowles, 1967b)
- 1970: Prefeasibility study (Magyar, 1970)
- 1975: Julienne Lake Deposit reverts to Exempt Mineral Land (EML)
- 1982: Offshore diamond drilling: 1 drillhole, 66.2 m (Simpson and Bird, 1982)
- 2001: Regional airborne magnetic surveys (Cotnoir *et al.*, 2002)
- 2010: Diamond drilling (42 drillholes, 9238 m), trenching, geological mapping, ground magnetometer survey, metallurgical studies and NI 43-101 compliant resource estimate (Coates *et al.*, 2012)
- 2011: Offshore ground gravity and magnetic survey (Seymour *et al.*, 2011)
- 2012: Offshore diamond drilling (9 drillholes, 1268 m, Seymour *et al.*, 2012; 2013)
- 2013: Concept development study (Churchill *et al.*, 2014)



## 18. KNIGHT

**Alternate Name:** Knights Brook, Knight Main, Northwest Canning Lake, Tup Lake East (and South)

**MODS Showing(s):** 023B/14/Fe028

**Status:** Prospect

**Structural Basin:** Carol

**UTM Zone:** 19

**NTS Area:** 23B/14

**Northing (NAD27):** 5868315

**Easting (NAD27):** 633501

**Latitude:** 52.9498

**Longitude:** -67.0130

**Object Located:** Drillhole KN-06-11

### Description of Occurrence

The Knight prospect is located to the north of Tup Lake (Figure 46), approximately 6.5 km west of Labrador City. Access to the area is by helicopter or by foot *via* a former lumber road off the TLH.

### Geology and Stratigraphy

The geology of the area north of Tup Lake consists of Sokoman Formation iron formation conformably underlain by quartzite of the Wishart Formation (Figure 46). The Sokoman Formation is intruded by Shabogamo Gabbro sills, particularly in areas close to the contacts between the UIF, MIF and LIF.

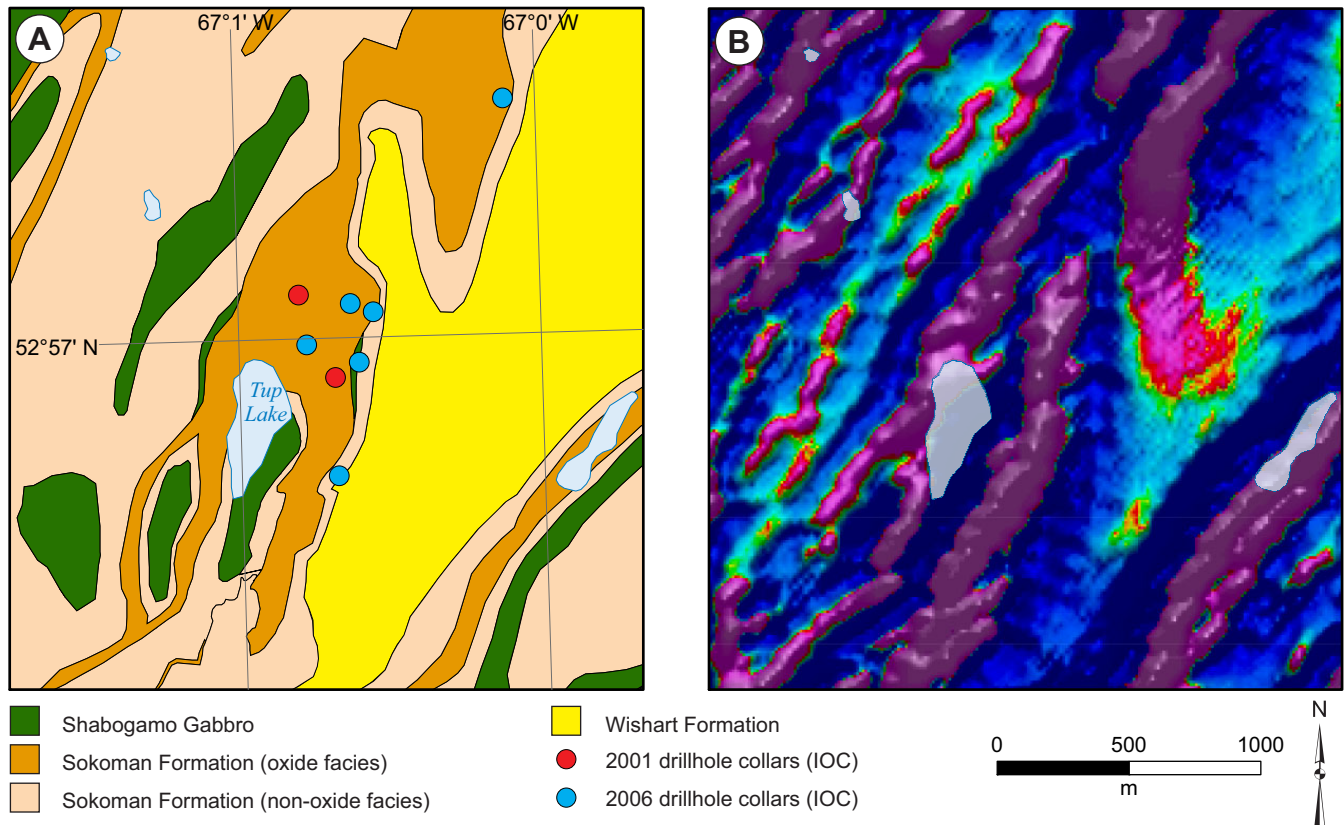


**Figure 46.** A) Geological map of the Knight prospect (adapted from Cotnoir et al., 2002), showing location of drillholes from 2001 and 2006 exploration programs (Cotnoir et al., 2002; Clark, 2007b); B) Airborne magnetics (second vertical derivative) showing extent of iron formation (data from Cotnoir et al., 2002).



Diamond drilling at the Knight prospect intersected significant thicknesses (>250 m) of Sokoman Formation (Clark, 2007b). Carbonate- and silicate-facies iron formation are recorded at the top of some drillholes, or as infolded sections in oxide-facies iron formation, and is interpreted as UIF. Oxide-facies iron formation of the MIF ranges in thickness from 32.6 to 227.75 m, with the thicker sequences interpreted to result from significant structural thickening (Clark, 2007b). Underlying carbonate- and silicate- facies iron formation can be greater than 50 m thick (drillhole KN-06-10), and is interpreted to represent the LIF, based on its stratigraphic position between the MIF and Wishart Formation (Clark, 2007b).

### ***Mineralization***

The oxide-facies iron formation is generally magnetite-rich (Plate 38B, C) with some sections of quartz–magnetite–hematite schists also recorded (Plate 38D–F; Cotnoir *et al.*, 2002; Clark, 2007b). Quartz–hematite schist with accessory anthophyllite and talc was also recorded in some drillholes (Clark, 2007b). Magnetite varies from being fine to coarse grained (Plate 38B), but very coarse-grained magnetite has also been recorded (Plate 38C). Specular hematite is medium to coarse grained. In outcrop, the oxide-facies iron formation is generally weathered, with secondary goethite and limonite staining, whereas in drillcore the oxide-facies iron formation is generally fresh and unaltered. Manganese contents of up to 2.7 wt. % have been recorded, but no pyrolusite or other Mn-oxides have been observed; suggesting that the Mn may be contained within as Mn-carbonate minerals.

Metallurgical testwork available from the Knight prospect includes RMI determination, minus 200 mesh weight fraction and iron weight recovery values from drillcore samples (Cotnoir *et al.*, 2002). Results indicate that oxide-facies iron formation from the Knight prospect is amenable for beneficiation, and has similar or slightly better than the chemical and physical characteristics of IOC ore from the Humphrey deposit (Cotnoir *et al.*, 2002).

Assay results from the Knight prospect have shown significant thickness of ore-grade oxide-facies iron formation, with the highlights including 42.5% Fe over 94.4 m in drillhole KN-01-01 (2.7 to 97.1 m), 37.6% Fe over 66 m in drillhole KN-06-10 (165 to 231 m) and 42.5% Fe over 82 m in drillhole KN-06-11 (151 to 258 m).

### ***Structure***

The structure in the area of the Knight prospect is complex, with an early generation of northwest–southeast-oriented isoclinal folds ( $F_1$ ) refolded by a later more open northeast–southwest structural event ( $F_2$ ) (Darch and Goodman, 2003). Rock units are moderately to steeply southeast dipping, and are interpreted to lie with a shallowly south-southwest-plunging (28–60°)  $F_2$  synclinal structure (Cotnoir *et al.*, 2002). This syncline refolds  $F_1$  isoclinal folds in a west-verging  $F_2$  fold, with the  $F_1$  and  $F_2$  fold axis' roughly parallel (Cotnoir *et al.*, 2002).

### ***Geophysics***

Regional aeromagnetic surveys show that the Knight prospect is located within a strong magnetic high, due to the high magnetite content of oxide-facies iron formation (Cotnoir *et al.*, 2002; Figure 46). Ground gravity surveys show a significant gravity high that is coincident with the aeromagnetic anomaly (Darch and Goodman, 2003).

### **Resource and/or Reserves**

No NI 43-101 compliant mineral resource or reserve estimate available.

Preliminary interpretation based on geological mapping, structural interpretation and regional aeromagnetic survey results have been used to estimate a possible geological resource of 450 Mt with grades ranging from 40 to 45% Fe (Cotnoir *et al.*, 2002).

### **History of Exploration**

- 1949: Geological mapping (Neal, 1950a)
- 1953: Geological mapping (Crouse, 1954)
- 1960: Geological mapping and prospecting, magnetic and gravity surveys (Love, 1961)
- 1972: Aeromagnetic survey (unpublished IOC report)

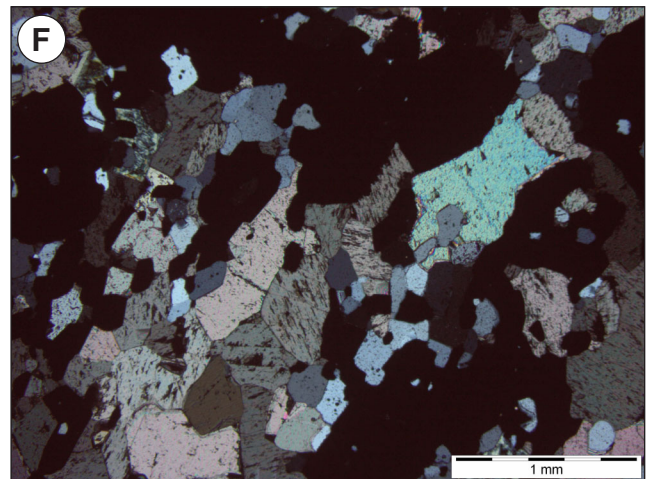
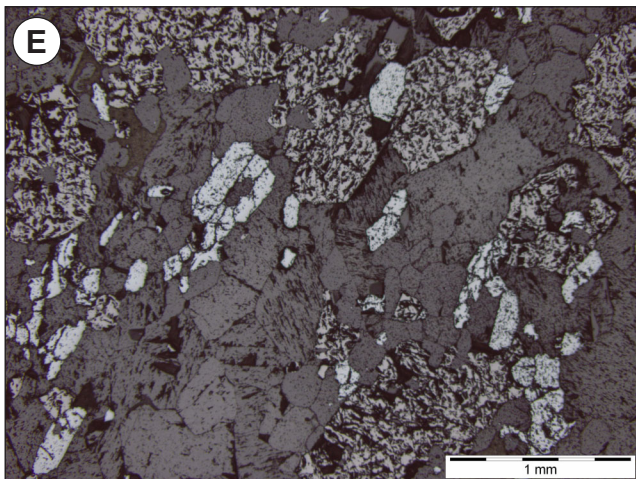


**Plate 38.** A) Typical carbonate-silicate-facies iron formation from the LIF (drillhole KN-06-A @ 227.7 m); B) Typical quartz-magnetite oxide-facies iron formation (drillhole KN-06-A @ 161.5 m); C) Quartz-magnetite oxide-facies iron formation with very coarse-grained clots of magnetite (drillhole KN-06-A @ 219.5 m); D) Quartz-carbonate-magnetite-hematite oxide-facies iron formation (drillhole KN-06-A @ 166.5 m); E) Photomicrograph of oxide-facies iron formation with magnetite and hematite and gangue quartz, carbonate and minor Fe-silicates (drillhole KN-06-A @ 166.5 m, reflected light); F) Same view as (E), in cross-polarized light.

- 1982: Airborne geophysical surveys (EM, magnetics, radiometrics, Johnson, 1982)
- 2000: Data compilation, structural synthesis (Hulstein and Lee, 2001)
- 2001: Data compilation, geological mapping and prospecting, diamond drilling (2 drillholes, 459 m), ground gravity survey, regional airborne magnetic surveys, structural/ stratigraphic interpretation (Cotnoir *et al.*, 2002)
- 2002: Geological mapping and prospecting, structural interpretation, ground gravity survey (Darch and Goodman, 2003)
- 2006: Diamond drilling (6 drillholes, 1373 m, Clark, 2007b)



## 19. KNIGHT NORTH

**Alternate Name:** Knights Brook, West Leg Lake, Leg Lake

**MODS Showing(s):** 023B/15/Fe006

**Status:** Showing

**Structural Basin:** Carol

**UTM Zone:** 19

**NTS Area:** 23B/15

**Northing (NAD27):** 5869906

**Easting (NAD27):** 634155

**Latitude:** 52.9639

**Longitude:** -67.0026

**Object Located:** 2001 IOC sample location

### Description of Occurrence

The Knight North showing is located west of Leg Lake (Figure 47), and approximately 6 km northwest of Labrador City. There is no road access, and access is by foot *via* a former lumber road off the TLH, or by helicopter.

### Geology and Stratigraphy

The Knight North showing is located ~3 km to the north of the Knight showing, along strike in the same belt of Sokoman Formation iron formation. The stratigraphy consists of Sokoman Formation conformably overlying Wishart Formation quartzite and schists of the Le Fer Formation. The Sokoman Formation is intruded by a number of Shabogamo Gabbro sills.

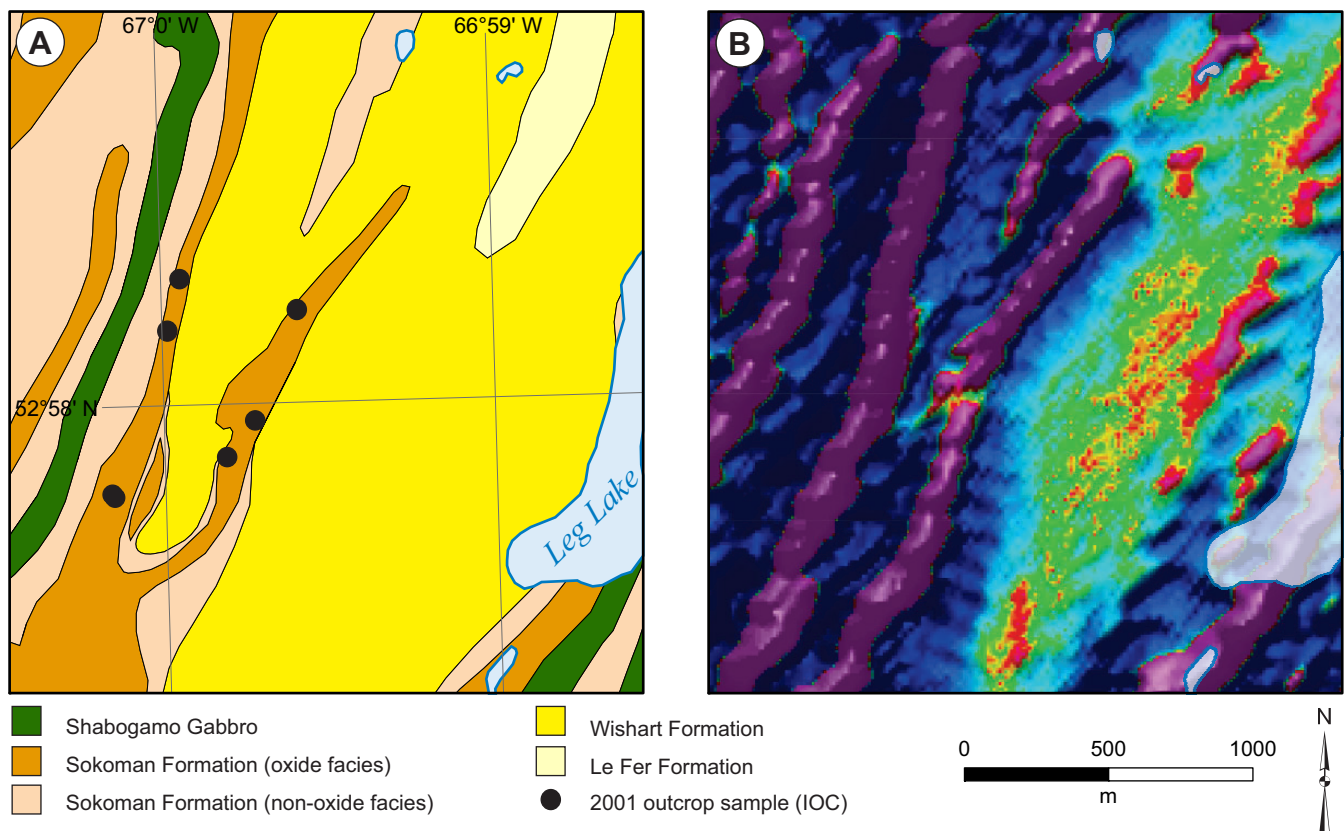


**Figure 47.** A) Geological map of the Knight North showing (adapted from Cotnoir et al., 2002), showing outcrop sample locations from 2001 exploration programs (Cotnoir et al., 2002); B) Airborne magnetics (second vertical derivative) showing extent of iron formation (data from Cotnoir et al., 2002).

No information is available on the stratigraphy of the Sokoman Formation at the Knight North showing, but it is likely similar to the stratigraphy described from the Knight showing (Cotnoir *et al.*, 2002).

### ***Mineralization***

Oxide-facies iron formation outcrops sporadically throughout the Knight North area, and consists of friable quartz–magnetite–hematite.

There is no published metallurgical testwork available from the Knight North showing, but the minus 200 mesh weight percent fraction and iron weight recovery of outcrop samples are similar to the Knight prospect, and within IOC’s chemical and physical crude-ore characteristics (Cotnoir *et al.*, 2002).

No drillholes have been completed on the Knight North showing. A number of oxide-facies iron formation samples were collected as part of a regional assessment in 2001 (Cotnoir *et al.*, 2002). A total of 7 samples were collected, with an average Fe content of 38.9% and 22.95% magnetite (determined by Satmagan).

### ***Structure***

Mapping and aeromagnetic data suggest that the Knight North showing occurs in a similar structural setting to the Knight showing, with oxide-facies iron formation located along the flank or limbs of  $F_2$  folds, within a northeast-plunging  $F_2$  synclinal structure. Cotnoir *et al.* (2002) suggested that the presence of tight  $F_1$ – $F_2$  interference structures at the Knight North showing may have resulted in structural thickening.

### ***Geophysics***

Regional aeromagnetic surveys show that the Knight North showing is located within a strong magnetic high (Cotnoir *et al.*, 2002; Figure 47). Ground gravity surveys show a gravity high that is coincident with the aeromagnetic anomaly (Darch and Goodman, 2003).

## **Resource and/or Reserves**

No NI 43-101 compliant mineral resource or reserve estimate available.

## **History of Exploration**

- 1949: Geological mapping (Neal, 1950a)
- 1953: Geological mapping (Crouse, 1954)
- 1960: Geological mapping and prospecting, magnetic and gravity surveys (Love, 1961)
- 1972: Aeromagnetic survey (unpublished IOC report)
- 1982: Airborne geophysical surveys (EM, magnetics, radiometrics, Johnson, 1982)
- 2000: Data compilation, structural synthesis (Hulstein and Lee, 2001)
- 2001: Data compilation, geological mapping and prospecting, regional airborne magnetic surveys, structural/stratigraphic interpretation (Cotnoir *et al.*, 2002)
- 2002: Structural interpretation, ground gravity survey (Darch and Goodman, 2003)

## 20. KNIGHT SOUTH

*Alternate Name:* n/a

*MODS Showing(s):* 023B/14/Fe019

*Status:* Prospect

*Structural Basin:* Carol

*UTM Zone:* 19

*NTS Area:* 23B/14

*Northing (NAD27):* 5866416

*Easting (NAD27):* 632802

*Latitude:* 52.9329

*Longitude:* -67.0242

*Object Located:* Drillhole KN-02-06

### Description of Occurrence

The Knight South prospect surrounds Throne Lake, approximately 8 km west of Labrador City. It is located ~1 km to the west of the TLH (Figure 48), with access on foot *via* small trails or by helicopter.

### Geology and Stratigraphy

The geology of the Knight South area is similar to that of the Knight area, located 2–3 km to the north along strike. The surface geology consists predominantly of Sokoman Formation iron formation, with the UIF and LIF intruded by gabbro sills

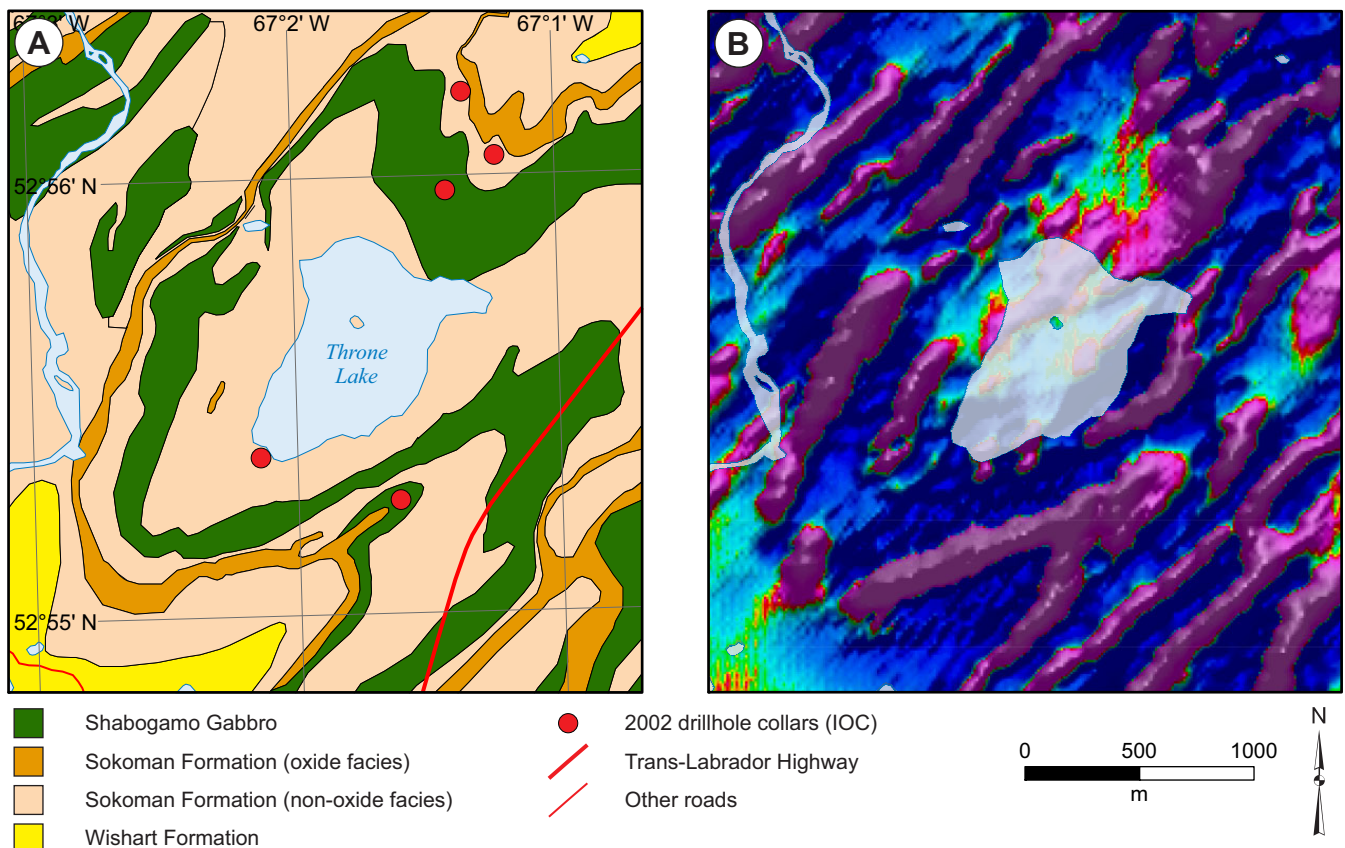


**Figure 48.** A) Geological map of the Knight South prospect (adapted from Cotnoir et al., 2002), showing location of drillholes from 2002 exploration program (Darch and Goodman, 2003); B) Airborne magnetics (second vertical derivative) showing extent of iron formation (data from Cotnoir et al., 2002).



of the Shabogamo Gabbro (Darch and Goodman, 2003). The Sokoman Formation conformably overlies the Wishart Formation south of Throne Lake (Figure 48).

Geological mapping and diamond drilling record a full sequence of Sokoman Formation iron formation at the Knight South prospect. The UIF intercepted in all of the drillholes completed in 2002, consists of quartz–carbonate–grunerite/ actinolite–magnetite schists. The upper and lower parts of the UIF are rich in Fe-silicates and fine-grained bands and disseminations of magnetite, and the middle portion of the UIF is rich in carbonate minerals with rare magnetite (Darch and Goodman, 2003). Thin (17.7 to 24 m) oxide-facies iron formation, interpreted as representing MIF, has been reported from four of the five 2002 drillholes. These intervals consist of well-banded, fine- to medium-grained quartz–magnetite–hematite schists. The LIF was not intercepted during drilling in 2002, but mapping shows the silicate and carbonate facies LIF outcrops to the south and west of Throne Lake, where it conformably overlies quartzite of the Wishart Formation (Darch and Goodman, 2003).

### ***Mineralization***

The oxide-facies iron formation is magnetite-rich, with only minor specular hematite (Darch and Goodman, 2003). The magnetite is generally fine to medium grained, and occurs in discrete bands alternating with quartz, carbonate, grunerite and actinolite. No significant alteration of the iron formation has been recorded, and assay data from drillcore show that the Mn content of oxide-facies iron formation is generally <1%.

Darch and Goodman (2003) reported on RMI determination, minus 200 mesh weight fraction and iron weight recovery values from drillcore samples. These data show that oxide-facies iron formation is relatively hard grinding (high RMI) and has lower minus 200 mesh weight fraction and iron weight recovery values than IOC's chemical and physical crude-ore characteristics (Cotnoir *et al.*, 2002).

Assay results from the 2002 drilling program indicate thick sequences of iron-rich rocks (up to 106.6 m of 35.4% Fe in drillhole KN-02-06; Darch and Goodman, 2003). However, these include thick sequences of silicate- and carbonate-facies iron formation. The best results from oxide-facies iron formation included 42.2% Fe over 24 m in drillhole KN-02-03 (67.9 to 91.9 m), 37.3% Fe over 20.3 m in drillhole KN-02-06 (232.3 to 252.6 m) and 40.2% Fe over 22.5 m in drillhole KN-02-07 (57.5 to 80 m).

### ***Structure***

The structural geology of the Knight South prospect has been described, in detail, by Darch and Goodman (2003). The prospect is located in the central portion of a  $F_1/F_2$  interference structure, which is a result of  $F_2$  folding of a large (several hundred metres wide), southwest-verging,  $F_1$  synclinorium (Darch and Goodman, 2003). The synclinorium is composed of a number of minor syncline/anticline pairs that follow the main structure around the broad  $F_2$  folds, with Shabogamo Gabbro sills and UIF occurring in the keels of isoclinal  $F_1$  folds. Although only thin sequences of MIF were encountered during drilling, this interpretation indicates that relatively thick sequences of MIF may have formed by structural thickening (Darch and Goodman, 2003).

### ***Geophysics***

Regional airborne magnetic surveys (Cotnoir *et al.*, 2002) have shown a large magnetic anomaly around Throne Lake (Figure 48), which coincides with abundant iron formation in outcrop. A ground gravity survey has identified a broad, strong gravity anomaly over Throne Lake representing a thick sequence of MIF (Darch and Goodman, 2003).

### **Resource and/or Reserves**

No NI 43-101 compliant mineral resource or reserve estimate available.

### **History of Exploration**

- 1949: Geological mapping (Neal, 1950a)
- 1953: Geological mapping (Crouse, 1954)

- 1960: Geological mapping and prospecting, magnetic and gravity surveys (Love, 1961)
- 1972: Aeromagnetic survey (unpublished IOC report)
- 1979: Diamond drilling (3 drillholes, 107 m) (Grant, 1979e)
- 1982: Airborne geophysical surveys (EM, magnetics, radiometrics; Johnson, 1982)
- 2000: Data compilation, structural synthesis (Hulstein and Lee, 2001)
- 2001: Data compilation, geological mapping and prospecting, regional airborne magnetic surveys, structural/stratigraphic interpretation (Cotnoir *et al.*, 2002)
- 2002: Geological mapping and prospecting, petrographic study, structural interpretation, ground gravity survey, diamond drilling (5 drillholes 1161.2 m, Darch and Goodman, 2003)

## 21. LORRAINE 4

**Alternate Name:** Lorraine No. 4

**MODS Showing(s):** 023G/02/Fe008

**Status:** Prospect

**Structural Basin:** Carol

**UTM Zone:** 19

**NTS Area:** 23G/02

**Northing (NAD27):** 5883410

**Easting (NAD27):** 642180

**Latitude:** 53.0832

**Longitude:** -66.8772

**Object Located:** MODS Occurrence

### Description of Occurrence

The Lorraine 4 prospect is located on a ridge between Lorraine Lake and Wabush Lake (Figure 49), to the west of IOC's Carol Lake Mine. It is approximately 15 km north of Labrador City. There is no road access to the area, and access is by boat from Wabush Lake, helicopter or by foot or ATV from the IOC mine area.

### Geology and Stratigraphy

The Lorraine 4 prospect occurs at the northern end of a belt of Sokoman Formation iron formation (Figure 49), which also encompasses the Wabush 6 deposit and Mill Basin, Wabush 4 and Canning prospects (Darch *et al.*, 2003a). The Sokoman

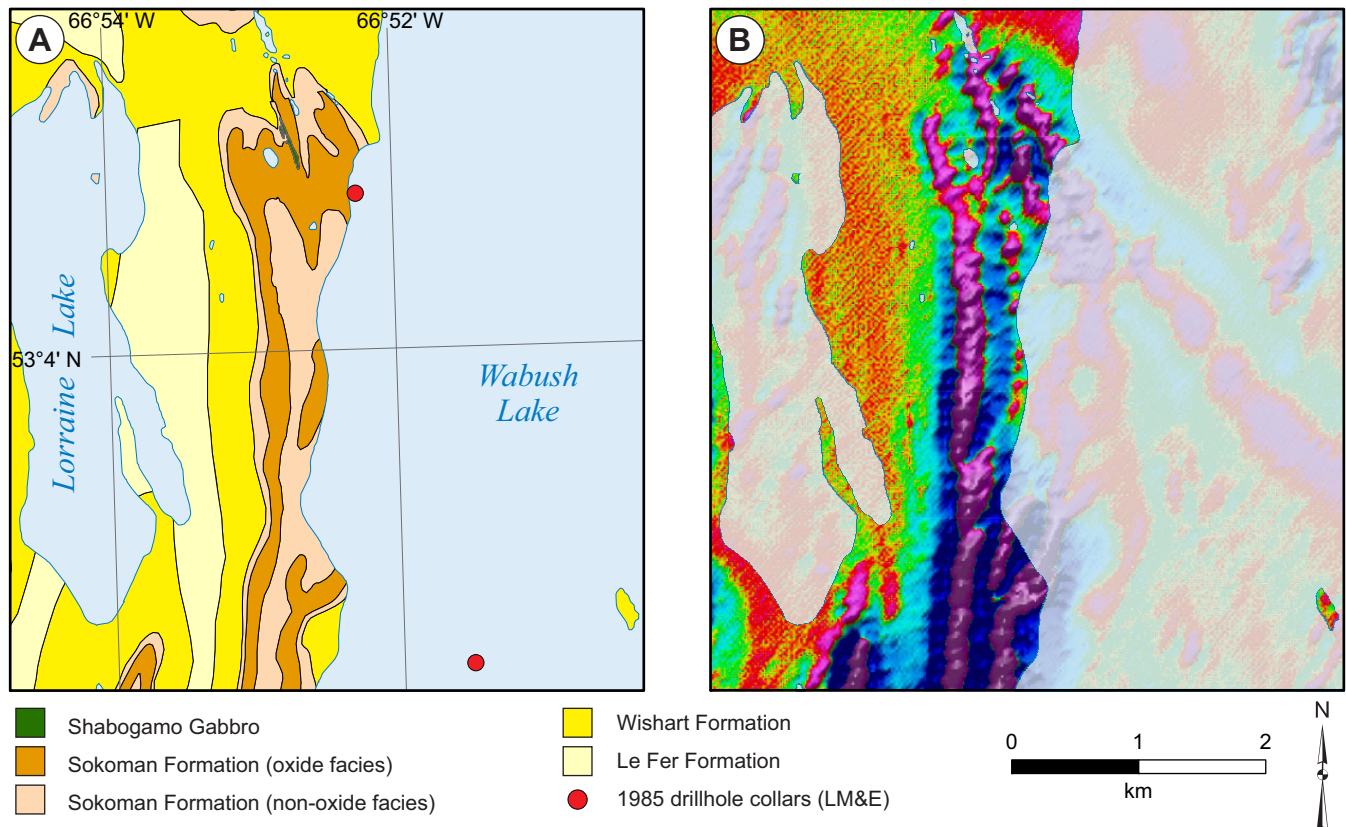


**Figure 49.** A) Geological map of the Lorraine 4 prospect (adapted from Cotnoir *et al.*, 2002), showing location of drillholes from 1985 exploration program (Simpson *et al.*, 1985); B) Airborne magnetics (second vertical derivative) showing extent of iron formation (data from Cotnoir *et al.*, 2002).



Formation is conformably underlain by Wishart Formation quartzite, which in turn overlies schist of the Le Fer Formation. A number of Shabogamo Gabbro sills occur to the north of the prospect.

Little is known about the stratigraphy of the Sokoman Formation in this area, but it is likely similar to the stratigraphy of the Sokoman Formation at the Wabush 6 deposit located 8 km south of the Lorraine 4 prospect.

### ***Mineralization***

Outcrops of oxide-facies iron formation in the Lorraine 4 area consist predominantly of quartz–hematite–magnetite schist, with hematite > magnetite (Neal, 1951; Thorniley, 1959). Diamond drilling in the Wabush Lake area to the east of the property has intersected predominantly oxide-facies iron formation over 112 m, with thin (<5 m) intervals of carbonate-facies iron formation and Shabogamo Gabbro (Simpson *et al.*, 1985).

Geological mapping and diamond drilling have shown that the Sokoman Formation is commonly moderately altered, with abundant goethite recorded in outcrop at the northern portion of the prospect (Thorniley, 1959) and Simpson *et al.* (1985) reporting on multiple goethite-rich zones intercepted during diamond drilling.

There is no published metallurgical testwork available from the Lorraine 4 prospect.

No assay data is available from drilling on the Lorraine 4 prospect. Thorniley (1959) reported assay data from 262 chip and outcrop samples from across the orebody, which averaged 37.88% Fe.

### ***Structure***

Geological mapping at Lorraine 4 indicates that the prospect is located in a north-trending F<sub>2</sub> syncline, with outcrops uniformly dipping to the east (Thorniley, 1959). Thorniley (1959) noted numerous drag folds in outcrop, and correlations with the Wabush 6 deposit suggest that F<sub>1</sub>/F<sub>2</sub> fold interference may be associated with structural thickening of the MIF.

### ***Geophysics***

The Lorraine 4 prospect is associated with a moderate magnetic anomaly on regional airborne magnetic surveys (Figure 49; Cotnoir *et al.*, 2002). However, the intensity of the magnetic anomaly decreases toward the north of the prospect, which is likely due to the relatively high proportion of hematite in the MIF. This is consistent with results of a ground magnetometer survey that identified a subdued anomaly across the Lorraine 4 prospect (Price, 1979).

### **Resource and/or Reserves**

No NI 43-101 compliant mineral resource or reserve estimate available.

Non 43-101 compliant historical estimates, based on limited data, of 218 Mt grading 37% Fe were reported by Elliot *et al.* (1980).

### **History of Exploration**

- 1949: Geological mapping (Neal, 1950a)
- 1950: Geological mapping (Neal, 1951)
- 1957: Geological mapping (Mumtazuddin, 1957)
- 1959: Geological mapping, sampling and dip needle survey (Thorniley, 1959)
- 1972: Aeromagnetic survey (unpublished IOC report)
- 1978: Ground magnetometer survey (Price, 1979g)
- 1985: Diamond drilling (1 drillhole, 112.1 m, Simpson *et al.*, 1985)
- 2000: Data compilation, structural synthesis (Hulstein and Lee, 2001)
- 2001: Data compilation, regional airborne magnetic surveys, structural/stratigraphic interpretation (Cotnoir *et al.*, 2002)

## 22. LUCE

**Alternate Name:** Luce No. 1, Hakim Lake Showing, Luce South, Luce Main, Luce Basin

**MODS Showing(s):** 023G/02/Fe005

**Status:** Producer

**Structural Basin:** Carol

**UTM Zone:** 19

**NTS Area:** 23G/02

**Northing (NAD27):** 5874676

**Easting (NAD27):** 637970

**Latitude:** 53.0058

**Longitude:** -66.9438

**Object Located:** Approximate centre of Luce Pit

### Description of Occurrence

The Luce deposit is located in IOC's Carol Lake Mine area, directly south of Luce Lake (Figure 50) and approximately 8 km north of Labrador City. Access to the deposit is *via* a series of mine roads that extend north from IOC's Concentrator and Pellet Plant. The deposit is subdivided into three pits, Luce South (Plate 39A), Luce Main and Luce Basin (Figure 50).

### Geology and Stratigraphy

The bedrock geology of the Luce deposit is dominated by Sokoman Formation iron formation, and is conformably underlain by quartzite of the Wishart Formation (Figure 51). The Sokoman Formation is intruded by a number of Shabogamo Gabbro sills.

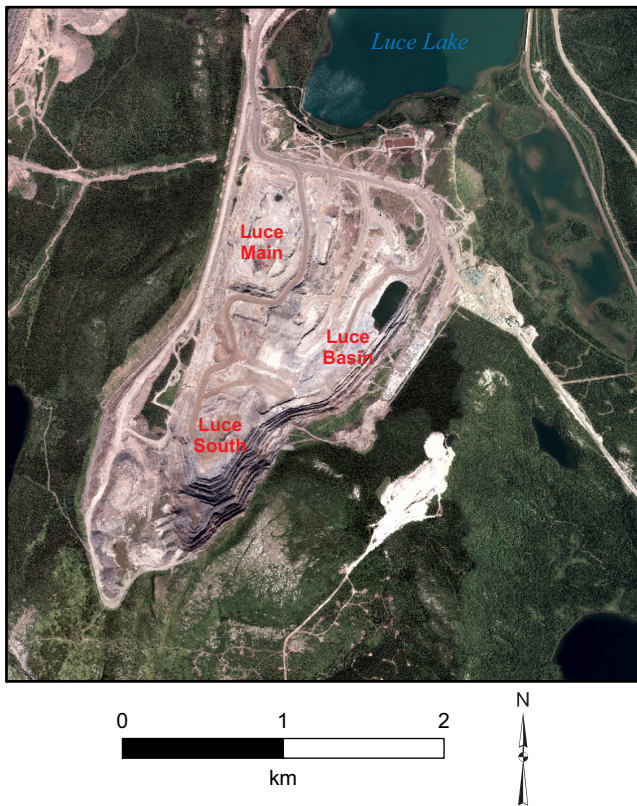


**Figure 50.** Aerial photograph of the Luce deposit, showing location of the Luce South, Luce Main and Luce Basin pits (image courtesy of IOC).

The stratigraphy of the Sokoman Formation has been described by Muwais (1974) and is similar to the stratigraphy of the Humphry deposit. The lower and upper iron formations are predominantly composed of carbonate- and silicate-facies iron formation, with a band of oxide-facies iron formation located in the LIF. The MIF is an oxide-facies unit, and has a vertical zonation with a magnetite-rich lower section and a hematite-rich upper section.

### Mineralization

Oxide-facies iron formation consists predominantly of hematite, magnetite and gangue quartz and carbonate minerals (Preziosi, 2001). The relative proportions of hematite and magnetite vary throughout the deposit. There is a general vertical zonation with high-magnetite ore (Plate 39B) at the base of the MIF and low-magnetite, hematite-rich ore (Plate 39C, D) in the upper part of the MIF. The Luce Main pit has a higher proportion of coarser grained, hematite-rich low-magnetite ore, whereas the Luce Basin and Luce South have a higher proportion of finer grained, high-magnetite ore (Preziosi, 2001; Bulled *et al.*, 2009).

Alteration is variable, with a high limonite (goethite-rich) zone in the western portion of the ore body (Plate 39E), possibly associated with late-stage fluid movement along faults.

Ore from the Luce deposit is processed at IOC's Concentrator and Pellet Plant. Preziosi (2001) stated that bulk



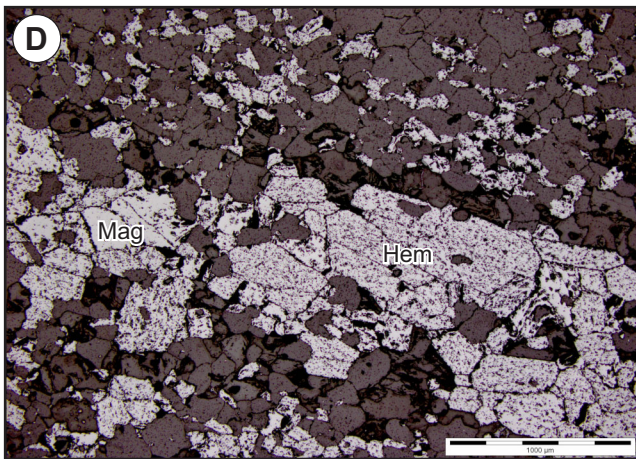


**Plate 39.** A) View of the Luce deposit, looking north from observation point above Luce South pit; B) Typical fine-grained, magnetite-rich oxide-facies iron formation (drillhole LU-10-62 @ 91 m); C) Medium-grained, friable hematite-rich oxide-facies iron formation (drillhole LU-10-77 @ 62 m); D) Photomicrograph of hematite-rich oxide-facies iron formation, with hematite (light grey) and magnetite (pink grey) crystals (drillhole LU-10-77 @ 62 m); E) Strongly altered, goethite-rich iron formation from west wall of Luce Main pit (drillhole LU-13-364 @ 207 m).



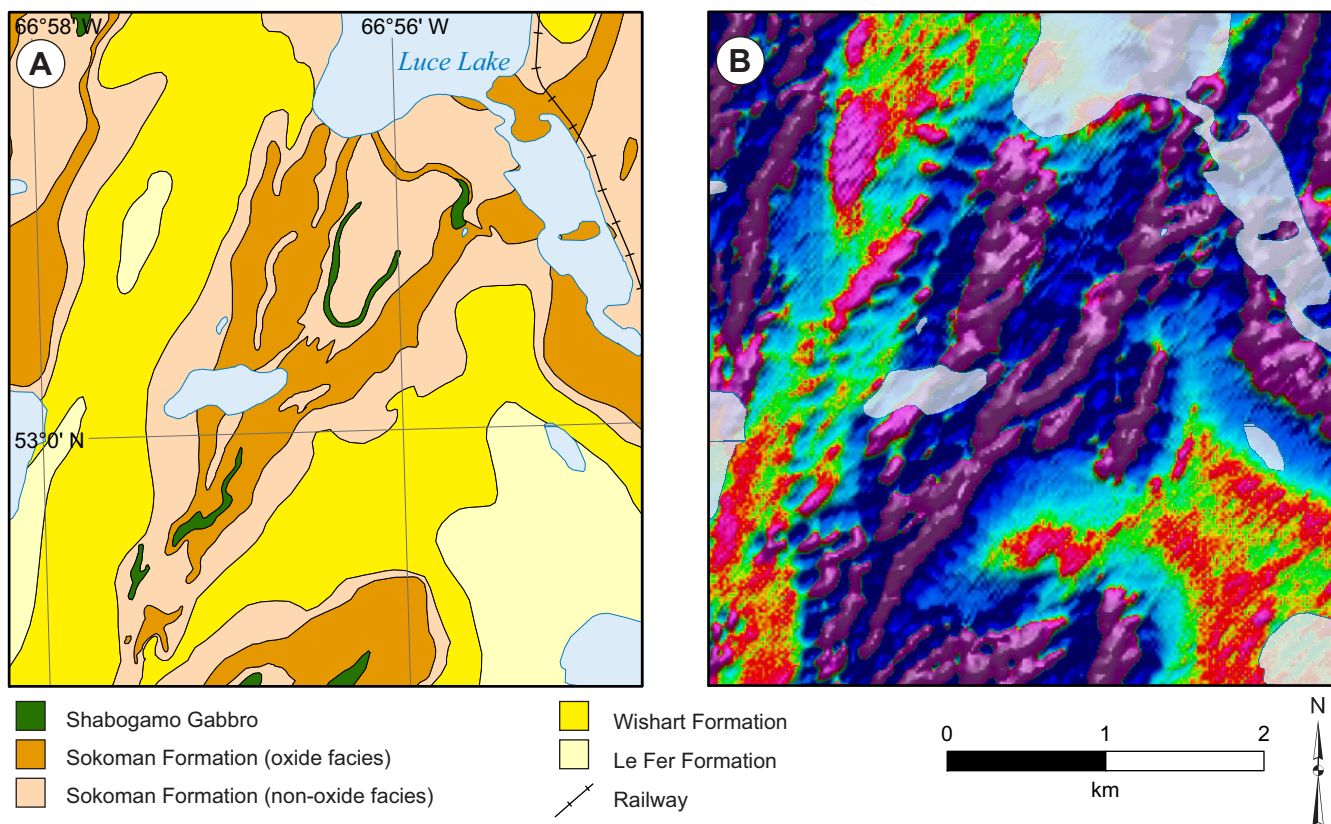


**Figure 51.** A) Geological map of the Luce deposit (adapted from Cotnoir et al., 2002); B) Airborne magnetics (second vertical derivative) showing extent of iron formation (data from Cotnoir et al., 2002).

sample testing in 1996 and 1997 indicated good mineral liberation, wet mill grinding and throughput parameters, and spiral concentrates had similar values to ore from the Humphrey deposit, with 67% Fe and low concentrations of SiO<sub>2</sub> (3.7%), Mn (0.1%), Al<sub>2</sub>O<sub>3</sub> (0.21%) and TiO<sub>2</sub> (0.05%). Bulled *et al.* (2009) reported that the coarser grained, low-magnetite ore was generally softer than the finer grained, high-magnetite ore (average SAG Power Index of 11 and 23 minutes, respectively).

### Structure

The Luce deposit is located in a broad, open north–northeast-trending syncline that plunges gently to the north, with a minor anticline separating the Luce Main pit to the west and the Luce Basin pit to the east. Detailed examination illustrates that the structure of the deposit is complex with interference of F<sub>1</sub> and F<sub>2</sub> folds resulting in significant structural thickening of the MIF oxide-facies iron formation in the keels of the synclines (Cotnoir *et al.*, 2002).

### Geophysics

The Luce deposit is associated with a strong magnetic anomaly on regional aeromagnetic surveys (Cotnoir *et al.*, 2002; Figure 51), which is due to the high magnetite content of the lower section of the MIF.

### Resource and/or Reserves

NI 43-101 compliant reserves (Iron Ore Company of Canada, 2014).

- Proven reserves: 350 Mt at 37% Fe
- Probable reserves: 212 Mt at 37% Fe

NI 43-101 compliant resource (Iron Ore Company of Canada, 2014). Mineral Resources exclude Mineral Reserves.

- Measured resources: 38 Mt at 37% Fe
- Indicated resources: 62 Mt at 37% Fe
- Inferred resources: 37 Mt at 36% Fe

### **History of Exploration**

- 1949: Geological mapping (Neal, 1950a)
- 1950: Geological mapping (Neal, 1951)
- 1957: Geological mapping (Mumtazuddin, 1957)
- 1958: Geological mapping (referenced in Klein, 1959)
- 1959: Sampling, dip needle survey (Klein, 1959)
- 1960: Diamond drilling (4 drillholes, 371 m, MacDonald, 1961)
- 1972: Aeromagnetic survey (unpublished IOC report)
- 1973: Geological mapping, diamond drilling (20 drillholes, 3262 m), clearing and overburden stripping (Stubbins, 1974), ground gravity and magnetometer surveys (Iron Ore Company of Canada, 1973)
- 1974: Diamond drilling (20 drillholes, 5292 m, Stubbins, 1975), stratigraphic interpretation (Muwais, 1974)
- 1975: Diamond drilling (28 drillholes, 6542 m, Stubbins, 1976), ground gravity and magnetometer survey (Iron Ore Company of Canada, 1975)
- 1995: Revised geological interpretation, diamond drilling (12 drillholes, 3189 m)
- 1996: Diamond drilling (26 drillholes, 4911 m)
- 1997: Diamond drilling (58 holes, 9408 m), bulk sample
- 1999: Production commences at Luce South Pit
- 2001: Development plan for Luce Pit registered (Preziosi, 2001), regional airborne magnetic surveys, structural/stratigraphic interpretation (Cotnoir *et al.*, 2002)

### 23. MILL BASIN

**Alternate Name:** Wabush 8, Wabush #8, Wabush No. 8, Mile 2, Mill

**MODS Showing(s):** 023B/15/Fe005, 023B/15/Fe011

**Status:** Prospect

**Structural Basin:** Carol

**UTM Zone:** 19

**NTS Area:** 23B/15

**Northing (NAD27):** 5871055

**Easting (NAD27):** 641925

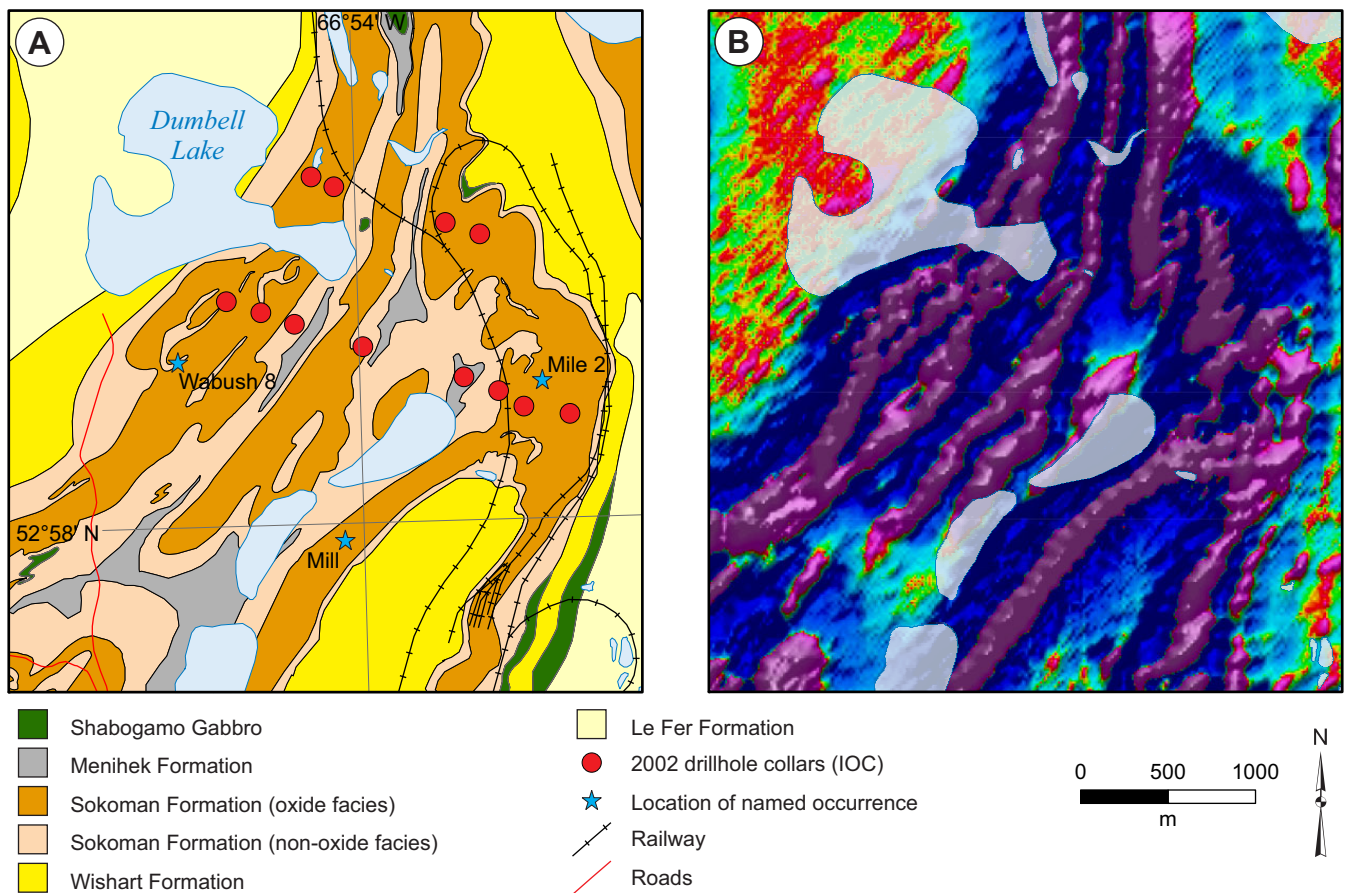
**Latitude:** 52.9722

**Longitude:** -66.8865

**Object Located:** Drillhole MD-02-02

#### Description of Occurrence

The Mill Basin prospect refers to a large exposure of iron formation that outcrops to the north and west of the IOC's Concentrator and Pellet Plant. It was previously subdivided into the Wabush 8, Mile 2 and Mill prospects (Figure 52), but as these represent limbs of the same syncline they are grouped together here as the Mill Basin prospect. The prospect is located approximately 3 km north of Labrador City, and access is *via* a series of gravel roads accessing the IOC's Concentrator and Pellet Plant (Mill and Mile 2 showings) and the Menihok Nordic Ski Club.





## ***Geology and Stratigraphy***

The Mill Basin prospect is located along strike from the Wabush 4 prospect to the south and Wabush 6 deposit to the north. The bedrock geology is dominated by Sokoman Formation iron formation (Figure 52), and diamond drilling has shown that it is conformably overlain by graphitic schist of the Menihek Formation (Darch *et al.*, 2003a). Wishart Formation quartzite conformably underlies the iron formation, and forms a series of prominent hills to the west of the Mill Basin prospect, whereas Le Fer Formation quartz–feldspar–biotite gneiss occurs at the base of the stratigraphy. Shabogamo Gabbro sills have been mapped to the east of the Mill Basin prospect, where they intrude the upper part of the Sokoman Formation.

The stratigraphy of the Sokoman Formation iron formation is similar to that recorded in the Wabush 4 prospect and Wabush 6 deposit. The UIF is predominantly composed of carbonate-facies iron formation, with minor silicate- and oxide-facies intervals. The MIF is subdivided into an upper unit of hematite-rich oxide-facies iron formation and a lower magnetite-rich unit (Darch *et al.*, 2003a). These are separated by a 15- to 35-m-thick interval of coarse-grained silicate-facies iron formation (Darch *et al.*, 2003a). The LIF consists of carbonate- and silicate-facies iron formation, with numerous thin (<10 m) intervals of oxide-facies iron formation (Darch *et al.*, 2003a).

## ***Mineralization***

Thick (>400 m) intervals of oxide-facies iron formation have been intersected during diamond drilling on the eastern part of the Mill Basin prospect, with drilling farther west intersecting only thin (typically <40 m) sequences of oxide-facies iron formation. This is consistent with structural thickening on the eastern limb of the syncline (*see below*). The upper, hematite-rich part of the MIF is generally lower grade (28–32% Fe), with the lower, magnetite section having higher grades (generally 36% Fe; Darch *et al.*, 2003a).

In drillcore, the oxide-facies iron formation is generally fresh and unaltered. Manganese-contents are highly variable, but generally increase toward the base of the MIF. Rhodochrosite was visually identified in drillcore and is associated with Mn values of 9.85% Mn over 8 m (drillhole MD-02-10 @ 29.5 m; Darch *et al.*, 2003a).

Metallurgical testwork available from the Mill Basin prospect includes RMI determination, minus 200 mesh weight fraction and iron weight recovery values from drillcore samples (Darch *et al.*, 2003a). These data show that oxide-facies iron formation has low to moderate –200 mesh weight fraction and iron weight recovery values and highly variable RMI values, with high values (hard grinding ore) associated with carbonate and Fe-silicate rich sections.

Assay results from the Mill Basin prospect have shown that the Fe grade is extremely variable, with the highlights including 35.8% Fe over 293.8 m in drillhole MD-02-01 (94.2 to 300 m) and 31.8% Fe over 161.8 m in drillhole MD-02-02 (240.2 to 400.2 m).

## ***Structure***

The Mill Basin prospect is located in a broad, open  $F_2$  synform, with the Wabush 8 prospect located on the western arm of the synform and the Mill and Mile 2 prospects located on the eastern arm. Geological mapping and diamond drilling have shown that the structure is complicated by interference of the  $F_1$  and  $F_2$  folds, with frequent in-folded sections of both LIF and UIF in the MIF. Structural thickening along the eastern limb of the synform has resulted in substantial thickening of the MIF (Darch *et al.*, 2003a).

## ***Geophysics***

A strong aeromagnetic anomaly coincides with the Mill Basin prospect (Figure 52; Cotnoir *et al.*, 2002). Ground gravity surveys have identified a strong gravity anomaly along the eastern limb of the synform that corresponds to the thickest intersections of oxide-facies iron formation encountered during drilling, and modelling of gravity data indicates that the greatest potential for a viable large tonnage iron deposit is along the structurally thickened eastern limb (Darch *et al.*, 2003a).

### **Resource and/or Reserves**

No NI 43-101 compliant mineral resource or reserve estimate available.

Non 43-101 compliant historical estimates, based on limited data, of 150 Mt grading 35% Fe for the Wabush 8 prospect and 39 Mt grading 32.8% Fe for the Mile 2 prospect were reported by Elliot *et al.* (1980). However, these estimates may underestimate the tonnage potential of Mill Basin prospect, particularly on the eastern limb of the synform where there is significant structural thickening of the MIF (Darch *et al.*, 2003a).

### **History of Exploration**

- 1949: Geological mapping (Neal, 1950a)
- 1950: Geological mapping (Neal, 1951)
- 1957: Geological mapping (Mumtazuddin, 1957)
- 1959: Geological mapping, dip needle survey (Leuner and Skimmer, 1959)
- 1961: Geological mapping, ground magnetometer survey (Macdonald and Hogg, 1962)
- 1972: Aeromagnetic survey (unpublished IOC report)
- 1977: Ground magnetometer survey (Price, 1977), diamond drilling (3 drillholes, 270 m, Atkinson, 1978)
- 1978: Ground magnetometer survey (Price, 1979)
- 2000: Data compilation, structural synthesis (Hulstein and Lee, 2001)
- 2001: Data compilation, regional airborne magnetic surveys, structural/stratigraphic interpretation (Cotnoir *et al.*, 2002)
- 2002: Geological mapping and prospecting, diamond drilling (12 drillholes, 2960 m), ground gravity survey (Darch *et al.*, 2003a)

## 24. MILLS LAKE

**Alternate Name:** Kami, Mills No. 1, Mills Lake No. 1, Kelly-Clavin Showing, Molar Lake

**MODS Showing(s):** 023B/14/Fe002

**Status:** Developed Prospect

**Structural Basin:** Mills Lake

**UTM Zone:** 19

**NTS Area:** 23B/14

**Northing (NAD27):** 5851399

**Easting (NAD27):** 634485

**Latitude:** 52.7976

**Longitude:** -67.0053

**Object Located:** Drillhole K-10-95

### Description of Occurrence

The Mills Lake deposit is located between Mills Lake and Molar Lake (Figure 53), approximately 17 km south of Labrador City and 6 km east of Fermont. The area is accessible *via* a number of small 4x4 roads from Labrador City.

### Geology and Stratigraphy

The area between Mills Lake and Molar Lake is predominantly underlain by Denault Formation marble and Sokoman Formation iron formation (Figure 53A). Previous geological mapping had indicated that the Le Fer Formation schist outcropped on the western shore of Mills Lake (Figure 53B); however, recent re-interpretations indicate that Le Fer Formation is not present (Figure 53A; Lyons and Velcic, 2013). The Wishart Formation, which conformably underlies the Sokoman Formation, is generally thin (<20 m; Grandillo *et al.*, 2012) and is not represented on the geological maps.

The base of the Sokoman Formation is defined by a thin (<20 m) silicate-facies iron formation member overlain by carbonate-facies iron formation with minor disseminated magnetite. Two main oxide-facies iron formation members can be traced through the deposit, a lower 30- to 130-m-thick oxide-facies iron formation member and an upper oxide-facies iron formation member, which is generally <25 m thick. These two oxide-facies iron formation members are separated by 20 to 50 m of carbonate-facies iron formation. The upper oxide-facies iron formation member is overlain by >50 m of carbonate-facies iron formation at the top of the Sokoman Formation. Zones of silicate-facies iron formation are reported from within the carbonate-facies iron formation, which are thought to represent products of metamorphic reactions (Lyons *et al.*, 2013a).

### Mineralization

The lower oxide member is subdivided into three stratigraphic domains or levels (Lyons *et al.*, 2013a) composed of magnetite-rich upper and lower domains separated by a middle domain containing abundant hematite (Lyons *et al.*, 2013a). The upper and lower magnetite domains are semi-massive to banded (Plate 40A), and contain fine- to medium-grained magnetite, quartz and minor hematite and carbonate minerals (Lyons *et al.*, 2013a). The middle, hematite-rich domain is much more variable, but hematite is >> magnetite (Plate 40A) and secondary martite has been recorded in thin section (Plate 40C). Quartz, rhodonite, rhodochrosite and Mn-rich aegirine are common gangue minerals (Plate 40D).

The upper oxide member is generally more diffuse, of a lower grade than the lower member and predominantly composed of fine- to medium-grained disseminated magnetite and quartz and carbonate gangue minerals.

In drillcore, the oxide-facies iron formation is generally fresh and unaltered. Manganese contents are variable throughout, with Mn contents of up to 18.4% in grab samples of the hematite-rich iron formation (Lyons *et al.*, 2013a), and Mn contents of hematite-rich measured and indicated resources averaging 4.58% Mn (Grandillo *et al.*, 2012). The magnetite-rich iron formation generally has lower Mn values (measured and indicated resources averaging 0.57% Mn; Grandillo *et al.*, 2012), although Mn contents are generally higher in the lower magnetite-rich domain of the lower oxide member (Lyons *et al.*, 2013).



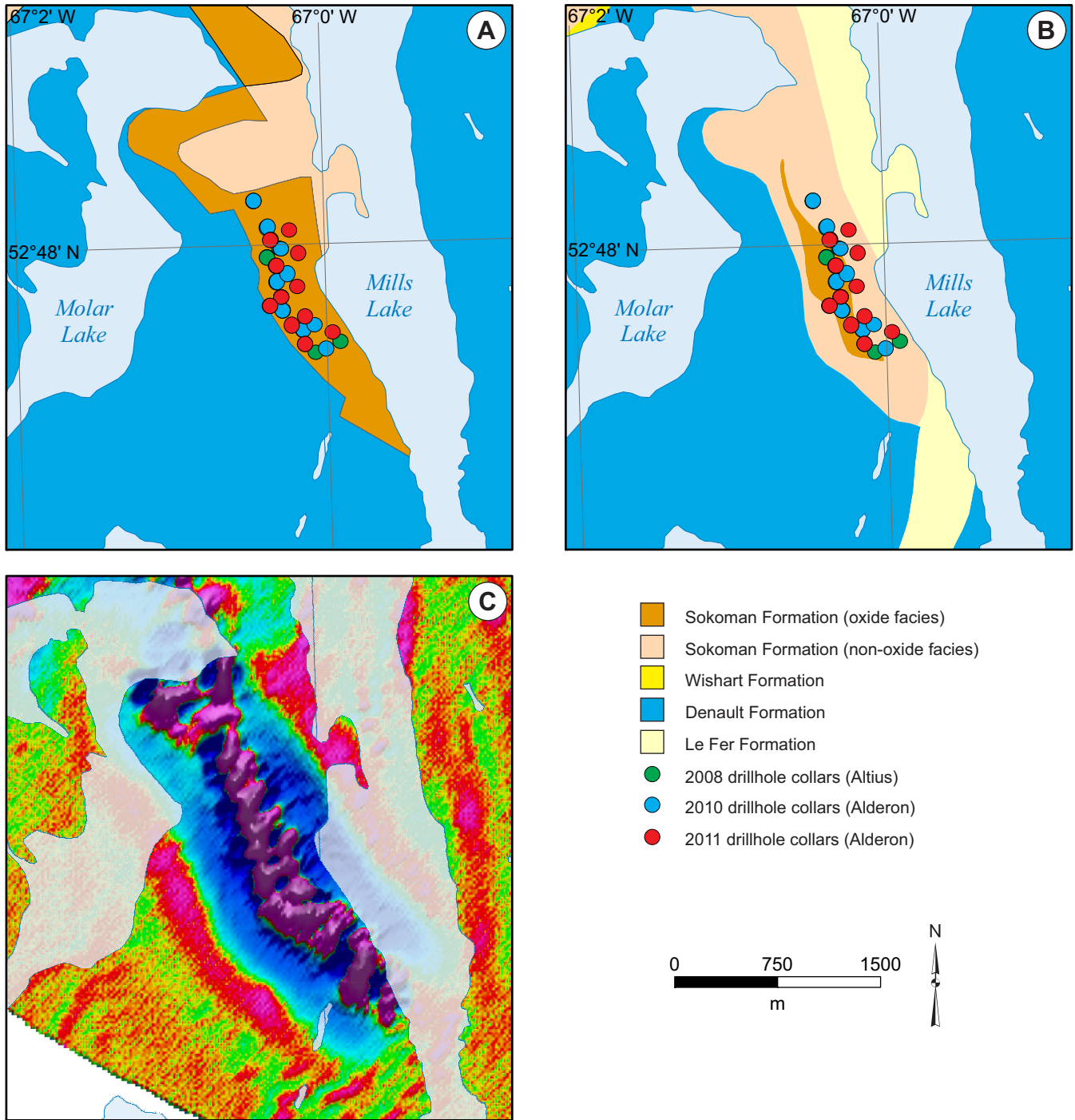


**Figure 53.** Geological maps and aeromagnetic data from the Mills Lake deposit (see text for discussion). A) Geological map based on Alderon mapping and diamond drilling (adapted from Lyons and Velcic, 2013); B) Geological map based on IOC mapping and interpretation of regional airborne magnetic surveys (adapted from Cotnoir et al., 2002); C) Airborne magnetics (second vertical derivative) showing extent of iron formation (data from Cotnoir et al., 2002).

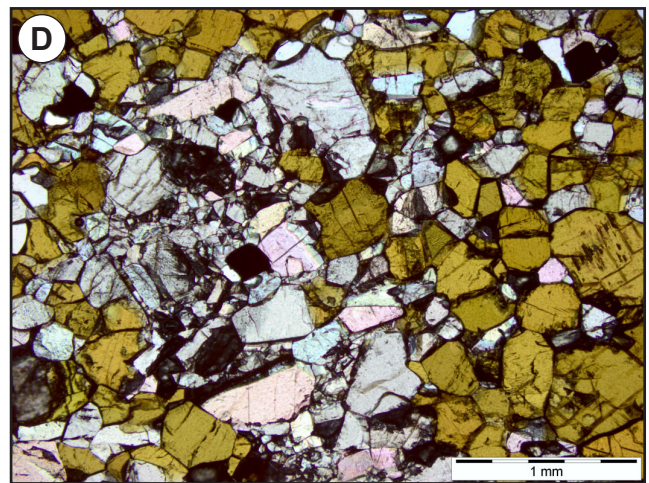
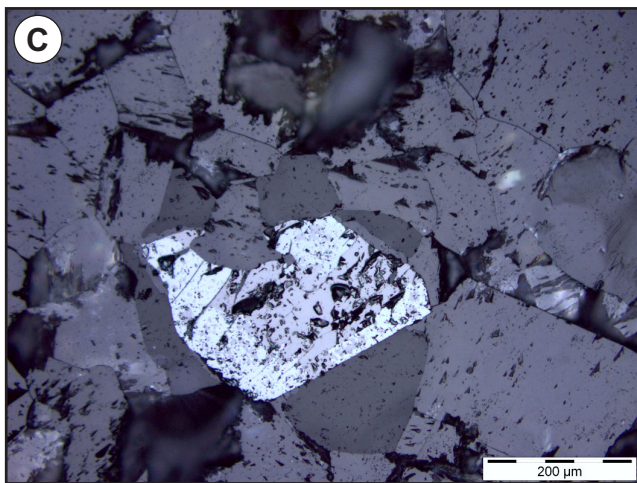


**Plate 40.** A) Banded, magnetite-rich oxide-facies iron formation from the lower domain of the lower oxide member (drillhole K-10-95 @ 93.6 m); B) Hematite-rich oxide-facies iron formation with pink rhodanite, from middle domain of lower oxide member (drillhole K-10-95 @ 76.25 m); C) Photomicrograph of hematite replacing a euhedral grain of magnetite, forming martite (rim) and kenomagnetite (core) (drillhole K-10-95 @ 76.25 m, reflected light); D) Photomicrograph of gangue carbonate and Mn-rich aegirine with minor hematite (drillhole K-10-95 @ 76.25 m, plane-polarized light).

Metallurgical testwork of a single composite drillcore sample is reported by Grandillo *et al.* (2011). This work included mineralogical analysis, Heavy Liquid Separation (HLS) and Davis Tube (DT) magnetic separation. The Fe-oxide liberation of 90% was achieved only at a particle size of less than 75 µm, and therefore no other metallurgical tests were carried out.

### Structure

Multiple generations of folding and faulting have been recognized in the Mills Lake area (Lyons and Velcic, 2013). The deposit is located in an east-northeast-trending asymmetrical open anticline that plunges to the east-northeast. The Elfie Lake Thrust, located approximately 3 km north of the Mills Lake Deposit, marks the northern limit of the Mills Lake Basin. A later, north-trending thrust fault is interpreted to run through Mill Lake, thrusting the Denault Formation marble over the Sokoman Formation from the east (Lyons and Velcic, 2013). A number of northwest-trending extensional faults have also been recorded in the Mills Lake area, which postdate Grenvillian deformation.

### Geophysics

Airborne magnetic surveys (Figure 53C) have identified significant anomalies associated with the Mills Lake deposit (Cotnoir *et al.*, 2002; Seymour *et al.*, 2008; Lyons *et al.*, 2011). The magnetic anomaly is strongest on the western side of the

deposit, where the highly magnetic lower oxide member is closest to the surface. Ground and airborne gravity surveys show that the Mills Lake deposit is also associated with a moderate gravity anomaly (Seymour *et al.*, 2009; Lyons *et al.*, 2011).

### **Resource and/or Reserves**

NI 43-101 compliant resource (Grandillo *et al.*, 2012).

- Measured resources: 50.7 Mt at 30.5% Fe, 0.97% Mn (cut-off grade = 15% Fe)
- Indicated resources: 130.6 Mt at 29.5% Fe, 0.80% Mn (cut-off grade = 15% Fe)
- Inferred resources: 74.8 Mt at 29.3% Fe, 0.67% Mn (cut-off grade = 15% Fe)

### **History of Exploration**

- 1949: Geological mapping (Neal, 1950a)
- 1953: Geological mapping and prospecting (Crouse, 1954)
- 1957: Diamond drilling (6 drillholes, Mathieson, 1957a)
- 1959: Geological mapping, magnetometer survey (Nincheri, 1959)
- 1972: Aeromagnetic survey (unpublished IOC report)
- 1979: Ground magnetometer survey (Price, 1979h)
- 2000: Data compilation, structural synthesis (Hulstein and Lee, 2001)
- 2001: Data compilation, regional airborne magnetic surveys, structural/stratigraphic interpretation (Cotnoir *et al.*, 2002)
- 2006: Geological mapping and prospecting (Way *et al.*, 2007)
- 2007: Geological mapping and prospecting, airborne magnetic survey (Seymour *et al.*, 2008)
- 2008: Diamond drilling (6 drillholes, 834.2 m), ground geophysical survey (gravity and total field magnetics) (Seymour *et al.*, 2009)
- 2010: Diamond drilling (16 drillholes, 4310.9 m), airborne geophysical survey (gravity and magnetics, Lyons *et al.*, 2011)
- 2011: Diamond drilling (18 drillholes, 2844.4 m, Lyons *et al.*, 2013a), metallurgical testwork and resource estimate (Grandillo *et al.*, 2011)
- 2012: Resource estimate (Grandillo *et al.*, 2012)
- 2013: Sterilization report (Lyons and Velcic, 2013)



## 25. NEAL 1

**Alternate Name:** Lac Viot, Neal #1, Neal No. 1

**MODS Showing(s):** 023B/14/Fe008

**Status:** Showing

**Structural Basin:** n/a

**UTM Zone:** 19

**NTS Area:** 23B/14

**Northing (NAD27):** 5868104

**Easting (NAD27):** 624167

**Latitude:** 52.9501

**Longitude:** -67.1519

**Object Located:** Drillhole LV-004

### Description of Occurrence

The Neal 1 showing is located to the northeast of Lac Viot (Figure 54), approximately 16 km west of Labrador City. There are no roads on the property, and access is *via* helicopter.

### Geology and Stratigraphy

The Neal 1 showing occurs in a thin (<700 m) thrust-bound band of Kaniapiskau Supergroup metasedimentary rocks (Sokoman and Menihek formations) surrounded by basement rocks of the Ashuanipi Complex (Figure 54). Garnet–biotite–graphite schist of the Menihek Formation stratigraphically overlies the Sokoman Formation iron formation. The base of the

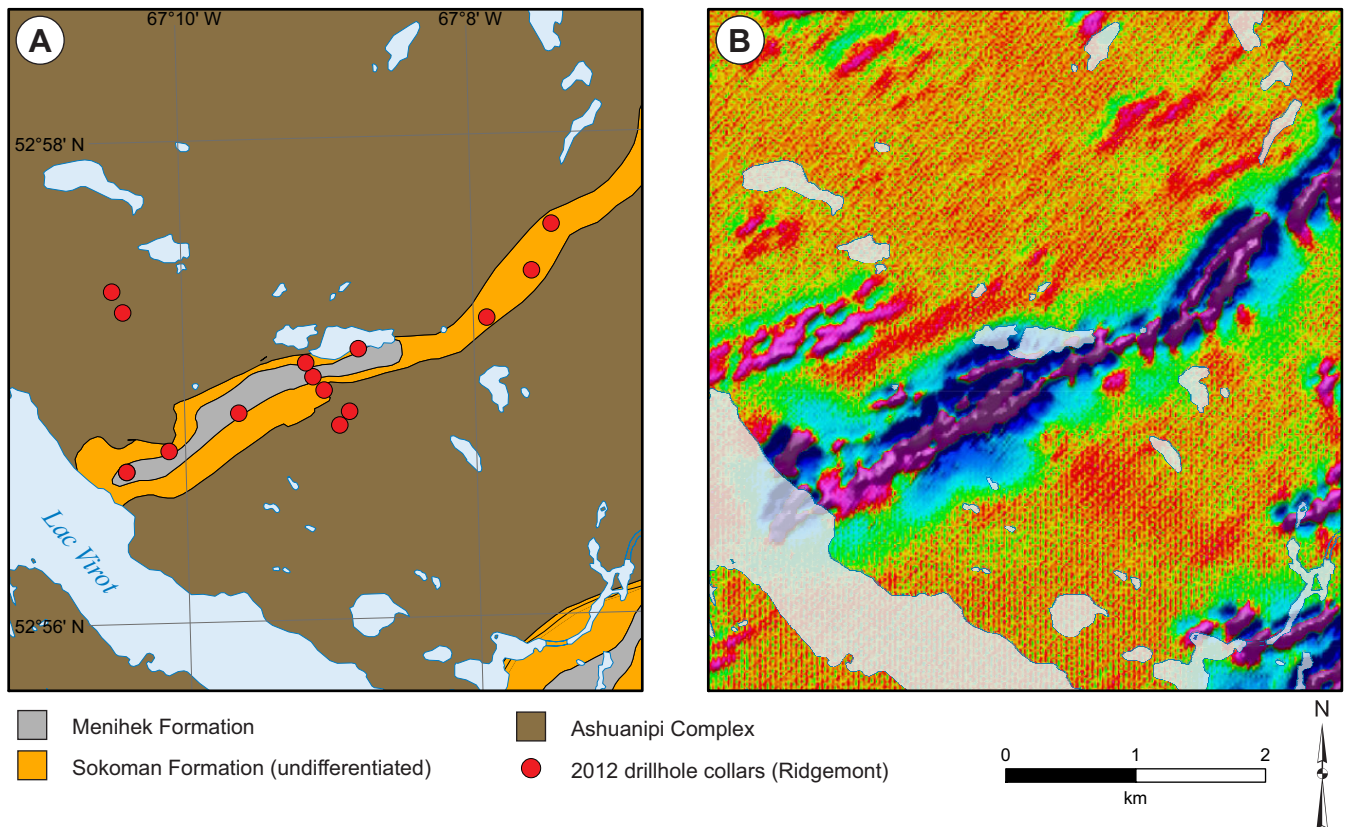


**Figure 54.** A) Geological map of the Neal 1 showing (adapted from Cotnoir et al., 2002), showing location of drillholes from 2012 exploration programs (Steele, 2013); B) Airborne magnetics (second vertical derivative), showing extent of iron formation (data from Cotnoir et al., 2002).

Sokoman Formation was not intercepted in any drillholes, and no outcrops of Wishart Formation quartzites have been recorded on the property (Steele, 2013). Thin (<10 m) Shabogamo Gabbro sills are rare, and intrude the Menihek and Sokoman formations as well as the Ashuanipi Complex basement rocks (Steele, 2013).

The Sokoman Formation is composed of carbonate, silicate and oxide-facies iron formation in varying proportions. The stratigraphy of the iron formation is difficult to determine due to complex folding, but silicate- and carbonate-facies iron formation predominately occur close to the contact with the Menihek Formation, whereas oxide-facies iron formation is more common with increasing stratigraphic depth (Steele, 2013).

### ***Mineralization***

Oxide-facies iron formation is composed of medium-grained quartz and magnetite, with lesser hematite, carbonate and Fe-silicate minerals (Steele, 2013). The oxide-facies members are generally <20 m thick with rare intervals up to 30 m thick, and are interbedded with thin (<5 m) silicate- and carbonate-facies members.

There is no published metallurgical testwork available from the Neal 1 showing.

Assay results show that most of the iron formation grades <30% Fe, with some intervals of higher grade oxide-facies iron formation (*e.g.*, 32.8% Fe from 82.8 to 116 m in drillhole LV-001). The thickest intervals of oxide-facies iron formation were recorded in drillhole LV-004 (24.6% Fe over 101.8 m at 4.5 m depth) and drillhole LV-011 (25.6% Fe over 106.6 m at 78 m depth).

### ***Structure***

Bedding and foliations at the Neal 1 showing dip moderately to the south, and the iron formation is located in an overturned F1 fold with axial planes dipping ~30–40° southeast (Steele, 2013). Menihek Formation schist forms the core of the fold, and the Sokoman and Menihek formations have been thrust onto the basement rocks by a series of regular-sequence, and out-of-sequence, thrusts (similar to the Emma Lake showing).

### ***Geophysics***

The Neal 1 showing is located within a prominent magnetic high, which is evident on regional aeromagnetic surveys (Coates *et al.*, 2011; Figure 54). An airborne gravity gradiometer survey showed that this magnetic high coincided with a large gravity anomaly, which was targeted by the 2012 drilling program (Steele, 2012).

### **Resource and/or Reserves**

No NI 43-101 compliant mineral resource or reserve estimate available.

Non 43-101 compliant historical estimates based on limited data of 15.84 Mt grading 36.9% Fe were reported by Hulstein and Lee (2001).

### **History of Exploration**

- 1950: Geological mapping (Neal, 1951)
- 1953: Geological mapping (Jackson, 1954)
- 1972: Aeromagnetic survey (unpublished IOC report)
- 1982: Airborne geophysical surveys (EM, magnetics, radiometrics, Johnson, 1982)
- 2000: Data compilation, structural synthesis (Hulstein and Lee, 2001)
- 2001: Regional airborne magnetic surveys (Cotnoir *et al.*, 2002)
- 2011: Airborne resolution magnetic, radiometric and VLF-EM survey, geological mapping and prospecting (Coates *et al.*, 2011)
- 2012: Airborne gravity gradiometer survey (Steele, 2012), diamond drilling (15 drillholes, 3744.1 m, Steele, 2013)

## 26. POLLY LAKE

**Alternate Name:** Polly No. 1, Duley No. 1, Kissing Lake

**MODS Showing(s):** 023B/14/Fe001, 023B/14/Fe025

**Status:** Developed Prospect

**Structural Basin:** Carol

**UTM Zone:** 19

**NTS Area:** 23B/14

**Northing (NAD27):** 5859963

**Easting (NAD27):** 631068

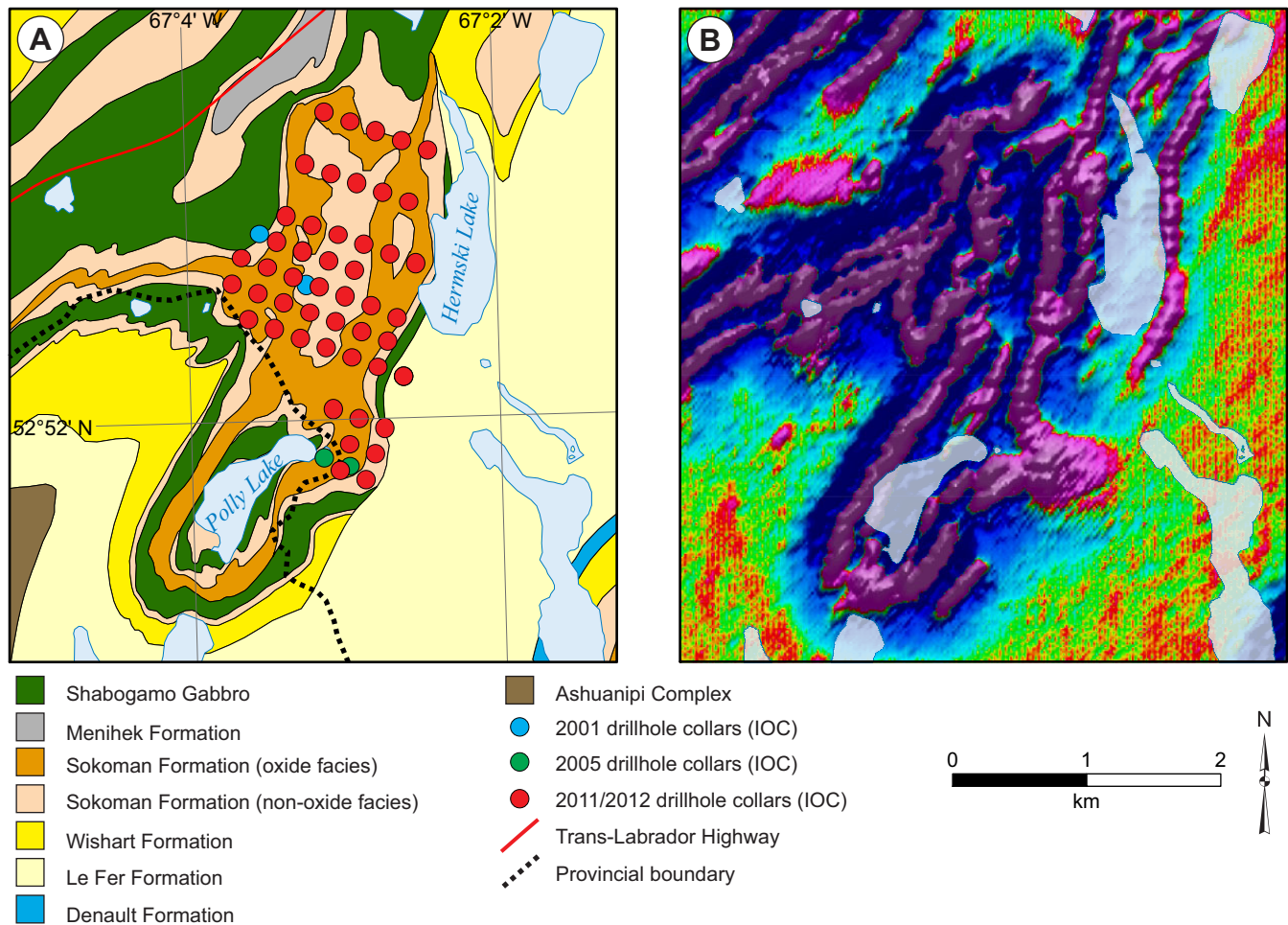
**Latitude:** 52.8755

**Longitude:** -67.0525

**Object Located:** Drillhole PL-11-24

### Description of Occurrence

The Polly Lake prospect straddles the Labrador–Québec border, with the southern part of the showing located around Polly Lake (Figure 55; Plate 41A). It is approximately 12 km southwest of Labrador City, and can be accessed *via* a series of gravel roads to the south of the TLH (access road to Exploration Québec/Labrador Inc. quartzite quarry).





## Geology and Stratigraphy

The Polly Lake area is predominantly underlain by Sokoman Formation iron formation (Figure 55). Menihek Formation schist has been recorded in drillcore conformably overlying the Sokoman Formation, but has not been recognized in outcrop (Darch, 2005b). The Sokoman Formation is conformably underlain by Wishart Formation quartzite, outcropping extensively to the east of the showing where a number of silica quarries are operational. The Wishart Quartzite is, in turn, conformably underlain by Le Fer Formation schist. A number of Shabogamo Gabbro sills (up to 70 m thick) intrude the Sokoman Formation, usually occurring stratigraphically above and below the MIF (Darch, 2005b).

The stratigraphy of the Sokoman Formation is similar to that described from the Humphrey deposit by Muwais (1974), but stratigraphic thicknesses are difficult to determine due to complex folding and structural thickening and attenuation. The UIF and LIF are composed of variable silicate- and carbonate-facies iron formation, with thin oxide-facies layers. The MIF is predominantly composed of oxide-facies iron formation, with a magnetite-rich basal section (Darch, 2005b).

## Mineralization

Diamond drilling has shown that thick (>300 m) sequences of oxide-facies iron formation occur at the Polly Lake prospect (Cotnoir *et al.*, 2002; Darch, 2005b; Bineli Betsi, 2012). Oxide-facies iron formation has variable magnetite and hematite con-

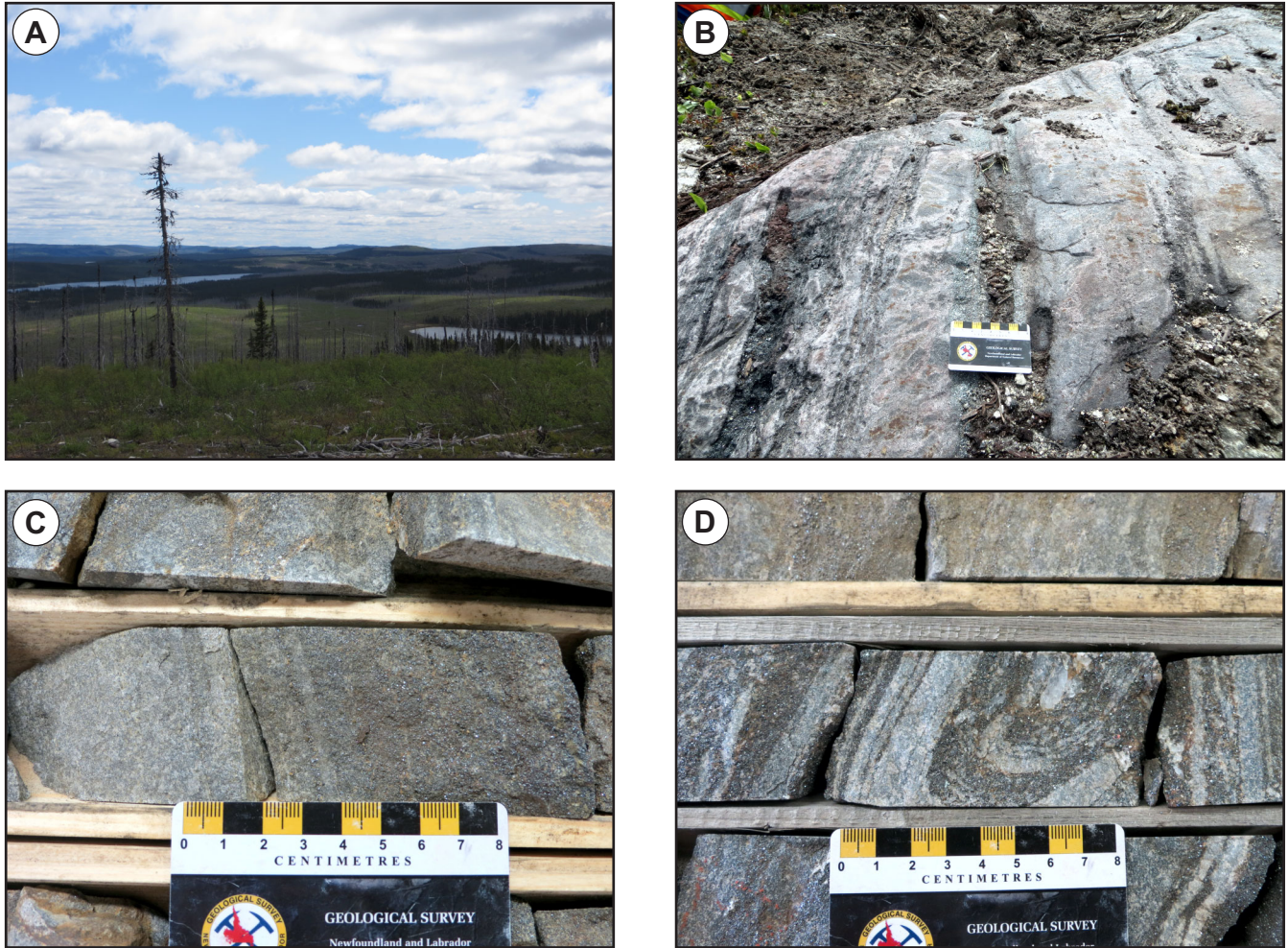


**Plate 41.** A) Overview of the Polly Lake area, overlooking Polly Lake; B) Outcrop of banded quartz-hematite-actinolite-carbonate iron formation (close to collar of drillhole PL-11-05); C) Banded magnetite-rich oxide-facies iron formation (drillhole PL-11-14 @ 41.2 m); D) Folded oxide-facies iron formation, with quartz-rich and magnetite-rich layers (drillhole PL-11-14 @ 71.2 m).

tents, with hematite-rich iron formation common near the top of the MIF (Plate 41B) and magnetite content increasing with depth (Plate 41C, D) (Darch, 2005b; Bineli Betsi, 2012). Magnetite and hematite range from fine grained to very coarse grained, and gangue minerals include quartz, Fe-silicate (grunerite and actinolite) and carbonate minerals.

Strong to moderate alteration is recorded in the upper 50–150 m of most drillholes. Manganese contents are generally high (>0.5 % Mn), with some intervals returning up to 8.45% Mn over 4 m (drillhole PL-11-24 from 214 to 218 m; Bineli Betsi, 2012).

Cotnoir *et al.* (2002) reported RMI determination, minus 200 mesh weight fraction and iron weight recovery values from a total assayed length of 288.7 m in two drillholes. These showed that weight recovery values are comparable to IOC's chemical and physical crude ore characteristics, but the RMI and minus 200 mesh weight fraction are higher. Despite this, Cotnoir *et al.* (2002) concluded that iron ore from the Polly Lake prospect should be amenable for beneficiation to produce a high-grade iron concentrate. During the 2011–2012 drilling program, 393 composite drillcore samples were sent for SAG Power index (SPI) and iron recovery testing (TT).

Assay data from diamond drilling show significant thicknesses of ore-grade iron formation, with highlights including 38.9% Fe over 258.3 m in drillhole PL-05-04 (38.7 to 297 m), 35% Fe over 309 m in drillhole PL-12-51 (39 to 348 m) and 31% Fe over 388.8 m in drillhole PL-12-53 (92 to 480.8 m).

### **Structure**

The Polly Lake prospect is located in a shallowly plunging (18 to 35°), northeast-trending and northwest-verging syncline (Cotnoir *et al.*, 2002). At least two generations of folding have been recorded, an early generation of northwest–southeast-oriented isoclinal folds (F<sub>1</sub>), which have been refolded by a broader, more open, northeast–southwest structural event (F<sub>2</sub>) (Cotnoir *et al.*, 2002; Darch, 2005b). Detailed structural analysis based on 2012 drilling indicates that the F<sub>2</sub> synform is composed of two different synforms, rather than one continuous synform (Bineli Betsi, 2012). This complex folding has resulted in numerous repetitions of the mineralized MIF horizon (Darch, 2005b).

### **Geophysics**

The Polly Lake prospect is located within a strong magnetic high on regional airborne magnetic surveys (Figure 55), which outline the synclinal structure of the showing and can be correlated with the magnetite-rich basal part of the MIF (Cotnoir *et al.*, 2002; Darch *et al.*, 2003b). Cotnoir *et al.* (2002) also recorded a number of large gravity anomalies in the Polly Lake area, with a 5-8 milligal anomaly surrounding Polly Lake and corresponding to the thickest intersections of ore-grade oxide-facies iron formation encountered during drilling.

### **Resource and/or Reserves**

No NI 43-101 compliant mineral resource or reserve estimate available.

Non 43-101 compliant historical estimates, based on limited data, of 115.5 Mt grading 38% Fe were reported by Hulstein and Lee (2001). Preliminary interpretation based on gravity data and assay results indicated the potential for a geological resource of greater than 300 Mt with grades ranging from 35 to 45% Fe (Cotnoir *et al.*, 2002), and geophysical modelling suggested that the Polly Lake prospect could host a geological resource of 1000 Mt of iron ore (Cotnoir *et al.*, 2002).

### **History of Exploration**

- 1949: Geological mapping (Neal, 1950a)
- 1953: Geological mapping and prospecting (Crouse, 1954)
- 1957: Diamond drilling (20 drillholes) and geological mapping (Mathieson, 1957a)
- 1958: Geological mapping and diamond drilling (12 drillholes, 286.1 m) on the Québec portion of deposit (Tuffy, 1958)
- 1972: Aeromagnetic survey (unpublished IOC report)
- 1973: Geological mapping, ground gravity and magnetic surveys (Hamilton, 1973)

- 1979: Ground magnetometer survey (Price, 1979i)
- 1982: Airborne geophysical surveys (EM, magnetics, radiometrics, Johnson, 1982)
- 2000: Data compilation, structural synthesis (Hulstein and Lee, 2001)
- 2001: Data compilation, geological mapping and prospecting, diamond drilling (2 drillholes, 621 m), ground gravity survey, regional airborne magnetic surveys, structural/stratigraphic interpretation (Cotnoir *et al.*, 2002)
- 2003: Geological mapping and prospecting (Darch *et al.*, 2003b)
- 2004: Geological mapping and prospecting (Darch, 2004)
- 2005: Diamond drilling (2 drillholes, 547 m, Darch, 2005b)
- 2011–2012: Diamond drilling (65 drillholes, including 48 drillholes in Labrador, 12 418 m, Bineli Betsi, 2012)



## 27. ROSE

**Alternate Name:** Rose Central, North Rose, Rose Lake, Elfie Lake, Narrow Lake South

**MODS Showing(s):** 023B/14/Fe020

**Status:** Developed Prospect

**Structural Basin:** Wabush

**UTM Zone:** 19

**NTS Area:** 23B/14

**Northing (NAD27):** 5855360

**Easting (NAD27):** 632907

**Latitude:** 52.8336

**Longitude:** -67.0271

**Object Located:** Drillhole K-10-39A

### Description of Occurrence

The Rose deposit is located north of Elfie Lake (Figure 56), approximately 14 km southwest of Labrador City and 6 km northeast of Fermont. The area is accessible *via* a number of small 4 x 4 roads from Labrador City.

### Geology and Stratigraphy

The area north of Elfie Lake has poor outcrop exposure, (Plate 42A) and most information on the geology and stratigraphy of the Rose deposit comes from diamond drilling and interpretation of geophysical data. Previous geological mapping had indicated that the Rose deposit was located in the same belt of Sokoman Formation iron formation as the Mills Lake deposit to the south (Figure 56B; Rivers, 1985; Cotnoir *et al.*, 2002). However, recent geological interpretations, based on exploration activity since 2006, have shown that the Rose deposit is located north of a major thrust fault (Elfie Lake Thrust; Figure 56A), which separates the Wabush Basin from the Mills Lake Basin to the south (Lyons and Velcic, 2013).

Diamond drilling has shown that a folded sequence of Kaniapiskau Supergroup metasedimentary rocks occurs north of the Elfie Lake Thrust (Lyons *et al.*, 2013b). Menihek Formation graphitic schist occurs at the top of the sequence, and is stratigraphically underlain by the Sokoman Formation with a transitional contact (Lyons *et al.*, 2013b). The Sokoman Formation conformably overlies Wishart Formation quartzite, which outcrops near the centre of the Rose deposit and has been recorded in drillcore along the northwestern boundary of the deposit (Lyons *et al.*, 2013b). Diamond drilling has also intersected Denault Formation dolomite below the Wishart Formation (Lyons *et al.*, 2013b), and numerous thin (<20 m) sills of Shabogamo Gabbro are also recorded intruding the Menihek, Sokoman and Wishart formations (Lyons *et al.*, 2013a, b).

The deposit is subdivided into three main zones (Rose North, Rose Central and South Rose/Elfie Lake zones), and the stratigraphy of the iron formation is correlated across these zones despite variations in the thickness of individual members and degrees of alteration (Lyons *et al.*, 2013b). The Sokoman Formation is strongly attenuated in the South Rose/Elfie Lake Zone (Lyons *et al.*, 2013b), and the following stratigraphic description is based on the Rose North and Central zones. A thin silicate-facies iron formation member marks the base of the Sokoman Formation, and is correlated with basal silicate-facies iron formation recorded along strike to the north at the Duley prospect and the Scully Mine deposit. There are three main oxide-facies members of the Sokoman Formation observed at the Rose deposit, and from the base to the top are called RC-1, RC-2 and RC-3 in the Rose Central Zone, and RN-1, RN-2 and RN-3 in the Rose North Zone (Lyons *et al.*, 2013b). These oxide-facies iron formation members are separated by thin (<10 m), discontinuous silicate and carbonate members with low contents of Fe-oxide minerals. The upper part of the Sokoman Formation is predominantly composed of silicate- and carbonate-facies with thin bands of oxide-facies iron formation.

### Mineralization

The three main oxide-facies members at the Rose Central (RC-1, RC-2 and RC-3) and Rose North (RN-1, RN-2, RN-3) zones are distinguished based on their various mineralogical contents and degrees of alteration. At Rose Central, the lower oxide-facies member (RC-1) is hematite-rich (Plate 42B) with <5% magnetite and gangue rhodonite (Grandillo *et al.*, 2012;

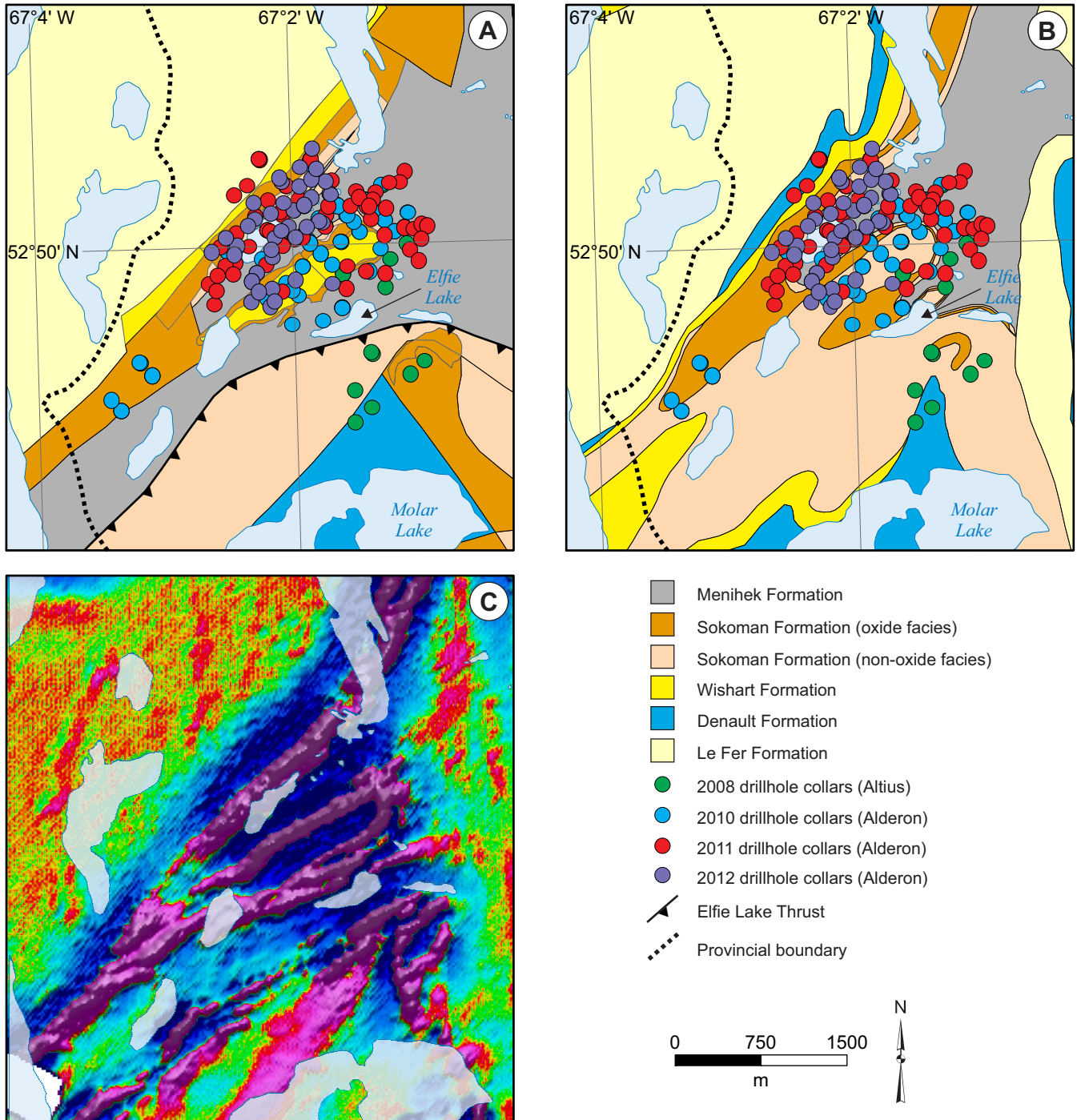


**Figure 56.** Geological maps and aeromagnetic data from the Rose deposit (see text for discussion). A) Geological map based on Alderon mapping and diamond drilling (adapted from Lyons and Velcic, 2013); B) Geological map based on IOC mapping and interpretation of regional airborne magnetic surveys (adapted from Cotnoir et al., 2002); C) Airborne magnetics (second vertical derivative) showing extent of iron formation (data from Cotnoir et al., 2002)



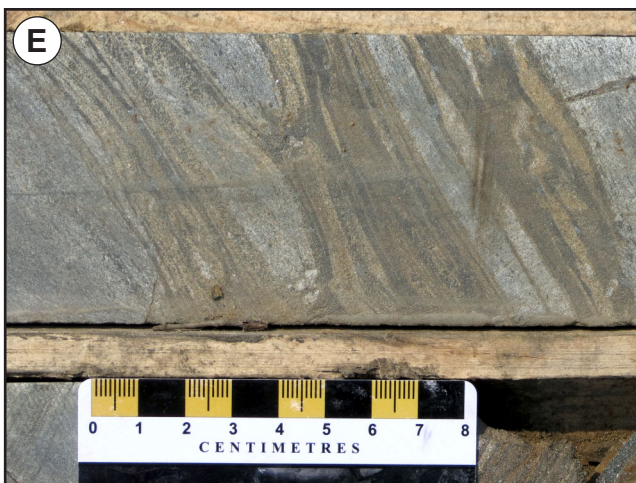
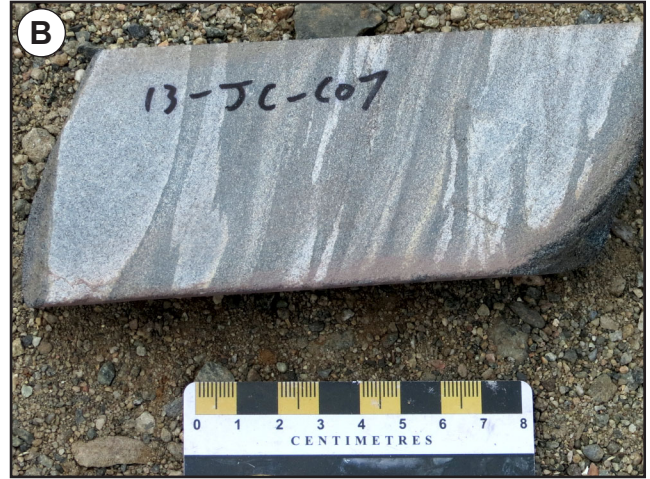


**Plate 42.** A) View of the Rose Central Zone of the Rose deposit, looking west; B) Banded quartz-hematite from RC-1 member (drillhole K-11-171 @ 232 m); C) Quartz-magnetite-hematite iron formation from RC-2 member (drillhole K-11-171 @ 205.6 m); D) Moderately altered quartz-hematite from RN-2 member (drillhole K-11-115 @ 329.2 m); E) Quartz-magnetite-carbonate iron formation from RC-3 member (drillhole K-11-171 @ 140.6 m); F) Strongly altered basal silicate-facies iron formation from Rose North Zone (drillhole K-11-115 @ 401.4 m).



Lyons *et al.*, 2013b). At Rose North the lowest oxide-facies member (RN-1) is moderately altered and friable with secondary goethite, psilomelane and, rarely, pyrolusite (Lyons *et al.*, 2013b).

The middle oxide-facies member at Rose Central (RC-2) is highly variable, with interlayered hematite-rich and magnetite-rich oxide-facies iron formation (Lyons *et al.*, 2013b). Magnetite-rich iron formation is more common than in RC-1, and gangue minerals are quartz, Fe-carbonate and Fe-silicate minerals and minor rhodochrosite (Plates 42C and 43A, B). In the Rose North zone, the RN-2 oxide member is moderately altered, with an increase in the hematite content compared to RC-2 (Plate 42D), and rhodochrosite commonly oxidized to psilomelane and pyrolusite.

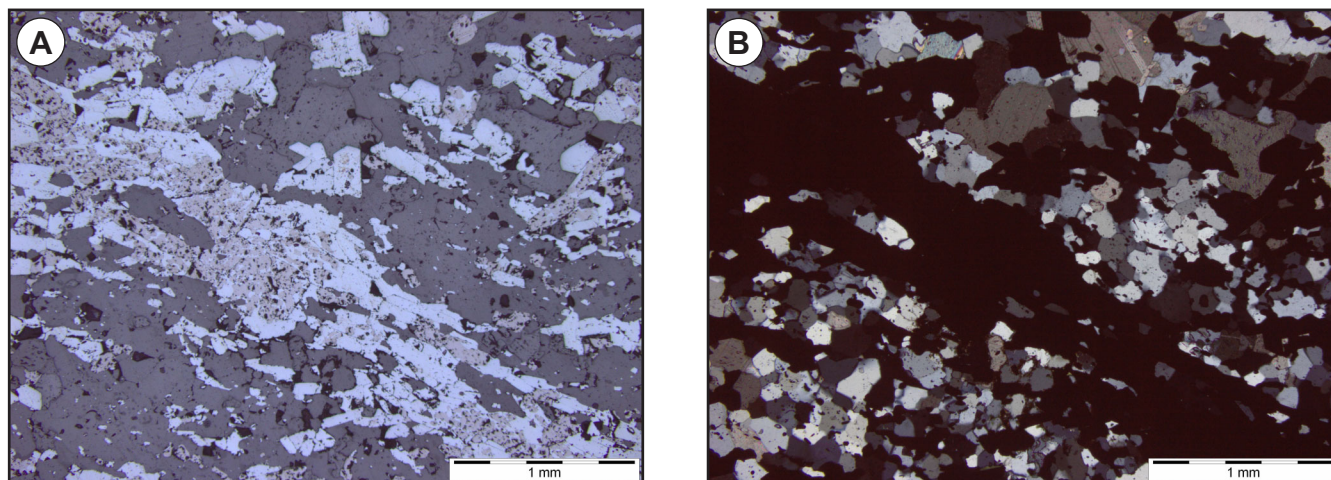


**Plate 43.** A) Photomicrograph of quartz–hematite–magnetite schist from RC-2, with hematite replacing magnetite and gangue quartz and carbonate (drillhole K-11-171 @ 205.1 m, reflected light); B) Same view as (A), in cross-polarized light.

RC-3 and RN-3 are the upper oxide members in the Rose Central and Rose North zones, respectively. These members are both similar with fine-grained magnetite >> hematite within a fine-grained Fe-silicate gangue (Plate 42E). RN-3 displays a much lower degree of secondary alteration compared to RN-2 and RN-1. Manganese-bearing minerals are rare in both RC-3 and RN-3, and the proportion of Fe-silicate and Fe-carbonate minerals increase toward the top of this member.

Manganese concentrations are highest in the lower and middle oxide-facies members in the Rose Central Zone, with Mn concentrations in Measured and Indicated resources of 2.59% in RC-1 and 1.52% in RC-2, dropping to 0.69% Mn in RC-3 (Grandillo *et al.*, 2012). Manganese is typically hosted in Mn-silicate and Mn-carbonate minerals, with >23% of the Mn chemically bonded to magnetite (Grandillo *et al.*, 2013). Manganese concentrations in the Rose North Zone are generally lower than the equivalent stratigraphic members in the Rose Central Zone, with Mn concentrations in Measured and Indicated resources of 1.21% in RN-1, 0.72% in RN-2 and 0.55% in RN-3 (Grandillo *et al.*, 2012). However, Mn as Mn-oxides is present in significant quantity in all three members at Rose North, which has metallurgical implications as Mn-oxides are generally heavy minerals, which will typically report to gravity concentrate in higher percentages than other Mn minerals (Grandillo *et al.*, 2012).

Extensive metallurgical work has been carried out at the Rose deposit, which is outlined in detail in recent feasibility studies (Grandillo *et al.*, 2012, 2018).

### **Structure**

The Rose North, Rose Central and South Rose/Elfie Lake zones of the Rose deposit occur on different limbs of a series of northeast–southwest-trending, upright to slightly overturned shallow northeast-plunging anticlines and synclines ( $F_2$ ) that re-fold smaller scale  $F_1$  folding (Lyons *et al.*, 2013b). The Rose Central and South Rose/Elfie Lake zones represent limbs of an anticline, the hinge of which has been outlined by diamond drilling (Lyons *et al.*, 2013b), whereas the Rose North zone is interpreted as representing the limb of a syncline (although the hinge of this syncline has not been intercepted during drilling; Lyons *et al.*, 2013). The oxide-facies iron formation is highly attenuated through the hinge into the South Rose/Elfie Lake zone, and the entire Rose system also appears to attenuate along strike to the southwest (Lyons *et al.*, 2013b).

The Rose deposit appears to be dismembered by thrust faulting parallel to the D<sub>1</sub> deformation from the south-southeast (Lyons *et al.*, 2013b). In addition, at least three, and possibly five, late extensional faults displace the folded iron formation, with displacements ranging from 50 to 100 vertical metres (Lyons and Velcic, 2013).

### **Geophysics**

Airborne magnetic surveys show that the Rose deposit is located within a strong magnetic high (Seymour *et al.*, 2008; Lyons *et al.*, 2011; Cotnoir *et al.*, 2002; Figure 56C), which correlates with the magnetite–hematite mineralization intersected during diamond drilling (Lyons *et al.*, 2013b). Ground and airborne gravity surveys show that the Rose deposit is also associated with a moderate gravity anomaly (Seymour *et al.*, 2009; Lyons *et al.*, 2011).

### **Resource and/or Reserves**

NI 43-101 compliant resource (Grandillo *et al.*, 2012).

#### Rose Central

- Measured resources: 249.9 Mt at 29.4% Fe, 1.60% Mn (cut-off grade = 15% Fe)
- Indicated resources: 294.5 Mt at 28.5% Fe, 1.28% Mn (cut-off grade = 15% Fe)
- Inferred resources: 160.7 Mt at 28.9% Fe, 1.43% Mn (cut-off grade = 15% Fe)

#### Rose North

- Measured resources: 236.3 Mt at 30.3% Fe, 0.87% Mn (cut-off grade = 15% Fe)
- Indicated resources: 312.5 Mt at 30.5% Fe, 0.96% Mn (cut-off grade = 15% Fe)
- Inferred resources: 287.1 Mt at 29.8% Fe, 0.76% Mn (cut-off grade = 15% Fe)

NI 43-101 compliant reserves (Grandillo *et al.*, 2018).

#### Rose Central and Rose North (combined)

- Proven reserves: 392.7 Mt at 29% Fe, 1.20% Mn (cut-off grade = 15% Fe)
- Probable reserves: 124.5 Mt at 28.2% Fe, 1.07% Mn (cut-off grade = 15% Fe)

### **History of Exploration**

- 1949: Geological mapping (Neal, 1950a)
- 1953: Geological mapping and prospecting (Crouse, 1954)
- 1959: Geological mapping, magnetometer survey (Nincheri, 1959)
- 1972: Aeromagnetic survey (unpublished IOC report)
- 1979: Diamond drilling (1 drillhole, 27.9 m, Grant, 1979f)
- 1983: Diamond drilling (1 drillhole, 51.2 m, Avison *et al.*, 1984)
- 2001: Data compilation, regional airborne magnetic surveys, structural/stratigraphic interpretation (Cotnoir *et al.*, 2002)
- 2006: Geological mapping and prospecting (Way *et al.*, 2007)
- 2007: Geological mapping and prospecting, airborne magnetic survey (Seymour *et al.*, 2008)
- 2008: Diamond drilling (12 drillholes, 3549.2 m), ground geophysical survey (gravity and total field magnetics, Seymour *et al.*, 2009)
- 2009: Metallurgical testwork (Seymour *et al.*, 2010)
- 2010: Diamond drilling (56 drillholes, 20 410.6 m at Rose Deposit; 10 drillholes, 1423.9 m southwest of Rose Deposit), airborne geophysical survey (gravity and magnetics, Lyons *et al.*, 2011)
- 2011: Diamond drilling (68 drillholes, 19 408.1 m, Lyons *et al.*, 2013a), metallurgical testwork and resource estimate (Grandillo *et al.*, 2011)
- 2012: Diamond drilling (44 drillholes, 12 169.4 m, Lyons *et al.*, 2013b), metallurgical testwork and feasibility study (including resource and reserve calculations, Grandillo *et al.*, 2012)
- 2013: Sterilization report (Lyons and Velcic, 2013)

## 28. SCULLY

**Alternate Name:** Scully Mine, Wabush Mine, Wabush (Lake) Iron Deposit, Burden No. 1

**MODS Showing(s):** 023B/15/Fe001

**Status:** Past Producer (Dormant)

**Structural Basin:** Wabush

**UTM Zone:** 19

**NTS Area:** 23B/15

**Northing (NAD27):** 5864970

**Easting (NAD27):** 640380

**Latitude:** 52.9180

**Longitude:** -66.9121

**Object Located:** MODS Showing (East Pit)

### Description of Occurrence

The Scully deposit is located between Little Wabush Lake and Long Lake (Figure 57), with access *via* the Wabush Mine operations. The deposit is located in a band of iron formation that continues to the south along strike to the Duley prospect and the Rose deposit (Kami property). The Scully deposit was in production from 1965 to 2014, during which time five individual open pits were in operation (East Pit (east), East Pit (west), South Pit, West Pit and West Pit Extension; Figure 58). In addition, an area to the north of the West Pit Ext called “The Boot” was stripped in preparation for mining.

### Geology and Stratigraphy

The bedrock geology of the Scully deposit is dominated by the Sokoman Formation iron formation (Figure 57). On the north side of the deposit, the iron formation is conformably underlain by Wishart Formation quartzite, which occurs above a thick sequence of coarse-grained schist of the Le Fer Formation (O’Leary *et al.*, 1972). To the south of the deposit, a thin sequence of quartzite (Wishart Formation) separates the iron formation from a thick sequence of Denault Formation dolomite (O’Leary *et al.*, 1972). Shabogamo Gabbro sills intrude the base of the iron formation to the east of the Scully deposit, but have not been recorded in the mine area (O’Leary, 1979). A number of fault-controlled dykes (strongly altered to chlorite) have also been recorded in the South Pit (O’Leary, 1973).

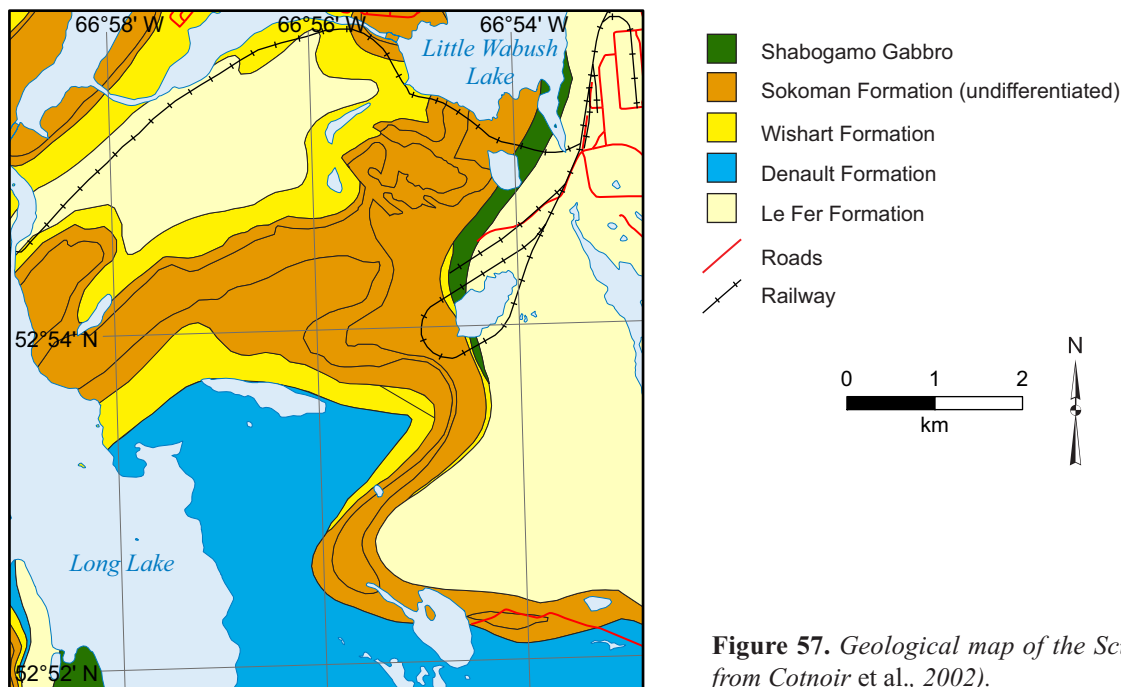


**Figure 57.** Geological map of the Scully deposit (adapted from Cotnoir *et al.*, 2002).



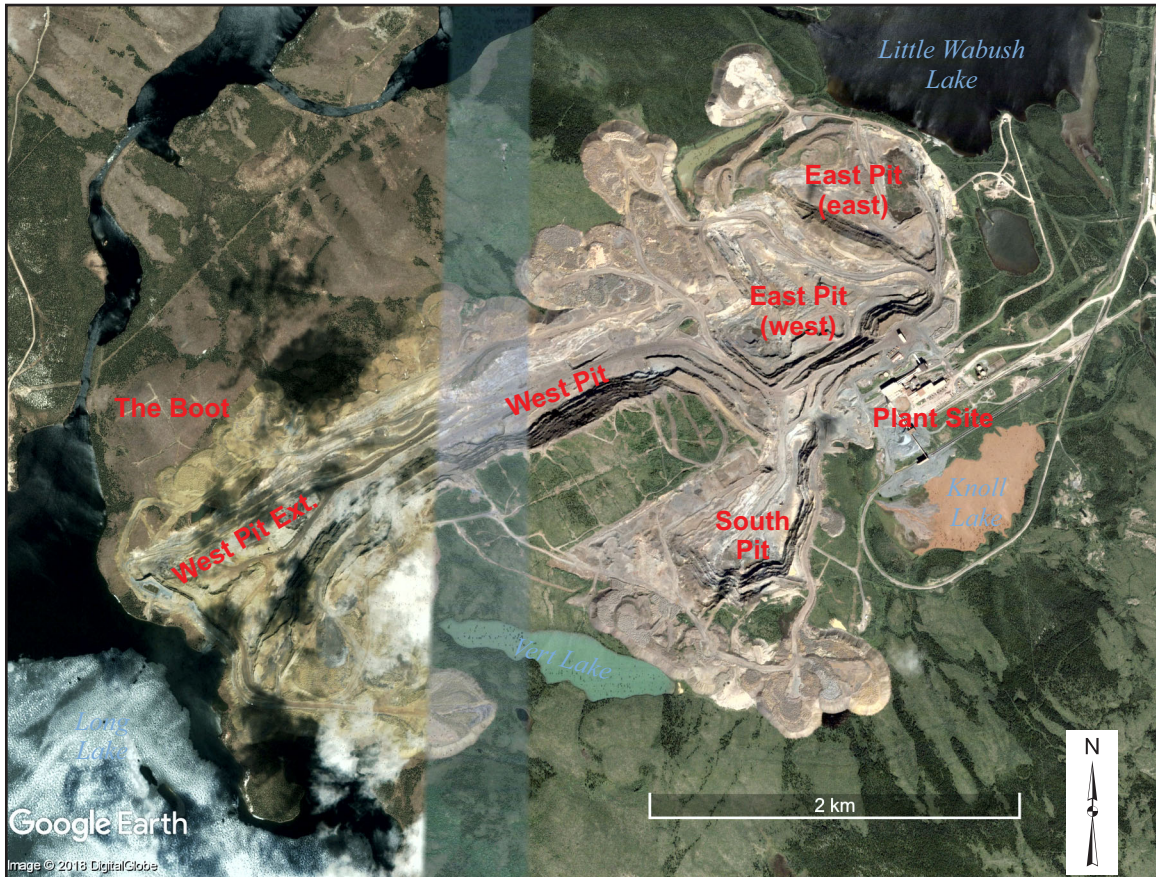


**Figure 58.** Google Earth image of mining operations at Scully deposit, showing location of active pits as well as undeveloped area (The Boot) and plant site. Images taken in 2002 (west) and 2004 (east).

The Sokoman Formation is subdivided into three main oxide-bearing members (Lower, Middle and Upper members) and two non-oxide members (Basal Silicate facies Iron Formation (BSIF) and Middle Quartzite (MQ) members). The non-oxide members can be traced throughout the mine area and act as important marker horizons. The BSIF member marks the base of the Sokoman Formation. It is ~25 m thick and is composed primarily of quartz and grunerite, commonly strongly altered to goethite (Plate 44A). The Lower Member of the Sokoman Formation is ~50 to 80 m thick and is subdivided into three sub-members (O’Leary, 1973; Farquharson and Thalenhorst, 2006). From base to top, these are Unit 53 (quartz–hematite ± magnetite with a relatively high Mn content; Plate 44B, C), Unit 52 (predominantly composed of quartz and goethite; Plate 44D), and Unit 51 (quartz–hematite–magnetite–Mn-oxides). This is overlain by the MQ member (Unit 41; Plate 44E). Conformably above this marker horizon the oxide-bearing Middle Member occurs, which is ~120 m thick and is divided into four sub-members. From the base to the top, these are Unit 34 (goethite-rich with occasional Fe-oxide and Mn-oxide bands), Unit 33 (quartz–hematite), Unit 32 (quartz with lesser magnetite and hematite), and Unit 31 (quartz–hematite; Plate 44F). The oxide-bearing Upper Member is ~135 m thick and has a much lower iron-oxide content than the Lower and Middle members. It is strongly altered, and likely represents carbonate-facies iron formation with minor oxide-facies iron formation (O’Leary, 1973).

### **Mineralization**

A number of ore-bearing units have been mined from the Lower and Middle members of the Sokoman Formation. In the Lower Member, Units 53 and 51 are considered ore units, with high iron weight recovery and relatively high Mn contents in concentrate (2.7% Mn; Farquharson and Thalenhorst, 2006). Ore from the Middle Member is considered the best quality ore, with high iron weight recoveries and lower Mn contents in concentrate than ore units in the Lower Member (Farquharson and Thalenhorst, 2006). Units 33 and 31 are the main ore units in the Middle Member, with high iron weight recoveries and Mn con-



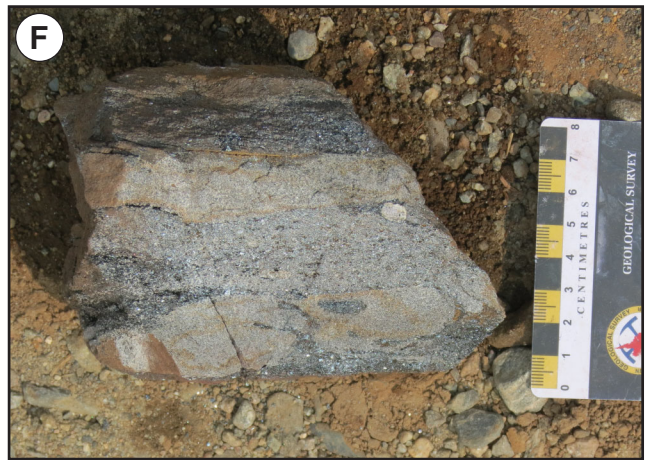


**Plate 44.** A) Strongly altered basal silicate-facies iron formation from West pit; B) Banded quartz-hematite-pyrolusite schist (Unit 53) from East pit (east); C) Quartz-hematite-pyrolusite schist with circular pits after leached carbonate minerals (Unit 53); East pit (east); D) Quartz-goethite waste unit (Unit 52) from East pit (east); E) Middle quartzite marker horizon from West pit; F) Banded quartz-hematite schist from West pit (Unit 31)



tents in concentrates consisting of 1.5 and 1.3% Mn, respectively (Farquharson and Thalenhorst, 2006). Unit 34 is normally considered waste, but is of ore grade in some places. In the Upper Member, the middle oxide unit (Unit 22) is locally ore grade, with generally low to medium iron weight recoveries and low Mn (0.8% Mn in concentrate; Farquharson and Thalenhorst, 2006).

Ore units are commonly strongly altered, and where silicate and carbonate minerals are completely leached, and magnetite oxidized to hematite. Secondary goethite (possibly an alteration product from Fe-carbonate and Fe-silicate minerals) is also common in some units. This alteration is related to late-stage fluid infiltration. Strongly altered ore is generally friable, except in areas proximal to late-stage faults (O'Leary, 1973). Remobilization of manganese during alteration is common, with high Mn grades (up to 7%) recorded close to the major fault zone in the East Pit (Gignac *et al.*, 2018). However, the higher Mn levels in some stratigraphic units indicates that the overall Mn distribution is controlled by the Mn content of the unaltered iron formation (Farquharson and Thalenhorst, 2006).

In the South Pit, alteration is much less pronounced, with relatively fresh equivalents of the units containing relatively higher magnetite contents and common Fe-silicate and Fe-carbonate minerals.

Ore from the Scully deposit was processed at the Scully Mine mineral processing facility and the ore characteristics and beneficiation processes have been summarized by Farquharson and Thalenhorst (2006) and Gignac *et al.* (2018).

### **Structure**

Three generations of folding have been identified in the Scully deposit (O'Leary *et al.*, 1972; O'Leary, 1973; Gignac *et al.*, 2018). In the West and South pit areas, east–west-trending  $F_2$  folds form broad open synclinal and anticlinal structures, which are superimposed on an early generation of tight to isoclinal  $F_1$  folds. In the East Pit, northwest-trending  $F_1$  and  $F_2$  folds form a complex interference pattern, which is evident in outcrop patterns (O'Leary *et al.*, 1972). The  $F_3$  folds have only been recognized in the West Pit, where a north–south-trending fold rotates the plunging fold axis of  $F_1$  and  $F_2$  folds from an easterly to a westerly direction over <100 m (O'Leary *et al.*, 1972).

Numerous late-stage faults have been recorded in the Scully deposit, divisible into two major sets consisting of an early set, which strikes  $030^\circ$  and dips at a high angle to the southeast, and a later set, which strikes  $150^\circ$  and dips steeply to the northeast (O'Leary, 1979). The later fault set is associated with significant displacement, observed by a major northwest-trending reverse fault in the East Pit that has a displacement of >75 m, resulting in the Middle Member of the Sokoman Formation (east of the fault) resting against Wishart Formation quartzite (west of the fault) (O'Leary *et al.*, 1972).

### **Geophysics**

There is only limited geophysical data available from the Scully deposit, which was not covered by aeromagnetic surveys of the Labrador City area (Cotnoir *et al.*, 2002). Gignac *et al.* (2018) reported on ground magnetometer surveys of the Boot Pit that outlined moderate magnetic anomalies that were used to provide detail for structural interpretation. In addition, ground gravity surveys on the Boot Pit area, south and north of West Pit Ext, West Pit, South Pit and east of South Pit, revealed several anomalies suggesting the presence of buried masses of iron beneath shallow cover sediments (Gignac *et al.*, 2018).

### **Resource and/or Reserves**

NI 43-101 compliant resource (Gignac *et al.*, 2018).

- Measured resources: 213.7 Mt at 35.1% Fe, 2.0% Mn (cut-off grade = 20% Fe)
- Indicated resources: 520.8 Mt at 34.3% Fe, 2.4% Mn (cut-off grade = 20% Fe)
- Inferred resources: 237.0 Mt at 34.1% Fe, 2.1% Mn (cut-off grade = 20% Fe)

NI 43-101 compliant reserves, Gignac *et al.* (2018).

- Proven reserves: 145.0 Mt at 35.1 % Fe, 2.4% Mn
- Probable reserves: 298.6 Mt at 34.7% Fe, 2.7% Mn



### **History of Exploration**

- 1953: Geological mapping and prospecting (Boyko, 1953), magnetometer survey (MacLeod, 1954), diamond drilling (Davidson, 1954)
- 1954: Diamond drilling and metallurgical testwork (Greer, 1954)
- 1957 to 1965: Exploration activity, development of pilot plant and construction of mine facilities
- 1965: Production begins at Scully Mine
- 2006: Ground gravity survey (described in Gignac *et al.*, 2018)
- 2010: Ground magnetometer survey (described in Gignac *et al.*, 2018)
- 2014: Cessation of mining activities at Scully Mine
- 2018: Feasibility study (Gignac *et al.*, 2018)

## 29. SHABO HILL

**Alternate Name:** Northwest Arm No 2, Northwest Arm No 3, Northwest Arm No 4

**MODS Showing(s):** 023G/02/Fe036, 023G/02/Fe037, 023G/ 07/Fe008

**Status:** Showing

**Structural Basin:** Carol

**UTM Zone:** 19

**NTS Area:** 23G/07

**Northing (NAD27):** 5902599

**Easting (NAD27):** 660827

**Latitude:** 53.2502

**Longitude:** -66.5895

**Object Located:** Drillhole 10LB0004

### Description of Occurrence

The Shabo Hill showing is located at the northern end of Northwest Arm, a major inlet of Shabogamo Lake (Figure 59). It is approximately 42 km northeast of Labrador City, and access is *via* helicopter or by boat from Julianne Lake.

### Geology and Stratigraphy

The Shabo Hill area is mostly till covered, with only a few scattered outcrops to the east of the northern end of Northwest Arm. These outcrops are of carbonate- and oxide-facies iron formation, and have been assigned to the UIF of the Sokoman

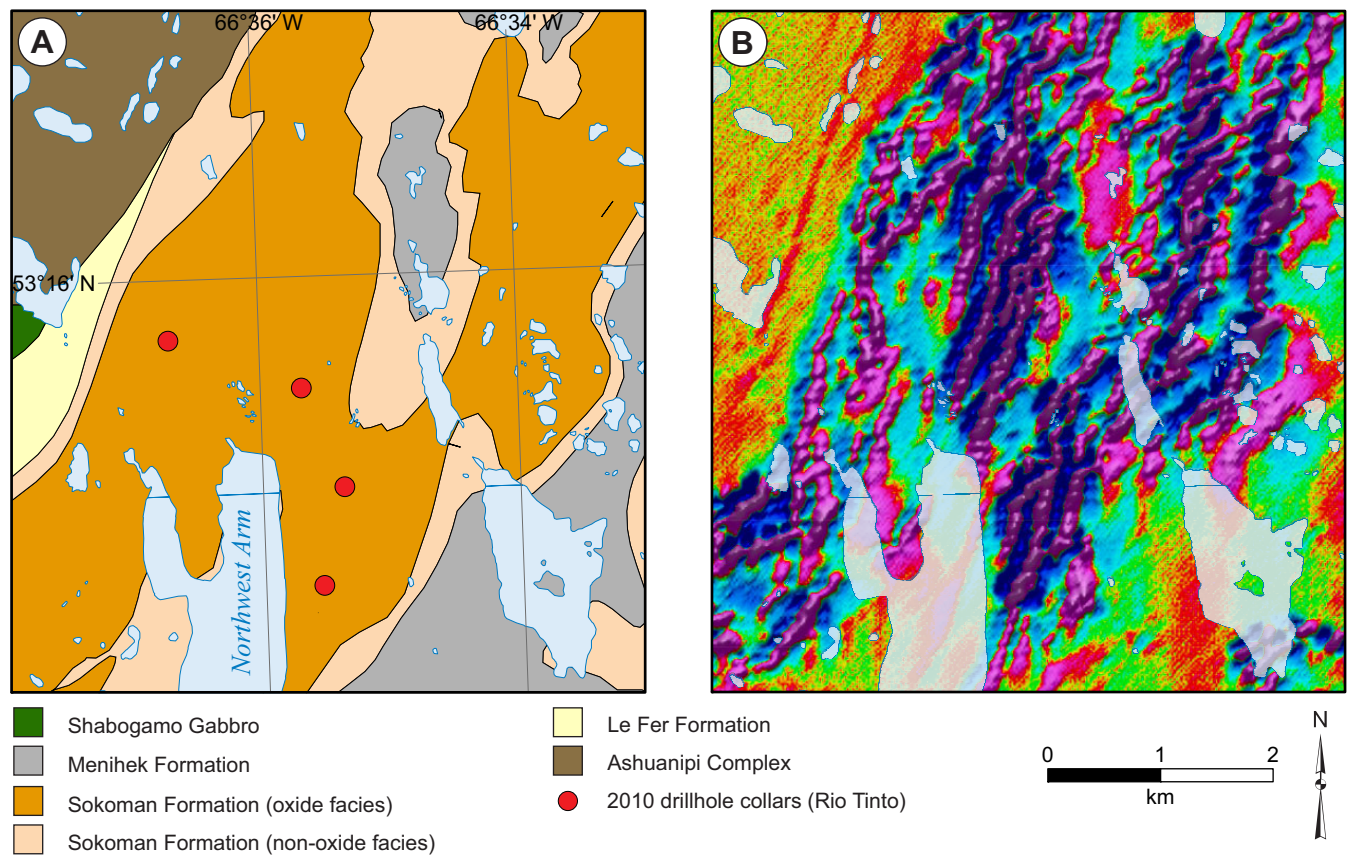


**Figure 59.** A) Geological map of the Shabo Hill showing (adapted from Cotnoir et al., 2002), showing location of drillholes from 2010 exploration program (Hovis and Broadbent, 2010; Hovis and Goldner, 2011b); B) Airborne magnetics (second vertical derivative) showing extent of iron formation (data from Cotnoir et al., 2002).

Formation. Interpretation of aeromagnetic data indicates that the Sokoman Formation is likely overlain by the Menihek Formation, whereas diamond drilling at the eastern portion of the showing intersected thick Shabogamo Gabbro sills intruding the Sokoman Formation. To the west of the showing, the Kanipiskau Supergroup metasedimentary rocks are in thrust contact with basement rocks of the Ashuanipi Complex (Darch *et al.*, 2003b).

The stratigraphy of the Sokoman Formation in the area is poorly understood, and information on the distribution of oxide-, silicate- and carbonate-facies is based on 4 diamond-drill holes (Hovis and Broadbent, 2010; Hovis and Goldner, 2011b). Thick (>85 m) sequences of carbonate- and silicate-facies iron formation occur above and below a package of dominantly oxide-facies iron formation (up to 38.5 m thick) that may represent the MIF.

### ***Mineralization***

Massive to banded oxide-facies iron formation generally contains <40% iron oxides, with magnetite > hematite and gangue minerals dominated by quartz and carbonate (Hovis and Broadbent, 2010). In drillcore, oxide-facies iron formation is generally fresh and unaltered, and Mn contents are generally low (<0.5% Mn).

There is no published metallurgical testwork available from the Shabo Hill showing.

Fe grades are generally low (<30% Fe), with the best assay results from drillhole 10LB0005 (38.5 m at 27.5% Fe from 13 to 51.5 m) and drillhole 10LB0004 (34.2 m at 26.2% Fe from 2.3 to 36.5 m).

### ***Structure***

Structural measurements from the few outcrops present display a northeast-striking foliation. Interpretation of aeromagnetic data indicates that the showing is located in a synclinal structure (Hovis and Broadbent, 2010).

### ***Geophysics***

The area north and east of Northwest Arm is characterized by a strong magnetic high (Figure 59), which likely correlates with the highly magnetic oxide-facies iron formation. Ground gravity surveys have identified a number of anomalies, one of which was tested by drilling in 2010 that intersected interlayered iron formation and Shabogamo Gabbro (Hovis and Goldner, 2011a).

### **Resource and/or Reserves**

No NI 43-101 compliant mineral resource or reserve estimate available.

### **History of Exploration**

- 1950: Geological mapping (Neal, 1951)
- 1952: Geological mapping and prospecting (Beemer, 1952)
- 1956: Geological mapping and prospecting (Shklanka, 1956)
- 1972: Aeromagnetic survey (unpublished IOC report)
- 1979: Prospecting (Grant, 1979g)
- 2000: Data compilation, structural synthesis (Hulstein and Lee, 2001)
- 2001: Data compilation, regional airborne magnetic surveys, structural/stratigraphic interpretation (Cotnoir *et al.*, 2002)
- 2003: Geological mapping, ground gravity survey (Darch *et al.*, 2003b)
- 2007: Prospecting, ground gravity survey (Reynolds and Mitchell, 2008)
- 2010: Prospecting, diamond drilling (4 drillholes, 568.2 m, Hovis and Broadbent, 2010; Hovis and Goldner, 2011b)
- 2011: Ground gravity survey (Hovis and Goldner, 2011c), magnetic and electromagnetic airborne survey (Smith *et al.*, 2012)
- 2012: Airborne gravity gradiometer survey (Sauve *et al.*, 2012)



### 30. SHABO PENINSULA NORTH

**Alternate Name:** Shabogamo South Zone, Block No. 41, Northwest Arm No. 1

**MODS Showing(s):** 023G/02/Fe035

**Status:** Showing

**Structural Basin:** Wabush

**UTM Zone:** 19

**NTS Area:** 23G/02

**Northing (NAD27):** 5897615

**Easting (NAD27):** 660955

**Latitude:** 53.2052

**Longitude:** -66.5902

**Object Located:** Drillhole 11LB0019

#### Description of Occurrence

The Shabo Peninsula North showing is located on the southern end of a peninsula between Shabogamo Lake and Northwest Arm (Figure 60). It is approximately 37 km northeast of Labrador City, and access is *via* helicopter or by boat from Julienne Lake.

#### Geology and Stratigraphy

Geological mapping indicates that the property is underlain by graphitic schist of the Menihek Formation, conformably overlain by the Sokoman Formation iron formation (Figure 60). Although Wishart Formation quartzite does not outcrop, it has been recorded in cores from diamond drilling to conformably underlie the Sokoman Formation.

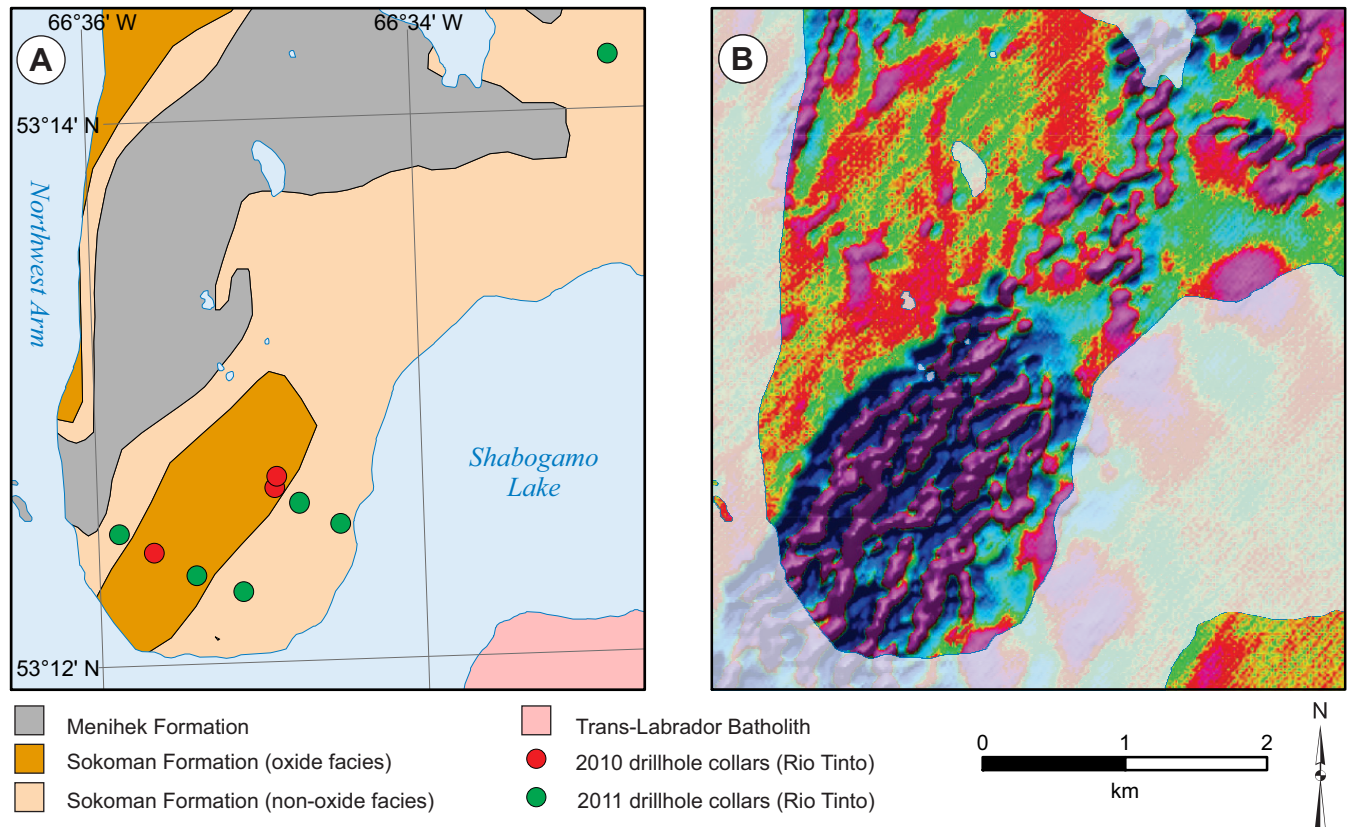


**Figure 60.** A) Geological map of the Shabo Peninsula North showing (adapted from Cotnoir et al., 2002), showing location of drillholes from 2010 and 2011 exploration programs (Hovis and Broadbent, 2010; Hovis and Goldner, 2011c); B) Airborne magnetics (second vertical derivative) showing extent of iron formation (data from Cotnoir et al., 2002).

Diamond drilling has intersected significant thicknesses of Sokoman Formation, but the stratigraphy is difficult to determine due to complex folding. The base of the Sokoman Formation, close to the contact with the Wishart Formation, is characterized by a thin (<10 m) silicate-rich member having large garnet porphyroblasts (Hovis and Goldner, 2011c), which is similar to the Basal Silicate Member recognized in the Rose and Scully deposits. Above this, the Sokoman Formation is composed of silicate-, carbonate- and oxide-facies iron formation in various proportions. Silicate- and carbonate-facies iron formation is more common close to the top and base of the Sokoman Formation, with oxide-facies iron formation more common in the middle of the formation.

### **Mineralization**

Oxide-facies iron formation is composed of fine- to medium-grained, disseminated to semi-massive magnetite and hematite (generally <30% Fe-oxides), with variable proportions of quartz, Fe-silicate (grunerite and actinolite) and carbonate minerals (Hovis and Goldner, 2011c). Magnetite is typically much more common than hematite, but some hematite-rich sections have been recorded (Hovis and Goldner, 2011c). Rhodochrosite is locally common, with up to 14.6% Mn over 3 m (drillhole 11LB0033 @ 402 m; Hovis and Goldner, 2011c).

There is no published metallurgical testwork available from the Shabo Peninsula North showing.

In general, Fe contents are low (<30% Fe) and include Fe contents in non-oxide minerals. However, some higher grade intervals of oxide-facies iron formation have been recorded. The best assay data from the main showing are from drillhole 11LB0019, which intersected 124 m of iron formation grading 27% Fe (from 182 to 306 m). Drillhole 11LB0033, located approximately 4 km northwest of the main showing, also intersected a significant thickness of iron formation at depth (100.7 m at 29.9% Fe from 248 to 348.7 m).

### **Structure**

Interpretation of diamond-drill hole data, as well as geophysical surveys and rare outcrops, indicate the Shabo Peninsula North showing is located in a northeast–southwest-trending, northwest-verging anticline (Hovis and Goldner, 2011c).

### **Geophysics**

A strong magnetic anomaly is located at the southern tip of the peninsula hosting the showing (Figure 60), illustrating that the Shabo Peninsula North showing is the northern extension of the Shabogamo showing. Ground gravity surveys show a strong positive gravity anomaly coincident with the high magnetic values (Reynolds and Mitchell, 2008).

### **Resource and/or Reserves**

No NI 43-101 compliant mineral resource or reserve estimate available.

### **History of Exploration**

- 1950: Geological mapping (Neal, 1951)
- 1952: Geological mapping and prospecting (Beemer, 1952)
- 1956: Geological mapping and prospecting (Shklanka, 1956)
- 1972: Aeromagnetic survey (unpublished IOC report)
- 1979: Ground magnetometer survey and prospecting (Price, 1979j)
- 2000: Data compilation, structural synthesis (Hulstein and Lee, 2001)
- 2001: Data compilation, regional airborne magnetic surveys, structural/stratigraphic interpretation (Cotnoir *et al.*, 2002)
- 2003: Geological mapping, ground gravity survey (Darch *et al.*, 2003b)
- 2007: Prospecting, ground gravity survey (Reynolds and Mitchell, 2008)
- 2010: Prospecting, diamond drilling (3 drillholes, 652.6 m, Hovis and Broadbent, 2010)
- 2011: Diamond drilling (6 drillholes, 2013.8 m), ground gravity survey (Hovis and Goldner, 2011c), magnetic and electromagnetic airborne survey (Smith *et al.*, 2012)
- 2012: Airborne gravity gradiometer survey (Sauve *et al.*, 2012)
- 2013: Mineralogical testwork (Sauve, 2014)

### 31. SHABOGAMO

**Alternate Name:** Scott Bay, Shabogamo No. 1, Shabogamo No. 2, Shabo Peninsula South

**MODS Showing(s):** 023G/02/Fe011, 023G/02/Fe012

**Status:** Prospect

**Structural Basin:** Wabush

**UTM Zone:** 19

**NTS Area:** 23G/02

**Northing (NAD27):** 5891514

**Easting (NAD27):** 657826

**Latitude:** 53.1518

**Longitude:** -66.6340

**Object Located:** Drillhole SB-01-01

#### Description of Occurrence

The Shabogamo prospect is located on a peninsula between Shabogamo Lake and Scott Bay (Figure 61). It is approximately 31 km northeast of Labrador City. Access is by boat from Julienne Lake, or by helicopter.

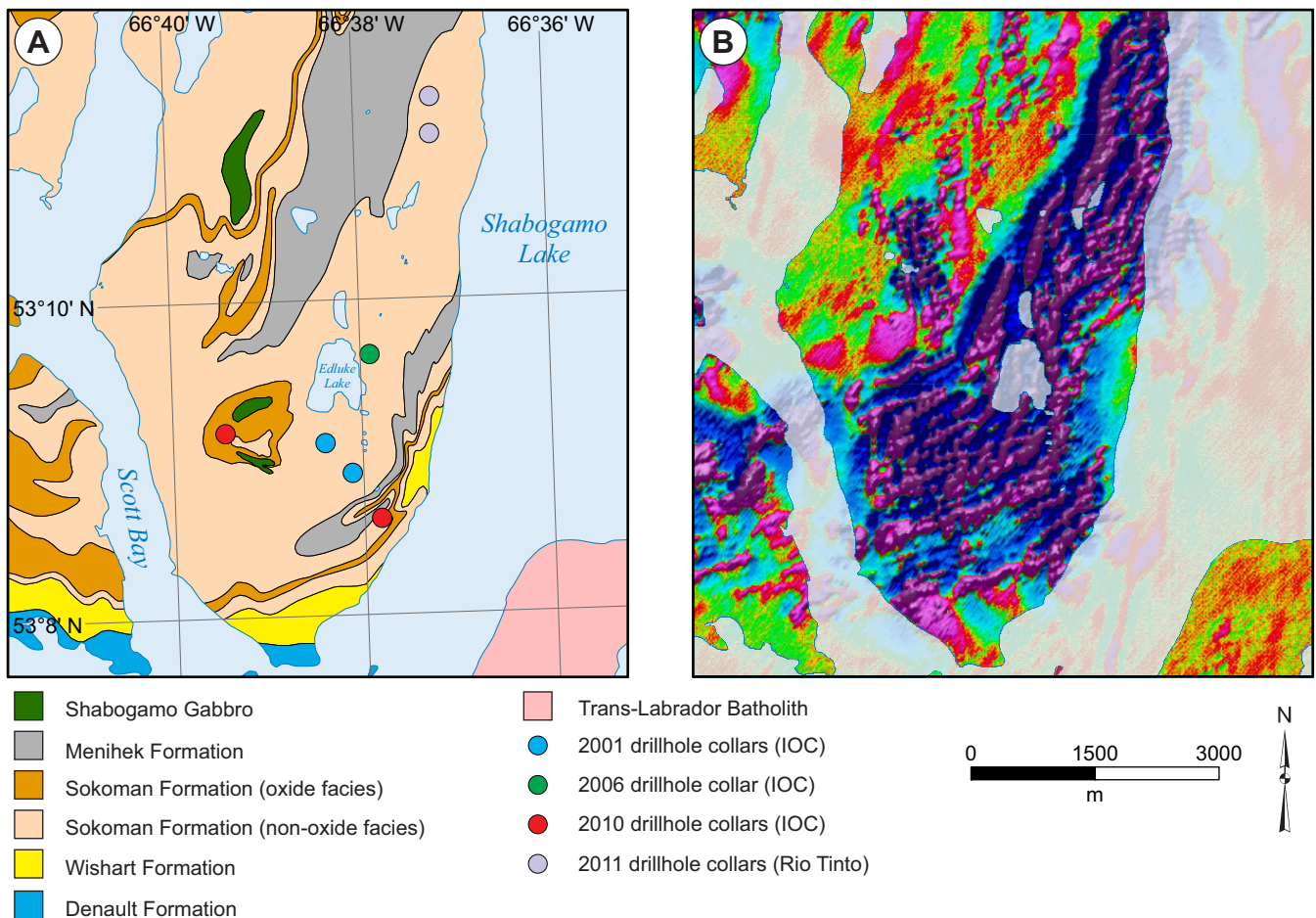


**Figure 61.** A) Geological map of the Shabogamo prospect (adapted from Cotnoir et al., 2002), showing location of drillholes from 2001, 2006, 2010 and 2011 exploration programs (Cotnoir et al., 2002; Clark, 2007; Carter, 2011d; Hovis and Goldner, 2011c); B) Airborne magnetics (second vertical derivative) showing extent of iron formation (data from Cotnoir et al., 2002).



## ***Geology and Stratigraphy***

The Shabogamo prospect is along strike from the Julienne 2 prospect. The bedrock is dominated by rocks of the Sokoman Formation, which are conformably overlain by Menihék Formation graphitic schist (Figure 61). The Sokoman Formation is underlain by quartzite of the Wishart Formation, which is present along the southern and eastern shores of the peninsula that hosts the prospect (Cotnoir *et al.*, 2002). Massive to foliated Shabogamo Gabbro sills outcrop to the north and west of Edluke Lake where they intrude the Sokoman Formation (Cotnoir *et al.*, 2002).

Outcrops of the Sokoman Formation are predominantly composed of silicate- and carbonate-facies iron formation, with some thin oxide-rich bands ranging up to 2 m thick (Cotnoir *et al.*, 2002; Darch, 2004); interpreted to represent the UIF. Thicker sequences of oxide-facies iron formation, representing the MIF, outcrop to the west of Edluke Lake as well on the southeast of the peninsula (Figure 61; Carter *et al.*, 2011f). A thin (<10 m) sequence of LIF has been recorded in drillhole SB-01-02, and is similar in composition to the UIF, but is differentiated due to its stratigraphic position above the Wishart Formation.

## ***Mineralization***

Oxide-facies iron formation is predominantly composed of quartz–magnetite schist, medium- to fine-grained disseminated to semi-massive magnetite, and rare hematite and gangue quartz ± actinolite–grunerite–carbonate. Rare pink carbonate (interpreted to be rhodochrosite) has also been recorded. In drillcore, the oxide-facies iron formation is generally fresh and unaltered.

There is no published metallurgical testwork available from the Shabogamo prospect.

Although significant thicknesses of oxide-facies iron formation have been reported from diamond drilling (>120 m in drill-hole SB-06-03), there is no available assay data from IOC's 2001, 2006 and 2010 drilling programs. A total of 28 grab and chip samples were collected during IOC's 2001 and 2004 mapping seasons, averaging 39.2% Fe, and 1.1% Mn (data from Cotnoir *et al.*, 2002, and Darch, 2004). Diamond drilling by Rio Tinto in 2011 targeted the northern limit of the prospect (Figure 61), and intersected 55 m of oxide-facies iron formation (25 to 70 m), which graded 29.7% Fe (Hovis and Goldner, 2011c).

## ***Structure***

The paucity of outcrop at the Shabogamo prospect makes structural interpretations difficult. At least two recorded folding events ( $F_1$  and  $F_2$ ) form a generally asymmetrical anticlinal–synclinal sequence of metasediments (Cotnoir *et al.*, 2002; Clark, 2007c). The axis of the anticline and syncline trends northeast–southwest through the property, and diamond drilling highlights the complex folding patterns, with sequences of UIF and LIF commonly infolded in MIF sequences (Cotnoir *et al.*, 2002; Clark, 2007c). Indications of possible thrusting have been observed in an area located approximately 1.5 km north of Edluke Lake where the UIF overlies the Menihék Formation (Cotnoir *et al.*, 2002).

## ***Geophysics***

The Shabogamo prospect is defined by a large aeromagnetic anomaly (Figure 61) that covers most of the peninsula and is the eastern extension of the magnetic anomaly observed at Julienne 1. Ground gravity surveys show that this magnetic anomaly coincides with a strong gravity anomaly of up to 17.5 milligals (Darch *et al.*, 2003b). This gravity anomaly was interpreted to represent a thick sequence of buried oxide-facies iron formation (Darch *et al.*, 2003b), and although subsequent drilling targeted this anomaly it has not been satisfactorily explained.

## **Resource and/or Reserves**

No NI 43-101 compliant mineral resource or reserve estimate available.

Non 43-101 compliant historical estimates, based on limited data, of 45 Mt grading 24% Fe were reported by Hulstein and Lee (2001), whereas a 2001 field evaluation by Cotnoir *et al.* (2002) suggested that the Shabogamo prospect could host a geological resource exceeding 500 Mt.

## History of Exploration

- 1950: Geological mapping (Neal, 1951)
- 1952: Geological mapping and prospecting (Beemer, 1952)
- 1953: Diamond drilling (15 drillholes, 330.7 m, Neal, 1953)
- 1957: Geological mapping (Crouse, 1957), 10 diamond-drill holes (described in Hulstein and Lee, 2001).
- 1972: Aeromagnetic survey (unpublished IOC report)
- 1979: Ground magnetometer survey (Price, 1979k), diamond drilling (2 drillholes, 77 m, Grant, 1979h)
- 1982: Diamond drilling (2 drillholes, 167.6 m, Simpson and Bird, 1982), airborne geophysical surveys (radiometrics, Johnson, 1982)
- 1985: Diamond drilling (1 drillhole, 112.8 m, Simpson *et al.*, 1985)
- 2000: Data compilation, structural synthesis (Hulstein and Lee, 2001)
- 2001: Data compilation, geological mapping and prospecting, diamond drilling (2 drillholes, 621 m), ground gravity survey, regional airborne magnetic surveys, structural/ stratigraphic interpretation (Cotnoir *et al.*, 2002)
- 2003: Geological mapping, ground gravity survey (Darch *et al.*, 2003b)
- 2004: Geological mapping and prospecting (Darch, 2004)
- 2006: Diamond drilling (1 drillhole, 151.5 m, Clark, 2007c)
- 2007: Ground gravity survey (Reynolds and Mitchell, 2008)
- 2010: Diamond drilling (2 drillholes, 246 m, Carter 2011e, f)
- 2011: Diamond drilling (2 drillholes, 414 m, Hovis and Goldner, 2011c), airborne electromagnetic, magnetic, and gravity surveys (Smith *et al.*, 2012; Wallace, 2012c)
- 2012: Airborne gravity gradiometer survey (Sauve *et al.*, 2012)
- 2013: Mineralogical testwork (Sauve, 2014)

## 32. SITTING BEAR

**Alternate Name:** Sitting Bear No. 1, Sitting Bear No. 2, Sudbury Lake West No. 2

**MODS Showing(s):** 023B/14/Fe005, 023B/14/Fe006

**Status:** Showing

**Structural Basin:** n/a

**UTM Zone:** 19

**NTS Area:** 23B/14

**Northing (NAD27):** 5859592

**Easting (NAD27):** 617940

**Latitude:** 52.8751

**Longitude:** -67.2476

**Object Located:** 2011 Rio Tinto sample location

### Description of Occurrence

The Sitting Bear showing is located to the north and to the east of Sitting Bear Lake (Figure 62), approximately 23 km west of Labrador City. There are no roads in the area, and access is *via* helicopter.

### Geology and Stratigraphy

The Sitting Bear showing is located to the southeast of the Green Water Lake showing, along strike (in the same belt) of Sokoman Formation iron formation. The Sokoman Formation outcrops to the north and east of Sitting Bear Lake, and geological

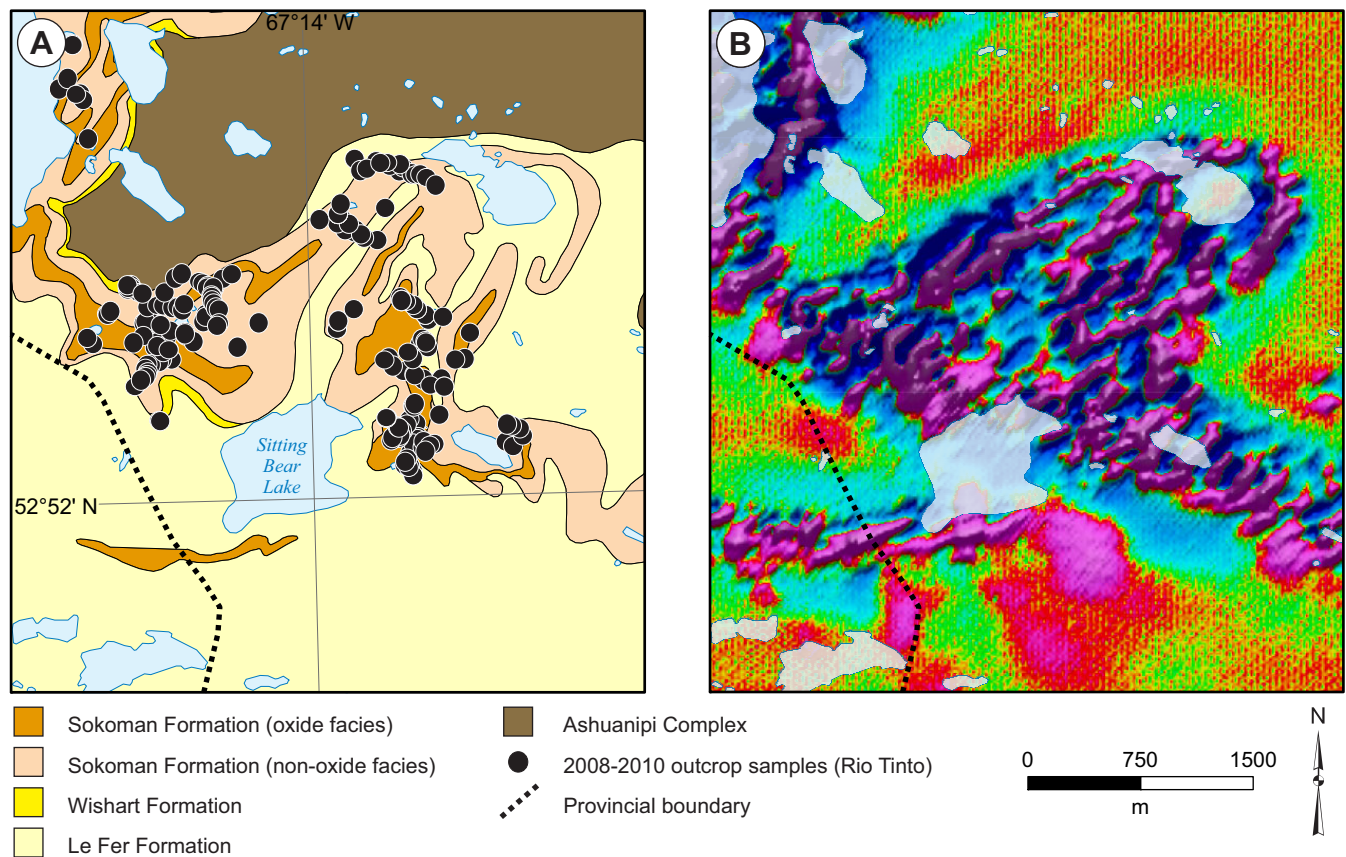


**Figure 62.** A) Geological map of the Sitting Bear showing (adapted from Cotnoir et al., 2002), showing outcrop sample locations from 2008, 2009 and 2010 exploration programs (Reynolds and Mitchell, 2008; Downing, 2009; Hovis and Goldner, 2011c); B) Airborne magnetics (second vertical derivative) showing extent of iron formation (data from Cotnoir et al., 2002).



mapping shows it is underlain by a thin sequence of Wishart Formation quartzite. Le Fer Formation schist forms the base of the stratigraphy in the Sitting Bear Lake area.

No information is available on the detailed stratigraphy of the Sokoman Formation at the Sitting Bear prospect, but geological mapping and prospecting has identified oxide-, silicate- and carbonate-facies iron formation (Reynolds and Mitchell, 2008).

### ***Mineralization***

Oxide-facies iron formation outcrops to the north and to the east of Sitting Bear Lake (Figure 62), with a section at least 20 m thick composed predominantly of oxide-facies iron formation exposed in a cliff face to the northeast of Sitting Bear Lake (Reynolds and Mitchell, 2008). Both hematite-rich and magnetite-rich oxide-facies iron formation, with up to 40–50% Fe-oxide minerals, have been recorded at the showing.

There is no published metallurgical testwork available from the Sitting Bear showing.

No drillholes have been completed on the Sitting Bear showing. Geochemical data from a single chip sample collected during the 2009 Rio Tinto exploration program returned 36.3% Fe (Downing, 2009).

### ***Structure***

Geological mapping indicates that the Sokoman Formation at the showing occurs in a syncline, and the area is crosscut by numerous faults (Hulstein and Lee, 2001).

### ***Geophysics***

The Sitting Bear showing is located within a prominent magnetic high on regional aeromagnetic surveys (Cotnoir *et al.*, 2002; Figure 62). Ground gravity surveys show a moderate gravity high northeast of Sitting Bear Lake (Reynolds and Mitchell, 2008).

## **Resource and/or Reserves**

No NI 43-101 compliant mineral resource or reserve estimate available.

Non 43-101 compliant historical estimates based on limited data of 4.05 Mt grading 26% Fe were reported by Hulstein and Lee (2001).

## **History of Exploration**

- 1953: Geological mapping and prospecting (Jackson, 1954)
- 1959: Gravity survey (Branch, 1959a)
- 1972: Aeromagnetic survey (unpublished IOC report)
- 1982: Airborne geophysical surveys (EM, magnetics, radiometrics, Johnson, 1982)
- 2000: Data compilation, structural synthesis (Hulstein and Lee, 2001)
- 2001: Data compilation, regional airborne magnetic surveys, structural/stratigraphic interpretation (Cotnoir *et al.*, 2002)
- 2008: Geological mapping and prospecting, gravity surveys (Reynolds and Mitchell, 2008)
- 2009: Geological mapping and prospecting (Downing, 2009)
- 2010: Geological mapping and prospecting, gravity surveys (Hovis and Goldner, 2011c)
- 2011: Magnetic and electromagnetic airborne survey (Smith *et al.*, 2012)
- 2012: Airborne gravity gradiometer survey (Suave *et al.*, 2012)

### 33. SMALLWOOD NORTH

**Alternate Name:** n/a

**MODS Showing(s):** n/a

**Status:** Prospect

**Structural Basin:** Carol

**UTM Zone:** 19

**NTS Area:** 23G/02

**Northing (NAD27):** 5879492

**Easting (NAD27):** 639555

**Latitude:** 53.0487

**Longitude:** -66.9181

**Object Located:** Drillhole SM-17-10

#### Description of Occurrence

The Smallwood North prospect is located in IOC's Carol Lake Mine area, approximately 13 km north of Labrador City and northeast of the past-producing Smallwood Mine (Figure 63). Access to the deposit is *via* a series of mine roads and bush roads that extend north from IOC's Concentrator and Pellet Plant.

#### Geology and Stratigraphy

The Smallwood North prospect is located in a broad syncline at the north end of the former Smallwood Mine (Figure 64). Wishart Formation quartzites are recorded stratigraphically below the Sokoman Formation iron formation. Shabogamo gabbro sills, ranging in thickness from <1 to 5 m, intrude the Sokoman Formation (IOC, personal communication).

The Sokoman Formation is subdivided into three units, the Lower Iron Formation (LIF), Middle Iron Formation (MIF) and Upper Iron Formation (UIF) (IOC, personal communication.). The LIF consists predominantly of carbonate-facies iron formation, and variable amounts of magnetite, hematite, grunerite, tremolite and actinolite. The MIF is predominantly composed of oxide-facies iron formation, and some stratigraphically conformable carbonate-facies units. The UIF is similar to the LIF and it consists of carbonate-facies iron formation with thin oxide-facies units and variable magnetite, hematite, grunerite, tremolite, and actinolite content.

#### Mineralization

Oxide-facies iron formation in the MIF consists of quartz–magnetite schist, with lesser amounts of hematite and siderite (IOC, personal communication). Magnetite grain size is coarser in the fold hinges and finer in the limbs (IOC, personal communication).

Alteration is variable across the prospect, with the degree of alteration increasing to the northwest (IOC, personal communication). This alteration occurs as abundant secondary goethite with leaching of carbonate.

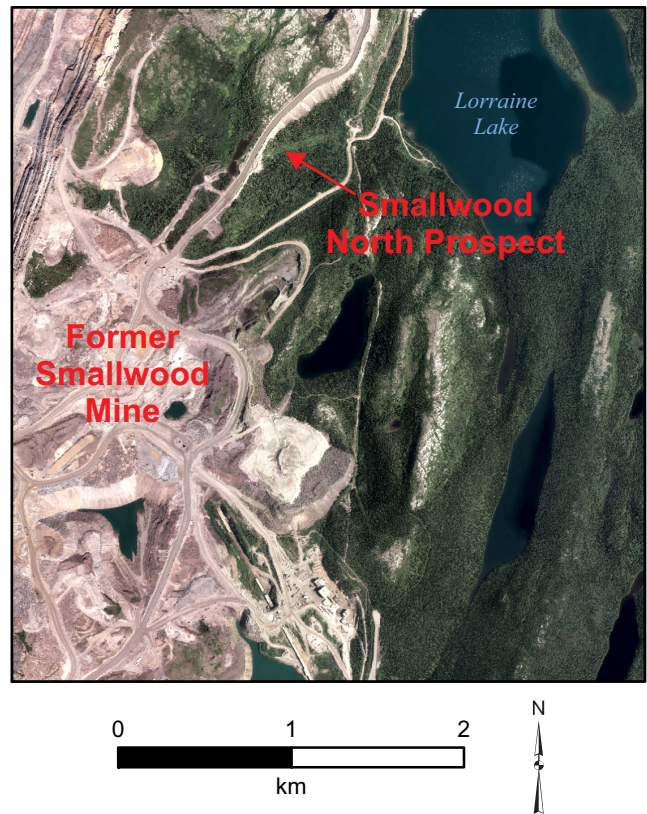


**Figure 63** Aerial photograph of the Smallwood North prospect, showing location of the former Smallwood Mine (image courtesy of IOC).

There is no published assay data or metallurgical testwork data from the Smallwood North prospect. However, most of the 2017 drillholes intersected significant intervals of oxide-facies iron formation in the MIF (IOC, personal communication).

**Structure**

The simplified structure of the Smallwood North prospect is that of a broad syncline, with an east limb approaching vertical in places. Interpretations suggest that there is a large fault which has superimposed the Wishart Formation over the Middle Iron Formation in the southeastern portion of the deposit (IOC, personal communication). It is postulated that the Smallwood North prospect is a faulted extension of the previously mined out Smallwood deposit to the southwest (IOC, personal communication).

**Geophysics**

The Smallwood North prospect is associated with a strong magnetic anomaly on regional aeromagnetic surveys (Cotnoir *et al.*, 2002; Figure 64), which is associated with the high magnetite content of the MIF.

**Resource and/or Reserves**

No NI 43-101 compliant mineral resource or reserve estimates are available.

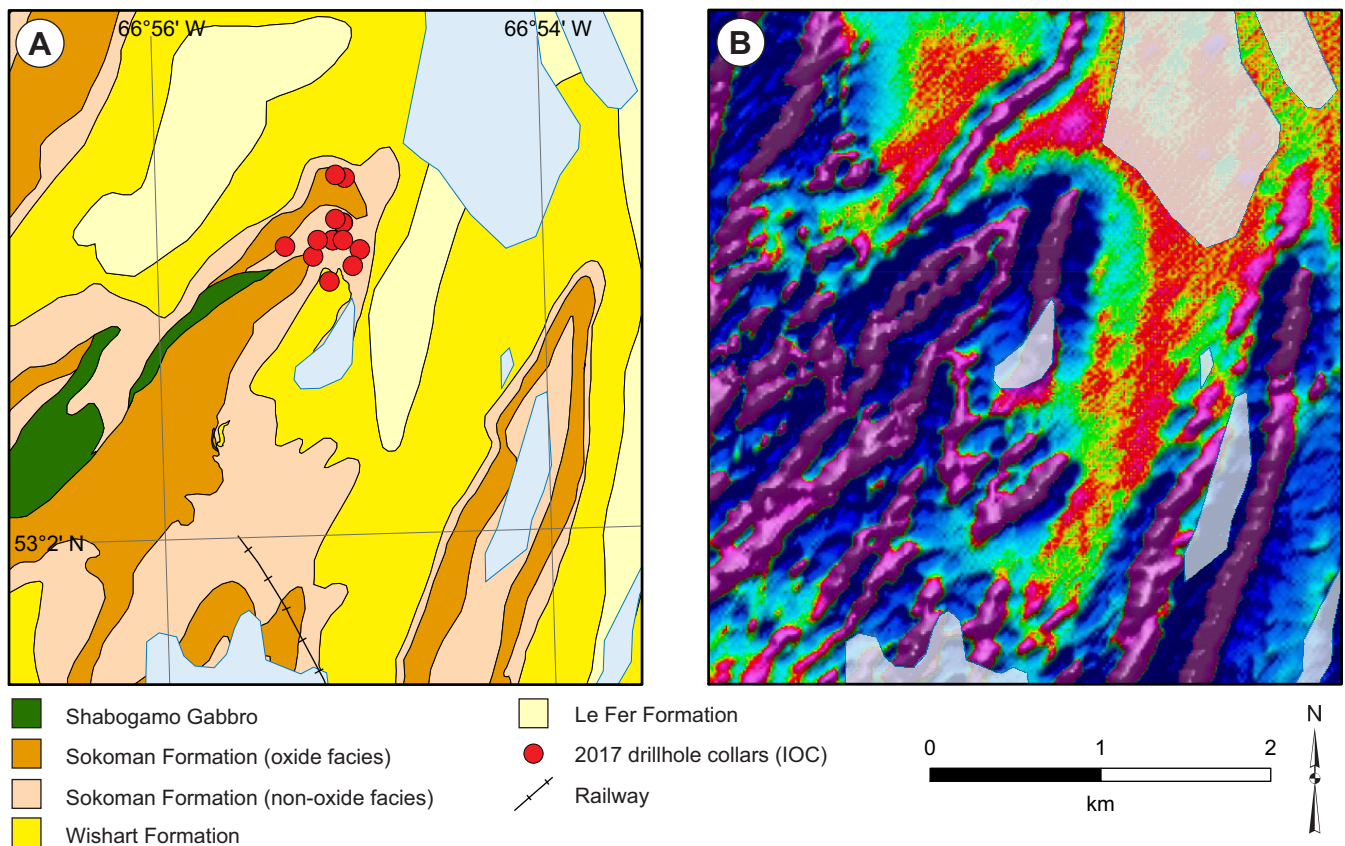


**Figure 64.** A) Geological map of the Smallwood North prospect (adapted from Cotnoir *et al.*, 2002), showing location of drill-holes from 2017 exploration programs (IOC, personal communication); B) Airborne magnetics (second vertical derivative) showing extent of iron formation (data from Cotnoir *et al.*, 2002).



### History of Exploration

- 1949: Geological mapping (Neal, 1950a)
- 1950: Geological mapping (Neal, 1951)
- 1953: Geological mapping and prospecting
- 1958: Geological mapping
- 1962: Production begins at Smallwood deposit (Smallwood Mine)
- 1972: Aeromagnetic survey (Unpublished IOC report)
- 1979: Ground magnetometer survey (Unpublished IOC report)
- 2000: Data compilation, structural synthesis (Hulstein and Lee, 2001)
- 2001: Data compilation, regional airborne magnetic surveys, structural/stratigraphic interpretation (Cotnoir *et al.*, 2002)
- Pre-2006: Diamond-drill program totalling 23 301 m drilled in 240 holes (IOC, personal communication)
- 2012: Diamond drilling (3 drillholes, 331 m, IOC, personal communication)
- 2017: Diamond drilling (14 drillholes, 1962 m, IOC, personal communication)

## 34. SQUID

**Alternate Name:** n/a

**MODS Showing(s):** 023B/14/Fe029

**Status:** Showing

**Structural Basin:** Carol

**UTM Zone:** 19

**NTS Area:** 23B/14, 23B/15

**Northing (NAD27):** 5873331

**Easting (NAD27):** 633627

**Latitude:** 52.9947

**Longitude:** -67.0087

**Object Located:** Drillhole SQ-11-01

### Description of Occurrence

The Squid showing (Figure 65) is located ~2 km west of the White Lake prospect, and ~9 km northwest of Labrador City. Access to the showing is by road and bush road from IOC's Carol Lake Mine, south of Sherwood dump (called the "Maggie Lake" road), then on foot from the White Lake prospect.

### Geology and Stratigraphy

The geology at the Squid showing comprises a series of anticlines and synclines cored by the Sokoman Formation iron formation, and is underlain by the Wishart and Le Fer formations (Figure 65). The Sokoman Formation is intruded by sills of Shabogamo Gabbro.

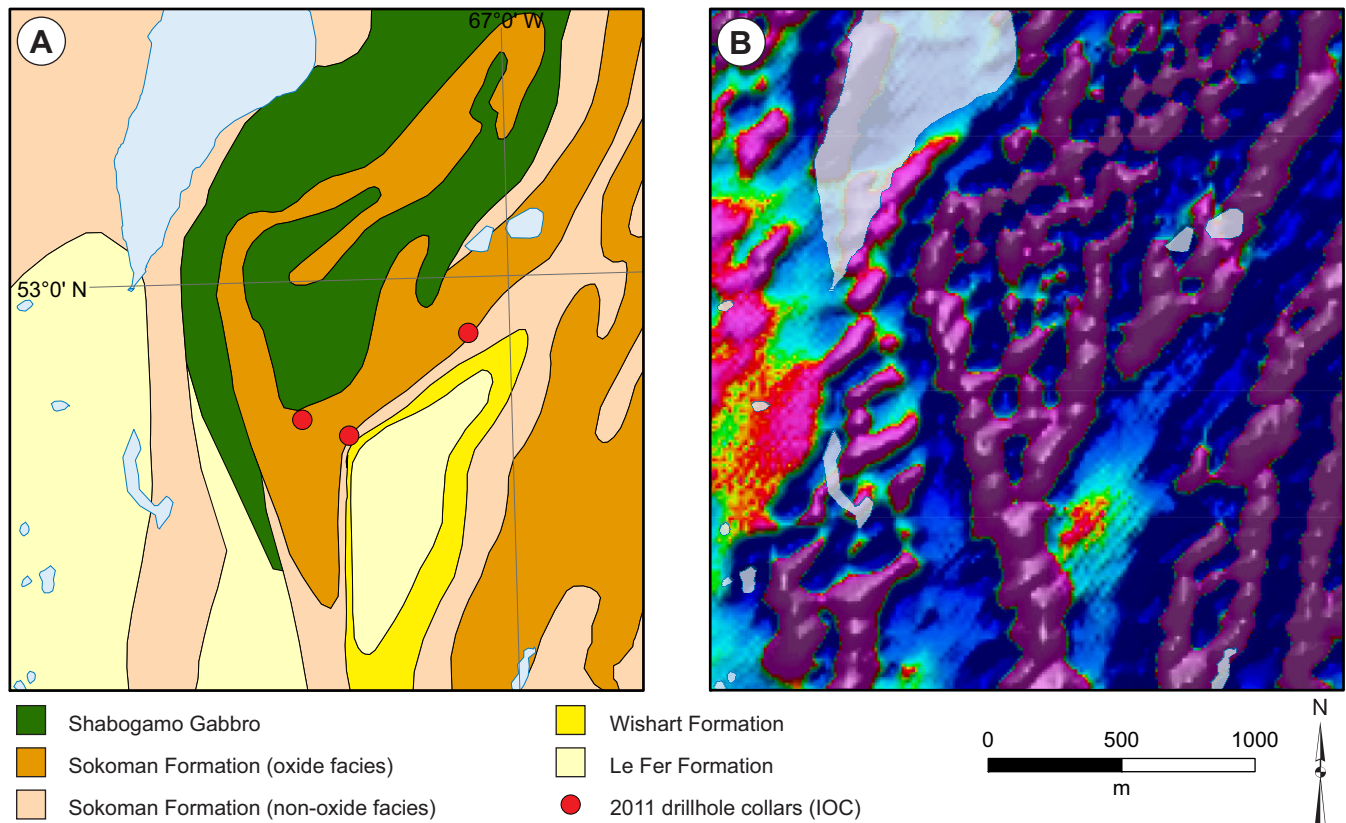


**Figure 65.** A) Geological map of the Squid showing (adapted from Cotnoir et al., 2002), showing location of drillholes from 2011 exploration programs (Duvergier, 2012); B) Airborne magnetics (second vertical derivative) showing extent of iron formation (data from Cotnoir et al., 2002).

The detailed stratigraphy of the Sokoman Formation at the Squid showing is poorly understood due the lack of drillhole data and structural complexity. Diamond drilling has identified oxide-, carbonate- and silicate-facies iron formation. Drillhole SQ-11-02 intersected a >175 m sequence of dominantly oxide-facies iron formation (and lesser carbonate- and silicate-facies iron formation), which likely represents the MIF (Duvergier, 2012). Other drillholes have intersected predominantly silicate- and carbonate-facies iron formation with thin (generally <15 m) intervals of oxide-facies iron formation (Duvergier, 2012), which may represent the LIF. The UIF was not intersected during diamond drilling, but geological mapping to the north of the Squid showing has identified quartz–grunerite–magnetite schist that has been interpreted as UIF in the core of a syncline (Cotnoir *et al.*, 2002).

### ***Mineralization***

Oxide-facies iron formation is predominantly composed of quartz–magnetite schist, where magnetite is concentrated in bands or as disseminations (Duvergier, 2012). Gangue Fe-silicate minerals (grunerite and actinolite) are common, and contacts between oxide- and carbonate-facies are generally gradational. In drillcore, the oxide-facies is generally fresh and unaltered. Manganese contents of up to 1.5 wt. % have been recorded (Duvergier, 2012), but no pyrolusite or other Mn-oxides have been visually observed.

Duvergier (2012) report on SAG Power index (SPI) and iron recovery testing (TT) on composite drillcore samples from the Squid showing, which show that ore samples have similar hardness (SPI) to ore from elsewhere in the Carol Lake Mine area, but have lower iron recovery.

Assay data from drillcore indicate that the oxide-facies iron formation is generally lower grade than ore material from the Carol Lake area (<30 wt. % Fe). Thin sequences of ore-grade material were encountered in drillhole SQ-11-02, with the best interval returning 31.7% Fe over 12 m (150 to 162 m).

### ***Structure***

Geological mapping and interpretation of regional aeromagnetic data indicate that the Squid showing lies within an east-dipping, north- to northeast-trending syncline that plunges to the northeast, and is flanked by two anticlines (Cotnoir *et al.*, 2002).

### ***Geophysics***

The Squid showing was identified based on regional airborne magnetic data, which recognized a north–northeast-trending moderate to high-intensity magnetic anomaly that is 150 to 700 m wide and 3000 m long (Cotnoir *et al.*, 2002; Figure 65).

### **Resource and/or Reserves**

No NI 43-101 compliant mineral resource or reserve estimate available.

### **History of Exploration**

- 1949: Geological mapping (Neal, 1950a)
- 1972: Aeromagnetic survey (unpublished IOC report)
- 2001: Data compilation, geological mapping and prospecting, regional airborne magnetic surveys, structural/ stratigraphic interpretation (Cotnoir *et al.*, 2002)
- 2011: Diamond drilling (3 drillholes, 625 m, Duvergier, 2012)



### 35. WABUSH 1

**Alternate Name:** Wabush #1, Wabush No. 1  
**MODS Showing(s):** 023B/15/Fe002  
**Status:** Prospect  
**Structural Basin:** Carol  
**UTM Zone:** 19  
**NTS Area:** 23B/15  
**Northing (NAD27):** 5869718  
**Easting (NAD27):** 636305  
**Latitude:** 52.9616  
**Longitude:** -66.9677  
**Object Located:** Drillhole W1-02-01

#### Description of Occurrence

The Wabush 1 prospect is located on a ridge to the east of Leg Lake (Figure 66), approximately 4 km northwest of Labrador City. It is located to the south of the Wabush 3 deposit, from which it is separated by a low-lying area with limited outcrop exposure. Access is on foot from a series of gravel roads that extend north from the TLH (Figure 66).

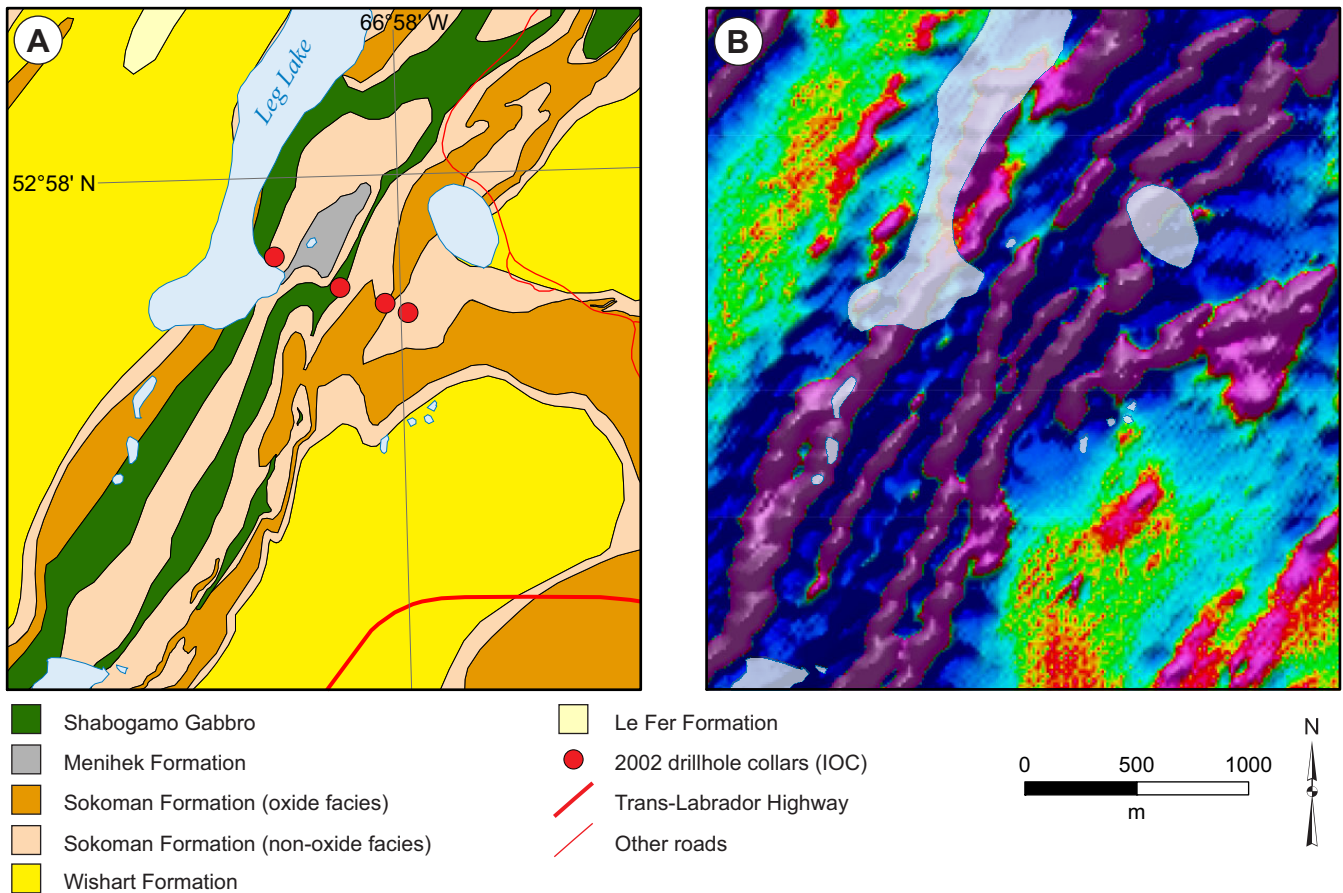


**Figure 66.** A) Geological map of the Wabush 1 prospect (adapted from Cotnoir et al., 2002), showing location of drillholes from 2002 exploration program (Darch et al., 2003a); B) Airborne magnetics (second vertical derivative) showing extent of iron formation (data from Cotnoir et al., 2002).

## ***Geology and Stratigraphy***

The Wabush 1 prospect occurs in the keel and eastern limb of a synclinal structure that preserves the upper part of the Kaniapiskau Supergroup stratigraphy. Menihek Formation graphitic schist is located in the core of the syncline, and conformably overlies the Sokoman Formation (Figure 66). Wishart Formation quartzite occurs stratigraphically below the iron formation. The upper part of the Sokoman Formation is intruded by thick Shabogamo Gabbro sills (Figure 66), with drilling intersecting >150 m of metagabbro (Darch *et al.*, 2003a).

The stratigraphy of the Sokoman Formation is similar to that at the Wabush 3 deposit. The UIF and LIF consist of carbonate- and silicate-facies iron formation with only minor oxide bands. The MIF is dominantly oxide-facies iron formation.

## ***Mineralization***

Drilling on the main mineralized outcrop intersected a 105.3-m-thick sequence of oxide-facies iron formation (Darch *et al.*, 2003a). The oxide-facies iron formation is coarse grained, with magnetite>hematite and gangue quartz, carbonate and actinolite. In drillcore, the MIF is generally fresh, but strongly altered oxide-facies iron formation has been recorded to the east of the prospect close to the Wabush 4 prospect (IOC, personal communication). Manganese contents are generally <1%.

Darch *et al.* (2003) reported RMI determination, minus 200 mesh weight fraction and iron weight recovery values. When compared to IOC's chemical and physical crude-ore characteristics (reported in Cotnoir *et al.*, 2002), these show that ore from the Wabush 1 deposit has similar or slightly better iron weight recovery values and minus 200 mesh weight. The RMI determination indicates a hard grinding ore (Darch *et al.*, 2003a).

The best assay results correspond to the thickest oxide-facies intervals in drillhole W1-02-01 (39.1% Fe over 113.3 m at 1.2 m depth).

## ***Structure***

The Wabush 1 prospect is located in a north-northeast-trending overturned syncline that extends northward along strike to the Wabush 3 deposit (Darch *et al.*, 2003a). The western limb of the fold dips to the east at 25 to 45° whereas the eastern limb has a much steeper dip (vertical to 70° to the east). The Wabush 1 prospect is located in the keel and eastern limb of the syncline, where structural thickening of the Sokoman Formation has occurred (Darch *et al.*, 2003a).

Geological mapping indicates that the normal fault observed crossing the Canning prospect may continue northeastward through the Wabush 1 prospect (Muwais and Broemling, 1971).

## ***Geophysics***

Regional airborne magnetic surveys (Figure 66; Cotnoir *et al.*, 2002) show that the Wabush 1 prospect is coincident with a strong magnetic anomaly that continues northward to the Wabush 3 deposit. Ground gravity surveys (Darch *et al.*, 2003a) have recorded the presence of a strong gravity anomaly that is coincident with the magnetic anomaly.

## **Resource and/or Reserves**

No NI 43-101 compliant mineral resource or reserve estimate available.

Non 43-101 compliant historical estimates based on limited data of 5 Mt grading 40.4% Fe for the Wabush 1 prospect were reported by Elliot *et al.* (1980).

### History of Exploration

- 1949: Geological mapping (Neal, 1950a)
- 1950: Geological mapping (Neal, 1951)
- 1972: Aeromagnetic survey (unpublished IOC report)
- 1978: Ground magnetic survey (Price, 1979g)
- 2000: Data compilation, structural synthesis (Hulstein and Lee, 2001)
- 2001: Data compilation, regional airborne magnetic surveys, structural/stratigraphic interpretation (Cotnoir *et al.*, 2002)
- 2002: Geological mapping and prospecting, diamond drilling (4 drillholes, 895 m), ground gravity survey (Darch *et al.*, 2003a)



### 36. WABUSH 3

**Alternate Name:** Moss Pit, Wabush #3, Wabush No. 3, Labrador Ridge

**MODS Showing(s):** 023B/15/Fe003

**Status:** Producer

**Structural Basin:** Carol

**UTM Zone:** 19

**NTS Area:** 23B/15

**Northing (NAD27):** 5872119

**Easting (NAD27):** 637949

**Latitude:** 52.9828

**Longitude:** -66.9459

**Object Located:** Approximate centre of proposed pit

#### Description of Occurrence

The Wabush 3 deposit is located approximately 5 km northwest of Labrador City and is directly south of the Luce Pit at IOC's Carol Lake Mine (Figure 67). Access is *via* a series of gravel and bush roads that extend north from the TLH.

#### Geology and Stratigraphy

The bedrock geology of the Wabush 3 deposit is dominated by the Sokoman Formation iron formation, which occupies the core of a large, open syncline (Figure 68). The Sokoman Formation is conformably underlain by Wishart Formation quartzite, which outcrops extensively on high ridges surrounding the deposit. At the southern end of the Wabush 3 deposit, the Sokoman Formation is intruded by a large unit of Shabogamo Gabbro, with drilling intersecting >200-m-thick intervals of gabbro.

The Sokoman Formation is subdivided into a lower silicate- and carbonate-facies unit (LIF), a middle oxide-facies unit (MIF) and an upper silicate- and carbonate-facies unit (UIF). The MIF is subdivided into an upper hematite-rich member and a lower magnetite-rich member.

#### Mineralization

Diamond drilling has recorded thick (>400 m) sequences of oxide-facies iron formation (MIF) at the Wabush 3 deposit (Pond, 2013). The upper part of the MIF is hematite-rich, with minor disseminated magnetite (Plate 45A). The lower part of the MIF is magnetite-dominated, with minor medium- to very coarse-grained specular hematite (Plate 45B–D). Gangue minerals include quartz, carbonate and Fe-silicate minerals (grunerite and actinolite).

Alteration of the iron formation is generally weak to moderate, with moderate to strong alteration (goethite-rich) associated with fault zones. Assay data from 2007–2012 drilling show that Mn contents of ore samples average 0.67% Mn (n = 4128, Pond, 2013). Manganese contents are generally higher (>1% Mn) at the base of the MIF and top of the LIF, with intervals ranging up to 5.2% Mn over 32 m (drillhole W3-11-62 from 22 m; Pond, 2013) and 3.3% Mn over 69 m (drillhole W3-12-117 from 19 m; Pond, 2013).

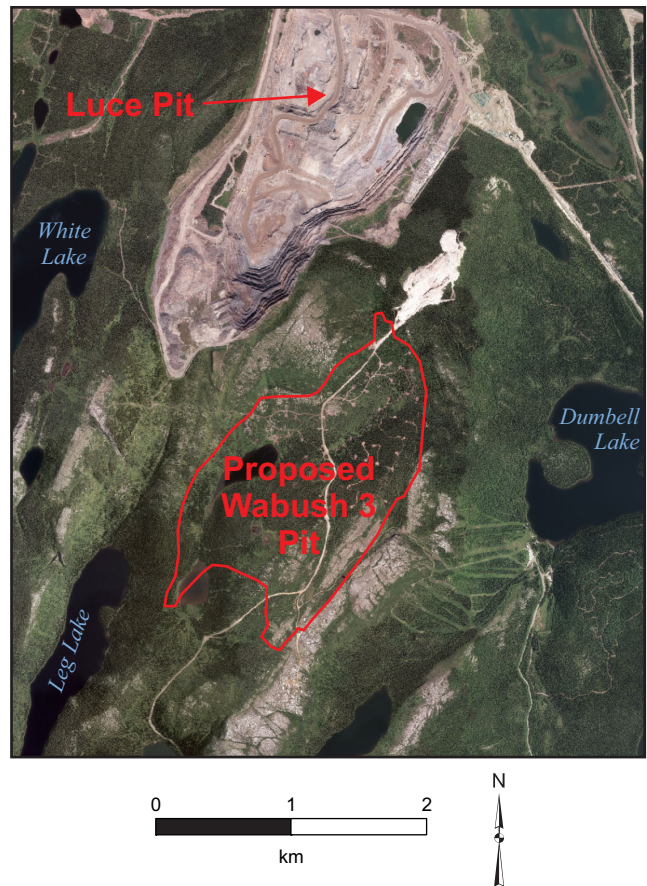


**Figure 67.** Aerial photograph of the Wabush 3 and Luce deposits, showing outline of the proposed Wabush 3 pit (image courtesy of IOC).

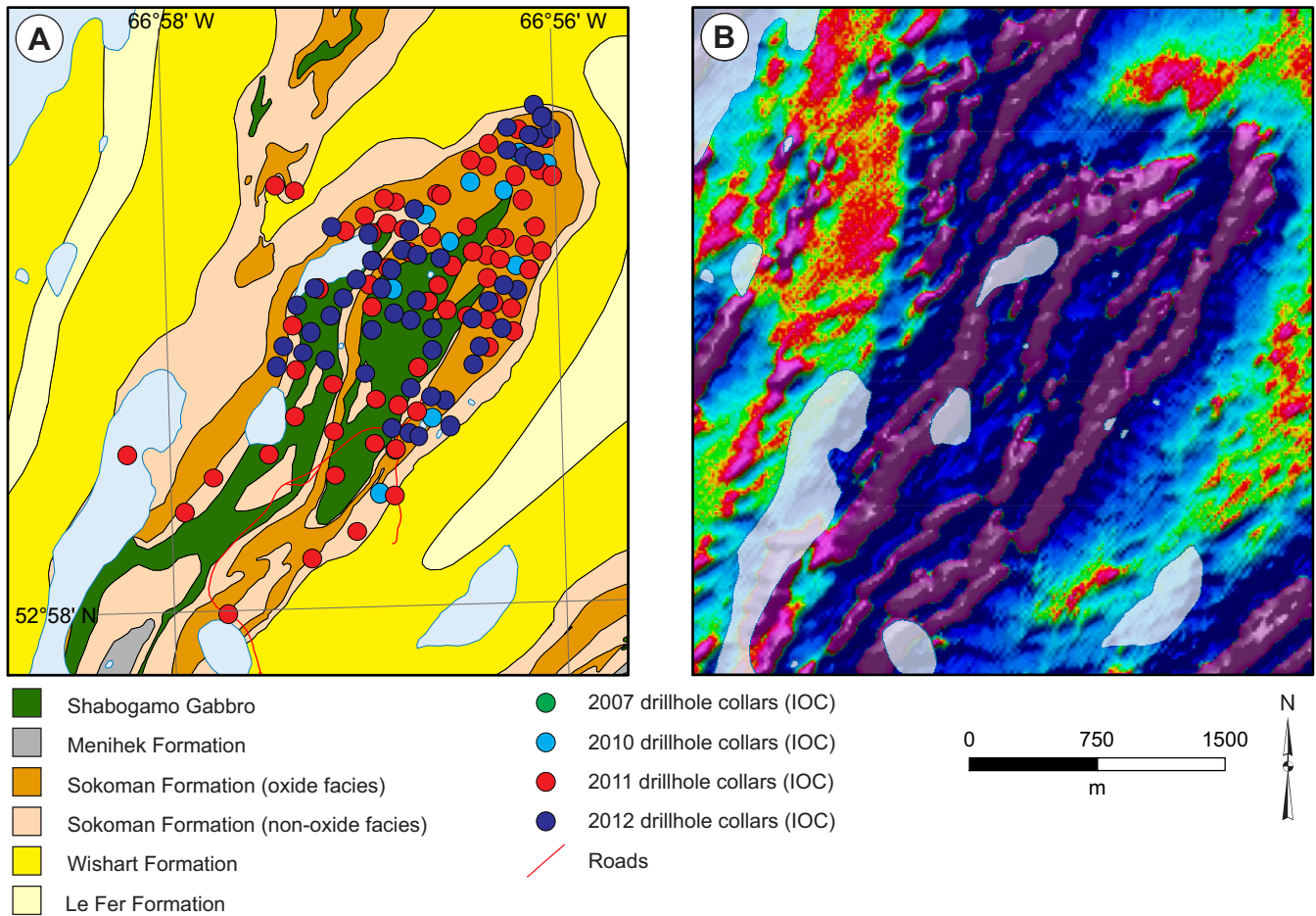


**Figure 68.** A) Geological map of the Wabush 3 deposit (adapted from Cotnoir et al., 2002), showing location of drillholes from 2007 and 2010–2012 exploration programs (Pond, 2013); B) Airborne magnetics (second vertical derivative) showing extent of iron formation (data from Cotnoir et al., 2002).

Metallurgical testwork from the 1965 feasibility study show that ore from the Wabush 3 deposit is amenable to simple beneficiation processes, producing a dry concentrate with 65.6% Fe and 4.5% silica, and dry pellets containing 64.8% Fe and 5.3% silica (Labrador Mining and Exploration Company Limited, 1965). Pond (2013) reported on SAG Power index (SPI) and iron recovery testing (TT) from 1182 composite samples from 2007 to 2012 drilling. These data show that magnetite-rich and hematite-rich ores have similar iron recovery, but magnetite-rich ore is a harder grinding ore (higher SPI values). Development plans for the Wabush 3 deposit envisage processing using IOC's existing processing facilities (Iron Ore Company of Canada, 2014).

Assay data from diamond drilling show significant thicknesses of ore-grade iron formation, with Fe contents of ore-grade samples from 2007–2012 drilling averaging 38.2% Fe (n = 4128). Highlights include 36.5% Fe over 316 m in drillhole W3-11-65 (15 to 331 m), 37.3% Fe over 315.6 m in drillhole W3-11-63 (2.4 to 318 m) and 39% Fe over 278.2 m in drillhole W3-12-139 (6.8 to 278.2 m).

### Structure

The Wabush 3 deposit is located in an open, broadly folded syncline (Pond, 2013). Fold limbs along the western margins dip approximately 30° to the east, whereas the eastern most limb of the fold is more steeply dipping with sub-vertical dips. The main synclinal fold axis plunges to the south at approximately 20°, with a reversal of the plunge toward the southern end of the deposit (Pond, 2013).



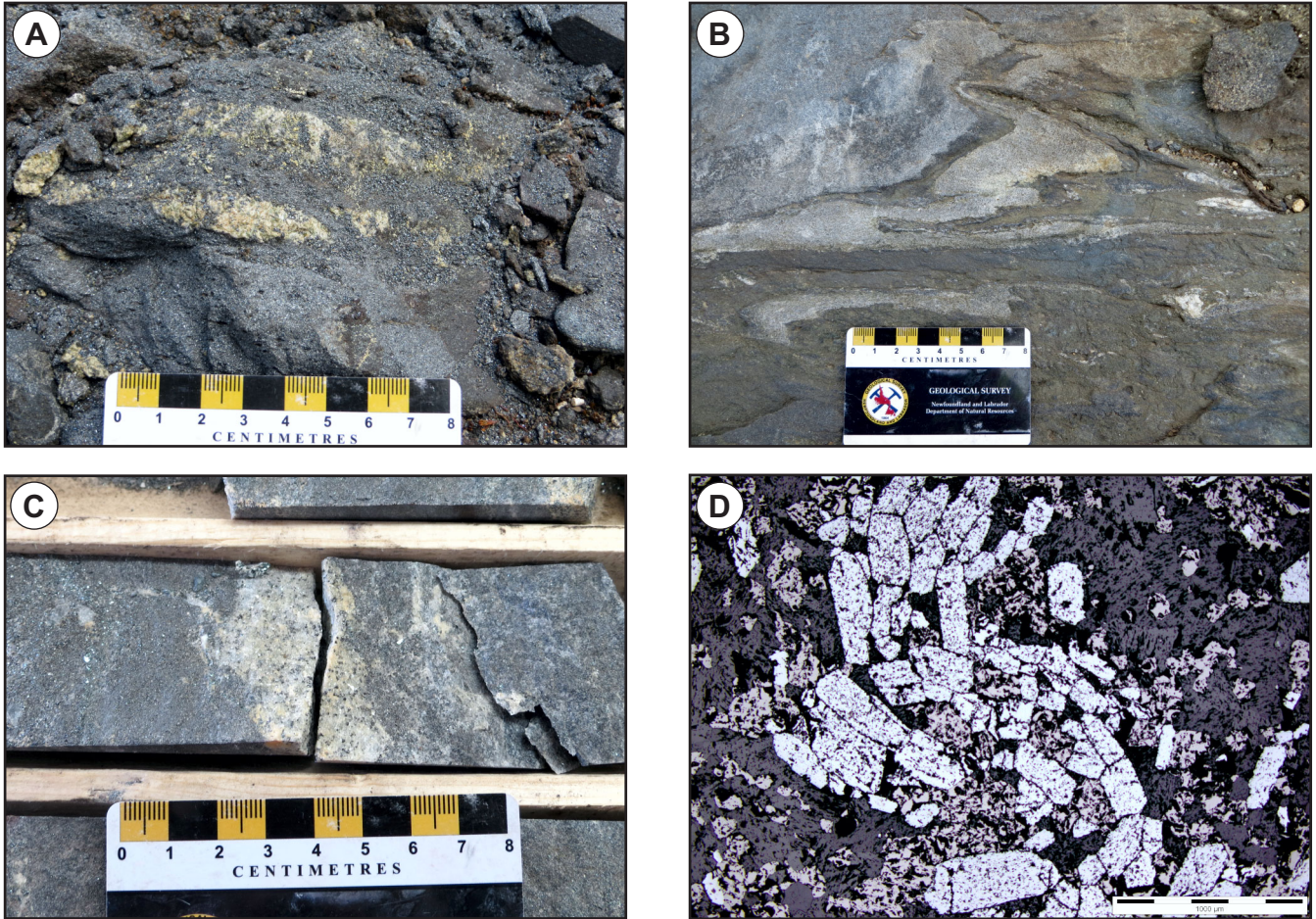


**Plate 45.** A) Outcrop of friable, hematite-rich oxide facies iron formation with folded band of Fe-silicates; B) Outcrop of folded oxide-facies iron formation, with magnetite-rich bands (dark grey) and quartz-rich bands (light grey); C) Banded magnetite-rich oxide-facies iron formation, with band of Fe-silicate-quartz and minor coarse-grained hematite (drillhole W3-11-101 @ 215.5 m); D) Photomicrograph of oxide-facies iron formation, with magnetite (pink grey) and tabular coarse-grained hematite crystals (light grey) (drillhole W3-11-101 @ 215.5 m).

Numerous small faults were recorded during diamond drilling, and are associated with moderate to strong alteration of the iron formation.

### **Geophysics**

Regional airborne magnetic surveys (Cotnoir *et al.*, 2002) show that the Wabush 3 orebody coincides with a strong magnetic anomaly (Figure 68). This strong anomaly can be correlated with the magnetite-rich unit in the lower part of the MIF. In addition, gravity surveys have identified a moderate to strong gravity anomaly at the Wabush 3 deposit (Darch *et al.*, 2003a).

### **Resource and/or Reserves**

NI 43-101 compliant resources (Iron Ore Company of Canada, 2014).

- Measured resources: 419 Mt at 38% Fe
- Indicated resources: 325 Mt at 38% Fe
- Inferred resources: 66 Mt at 38% Fe



## History of Exploration

- 1949: Regional geological mapping, bulk sample (Neal, 1950a)
- 1950: Prospecting and metallurgical testwork (Neal, 1950b)
- 1951: Diamond drilling (2 drillholes, 60.4 m, Moss, 1952)
- 1958: Geological mapping and prospecting, dip needle surveys (referenced in Labrador Mining and Exploration Company Limited, 1965)
- 1959: Gravity survey (Branch, 1959b), diamond drilling (20 drillholes, 1362 m, Tuffy, 1960)
- 1961: Diamond drilling (48 drillholes, 6582 m) (referenced in Labrador Mining and Exploration Company Limited, 1965), ground magnetometer survey (Tuffy, 1962)
- 1949-1963: Metallurgical testwork (referenced in Labrador Mining and Exploration Company Limited, 1965)
- 1965: Feasibility study (Labrador Mining and Exploration Company Limited, 1965)
- 1972: Aeromagnetic survey (unpublished IOC report)
- 1978: Ground magnetometer survey (Price, 1979g)
- 2000: Data compilation, structural synthesis (Hulstein and Lee, 2001)
- 2001: Data compilation, regional airborne magnetic surveys, structural/stratigraphic interpretation (Cotnoir *et al.*, 2002)
- 2006: Diamond drilling (19 drillholes, 3582.8 m, referenced in Pond, 2013)
- 2007: Diamond drilling (2 drillholes, 740 m, Pond, 2013)
- 2010: Diamond drilling (12 drillholes, 2561.7 m), metallurgical testwork (Pond, 2013)
- 2011: Diamond drilling (71 drillholes, 14 663.25 m), metallurgical testwork (Pond, 2013)
- 2012: Diamond drilling (50 drillholes, 11 925.7 m), metallurgical testwork (Pond, 2013)
- 2013: Diamond drilling (9 drillholes, 1147 m)
- 2014: Diamond drilling (78 drillholes, 18 321 m)
- 2015: Diamond drilling (69 drillholes, 13 540 m)
- 2018: Production begins at Wabush 3 deposit (Moss Pit)

### 37. WABUSH 4

**Alternate Name:** Wabush #4, Wabush No. 4  
**MODS Showing(s):** 023B/15/Fe004  
**Status:** Prospect  
**Structural Basin:** Carol  
**UTM Zone:** 19  
**NTS Area:** 23B/15  
**Northing (NAD27):** 5868890  
**Easting (NAD27):** 638330  
**Latitude:** 52.9537  
**Longitude:** -66.9409  
**Object Located:** MODS Occurrence

#### Description of Occurrence

The Wabush 4 prospect is located 1.5 km northwest of Labrador City, on a hill directly behind the Labrador West Health Centre. Access is *via* numerous gravel roads that extend north from the TLH (Figure 69).

#### Geology and Stratigraphy

The Wabush 4 prospect is located south along strike from the Mill Basin prospect and Wabush 6 deposit. The bedrock geology of the Wabush 4 prospect is predominately composed of the Sokoman Formation iron formation, and is conformably

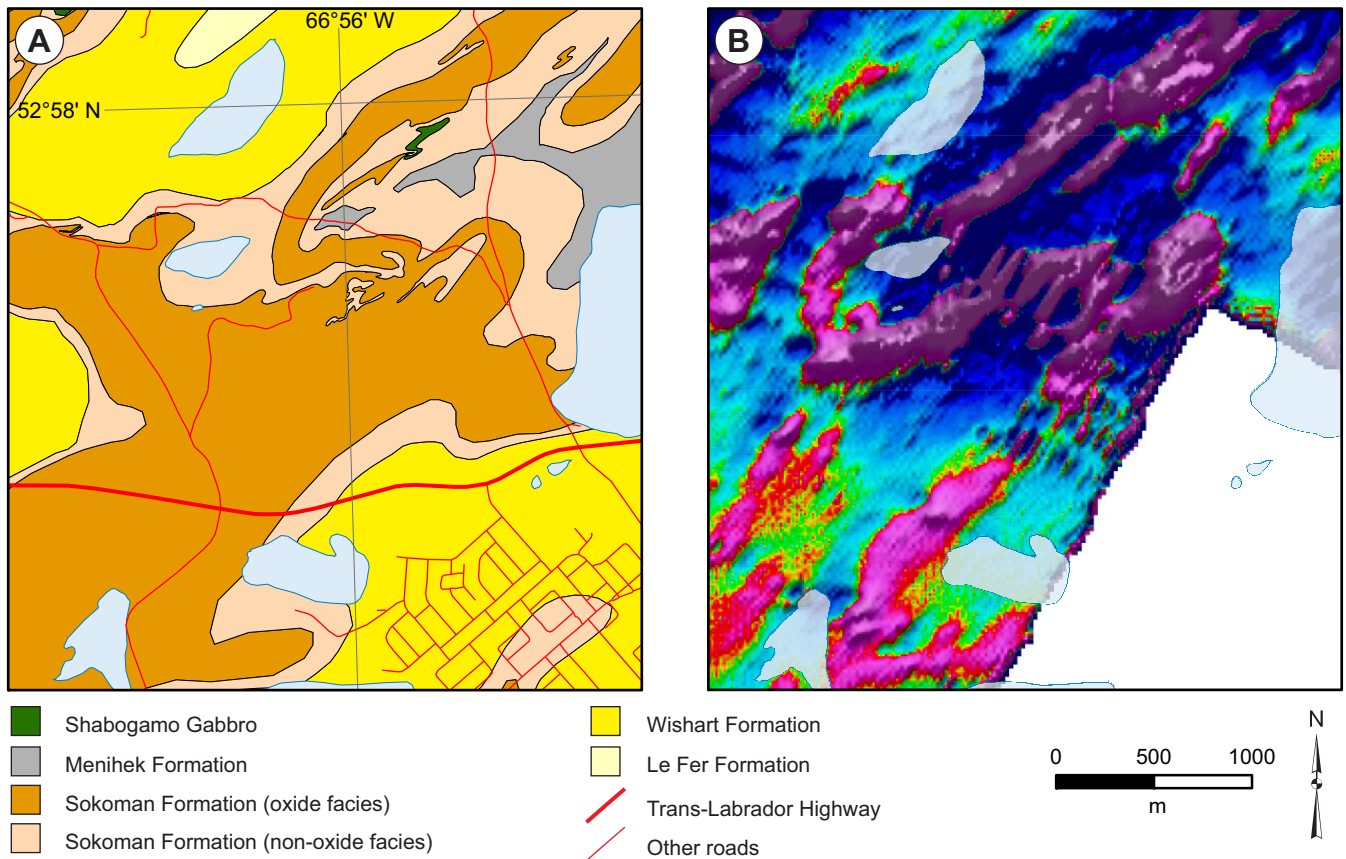


**Figure 69.** A) Geological map of the Wabush 4 prospect (adapted from Cotnoir et al., 2002); B) Airborne magnetics (second vertical derivative) showing extent of iron formation (data from Cotnoir et al., 2002).

overlain by Menihok Formation schist and underlain by quartzite of the Wishart Formation (Figure 69). Shabogamo Gabbro sills north of the Wabush 4 prospect, intrude the upper part of the Sokoman Formation.

Stratigraphy of the Sokoman Formation at the Wabush 4 deposit is taken from Darch *et al.* (2003a) and McDonald (2015), and is similar to the Mill Basin prospect and Wabush 6 deposit. The LIF is dominantly carbonate-facies iron formation, consisting of quartz–carbonate  $\pm$  grunerite. The MIF is the main ore-bearing unit, and is subdivided into a lower, high magnetite unit (Plate 46A) and an upper hematite-rich unit; it is overlain by an upper carbonate-facies unit of quartz–carbonate  $\pm$  grunerite (UIF).

### Mineralization

Oxide-facies iron formation is predominantly magnetite-rich (Plate 46B), with hematite content increasing in some sections. Magnetite is generally fine to coarse grained, but very coarse-grained magnetite has also been recorded (Plate 46C). The main gangue mineral is quartz, with minor Fe-silicate and carbonate minerals. In outcrop, the iron formation is moderately weathered, with secondary goethite after Fe-silicate and carbonate minerals and limonite staining. In drillcore, the iron formation is generally fresh to moderately altered in areas with no faulting, but alteration is strong to intense around fault zones. Some intervals have high Mn contents, with a drillcore sample collected for this study returning 10% Mn (Plate 46D).

There is no published metallurgical testwork available from the Wabush 4 prospect.

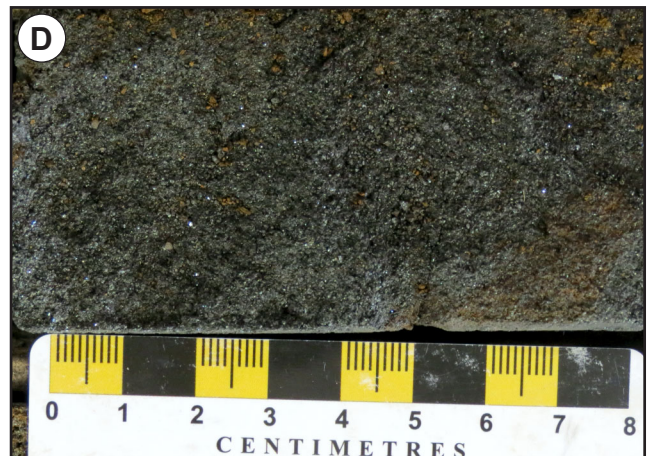
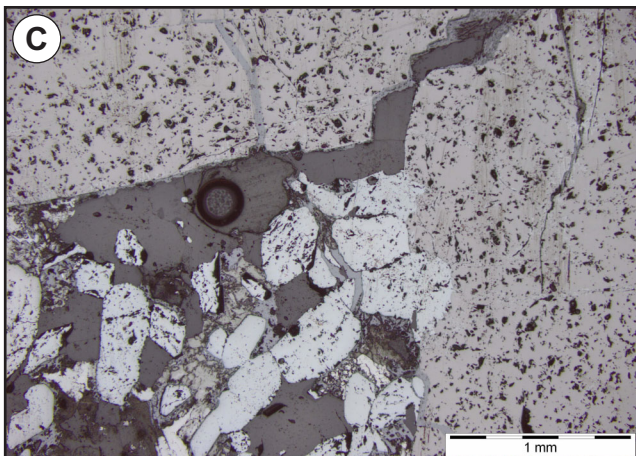
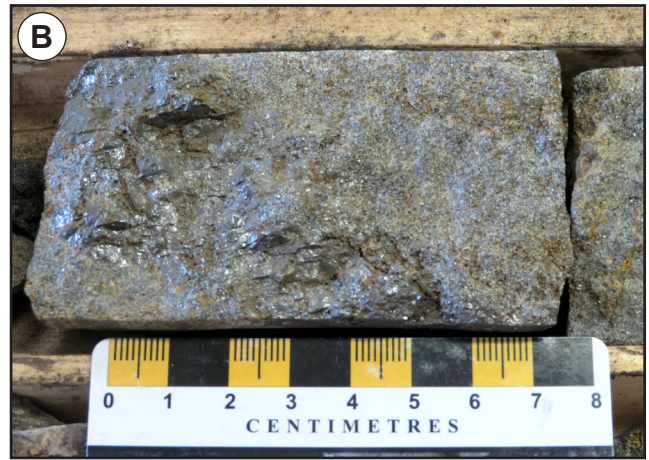


**Plate 46.** A) Outcrop of folded quartz–magnetite–hematite oxide-facies iron; B) Quartz–magnetite–hematite oxide-facies iron formation with coarse-grained magnetite (drillhole W4-10-01 @ 12.8 m); C) Photomicrograph of oxide-facies iron formation with coarse-grained magnetite bands and fine-grained hematite and quartz (drillhole W4-10-01 @ 12.8 m); D) Moderately altered, friable oxide-facies iron formation with abundant Mn-oxides (drillhole W4-10-01 @ 74.1 m).



Assay data from drillcore are not available. Outcrop samples (eight in total), which were collected in 2002 as part of an assessment of mineral resources in the Carol Lake mine area (Darch *et al.*, 2003a), returned Fe contents of 26.4 to 62.2% Fe (average 37.4% Fe).

### ***Structure***

The Wabush 4 prospect is interpreted to occur within a tightly folded syncline that is overturned to the west, and plunging toward the south. Smaller scale folding is also present, complicating the overall structure (McDonald, 2015). The Wabush 4 prospect is also cut by a number of faults that have been identified in drillcore.

### ***Geophysics***

Regional aeromagnetic surveys show that the Wabush 4 deposit is associated with a strong magnetic anomaly (Figure 69; Cotnoir *et al.*, 2002), which corresponds to the high magnetite content of the oxide-facies iron formation. Ground gravity surveys have also recognized a moderate to strong gravity anomaly that is coincident with the aeromagnetic anomaly (Darch *et al.*, 2003a).

### **Resource and/or Reserves**

No NI 43-101 compliant mineral resource or reserve estimate available.

Elliot *et al.* (1980) reported proven and probable reserves (as of January 1, 1979) of 122.9 Mt at 37.9% Fe. However, no details were provided on how this reserve estimate was calculated.

### **History of Exploration**

- 1949: Geological mapping (Neal, 1950a)
- 1950: Geological mapping (Neal, 1951)
- 1959: Geological mapping, dip needle survey (Leuner and Skimmer, 1959; Hird, 1960)
- 1972: Aeromagnetic survey (unpublished IOC report)
- 1978: Ground magnetometer survey (Price, 1979g)
- 1985: Diamond drilling (1 drillhole, 51.8 m, Simpson *et al.*, 1985)
- 2000: Data compilation, structural synthesis (Hulstein and Lee, 2001)
- 2001: Data compilation, regional airborne magnetic surveys, structural/stratigraphic interpretation (Cotnoir *et al.*, 2002)
- 2002: Geological mapping and prospecting, ground gravity survey (Darch *et al.*, 2003a)
- 2010: Diamond drilling (2 drillholes, 540 m, referenced in McDonald, 2015)
- 2011: Diamond drilling (4 drillholes, 890 m, referenced in McDonald, 2015)
- 2014: Geophysical surveys (direct current resistivity and induced polarization chargeability, McDonald, 2015)

### 38. WABUSH 6

**Alternate Name:** Wabush #6, Wabush No. 6  
**MODS Showing(s):** 023G/02/Fe006  
**Status:** Developed Prospect  
**Structural Basin:** Carol  
**UTM Zone:** 19  
**NTS Area:** 23G/02, 23B/15  
**Northing (NAD27):** 5874670  
**Easting (NAD27):** 640919  
**Latitude:** 53.0050  
**Longitude:** -66.8999  
**Object Located:** Drillhole W6-08-47

#### Description of Occurrence

The Wabush 6 deposit is located in IOC’s Carol Lake Mine, between the Luce deposit and Wabush Lake (Figure 70). It is approximately 5 km north of IOC’s Concentrator and Pellet plant, and approximately 7 km north of Labrador City. Access is via a series of gravel roads.

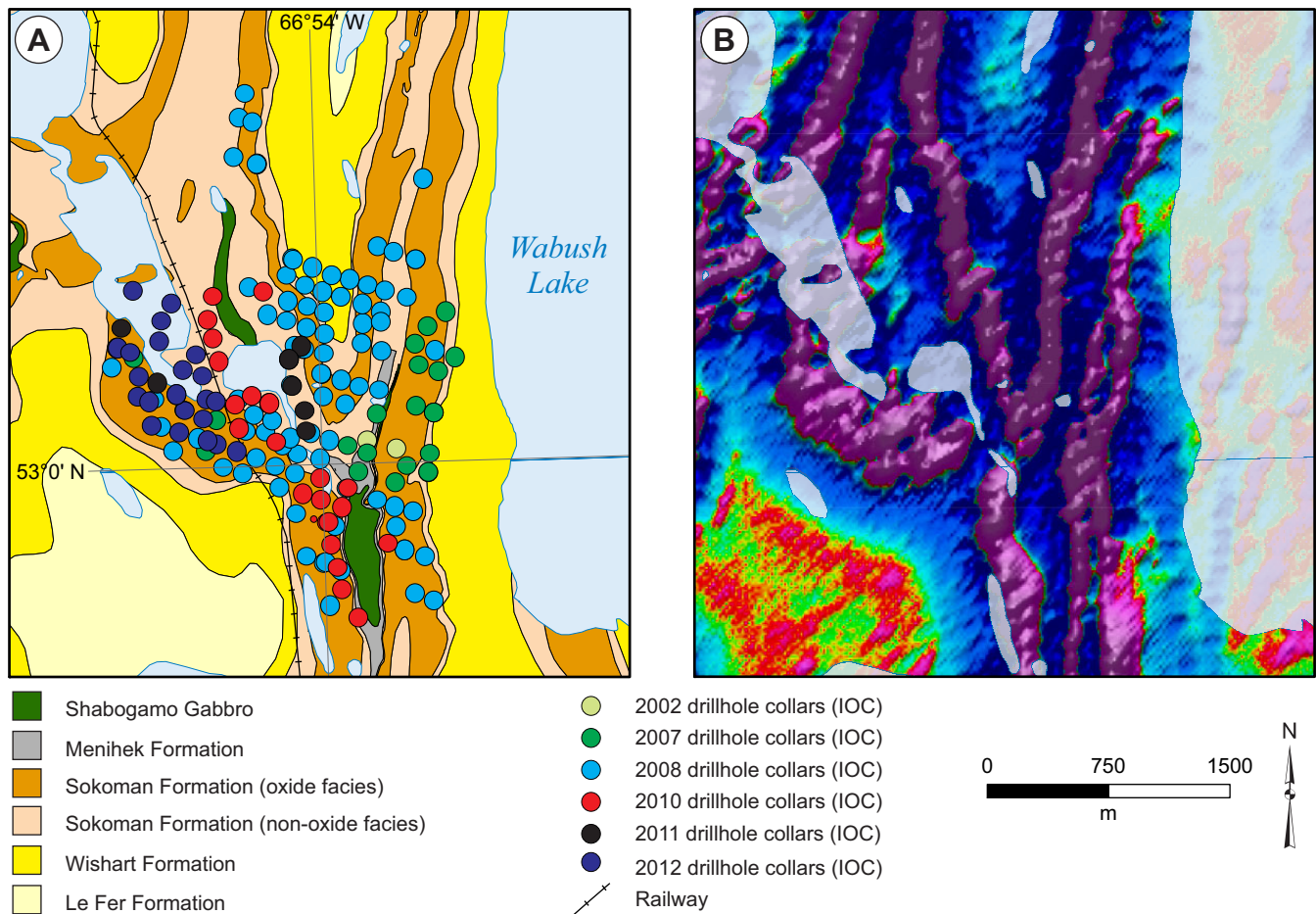


**Figure 70.** A) Geological map of the Wabush 6 deposit (adapted from Cotnoir et al., 2002), showing location of drillholes from 2002 and 2007–2012 exploration programs (Darch et al., 2003a; Marshall, 2012b); B) Airborne magnetics (second vertical derivative) showing extent of iron formation (data from Cotnoir et al., 2002).

## Geology and Stratigraphy

The Wabush 6 deposit is located in a syncline that preserves a complete sequence of Kaniapiskau Supergroup metasediments (Figure 70). Le Fer Formation quartz–feldspar–biotite gneiss occurs at the base of the stratigraphy and is conformably overlain by Wishart Formation quartzite, which forms prominent ridges. The Sokoman Formation occurs stratigraphically above the Wishart Formation, and a thin sequence of graphitic Menihek Formation schist has been recorded in the core of the syncline. Shabogamo Gabbro sills intrude the Sokoman Formation.

The stratigraphy of the Sokoman Formation is believed to be similar to the stratigraphy described from the Humphrey deposit by Muwais (1974) and the Mill Basin prospect along strike to the south (Darch *et al.*, 2003a). However, stratigraphic thicknesses are difficult to determine because the stratigraphy is complicated by complex folding and structural thickening and attenuation (Darch *et al.*, 2003a; Marshall, 2012b). The UIF is dominantly composed of silicate-facies iron formation, with subordinate carbonate-facies iron formation. The MIF is predominantly composed of oxide-facies iron formation, with a hematite-rich upper zone and a magnetite-rich lower zone (Darch *et al.*, 2003a). The LIF consists of carbonate-facies iron formation, with lesser silicate-facies and rare oxide-facies iron formation.

## Mineralization

Diamond drilling has intersected thick (>300 m) intervals of oxide-facies iron formation at the Wabush 6 deposit (Marshall, 2012b). The oxide-facies iron formation has highly variable hematite and magnetite contents, generally displaying a hematite-rich upper zone (Plate 47A) and a magnetite-rich lower zone (Plate 47B). Gangue includes quartz, carbonate and Fe-silicate minerals (grunerite and actinolite).

Generally, the iron formation is fresh and unaltered, but some zones display moderate to strong alteration with abundant secondary goethite. Manganese contents are generally low (<1%), with assay data from 2007–2012 drilling returning Mn contents of ore samples averaging 0.48% Mn (n = 3167, Marshall, 2012b). However, some drillholes show elevated Mn concentrations over significant intervals (*e.g.*, 1.79% Mn over 184.2 m in drillhole W6-12-151, 1.29% Mn over 157 m in drillhole W6-12-171). These intervals of higher Mn concentrations occur where ore horizons are interbedded with lower grade carbonate- and silicate-facies iron formation, and may represent infolded sections of oxide-facies iron formation from the base of the MIF or the LIF, which are known to have higher Mn contents (Marshall, 2012b).

Marshall (2012b) reported on SAG Power Index (SPI) and iron recovery testing (TT) from 540 composite samples from 2010 to 2012 drilling. These data show that magnetite-rich and hematite-rich ores have similar iron recovery, but magnetite-rich ore is a harder grinding ore (higher SPI values).

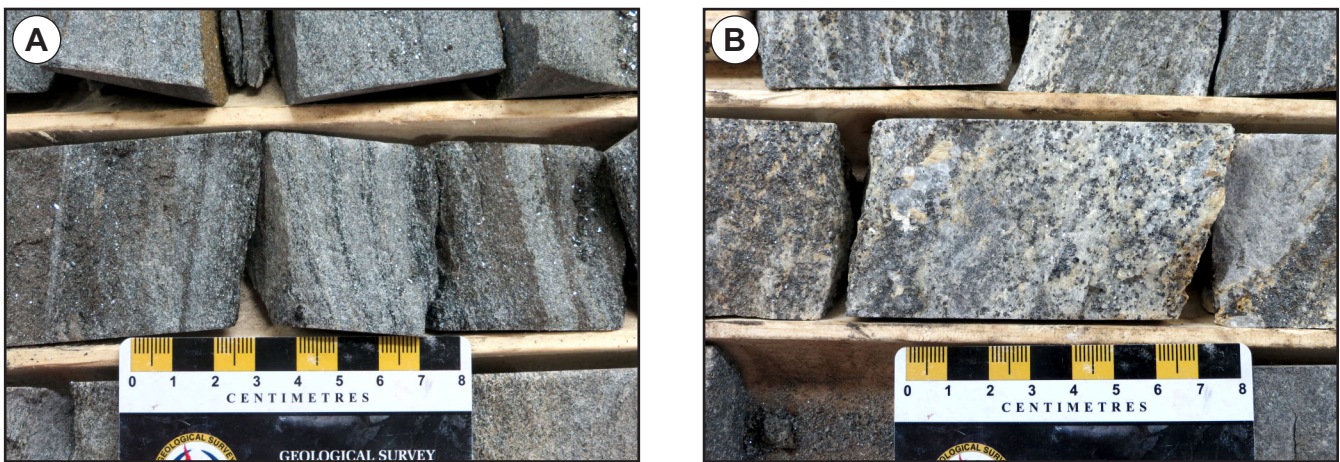


**Plate 47.** A) Hematite-rich oxide-facies iron formation (drillhole W6-10-135 @ 31.2 m); B) magnetite-rich oxide-facies iron formation with gangue quartz and carbonate (drillhole W6-10-135 @ 50.5 m).



The Fe contents of ore-grade samples from the 2007–2012 drilling averaged 37.3% Fe (n = 3167, Marshall, 2012b). Highlights from diamond drilling include 36% Fe over 334 m in drillhole W6-08-47 (5 to 339 m), 36.7% Fe over 308 m in drillhole W6-12-153 (14 to 308 m), 35.6% Fe over 298.4 m in drillhole W6-12-157 (17.6 to 316 m) and 36.9% Fe over 289.9 m in drillhole W6-12-154 (122.4 to 412.3 m).

### ***Structure***

The Wabush 6 deposit occurs at the northern end of a broad open basin (Mill Structural Basin). This broad open basin is the result of a larger amplitude overturned  $F_2$ -synclinal fold trend intersecting a series of smaller amplitude  $F_1$ -synform dominated folds (Marshall, 2012b). The southern part of the deposit occurs within an open synform, cored by Menihek Formation graphitic schist, plunging to the north. At the northern end of the deposit, the iron formation occurs in an eastern and western synform, which are separated by an antiform. On a local scale, the structure of the iron formation is complex due to the interference of the  $F_1$  and  $F_2$  folds and the high frequency of parasitic and disharmonic folds occurring in the iron formation (Darch *et al.*, 2003a).

### ***Geophysics***

Regional aeromagnetic surveys show that the Wabush 6 deposit corresponds to a strong magnetic anomaly, which clearly show the eastern and western synforms at the northern portion of the deposit (Figure 70; Cotnoir *et al.*, 2002). Ground gravity surveys show strong gravity anomalies associated with the Wabush 6 deposit, consistent with diamond drilling, which shows significant thicknesses of oxide-facies iron formation (Darch *et al.*, 2003a).

### **Resource and/or Reserves**

NI 43-101 compliant resources (Iron Ore Company of Canada, 2014).

- Measured resources: 156 Mt at 37% Fe
- Indicated resources: 878 Mt at 37% Fe
- Inferred resources: 268 Mt at 35% Fe

### **History of Exploration**

- 1949: Geological mapping (Neal, 1950a)
- 1950: Geological mapping (Neal, 1951)
- 1957: Geological mapping (Mumtazuddin, 1957)
- 1959: Geological mapping, sampling and dip needle survey (Thorniley, 1959)
- 1972: Aeromagnetic survey (unpublished IOC report)
- 1977: Ground magnetometer survey (Price, 1977)
- 1978: Ground magnetometer survey (Price, 1979g)
- 2000: Data compilation, structural synthesis (Hulstein and Lee, 2001)
- 2001: Data compilation, regional airborne magnetic surveys, structural/stratigraphic interpretation (Cotnoir *et al.*, 2002)
- 2002: Geological mapping and prospecting, diamond drilling (2 drillholes, 555 m), ground gravity survey (Darch *et al.*, 2003a)
- 2005: Diamond drilling (10 drillholes, 2419 m)
- 2006: Diamond drilling (7 drillholes, 1814 m)
- 2007: Diamond drilling (21 drillholes, 5287 m, Marshall, 2012b)
- 2008: Diamond drilling (93 drillholes, 16 677 m, Marshall, 2012b)
- 2010: Diamond drilling (23 drillholes, 4640 m, Marshall, 2012b)
- 2011: Diamond drilling (9 drillholes, 1941 m, Marshall, 2012b; Wallace, 2012d)
- 2012: Diamond drilling (23 drillholes, 5890 m, Marshall, 2012b)

### 39. WABUSH MOUNTAIN

**Alternate Name:** n/a

**MODS Showing(s):** 023B/15/Fe010

**Status:** Showing

**Structural Basin:** Wabush

**UTM Zone:** 19

**NTS Area:** 23B/15

**Northing (NAD27):** 5869120

**Easting (NAD27):** 644130

**Latitude:** 52.9543

**Longitude:** -66.8545

**Object Located:** Approximate location of 1962 drilling

#### Description of Occurrence

The Wabush Mountain showing (Figure 71) is located on the top of Wabush Mountain, a prominent hill overlooking Labrador City and Wabush. It is located to the east of Wabush Lake, and is approximately 5 km east of Labrador City and 6.5 km north of Wabush. Access is *via* a well-maintained secondary road.

#### Geology and Stratigraphy

The Sokoman Formation iron formation outcrops on the western slopes of Wabush Mountain, and diamond drilling shows that the iron formation is conformably underlain by Wishart Formation quartzite (Hartopp, 1962a). Denault Formation dolomite underlies this, and is mapped to the east of the mountain. Le Fer Formation schist occurs at the base of the stratigraphic sequence, and is intruded by Shabogamo Gabbro sills.

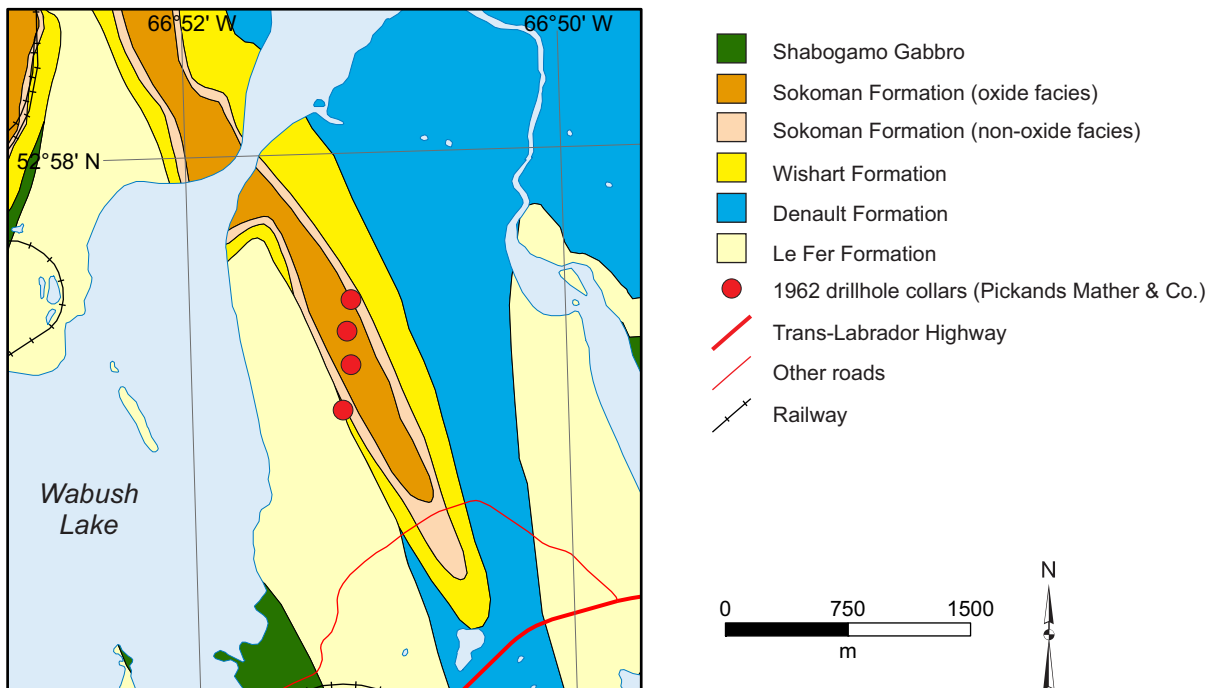


**Figure 71.** Geological map of the Wabush Mountain area (adapted from Cotnoir et al., 2002), showing approximate location of drillholes from 1962 drilling programs (Hartopp, 1962a).

Little is known about the stratigraphy of the Sokoman Formation, due to limited data from diamond drilling and extensive alteration of the iron formation. However, the description of drillcore in Hartopp (1962a) suggests that the stratigraphy is similar to that in the Scully deposit, which is located along strike to the south of the Wabush Mountain showing.

### ***Mineralization***

The Sokoman Formation is composed predominantly of quartz–hematite schist, with minor magnetite, in places. Manganese contents are highly variable, with some intervals strongly enriched in Mn (up to 14.4% Mn over 6.1 m in drillhole WM-4). The core is generally friable and moderately to strongly altered, with abundant secondary goethite throughout and pyrolusite and psilomelane common in Mn-rich intervals. Alteration may be associated with late-stage (post-metamorphic) fluid flow, secondary leaching and/or deep weathering, possibly related to fluid infiltration along the adjacent Flora Lake shear zone.

There is limited metallurgical testwork available from the Wabush Mountain showing, with Hartopp (1962b) reporting on results from table tests and magnetic tube tests.

The best assay results are from drillholes WM-2 (31.6% Fe over 85.7 m from 28.3 to 114 m) and WM-4 (30.6% Fe over 69.8 m from 7.3 to 87.5 m).

### ***Structure***

Geological mapping indicates that the showing is located in a northwest–southeast-trending, northwest-plunging syncline. The Flora Lake shear zone, a major north-northeast-trending shear zone, is located approximately 1 km east of Wabush Mountain (van Gool, 1992)

### ***Geophysics***

Regional aeromagnetic data for Labrador conducted by the Geological Survey of Canada suggest a strong aeromagnetic high coincident with the Wabush Mountain showing.

### **Resource and/or Reserves**

No NI 43-101 compliant mineral resource or reserve estimate available.

### **History of Exploration**

- 1953: Geological mapping and prospecting (Boyko, 1953)
- 1962: Diamond drilling (4 drillholes, 397.9 m, Hartopp, 1962a, b)



#### 40. WHITE LAKE

**Alternate Name:** Wabush No. 2, Carol West No. 2

**MODS Showing(s):** 023B/15/Mn001, 023B/15/Mn002, 023G/02/Mn001, 023G/02/Mn002, 023G/02/Mn003

**Status:** Prospect

**Structural Basin:** Carol

**UTM Zone:** 19

**NTS Area:** 23B/15, 23G/02

**Northing (NAD27):** 5873457

**Easting (NAD27):** 634974

**Latitude:** 52.9956

**Longitude:** -66.9889

**Object Located:** Drillhole WL-10-02

#### Description of Occurrence

The White Lake prospect is located to the west of White Lake (Figure 72), approximately 8.5 km northwest of Labrador City, and 2 km southeast of the Sherwood Pit of IOC's Carol Lake mining operation. Access to the prospect is by road and bush road from IOC Carol Lake Mine, south of Sherwood dump (called the Maggie Lake road), then on foot.

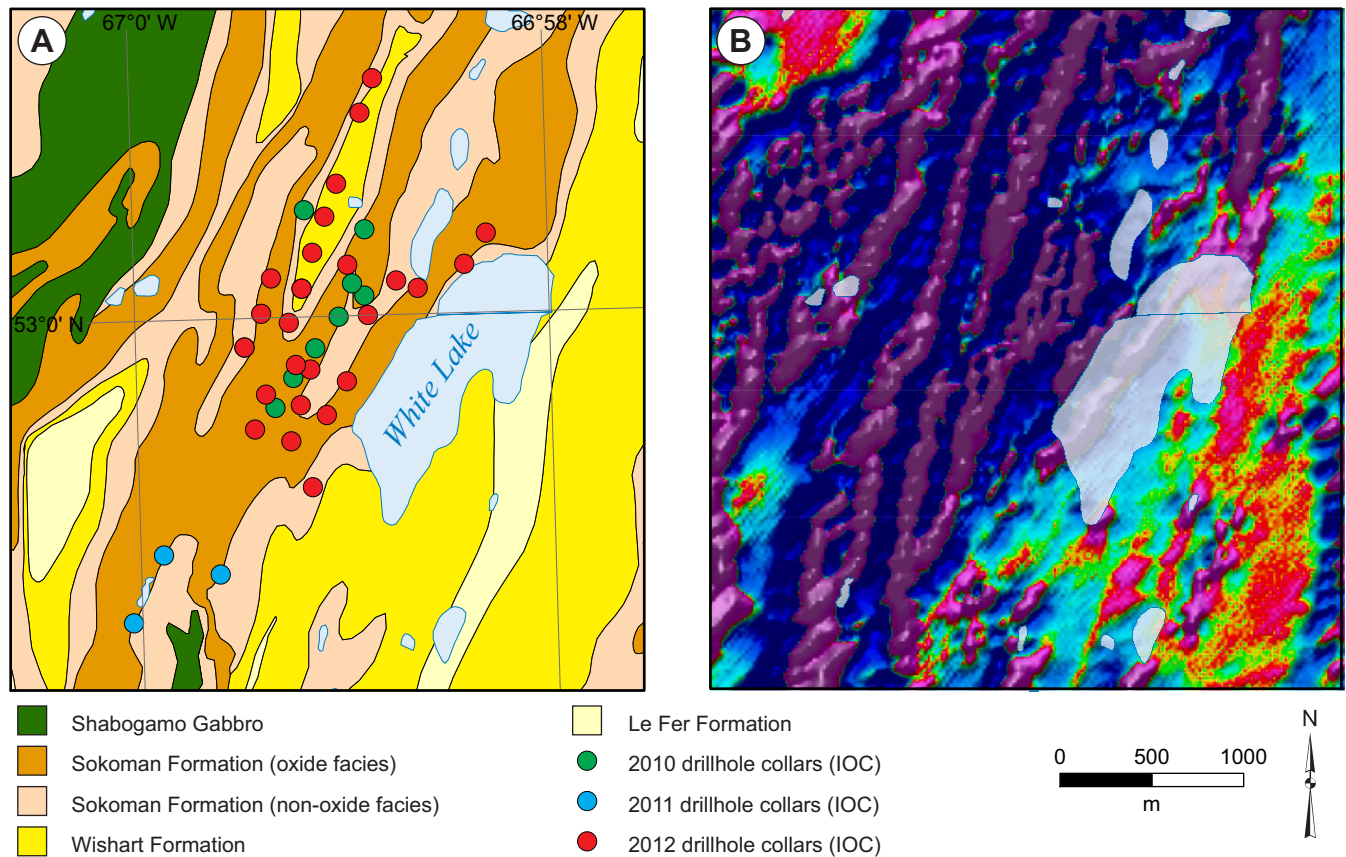


**Figure 72.** A) Geological map of the White Lake prospect (adapted from Cotnoir et al., 2002), showing location of drillholes from 2010, 2011 and 2012 IOC exploration programs (Duvergier, 2012); B) Airborne magnetics (second vertical derivative) showing extent of iron formation (data from Cotnoir et al., 2002).

## ***Geology and Stratigraphy***

The geology to the west of White Lake is composed of Sokoman Formation iron formation, which conformably overlies quartzite of the Wishart Formation. Le Fer Formation schist occurs in the cores of anticlines, conformably below the Wishart Formation. Minor Shabogamo Gabbro sills (generally <1 m thick) intrude the Sokoman and Wishart formations.

Geological mapping and diamond drilling show that Sokoman Formation can be subdivided into LIF, MIF and UIF, and has a similar stratigraphy to that described by Muwais (1974) from the Humphrey deposit. The LIF and UIF are predominantly composed of silicate- and carbonate-facies iron formation, with lesser oxide-facies iron formation, whereas the MIF is primarily oxide-facies iron formation (quartz–magnetite–hematite schist; Duvergier, 2012).

## ***Mineralization***

Thick sequences of oxide-facies MIF (>175 m) have been recorded during diamond drilling (Duvergier, 2012). The oxide-facies iron formation consists of hematite–magnetite schist, with variable proportions of hematite and magnetite. Gangue includes quartz, Fe-silicate (grunerite and actinolite) and carbonate minerals.

Alteration across the deposit is highly variable, with strong to moderate alteration common in the northeast portion of the showing, and generally decreasing to the southwest (Cotnoir *et al.*, 2002; Duvergier, 2012). This alteration is identified by the leaching of carbonate and Fe-silicate minerals, precipitation of secondary goethite and transformation of magnetite to hematite (martite). The alteration is attributed to fluid flow along late-stage faults that have been recognized during diamond drilling (Duvergier, 2012), and is similar to alteration observed in the Canning prospect and Scully deposit. Manganese-contents of oxide-facies iron formation are generally low (<1 % Mn), but values of up to 4% Mn have been recorded around faults in some drillholes, interpreted to represent the secondary migration of Mn-oxides during late-stage alteration.

Duvergier (2012) report on SAG Power index (SPI) and iron recovery testing (TT) from 233 composite samples from 2010 to 2012 drilling, which show that the ore has similar physical characteristics to ore from other deposits in IOC's Carol Lake Mine area.

Assay data from diamond drilling show significant thicknesses of ore-grade iron formation. The thickest sequence of oxide-facies iron formation is in drillhole WL-10-02, with mineralized intervals of 37.9% Fe over 51.5 m (5.5 to 57 m) and 38.7% Fe over 90.6 m (87.4 to 186 m). These mineralized intervals are separated by oxide-facies iron formation that was not selected for assay due to the presence of fibrous amphiboles (Duvergier, 2012). Other highlights from diamond drilling include 39.0% Fe over 107 m in drillhole WL-12-19 (40 to 147 m), 40.1% Fe over 85.3 m in drillhole WL-12-35 (3 to 92 m) and 42.8% Fe over 87 m in drillhole WL-12-29 (32 to 122 m, very poor core recovery over upper 15.5 m).

## ***Structure***

The White Lake prospect is located in a series of northeast-trending, northwest-verging  $F_2$  anticlines and synclines, imparting repetition of the MIF stratigraphy (Cotnoir *et al.*, 2002). The  $F_1$  folds have also been recognized based on the presence of doubly plunging  $F_2$  fold structures, with interference between  $F_1$  and  $F_2$  folds believed to be associated with structural thickening (Cotnoir *et al.*, 2002). North–south-trending faults have been recorded in the eastern portion of the prospect and are associated with strong to moderate alteration of the iron formation. These faults are likely part of a major fault system, which has been recognized to the east of White Lake (Azomani and Bineli Betsi, 2012).

## ***Geophysics***

Regional airborne magnetic data shows that the White Lake prospect is located within a strong magnetic high, related to the high magnetite content of oxide-facies iron formation (Cotnoir *et al.*, 2002; Figure 72). A ground gravity survey across the White Lake prospect produced a gravity anomaly of 8–10 milligals on the west side of White Lake representing a significant thickness of iron formation (Cotnoir *et al.*, 2002).

### **Resource and/or Reserves**

No NI 43-101 compliant mineral resource or reserve estimate available.

Preliminary interpretation based on geological mapping, structural interpretation and regional aeromagnetic survey results have been used to estimate a possible geological resource of 500 Mt at plus 35% Fe (Cotnoir *et al.*, 2002).

### **History of Exploration**

- 1949: Geological mapping (Neal, 1950a)
- 1950: Geological mapping (Neal, 1951)
- 1957: Geological mapping and prospecting (Duquette, 1957)
- 1958: Geological mapping, diamond drilling (52 drillholes, 732 m, referenced in Duvergier, 2012)
- 1972: Aeromagnetic survey (unpublished IOC report)
- 1979: Ground magnetometer survey (referenced in Duvergier, 2012)
- 2000: Data compilation, structural synthesis (Hulstein and Lee, 2001)
- 2001: Data compilation, geological mapping and prospecting, ground gravity survey, regional airborne magnetic surveys, structural/stratigraphic interpretation (Cotnoir *et al.*, 2002)
- 2002: Geological sampling program (referenced in Duvergier, 2012)
- 2006: Diamond drilling (referenced in Duvergier, 2012)
- 2010: Diamond drilling (8 drillholes, 1729.6 m, Duvergier, 2012)
- 2011: Diamond drilling (3 drillholes, 621 m, Duvergier, 2012)
- 2012: Diamond drilling (27 drillholes, 5051.3 m, 2012)



## ACKNOWLEDGMENTS

Garrett Martin and Alex Calon are thanked for their able assistance during summer fieldwork, constant enthusiasm and cheerful demeanor in sometimes trying conditions. Wayne Tuttle provided vital assistance and logistical support without which this project would be impossible. Staff and geologists at the Iron Ore Company of Canada, Alderon Iron Ore, Cliffs Natural Resources, Champion Iron, Ridgemont Iron Ore Corp. and ArcelorMittal provided access to drillcore and mine sites, as well as information on the geology of individual deposits and numerous thought-provoking discussions. Staff at the Mineral Development Division and Mineral Lands Division of the Department of Natural Resources provided information on the Julienne Lake deposit, as well as access to drillcore. Sample preparation and geochemical analyses were carried out under the supervision of Chris Finch of the GSNL Geochemistry Laboratory. Gerry Kilfoil is thanked for helping to interpret geophysical data. John Hinchey provided a helpful review of an early draft of this contribution.

## REFERENCES

- Almond, P.  
1953: Exploration report on Julienne Lake-North Wabush Lake area, Labrador. Iron Ore Company of Canada. Newfoundland and Labrador Geological Survey, Assessment File 23G/0008, 29 pages.
- Atkinson, T.  
1978: Diamond drilling data for mining lease block 22-8 in the Labrador City area, Labrador. Iron Ore Company of Canada and Labrador Mining and Exploration Company Limited. Newfoundland and Labrador Geological Survey, Assessment File 23B/15/0104, 20 pages.
- Avison, A.T., Alcock, P.W., Poisson, P. and Connell, E.  
1984: Assessment report on geological, geochemical and geophysical exploration for 1983 submission on Labrador Mining and Exploration Company Limited blocks 4, 8 to 18, 20, 21, 26 to 31, 33, 43, 44, 45, 53, 55, 57, 63, 68, 78, 79, 80, 84 to 87, 92, 94, 95, 96, 100, 103 to 108, 110, 115 to 118, 120 to 125, 127 to 131, 134, 136, 138, 139, 140 and 142 in the Labrador City and Scheferville areas, Labrador, 4 reports. Labrador Mining and Exploration Company Limited. Newfoundland and Labrador Geological Survey, Assessment File LAB/0719, 396 pages.
- Azomani, E. and Bineli Betsi, T.  
2012: First year assessment report on geological exploration and aerial photography for licences 17886M and 17889M on claims in the White Lake area, near Labrador City, western Labrador. Iron Ore Company of Canada. Newfoundland and Labrador Geological Survey, Assessment File LAB/1706, 27 pages.
- Babechuk, M.G., Widdowson, M. and Kamber, B.S.  
2014: Quantifying chemical weathering intensity and trace element release from two contrasting basalt profiles, Deccan Traps, India. *Chemical Geology*, Volume 363, pages 56-75.
- Baragar, W.R.A.  
1967: Wakuach Lake, Quebec - Labrador. Geological Survey of Canada, Memoir 344, 174 pages.
- Bau, M.  
1993: Effects of syn- and post-depositional processes on the rare-earth element distribution in Precambrian iron-formations. *European Journal of Mineralogy*, Volume 5, pages 257-267.
- Bau, M. and Dulski, P.  
1996: Distribution of yttrium and rare-earth elements in the Penge and Kuruman iron-formations, Transvaal Supergroup, South Africa. *Precambrian Research*, Volume 79, pages 37-55.
- Beemer, E.F., Jr  
1952: Field report on Lake Shabogamo area, Labrador. Iron Ore Company of Canada. Newfoundland and Labrador Geological Survey, Assessment File 23G/0006, 28 pages.
- Bineli Betsi, T.  
2012: Fourth and seventh year assessment report on diamond drilling exploration for licences 8928M and 15685M on claims in the Polly Lake area, western Labrador. Iron Ore Company of Canada and Labrador Iron Ore Royalty Corporation, Newfoundland and Labrador Geological Survey, Assessment File 23B/14/0221, 799 pages.
- Blakeman, W.B. and Knowles, D.M.  
1963: The Julian Deposit and its extensions. Canadian Javelin Limited. Newfoundland and Labrador Geological Survey, Assessment File 023G/0117, 25 pages.
- Bolhar, R., Kamber, B.S., Moorbath, S., Fedo, C.M. and Whitehouse, M.J.  
2004: Characterisation of early Archaean chemical sediments by trace element signatures. *Earth Planetary Science Letters*, Volume 222, pages 43-60.
- Boyko, W.P.  
1953: Geological report on the Wabush Lake area, Labrador. Newfoundland and Labrador Corporation

Limited. Newfoundland and Labrador Geological Survey, Assessment File LAB/0688, 11 pages.

Branch, C.

1959: Gravity profile maps for Sitting Bear Lake, Labrador. Labrador Mining and Exploration Company Limited. Newfoundland and Labrador Geological Survey, Assessment File 23G/0036, 19 pages.

1959a: Gravity profiles maps for Julienne West, Labrador. Labrador Mining and Exploration Company Limited. Newfoundland and Labrador Geological Survey, Assessment File 23G/0035, 11 pages.

1959b: Report of gravity survey of Wabush No. 3, Labrador. Labrador Mining and Exploration Company Limited. Newfoundland and Labrador Geological Survey, Assessment File 23G/0033, 2 pages.

Brown, D.L.

1991: A structural analysis of the Grenville Front Zone, northeast Gagnon Terrance, Labrador. Unpublished M.Sc. Thesis, Memorial University of Newfoundland, St. John's 203 pages.

Brown, D., Rivers, T. and Calon T.

1992: A structural analysis of a metamorphic fold-thrust belt, northeast Gagnon terrane, Grenville Province. Canadian Journal of Earth Sciences, Volume 29, pages 1915-1927.

Brown, D., van Gool, J., Calon, T. and Rivers, T.

1991: The geometric and kinematic development of the Emma Lake Thrust Stack, Grenville Front, southwestern Labrador. Canadian Journal of Earth Sciences, Volume 28, No. 1, pages 136-144.

Bruneau, Y.

1960: Report on diamond drilling exploration on property in the Goethite Bay and Scott Bay areas, Labrador. Labrador Mining and Exploration Company Limited. Newfoundland and Labrador Geological Survey, Assessment File 23G/0236, 53 pages.

Bulled, D., Leriche, T., Blake, M., Thompson, J. and Wilkie, T. 2009: Improved production forecasting through geomet-allurgical modelling at Iron Ore Company of Canada. SGS Mineral Services, Technical Paper 2009-01, 9 pages.

Canadian Javelin Limited

1959: Ore reserve estimates for the Julienne Lake Deposit, Julienne Lake area, Labrador. Canadian Javelin

Limited. Newfoundland and Labrador Geological Survey Assessment File 023G/02/0247, 15 pages.

Carter, L.

2011a: Eighth year assessment report on diamond drilling exploration for licence 8927M on claims in the Canning Lake area, near Labrador City, western Labrador. Labrador Mining and Exploration Company Limited and Iron Ore Company of Canada. Newfoundland and Labrador Geological Survey, Assessment File 23B/0207, 50 pages.

2011b: Sixth and eighth year assessment report on diamond drilling exploration for licences 8931M and 9284M on claims in the D'Aigle Bay area, Wabush Lake, western Labrador. Labrador Mining Company Limited and Iron Ore Company of Canada. Newfoundland and Labrador Geological Survey, Assessment File 23G/02/0303, 109 pages.

2011c: Fifth year assessment report on diamond drilling exploration for licence 9835M on claims in the Duley Lake area, near Labrador City, western Labrador. Labrador Mining Company Limited. Newfoundland and Labrador Geological Survey, Assessment File 23B/0208, 77 pages.

2011d: Seventh and eighth year assessment report on diamond drilling exploration for licences 7799M and 8930M on claims in the Throne Lake area, near Labrador City, western Labrador. Labrador Mining Company Limited and Iron Ore Company of Canada. Newfoundland and Labrador Geological Survey, Assessment File 23G/02/0209, 47 pages.

2011e: First and sixth year assessment report on diamond drilling exploration for licences 10380M and 16049M on claims in the Julienne Lake area, western Labrador. Labrador Mining Company Limited and Iron Ore Company of Canada. Newfoundland and Labrador Geological Survey, Assessment File 23G/02/0300, 101 pages.

2011f: Eighth year assessment report on diamond drilling exploration for licence 7795M on claims in the Shabogamo Lake area, western Labrador. Iron Ore Company of Canada. Newfoundland and Labrador Geological Survey, Assessment File 23G/02/0302, 33 pages.

Campbell, D.S. and Simpson, H.

1987: Second year assessment report on diamond drilling and trenching exploration for the dolomite project for licences 223m-224m on claims in the Wynne Lake and Wabush Lake areas, Labrador. Iron Ore Company of

- Canada. Newfoundland and Labrador Geological Survey, Assessment File 23G/02/0230, 82 pages.
- Churchill, R., Seymour, C., Allaire, A., Giddens, H., Greenwood, J., Kociumbas, M. and Contreras, I.A.  
2014: First and sixth year assessment report on development proposals and remote sensing for licences 20499M, 20636M-20637M and 21047M on claims in the Julienne Lake area, western Labrador, 3 reports. Altius Resources Incorporated. Newfoundland and Labrador Geological Survey, Assessment File 23G/02/0307, 435 pages.
- Clark, D.  
2006: Sixth year assessment report on diamond drilling exploration for licence and 9284M on claims in the D'Aigle Bay, Wabush Lake area, western Labrador. Iron Ore Company of Canada and Labrador Mining and Exploration Company. Newfoundland and Labrador Geological Survey, Assessment File 23B/0185, 65 pages.  
2007a: Second year supplementary assessment report on diamond drilling exploration for licence 10380M on claims in the Julienne Lake area, western Labrador. Iron Ore Company of Canada and Labrador Mining and Exploration Company. Newfoundland and Labrador Geological Survey, Assessment File 23G/02/0264, 34 pages.  
2007b: Fifth year assessment report on diamond drilling exploration for licence 8927M on claims in the Tup Lake area, near Labrador City, western Labrador. Iron Ore Company of Canada and Labrador Mining and Exploration Company Newfoundland and Labrador Geological Survey, Assessment File 23B/0185, 65 pages.  
2007c: Seventh year assessment report on diamond drilling exploration for licence 7795M on claims in the Shabogamo Lake area, western Labrador. Iron Ore Company of Canada and Labrador Mining and Exploration Company. Newfoundland and Labrador Geological Survey, Assessment File 23G/02/0263, 26 pages.
- Clark, T., Leclair, A., Pufahl, P. and David, J.  
2006: Recherche géologique et métallogénique dans les régions de Schefferville (23J15) et du lac Zeni (23I16). Ministère des Ressources naturelles et de la Faune, Québec; RP 2008-01, 17 pages.
- Clark, D. and Tshimbalanga, S.  
2006: Second year assessment report on geophysical exploration for licence 9835M on claims in the Duley Lake area, near Labrador City, western Labrador, 2 reports. Iron Ore Company of Canada and Labrador Mining Company Limited. Newfoundland and Labrador Geological Survey, Assessment File 23B/018326 pages.
- Clark, T. and Wares, M.  
2005: Lithotectonic and metallogenic synthesis of the New Québec Orogen (Labrador Trough). Ministère des Ressources naturelles, Québec, MM 2005-01, 175 pages.
- Clarke, P.J.  
1965: Geology of Silicates Lake area, Saguenay County. Preliminary Report 539, Ministère des Richesses Naturelles du Québec, 12 pages.
- Cliffs Natural Resources Annual Report  
2012: Annual Report: Cliffs Natural Resources Inc. Available online at <http://www.cliffsnaturalresources.com/English/investors/financial-information/annual-reports>
- Coates, H.J., Cote, M., Brett, J. and Barrie, C.  
2011: First year assessment report on geological, geochemical and geophysical exploration for licences 17737M, 18381M, 18383M-18384M, 18487M, 18495M, 18540M, 18611M, 18613M-18614M, 18693M-18694M, 19112M and 19114M-19115M on claims in the Lac Virot area, western Labrador, 2 reports. Iron One Incorporated, Hicks, D and Malhi, K. Newfoundland and Labrador Geological Survey, Assessment File LAB/1666, 126 pages.
- Coates, H., Thein, A.M. and Cote, M.  
2012: Report on the 2010 exploration program, Julienne Lake iron deposit, western Labrador, 4 volumes. Newfoundland and Labrador Geological Survey, Internal Collection, Company or Consultant Report, 894 pages [023G/02/0287].
- Conliffe, J.  
2013: The geological setting of the Julienne Lake iron-ore deposit, western Labrador. *In* Current Research. Government of Newfoundland and Labrador, Department of Natural Resources, Geological Survey, Report 13-1, pages 83-97.  
2015: Geological setting and genesis of high-grade iron-ore deposits in the eastern Labrador Trough. *In* Current Research. Government of Newfoundland and Labrador, Department of Natural Resources, Report 15-1, pages 1-25.  
2016a: Geochemical data from high-grade iron-ore deposits and altered and unaltered iron formation in the Labrador Trough (NTS 23J and 23O). Government of Newfoundland and Labrador, Department of Natural Resources, Geological Survey, Open File LAB/1667, 35 pages



- 2016b: Geology and geochemistry of high-grade iron-ore deposits in the Kivivic, Timmins and Ruth Lake areas, western Labrador. *In* Current Research. Government of Newfoundland and Labrador, Department of Natural Resources, Geological Survey, Report 16-1, pages 1-26.
- 2017: Geology and geochemistry of the Sokoman Formation in the Gabbro Lake area, eastern Labrador Trough. *In* Current Research. Government of Newfoundland and Labrador, Department of Natural Resources, Geological Survey, Report 17-1, pages 147-168.
- Connelly, J.N.  
1991: The thermotectonic history of the Grenville Province, western Labrador. Unpublished Ph.D. thesis, Memorial University of Newfoundland, 316 pages.
- Connelly, J.N. and Heaman, L.M.  
1993: U-Pb geochronological constraints on the tectonic evolution of the Grenville Province, western Labrador. *Precambrian Research*, Volume 63, pages 123-142.
- Connelly, J.N., Rivers, T. and James D.T.  
1995: Thermotectonic evolution of the Grenville Province of western Labrador. *Tectonics*, Volume 14, pages 202-217.
- Connelly, J.N., van Gool, J., Rivers, T. and James D.T.  
1996: Field Guide to the Geology of the Grenville Province of Western Labrador. Pre-conference field excursion; Proterozoic Evolution in the North Atlantic Realm, COPENA-ECSOOT-IBTA Conference, Goose Bay, Labrador, July 29-August 2, 1996, Field Excursion Guide 1, 86 pages.
- Cotnoir, A., Goodman, S., Granger, B., Cowan, D.R., Barrie, C.Q. and Lee, C.  
2002: Assessment report on geological, geochemical, geophysical and diamond drilling exploration for 2001 submission for Mining Leases 114 [224M], 116 [224M], 125 [223M] and 132 [223M], Labrador Mining and Exploration Company Limited Blocks 22-1, 22-2, 22-3, 22-4, 22-6, 22-7, 22-8, 22-9, 22-10, 64-1, 64-2 and 22 to 42 and for first year supplementary, fifth and sixth year assessment for licences 6695M and 7782M-7803M on claims in the Labrador City area, western Labrador, 7 reports. Iron Ore Company of Canada. Newfoundland and Labrador Geological Survey, Assessment File LAB/1369, 554 pages.
- Crouse, R.A.  
1954: Report on the Mills Lake-Dispute Lake area, Labrador. Iron Ore Company of Canada. Newfoundland and Labrador Geological Survey, Assessment File 023B/0006, 22 pages.
- 1957: Lorraine Lake-Daigle Bay area and Shabogamo Anomaly. Labrador Mining and Exploration Company Limited. Newfoundland and Labrador Geological Survey, Assessment File 23G/0022, 13 pages.
- Darch, D.  
2004: First, second and fourth year assessment report on geological and geochemical exploration for licences 7795M, 8928M, 8931M, 9284M, 9835M and 10380M on claims in the Wabush Lake area, western Labrador. Iron Ore Company of Canada, Labrador Mining and Exploration Company and Labrador Iron Ore Royalty Income Fund. Newfoundland and Labrador Geological Survey, Assessment File LAB/1396, 51 pages.
- Darch, D. and Clark, D.  
2003: First year assessment report on geological and geochemical exploration for licence 8929M on claims in the Sudbury Lake area, western Labrador. Iron Ore Company of Canada and Labrador Mining Company. Newfoundland and Labrador Geological Survey, Assessment File 23B/14/0180, 20 pages.
- Darch, D. and Goodman, S.  
2003: First and second year assessment report on geological, geochemical, geophysical and diamond drilling exploration for licences 7799M-7800M, 8927M and 8930M on claims in the Huguette Lake - Leg Lake area, near Labrador City, western Labrador, 3 reports. Iron Ore Company of Canada and Labrador Mining and Exploration Company Limited. Newfoundland and Labrador Geological Survey, Assessment File 23B/0179, 169 pages.
- Darch, D., Tshimbalanga, S. and Clark, D.  
2003b: First and third year assessment report on geological, geochemical and geophysical exploration for licences 7795M, 8928M, 8931M-8935M and 9284M on claims in the Wabush Lake area, western Labrador, 2 reports. Labrador Iron Ore Royalty Income Fund, Labrador Mining and Exploration Company Limited and Iron Ore Company of Canada. Newfoundland and Labrador Geological Survey, Assessment File LAB/1389, 95 pages.
- Darch, W.  
2005a: Third and fifth year assessment report on diamond drilling exploration for licences 8931M and 9284M on claims in the Lost Lake area, near Wabush Lake, western Labrador. Iron Ore Company of Canada and Labrador Mining Company Limited. Newfoundland

- and Labrador Geological Survey, Assessment File 23G/02/0258, 109 pages.
- 2005b: Third year assessment report on diamond drilling exploration for licence 8928M on claims in the Polly Lake area, western Labrador. Labrador Mining Company Limited and Iron Ore Company of Canada. Newfoundland and Labrador Geological Survey, Assessment File 23B/14/0181, 58 pages.
- Darch, W., Tshimbalanga, S. and Goodman, S.  
2003a: Assessment report on geological, geochemical, geophysical and diamond drilling exploration for 2002 submission for Mining Lease 16 [LME Block 22-6] and Mining Lease 18 [LME Block 22-8] in the Labrador City area, western Labrador. Labrador Mining and Exploration Company and Iron Ore Company of Canada. Newfoundland and Labrador Geological Survey, Assessment File LAB/1388, 178 pages.
- Davidson, D.M.  
1954: Report on the Burden No 1 iron ore deposit in the Wabush Lake area, Labrador. Newfoundland and Labrador Corporation Limited. Newfoundland and Labrador Geological Survey, Assessment File 23G/0016, 70 pages.
- Dimroth, E. Baragar, W.R.A., Bergeron, R. and Jackson, G.D.  
1970: The Filling of the Circum-Ungava Geosyncline. *In* Symposium on Basins and Geosynclines of the Canadian Shield. Geological Survey of Canada, Paper 70-40, pages 45-142.
- Downing, K.  
2009: Second year assessment report on remote sensing and geological and geophysical exploration for licences 13953M and 13958M-13964M on claims in the Shabogamo Lake to Lac Virot area, near Labrador City, Labrador, 2 reports. Kennecott Canada Exploration Incorporated. Newfoundland and Labrador Geological Survey, Assessment File LAB/1546, 95 pages.
- 2010: First and second year assessment report on geological and geochemical exploration for licences 14804M, 14807M-14812M, 14816M, 14819M, 14822M-14823M, 14970M, 14984M-14985M, 14988M and 15041M-15042M on claims in the Lac Virot to Pegrum Lake area, western Labrador. Rio Tinto Exploration Incorporated. Newfoundland and Labrador Geological Survey, Assessment File LAB/1622, 50 pages.
- Downing, K. and Mitchell, T.  
2009a: First year assessment report on prospecting, remote sensing and geochemical and geophysical exploration for licences 14970M, 14984M-14985M, 14988M and 15041M-15042M on claims in the Wahnahnish Lake, Shabogamo Lake, Carol Lake, and Lac Virot areas, western Labrador, 2 reports. Kennecott Canada Exploration Incorporated. Newfoundland and Labrador Geological Survey, Assessment File LAB/1523, 69 pages.
- 2009b: First year assessment report on prospecting, remote sensing and geophysical exploration for licences 14816M, 14819M and 14822M-14823M on claims in the Pegrum Lake, Shabogamo Lake and Green Water Lake areas, western Labrador, 2 reports. Kennecott Canada Exploration Incorporated. Newfoundland and Labrador Geological Survey, Assessment File LAB/1512, 71 pages.
- Duquette, G.  
1957: Geology of Carol 1 west deposit, White Lake area, Labrador. Iron Ore Company of Canada. Newfoundland and Labrador Geological Survey, Assessment File 23G/0023, 16 pages.
- Duvergier, C.  
2012: Assessment report on diamond drilling exploration for 2010-2012 submission for mining lease 13-B22-3 in the White lake area, near Labrador City, western Labrador. Iron Ore Company of Canada and Labrador Iron Ore Royalty Corporation. Newfoundland and Labrador Geological Survey, Assessment File LAB/1727, 550 pages.
- Dymond, J., Suess, E. and Lyle, M.  
1992: Barium in deep-sea sediment: a geochemical proxy for paleoproductivity. *Paleoceanography*, Volume 7, pages 163-181.
- Eade, J.R.  
1958: Report on diamond drilling exploration on property in the Tuffy Lake, Stevens Lake and Riviere aux Fraises areas, Labrador. Labrador Mining and Exploration Company Limited. Newfoundland and Labrador Geological Survey, Assessment File 23G/02/0237, 34 pages.
- Eckstrand, O.R.  
1956: Report on the Scott Bay-Flat Rock Lake area, Labrador. Iron Ore Company of Canada. Newfoundland and Labrador Geological Survey, Assessment File 023G/0019, 17 pages.
- Elliott, R.A., McVeigh, H.G., Neal, H.E. and Rolling, F.J.  
1980: Potential for further iron ore development in Newfoundland and Labrador. Department of Mines and Energy, Government of Newfoundland and Labrador,

- Newfoundland and Labrador Geological Survey, Internal Collection, Company or Consultant Report LAB/0523, 175 pages.
- Emslie, R.F., Hamilton, M.A. and Gower, C.F.  
1997: The Michael Gabbro and other Mesoproterozoic lithospheric probes in southern and central Labrador. *Canadian Journal of Earth Sciences*, Volume 34, pages 1566-1580.
- Evans, J.L.  
1978: The geology and geochemistry of the Dyke Lake area (parts of 23J/8, 9), Labrador. Government of Newfoundland and Labrador, Department of Mines and Energy, Mineral Development Division, Report 78-4, 43 pages.
- Ewers, W.E. and Morris, R.C.  
1981: Studies of the Dales Gorge Member of the Brockman Iron Formation, Western Australia. *Economic Geology*, Volume 76, pages 1929-1953.
- Fahrig, W.F.  
1960: Shabogamo Lake, Newfoundland-Quebec. Geological Survey of Canada, Preliminary Map 9-1960.  
  
1967: Shabogamo Lake map area, Newfoundland-Labrador and Quebec, 23G (east half). Geological Survey of Canada, Memoir 354, 23 pages.
- Farquharson, G. and Thalenhorst, H.  
2006: Wabush Mines, Review of Scully Mine Reserves, by Strathcona Mineral Services Limited, for Department of Natural Resources, Government of Newfoundland and Labrador, 27 pages.
- Finch, C., Roldan, R., Walsh, L., Kelly, J. and Amor S.  
2018: Analytical methods for chemical analysis of geological materials. Government of Newfoundland and Labrador, Department of Natural Resources, Geological Survey, Open File NFLD/3316, 67 pages.
- Findlay, J.M., Parrish, R.R., Birkett, T.C. and Watanabe, D.H.  
1995: U-Pb ages from the Nimish Formation and Montagnais glomeroporphyritic gabbro of the central New Québec Orogen, Canada. *Canadian Journal of Earth Sciences*, Volume 32, pages 1208-1220.
- Gastil, R.G.  
1956: Report on geological and magnetic surveys of the Julienne Lake deposit, Labrador, Canadian Javelin Limited. Newfoundland and Labrador Geological Survey, Assessment File 23G/0154, 29 pages.
- Gastil, G. and Knowles, D.M.  
1960: Geology of the Wabush Lake area, southwestern Labrador and eastern Quebec, Canada. *Geological Society of America Bulletin*, Volume 71, pages 1243-1254.
- Geren, R.D. and McCullough, W.B.  
1990: Cain's Legacy, The Building of Iron Ore Company of Canada. Ramsay Derry, Metropole Litho Inc, 349 pages.
- Gignac, L-P., Sirois, R., Bernier, E., Giroux, K-E., Lapointe, R., St-Amour, M., Sims, D. and Bugden, C.  
2018: Amended and restated feasibility study Technical Report for the Scully Mine Re-Start Project Wabush, Newfoundland & Labrador. Prepared for Tacora Resources Inc. 43-101 Technical report, available online at [www.sedar.com](http://www.sedar.com).
- Gill, J.E., Bannerman, H.M. and Tolman, C.  
1937: Wapussakatoo Mountains, Labrador. *Geological Society of America Bulletin*, Volume 48, pages 567-585.
- Gill, J.E. and James, W.F.  
1933: Labrador report on the Kayak concession, Labrador. Newfoundland and Labrador Geological Survey, Internal Collection, Individual Report, 023G/02/0070.
- Goldner, B. and Sauve, M.  
2012: Fourth year assessment report on geophysical and diamond drilling exploration for licences 14970M, 14985M and 14988M on claims in the Wahnahnish Lake, Carol Lake, and Lac Virot areas, western Labrador, 2 reports. Rio Tinto Exploration Canada Incorporated. Newfoundland and Labrador Geological Survey, Assessment File LAB/1596, 249 pages.
- Goldner, B, Smith, L and Sauve, M  
2013: First year supplementary, second year supplementary, third year, fifth year supplementary and sixth year assessment report on remote sensing, metallurgical testing and diamond drilling exploration for licences 13954M, 13958M-13960M, 14808M-14809M, 14812M, 14985M, 14988M, 18241M, 18243M, 18675M-18676M, 18769M-18770M, 18774M-18775M, 18777M-18781M, 18784M-19785M, 18788M-18790M, 19359M-19360M, 19363M and 20385M on claims in the Shabogamo Lake to Lac Virot area, near Labrador City, Labrador. Rio Tinto Exploration Canada Incorporated, Newfoundland and Labrador Geological Survey, Assessment File LAB/1747, 1036 pages.
- Gower, C.F., Rivers, T. and Brewer, T.S.  
1990: Middle Proterozoic mafic magmatism in Labrador, eastern Canada. *In* Mid-Proterozoic Laurentia-Baltica.



*Edited by C.F. Gower, T. Rivers and A.B. Ryan. Geological Association of Canada, Special Paper 38, pages 485-506.*

Grandillo, A., Live, P., Deering, P., Koclumbas, M. and Risto, R.W.

2012: Feasibility study of the Rose Deposit and resource estimate for the Mills Lake of the Kamistiatasset (Kami) iron ore property, Labrador, for Alderon Iron Ore Corporation. 43-101 Technical Report, available online at [www.sedar.com](http://www.sedar.com).

Grandillo, A., Powell, J.K., Koclumbas, M. and Risto, R.W.

2011: Preliminary economic assessment report of the Kamistiatasset (Kami) iron ore property, Labrador, for Alderon Iron Ore Corp. 43-101 Technical report, available online at [www.sedar.com](http://www.sedar.com).

Grant, J.M.

1979a: Drill report on block 65 in the Wabush area, Labrador. Iron Ore Company of Canada and Labrador Mining and Exploration Company Limited. Newfoundland and Labrador Geological Survey, Assessment File 23G/02/0190, 6 pages.

1979b: Rock sampling report on block 84 in the Wabush area, Labrador. Iron Ore Company of Canada and Labrador Mining and Exploration Company Limited. Newfoundland and Labrador Geological Survey, Assessment File 23G/03/0196, 5 pages.

1979c: Rock sampling report on block 75 in the Wabush area, Labrador. Iron Ore Company of Canada and Labrador Mining and Exploration Company Limited. Newfoundland and Labrador Geological Survey, Assessment File 23G/02/0192, 6 pages.

1979d: Rock sampling report on block 76 in the Wabush area, Labrador. Ore Company of Canada and Labrador Mining and Exploration Company Limited. Newfoundland and Labrador Geological Survey, Assessment File 23G/02/0193, 9 pages.

1979e: Drill report on block 55 in the Wabush area, Labrador. Iron Ore Company of Canada and Labrador Mining and Exploration Company Limited. Newfoundland and Labrador Geological Survey, Assessment File 23B/14/0122, 10 pages.

1979f: Drill report on block 57 in the Wabush area, Labrador. Iron Ore Company of Canada and Labrador Mining and Exploration Company Limited. Newfoundland

and Labrador Geological Survey, Assessment File 23B/14/0121, 6 pages.

1979g: Rock sampling report on block 89 in the Wabush area, Labrador. Iron Ore Company of Canada and Labrador Mining and Exploration Company Limited. Newfoundland and Labrador Geological Survey, Assessment File 23G/0198, 8 pages.

1979h: Drill report on block 74 in the Wabush area, Labrador. Iron Ore Company of Canada and Labrador Mining and Exploration Company Limited. Newfoundland and Labrador Geological Survey, Assessment File 23G/02/0204, 7 pages

1980a: Report on a ground geophysical survey on block 23 in the Labrador City-Wabush area, Labrador. Labrador Mining and Exploration Company Limited. Newfoundland and Labrador Geological Survey, Assessment File 23B/0124, 6 pages.

1980b: Report on a ground geophysical survey on block 58 in the Labrador City-Wabush area, Labrador. Labrador Mining and Exploration Company Limited. Newfoundland and Labrador Geological Survey, Assessment File LAB/0593, 28 pages.

Greer, W.L.C.

1954: Report on Nalco iron deposit of the Wabush Lake area, Labrador. Newfoundland and Labrador Corporation Limited. Newfoundland and Labrador Geological Survey, Assessment File 23G/0014, 6 pages.

Grimaldi, S.

1959a: Gravity profiles maps for North Carol Lake, Labrador. Labrador Mining and Exploration Company Limited. Newfoundland and Labrador Geological Survey, Assessment File 23G/0038, 1959, 14 maps.

1959b: Gravity and magnetic profiles maps for Goethite Bay, Labrador. Labrador Mining and Exploration Company Limited. Newfoundland and Labrador Geological Survey, Assessment File 23G/0042, 3 pages.

Gross, G.A.

1955: The metamorphic rocks of the Mount Wright and Matonipi Lake areas of Québec. Unpublished Ph.D. Thesis, University of Wisconsin, 152 pages.

1968: Geology of Iron Deposits of Canada, Volume III. Iron Ranges of the Labrador Geosyncline. Geological Survey of Canada, Economic Geology Report 22, 179 pages.

- Gutzmer, J., Chisonga, B.C., Beukes, N.J. and Mukhopadhyay, J.  
2008: The geochemistry of banded iron formation-hosted high-grade hematite-martite iron ores. *Reviews in Economic Geology*, Volume 15, pages 157-183.
- Hamilton, C.G.  
1973: Polly Lake Claims Group. *Énergie et Ressources naturelles*, Québec, Assessment Report GM 29166, 41 pages.
- Harrison, J.M.  
1952: The Quebec-Labrador iron belt, Quebec and Newfoundland. *Geological Survey of Canada*, Paper 52-20, 21 pages.
- Harrison, J.M., Howell, J.E. and Fahrig, W.F.  
1972: A geological cross section of the Labrador miogeosyncline near Schefferville, Quebec. *Geological Survey of Canada*, Report 70-37, 34 pages.
- Hartopp, P.G.  
1962a: Diamond drilling data from Wabush mines, Labrador. Newfoundland and Labrador Corporation Limited. Newfoundland and Labrador Geological Survey, Assessment File 23B/15/0038, 7 pages.  
  
1962b: Diamond drilling data from the Wabush Mountain area, western Labrador. Wabush Mines and Wabush Iron Company Limited. Newfoundland and Labrador Geological Survey, Assessment File 23B/15/0131, 52 pages.
- Haugaard, R., Frei, R., Stendal, H. and Konhauser, K.  
2013: Petrology and geochemistry of the ~2.9 Ga Itilliarsuk banded iron formation and associated supracrustal rocks, West Greenland: source characteristics and deposition. *Precambrian Research*, Volume 229, pages 150-176.
- Hird, J.M.  
1960: Report on the Wabush iron ore deposits. Iron Ore Company of Canada and Michigan College of Mining and Technology. Newfoundland and Labrador Geological Survey, Internal Report 023B/0033, 35 pages.
- Horstmann, U.E. and Hälbich, I.W.  
1995: Chemical composition of banded iron-formations of the Griqualand West Sequence, Northern Cape Province, South Africa, in comparison with other Precambrian iron formations. *Precambrian Research*, Volume 72(1), pages 109-145.
- Hovis, S. and Broadbent, G.C.  
2010: Third year assessment report on remote sensing and geological, geochemical, geophysical and diamond drilling exploration for licences 13953M-13954M and 13958M-13964M on claims in the Shabogamo Lake to Lac Virot area, near Labrador City, Labrador, 3 reports. Kennecott Canada Exploration Incorporated and Rio Tinto Exploration Canada Incorporated. Newfoundland and Labrador Geological Survey, Assessment File LAB/1580, 288 pages.
- Hovis, S. and Goldner, B.  
2011a: Second and third year assessment report on prospecting and geochemical, geophysical and diamond drilling exploration for licences 14970M, 14984M-14985M, 14988M and 15041M-15042M on claims in the Pegrum Lake to Lac Virot area, western Labrador. Rio Tinto Exploration Canada Incorporated. Newfoundland and Labrador Geological Survey, Assessment File LAB/1662, 108 pages.  
  
2011b: Second and third year assessment report on prospecting, remote sensing, and geochemical, geophysical and diamond drilling exploration for licences 14804M, 14807M-14812M, 14819M and 14822M-14823M on claims in the Shabogamo Lake to Green Water Lake area, western Labrador. Rio Tinto Exploration Canada Incorporated. Newfoundland and Labrador Geological Survey, Assessment File LAB/1661, 218 pages.  
  
2011c: Fourth year assessment report on geological, geochemical, geophysical and diamond drilling exploration for licences 13954M, 13958M-13962M and 19361M-19363M on claims in the Shabogamo Lake to Lac Virot area, near Labrador City, Labrador. Rio Tinto Exploration Canada Incorporated. Newfoundland and Labrador Geological Survey, Internal Report, Miscellaneous LAB/1650, 322 pages.  
  
2012: First and fourth year assessment report on prospecting, and geophysical and diamond drilling exploration for licences 14808M-14809M, 14812M, 14819M, 18770M-18791M, 18797M-18798M and 19359M-19360M on claims in the Shabogamo Lake to Green Water Lake area, western Labrador. Rio Tinto Exploration Canada Incorporated. Newfoundland and Labrador Geological Survey, Assessment File LAB/1679, 560 pages.
- Hulstein, R. and Lee, C.  
2001: Assessment report on compilation and structural analysis for 2000-2001 submission for Labrador Mining

- and Exploration Company Limited Blocks 22 to 38, 41 and 42 and for first year assessment for licences 7782M-7803M on claims in the Labrador City area, western Labrador, 5 reports. Iron Ore Company of Canada. Newfoundland and Labrador Geological Survey, Assessment File LAB/1412, 212 pages.
- Indares, A. and Rivers, T.  
1995: Textures, metamorphic reactions and thermobarometry of eclogitized metagabbros: A Proterozoic example. *European Journal of Mineralogy*, Volume 7, pages 43-56.
- Iron Ore Company of Canada  
1973: Gravity and magnetic profiles from the Luce No 1 deposit, Labrador City, Labrador. Iron Ore Company of Canada. Newfoundland and Labrador Geological Survey, Assessment File 23G/02/0099, 15 pages.  
  
1975: Gravity and magnetic profiles from the Luce No 1 deposit, Labrador City, Labrador. Iron Ore Company of Canada. Newfoundland and Labrador Geological Survey, Assessment File 23G/02/0101.  
  
2014: Wabush 3 Open Pit Mine Project: Environmental Impact Statement.  
  
2015: Wabush 3 Open Pit Mine Project: Environmental Impact Statement. Available online at [http://www.mae.gov.nl.ca/env\\_assessment/projects/Y2013/1711](http://www.mae.gov.nl.ca/env_assessment/projects/Y2013/1711)  
  
2017: Sherwood North Pit Project, Labrador West. Environmental Assessment Registration.  
  
2018: Magy Pit Extension Project, Labrador West. Environmental Assessment Registration.
- Jackson, G.  
1954: Exploration report on the Nip Lake-Reid Lake area, Labrador. Iron Ore Company of Canada. Newfoundland and Labrador Geological Survey, Assessment File 23G/0015, 45 pages.  
  
1963: The geology of the Neal (Virot) Lake area, west of Wabush Lake, Labrador, with special reference to iron deposits. Unpublished Ph. D. thesis, McGill University, 337 pages.  
  
1976: Geology, Opocopa Lake (east half), Quebec-Newfoundland. Geological Survey of Canada, "A" Series Map 1417A.
- James, D.T.  
1997: Geology of the Archean Ashuanipi Complex, western Labrador. Government of Newfoundland and Labrador, Department of Mines and Energy, Geological Survey, Report 97-2, 27 pages.
- Johnson, I.  
1982: Assessment report on airborne geophysical surveys for 1982 submission on Labrador Mining and Exploration Company Limited blocks 26 to 31, 33, 51 to 58, 64, 65, 66, 69 to 77, 83 to 92, 134 and 135 in the Schefferville and Wabush areas, northwestern Labrador. Labrador Mining and Exploration Company Limited. Newfoundland and Labrador Geological Survey, Assessment File LAB/0630, 142 pages.
- Jury, R.  
1957: Report on the Emma Lake-O'Brien Lake area, Labrador. Labrador Mining and Exploration Company Limited. Newfoundland and Labrador Geological Survey, Assessment File 23G/0024, 15 pages.
- Kaul, A., Sylvester, P.J. and Blake, M.  
2012: New insights into the formation processes of superior-type banded iron formations: Carbonates, an additional source of Keno-magnetite from the Luce iron ore deposits, Labrador City, Newfoundland and Labrador. Geological Association of Canada–Mineralogical Association of Canada, 2012 Joint Annual Meeting, St. John's, Newfoundland. Abstract Volume, page 65.
- Klein, C.  
1959: Summary report on the geology of Carol west, Luce 1 extension and Wabush No 7 in the Wabush Lake area, Labrador. Labrador Mining and Exploration Company Limited. Newfoundland and Labrador Geological Survey, Assessment File 23G/0044, 33 pages.  
  
1966: Mineralogy and petrology of the metamorphosed Wabush Iron Formation, southwestern Labrador. *Journal of Petrology*, Volume 7, pages 246-305.  
  
1973: Changes in mineral assemblages with metamorphism of some banded Precambrian iron-formations. *Economic Geology*, Volume 68, pages 1075-1088.  
  
1978: Regional metamorphism of Proterozoic iron-formation, Labrador Trough, Canada. *American Mineralogist*, Volume 63, pages 898-912.



- Klein, C. and Fink, R.P.  
1976: Petrology of the Sokoman Iron-Formation in the Howells River area, at the western edge of the Labrador Trough. *Economic Geology*, Volume 71, pages 453-487.
- Knowles, D.M.  
1955: Geology and petrology of the Wabush Lake Iron Formation, Labrador, Unpublished M.Sc. thesis, Michigan College of Mining and Technology, 109 pages.  
1960: A report of studies conducted during 1959-1960 on the Julienne Lake Deposit, Labrador. Canadian Javelin Limited. Newfoundland and Labrador Geological Survey, Assessment File 023G/0124, 59 pages.  
1963: Review of the geology and mineralogy of the Julian Lake Deposit, Labrador. Canadian Javelin Limited. Newfoundland and Labrador Geological Survey, Assessment File 023G/0126, 14 pages.  
1967a: Report concerning the 1963 bulk sample analysis project on the Julienne Lake deposit, Labrador, Canadian Javelin Limited. Newfoundland and Labrador Geological Survey, Assessment File 023G/02/0112, 6 pages.  
1967b: Report concerning the 1966 sample project Julienne Lake deposit, Canadian Javelin Limited. Newfoundland and Labrador Geological Survey, Assessment File 023G/0125, 24 pages.
- Knowles D.M. and Gastil R.G.  
1959: Metamorphosed iron formation in southwestern Labrador. *Canadian Mining and Metallurgical Bulletin*, pages 1-8.
- Knowles, D.M., MacPherson, W., Blakeman, W. and LaRush, P.  
1962: Report on the geology and trench stripping project of the Julian Lake deposit, Labrador, Canadian Javelin Limited. Newfoundland and Labrador Geological Survey, Assessment File 023G/0152, 17 pages.
- Labrador Mining and Exploration Company Limited  
1965: Feasibility study Labrador Ridge Mine. Labrador Mining and Exploration Company Limited. Newfoundland and Labrador Geological Survey, Assessment File 23B/0052, 73 pages.
- Lachance, N.  
2015: Genesis of iron ore in the Snelgrove Lake area, Labrador Trough, western Labrador. Unpublished M.Sc. thesis, Memorial University of Newfoundland, St. John's, 76 pages.
- Le Gallais, C.J. and Lavoie, S.  
1982: Basin evolution of the Lower Proterozoic Kaniapiskau Supergroup, central Labrador Miogeocline (Trough), Quebec. *Bulletin of Canadian Petroleum Geology*, Volume 30, pages 150-160.
- Leuner, W.R. and Skimming, T.  
1959: Summary report on the geology of Beverley Lake and Wabush No 4 and No 8 orebodies in the Wabush Lake area, Labrador. Iron Ore Company of Canada. Newfoundland and Labrador Geological Survey, Assessment File 23G/0048, 17 pages.
- Love, H.D.  
1959: Geological report of Grace and Bruce Lake areas, Labrador. Labrador Mining and Exploration Company Limited. Newfoundland and Labrador Geological Survey, Assessment File 023G/0046, 22 pages.  
1961: Geological and geophysical report of the Haguette, Throne and Jackman Lake areas, Labrador. Labrador Mining and Exploration Company Limited. Newfoundland and Labrador Geological Survey, Assessment File 23B/14/0014, 24 pages.
- Lyons, E., Dube, V., Grandillo, A., Live, P., Deering, P., Kociumbas, M.W. and Risto, R.W.  
2013: Second year assessment report on feasibility studies, remote sensing, geotechnical drilling and geological exploration for licences 17926M and 17948M on claims in the Mills Lake area, western Labrador, 3 reports. Alderon Iron Ore Corporation. Newfoundland and Labrador Geological Survey, Assessment File 23B/15/0211, 699 pages.
- Lyons, E., Dube, V., Grandillo, A., Live, P., Deering, P., Kociumbas, M.W. and Risto, R.W.  
2013b: Eighth year assessment report on feasibility studies, remote sensing, and diamond drilling exploration for licence 15980M on claims in the Rose Lake area, western Labrador, 3 reports. Alderon Iron Ore Corporation. Newfoundland and Labrador Geological Survey, Assessment File 23B/0219, 1492 pages.
- Lyons, E., Fox, D. and Selman, D.  
2011: First and sixth year assessment report on geochemical, geophysical and diamond drilling exploration for licences 15980M, 17926M and 17948M on claims in the Mills Lake area, western Labrador, 5 reports. Alderon Resource Corporation and Altius Resources Incorporated. Newfoundland and Labrador Geological Survey, Assessment File 23B/0197, 215 pages.

- Lyons, E., Grandillo, A., Deering, P., Kociumbas, M.W. and Risto, R.W.  
2013a: Seventh year assessment report on economic assessment, resource estimation, remote sensing, and diamond drilling exploration for licence 15980M on claims in the Rose Lake area, western Labrador, 2 reports. Alderon Iron Ore Corporation. Newfoundland and Labrador Geological Survey, Assessment File 23B/0218, 4845 pages.
- Lyons, E., Velcic, N. and Haack, E.  
2014: Ninth year assessment report on geotechnical drilling, environmental work and mineral potential for licence 15980M on claims in the Rose Lake area, western Labrador, 2 reports. The Kami Mine Limited Partnership and Alderon Iron Ore Corporation. Newfoundland and Labrador Geological Survey, Assessment File 23B/0225, 274 pages.
- MacDermott, D.B.  
1958: Evaluation of an anomaly in the northeast of Wabush Lake, Labrador. Labrador Mining and Exploration Company Limited. Newfoundland and Labrador Geological Survey, Assessment File 23G/0026, 34 pages.
- Macdonald, R.D.  
1961: Report of operations for 1960 in Labrador. Iron Ore Company of Canada and Labrador Mining and Exploration Company Limited. Newfoundland and Labrador Geological Survey, Assessment File LAB/0264, 12 pages.  
  
1963: Report on operations for 1962 for Labrador. Labrador Mining and Exploration Company Limited. Newfoundland and Labrador Geological Survey, Assessment File LAB/0525, 19 pages.
- Macdonald, R.D. and Hogg, C.M.  
1962: Report on operations for 1961 for Labrador. Labrador Mining and Exploration Company Limited. Newfoundland and Labrador Geological Survey, Assessment File LAB/0524, 23 pages.
- MacLeod, K.  
1954: Magnetometer survey map of the Wabush iron ore deposit, Labrador. Canadian Javelin Limited. Newfoundland and Labrador Geological Survey, Assessment File 23B/0008.
- Machado, N., Clark, T., David, J. and Goulet, N.  
1997: U-Pb ages for magmatism and deformation in the New Quebec Orogen. *Canadian Journal of Earth Sciences*, Volume 34, pages 716-723.
- Magyar, W.B.  
1970: The Julian-Star-O'Keefe project feasibility assessment. Julco Iron Corporation Limited, Dominion Jubilee Corporation Limited and Newfoundland & Labrador Corporation. Newfoundland and Labrador Geological Survey, Assessment File LAB/0414, 40 pages.
- Malchelosse, B.  
1957: Report on Carol 1 E-Lorraine 2 and Wabush 5 deposits, Labrador. Iron Ore Company of Canada. Newfoundland and Labrador Geological Survey, Assessment File 23G/0025.
- Marshall, L.  
2012: Assessment report on diamond drilling exploration for 2007-2012 submission for mining leases 17-822-7 and 18-B22-8 in the Labrador City area, western Labrador. Labrador Iron Ore Royalty Corporation and the Iron Ore Company of Canada, Newfoundland and Labrador Geological Survey, Assessment File LAB/1728, 550 pages.  
  
2012a: Tenth year assessment report on diamond drilling exploration for licence 8927M on claims in the Canning Lake area, near Labrador City, western Labrador. Iron Ore Company of Canada and Labrador Iron Ore Royalty Corporation. Newfoundland and Labrador Geological Survey, Assessment File 23B/0220, 53 pages.  
  
2012b: Assessment report on diamond drilling exploration for 2007-2012 submission for Mining Leases 17-B22-7 and 18-B22-8 in the Labrador City area, western Labrador. Labrador Iron Ore Royalty Corporation and Iron Ore Company of Canada. Newfoundland and Labrador Geological Survey, Assessment File LAB/1728, 550 pages.
- Mathieson, R.D.  
1957: Report on the Wabush project for 1956 in the Carol Lake area, Labrador. Iron Ore Company of Canada. Newfoundland and Labrador Geological Survey, Assessment File 23G/0020, 18 pages.  
  
1957a: Report of exploratory drilling of the Wabush project in the Duley Lake-Mills Lake area, Labrador. Iron Ore Company of Canada. Newfoundland and Labrador Geological Survey, Assessment File 23B/0011, 32 pages.
- McLennan, S.M.  
1989: Rare earth elements in sedimentary rocks: influences of provenance and sedimentary processes. *In Geochemistry and Mineralogy of Rare Earth Elements. Edited by B.R. Lipin and G.A. McKay. Reviews in Mineralogy*, Volume 21, pages 169-200.

- McDonald, M.  
2015: Assessment report on geophysical exploration for 2014 submission for Mining Lease 16 [LME Block 22-6] in the Labrador City area, western Labrador, 2 reports. Labrador Iron Ore Royalty Corporation and Iron Ore Company of Canada, Newfoundland and Labrador Geological Survey, Assessment File 23B/15/0233, 136 pages.
- Meyer, J.R. and Dean, P.L.  
1987: Silica in western Labrador. *In* Current Research. Government of Newfoundland and Labrador, Department of Mines and Energy, Mineral Development Division, Report 87-1, pages 71-75.
- Mloszewska, A.M., Pecoits, E., Cates, N.L., Mojzsis, S.J., O'Neil, J., Robbins, L.J. and Konhauser, K.O.  
2012: The composition of Earth's oldest iron formations: the Nuvvuagittuq Supracrustal Belt (Québec, Canada). *Earth and Planetary Science Letters*, Volumes 317-318, pages 331-342.
- Moss, A.E.  
1952: Report on operations for 1951 for Labrador. Labrador Mining and Exploration Company Limited. Newfoundland and Labrador Geological Survey, Assessment File LAB/0505, 8 pages.
- Mumtazuddin, M  
1957: Geology of the Wabush area, Labrador. Newfoundland and Labrador Geological Survey, Internal Report 023B/0010, 14 pages.
- Muwais, W.  
1974: Stratigraphy of the Wabush Lake area with special reference to the Wabush Iron Formation. Iron Ore Company of Canada. Newfoundland and Labrador Geological Survey, Assessment File 23G/02/0281, 149 pages.
- Muwais, W. and Broemling, A.  
1971: Geological exploration map and diamond drillhole logs from the Labrador City area, Labrador. Iron Ore Company of Canada. Newfoundland and Labrador Geological Survey, Assessment File 23B/0171, 149 pages.
- Neal, H.E.  
1950a: Report on the geology of the Duley Lake-Wabush Lake area, Labrador. Labrador Mining and Exploration Company Limited. Newfoundland and Labrador Geological Survey, Assessment File 23B/0002, 56 pages.  
  
1950b: Economic geology of Wabush No 3 and Lorraine No 1 magnetite-specularite showings in the Wabush Lake area, Labrador. Labrador Mining and Exploration Company Limited. Newfoundland and Labrador Geological Survey, Assessment File 23B/0001, 10 pages.
- 1951: Exploration report on the Wabush Lake-Shabogamo Lake area, Labrador. Newfoundland and Labrador Geological Survey, Assessment File 23G/0004, 47 pages.
- 1953: Monthly and summary report for the Wabush Lake area, Labrador. Iron Ore Company of Canada. Newfoundland and Labrador Geological Survey, Assessment File 23G/0011, 13 pages.
- 1998: Early history and recollections of the Labrador City area. *Dialogue for Engineers and Geoscientists, Association of Professional Engineers and Geoscientists of Newfoundland*, Issue 70, pages 9-14.
- 2000: Iron deposits of the Labrador Trough. *Exploration and Mining Geology*, Volume 9(2), pages 113-121.
- Nesbitt, H.W.  
1979: Mobility and fractionation of rare earth elements during weathering of a granodiorite. *Nature*, Volume 279, pages 206-210.
- Nincherie, R.  
1959: Geological and geophysical report of the Duley-Mills Lake area, Labrador. Labrador Mining and Exploration Company Limited. Newfoundland and Labrador Geological Survey, Assessment File 23G/0047, 28 pages.
- Noel, N.T.  
1992: The geology and geochemistry of the McKay River area volcanic rocks, western Labrador. Unpublished M.Sc. thesis, Memorial University of Newfoundland, St. John's, 149 pages.
- O'Leary, J.  
1973: Application of geology and geostatistics at the Scully Mine orebody, Wabush, Labrador. Unpublished Ph.D. thesis, Royal School of Mines, 199 pages.  
  
1979: Ore reserve estimation methods and grade control at the Scully Mine, Canada – an intergrated geological/geostatistical approach. *Mining Magazine*, pages 300-314.
- O'Leary, J., Cannell, R. and Honsberger, D.  
1972: Geology at the Scully mine. *Canadian Institute of Mining Bulletin*, Volume 65, pages 25-29.
- Parrent, M.D.  
2012: Separation of pyrolusite and hematite by froth flotation. Unpublished M.Sc. thesis, University of Alberta, 179 pages.



- Pecoits, E., Gingras, M.K., Barley, M.E., Kappler, A., Posth, N.R. and Konhauser, K.O.  
2009: Petrography and geochemistry of the Dales Gorge banded iron formation: paragenetic sequence, source and implications for palaeo-ocean chemistry. *Precambrian Research*, Volume 172, pages 163-187.
- Percival, J.A.  
1987: Geology of the Ashuanipi Granulite Complex in the Schefferville area, Quebec. *In Current Research, Part A. Geological Survey of Canada, Paper 87-1A*, pages 1-10.
- Pickands Mather and Company  
1959a: Report on exploration of the Julian ore deposit, Labrador. Pickands Mather and Company. Newfoundland and Labrador Geological Survey, Assessment File 023G/02/0066, 49 pages.  
  
1959b: Report on exploration of the Julian Lake area and North Concession areas, Labrador. Pickands Mather and Company. Newfoundland and Labrador Geological Survey, Assessment File 023G/0067, 25 pages.
- Pickard, A.L.  
2002: SHRIMP U-Pb zircon ages of tuffaceous mudrocks in the Brockman Iron Formation of the Hamersley Range, Western Australia. *Australian Journal of Earth Science*, Volume 49, pages 491-507.
- Planavsky, N., Bekker, A., Rouxel, O.J., Kamber, B., Hofmann, A., Knudsen, A. and Lyons, T.W.  
2010: Rare earth element and yttrium compositions of Archean and Paleoproterozoic Fe formations revisited: new perspectives on the significance and mechanisms of deposition. *Geochimica et Cosmochimica Acta*, Volume 74, pages 6387-6405.
- Pond, S.  
2013: Assessment report on diamond drilling exploration for 2007-2012 submission for mining lease 15-B22-5 in the Labrador City area, western Labrador. Labrador Iron Ore Royalty Corporation and Iron Ore Company of Canada, Newfoundland and Labrador Geological Survey, Assessment File 23B/15/0226, 1749 pages.
- Preziosi, L.  
2001: Luce Pit, continuation of the Carol mining project, registration/referral. Iron Ore Company of Canada. Newfoundland and Labrador Geological Survey, Internal Collection, Company or Consultant Report LAB/1329, 98 pages.
- Price, J.  
1977: Report on magnetic investigation and diamond drilling in the Labrador City area, Labrador. Iron Ore Company of Canada. Newfoundland and Labrador Geological Survey, Assessment File 23G/02/0092, 14 pages.
- Price, J.B.  
1979a: Report on a ground magnetometer survey on block 22, Labrador. Labrador Mining and Exploration Company Limited. Newfoundland and Labrador Geological Survey, Assessment File 23B/0106, 18 pages.  
  
1979b: Report on geochemistry and geophysics of block 35, Labrador. Labrador Mining and Exploration Company Limited. Newfoundland and Labrador Geological Survey, Assessment File 23G/02/0180, 20 pages.  
  
1979c: Report on geochemistry, geophysics and petrography of block 37, Labrador. Iron Ore Company of Canada and Labrador Mining and Exploration Company Limited. Newfoundland and Labrador Geological Survey, Assessment File 23G/02/0182, 19 pages.  
  
1979d: Report on geochemistry, geophysics and petrography of block 30, Labrador. Iron Ore Company of Canada and Labrador Mining and Exploration Company Limited. Newfoundland and Labrador Geological Survey, Assessment File 23B/14/0112, 29 pages.  
  
1979e: Report on ground magnetometer survey on block 27, Labrador. Labrador Mining and Exploration Company Limited. Newfoundland and Labrador Geological Survey, Assessment File 23B/14/0110, 13 pages.  
  
1979f: Report on ground magnetometer survey on block 36, Labrador. Labrador Mining and Exploration Company Limited. Newfoundland and Labrador Geological Survey, Assessment File 23G/02/0181, 20 pages.  
  
1979g: Report on 1978 magnetite investigation of lease blocks in the Labrador City area, Labrador. Iron Ore Company of Canada. Newfoundland and Labrador Geological Survey, Assessment File 23B/15/0132, 45 pages.  
  
1979h: Report on a ground magnetometer survey on block 24, Labrador. Labrador Mining and Exploration Company Limited. Newfoundland and Labrador Geological Survey, Assessment File 23B/0107, 15 pages.  
  
1979i: Report on a ground magnetometer survey on block 25, Labrador. Labrador Mining and Exploration Company Limited. Newfoundland and Labrador Geological Survey, Assessment File 23B/14/0108, 13 pages.

- 1979j: Report on geochemistry and geophysics of block 41, Labrador. Labrador Mining and Exploration Company Limited. Newfoundland and Labrador Geological Survey, Assessment File 23G/02/0184, 18 pages.
- 1979k: Report on a ground magnetometer survey on block 38, Labrador. Labrador Mining and Exploration Company Limited. Newfoundland and Labrador Geological Survey, Assessment File 23G/02/0183, 13 pages.
- Pufahl, P.K., Anderson, S.L. and Hiatt, E.E.  
2014: Dynamic sedimentation of Paleoproterozoic continental margin iron formation, Labrador Trough, Canada: Paleoenvironments and sequence stratigraphy. *Sedimentary Geology*, Volume 309, pages 48-65.
- Reynolds, J. and Mitchell, T.  
2008: First year assessment report on sampling and geophysical exploration for licences 13953M-13964M on claims in the Shabogamo Lake to Lac Virot area, near Labrador City, Labrador, 2 reports. Kennecott Canada Exploration Incorporated. Newfoundland and Labrador Geological Survey, Assessment File LAB/1477, 86 pages.
- Rivers, T.  
1980a: Wabush Lake, NTS 23G/2, with marginal notes. Government of Newfoundland and Labrador, Department of Mines and Energy, Mineral Development Division, Map 80-001.  
1980b: Sawbill Lake, NTS 23G/7, with marginal notes. Government of Newfoundland and Labrador, Department of Mines and Energy, Mineral Development Division, Map 80-002.  
1980c: Flora Lake, NTS 23B/15, with marginal notes. Government of Newfoundland and Labrador, Department of Mines and Energy, Mineral Development Division, Map 80-282.  
1980d: Revised stratigraphic nomenclature for Aphebian and other rock units, southern Labrador Trough, Grenville Province. *Canadian Journal of Earth Sciences*, Volume 17, pages 668-670.  
1983a: The northern margin of the Grenville Province in western Labrador - anatomy of an ancient orogenic front. *Precambrian Research*, Volume 22, pages 41-73.  
1983b: Progressive metamorphism of pelitic and quartzofeldspathic rocks in the Grenville Province of western Labrador-tectonic implications of bathozone 6 assemblages. *Canadian Journal of Earth Sciences*, Volume 20, pages 1791-1804.
- 1985a: Geology of the Opocopa Lake area, Labrador/Quebec. Government of Newfoundland and Labrador, Department of Mines and Energy, Mineral Development Division, Map 85-024.  
1985b: Geology of the Lac Virot area, Labrador/Quebec. Government of Newfoundland and Labrador, Department of Mines and Energy, Mineral Development Division, Map 85-025.
- Rivers, T., Ketchum, J., Indares, A. and Hynes A.  
2002: The high pressure belt in the Grenville Province: Architecture, timing and exhumation models. *Canadian Journal of Earth Sciences*, Volume 39, pages 867-893.
- Rivers, T. and Massey, N.  
1985: Geology of the Wightman Lake area, Labrador. Government of Newfoundland and Labrador, Department of Mines and Energy, Mineral Development Division, Map 85-028.
- Rivers, T., van Gool, J.A.M. and Connelly J.N.  
1993: Contrasting tectonic styles in the northern Grenville Province: Implications for the dynamics of orogenic fronts. *Geology*, Volume 21, pages 1127-1130.
- Rohon, M.-L., Vialette, Y., Clark, T., Roger, G., Ohnenstetter, D. and Vidal P.  
1993: Aphebian mafic-ultramafic magmatism in the Labrador Trough (New Quebec): its age and the nature of its mantle source. *Canadian Journal of Earth Sciences*, Volume 30, pages 1582-1593.
- Sauve, M.  
2014: Mineralogical characteristics of polished thin sections on the Labrador Iron Project. Rio Tinto Exploration Canada Incorporated. Newfoundland and Labrador Geological Survey, Assessment File 023G/0314, 27 pages.
- Sauve, M., Smith, L. and Goldner, B.  
2012: First year, second year, second year supplementary, fifth year, fifth year supplementary, eleventh and twelfth year assessment report on geophysical exploration for licences 7795M, 7799M-7800M, 8930M-8931M, 10380M, 13954M, 13958M-13962M, 14808M-14809M, 14812M, 14819M, 14985M, 14988M, 15780M-15781M, 15924M, 18240M-18244M, 18467M, 18672M-18679M, 18769M-18786M, 18788M-18791M, 18797M-18798M, 19359M-19363M and 20385M on claims in the Shabogamo Lake to Lac Virot area, near Labrador City, Labrador, 2 reports.

- Rio Tinto Exploration Canada Incorporated, Iron Ore Company of Canada and Labrador Iron Ore Royalty Corporation. Newfoundland and Labrador Geological Survey, Assessment File LAB/1683, 77 pages.
- Seymour, C., Churchill, R., Simoneau, P. and Tshimbalanga, S. 2011: First year assessment report on geophysical exploration for licences 16266M and 17390M-17391M on claims in the Julienne Lake area, western Labrador, 2 reports. Altius Resources Incorporated. Newfoundland and Labrador Geological Survey, Assessment File 23G/02/0324, 44 pages.
- Seymour, C., Churchill, R., Winter, L. and Grand, T. 2008: First year assessment report on geological, geochemical and geophysical exploration for licences 10501M, 11927M, 12853M-12854M, 13935M and 13937M on claims in the Mills Lake area, western Labrador. Altius Resources Incorporated. Newfoundland and Labrador Geological Survey, Assessment File 23B/0195, 127 pages.
- Seymour, C., Churchill, R., Winter, L., O'Driscoll, J., Tshimbalanga, S. and Mira Geoscience 2009: First and fourth year assessment report on geophysical and diamond drilling exploration for licences 14957M, 14962M, 14967M-14968M and 15037M on claims in the Mills Lake area, western Labrador, 3 reports. Altius Resources Incorporated. Newfoundland and Labrador Geological Survey, Assessment File 23B/0192, 453 pages.
- Seymour, C., Winter, L. and Churchill, R. 2012: Fourth year assessment report on diamond drilling exploration for licence 20499M on claims in the Julienne Lake area, western Labrador, 3 reports. Altius Resources Incorporated. Newfoundland and Labrador Geological Survey, Assessment File, 023G/02/0306, 284 pages.
- 2013: Fifth year assessment report on analytical results from the 2012 diamond drilling program for map staked license 20499M, Julienne Lake Property, western Labrador, NTS 23G02 & 23B15. Altius Resources Incorporated. Newfoundland and Labrador Geological Survey, Assessment File 023G/02/0308, 72 pages.
- Shklanka, R. 1956: Field report on the Shabogamo Lake area, Labrador. Iron Ore Company of Canada, Newfoundland and Labrador Geological Survey, Assessment File 23G/0021, 1956, 18 pages.
- Simpson, H.J. and Bird, D. 1982: Assessment report on geological, geochemical and geophysical exploration for 1982 submission on Labrador Mining and Exploration Company Limited blocks 26 to 31, 33, 51 to 59, 62, 64 to 67, 69 to 77 and 83 to 92 in the Labrador City, Wabush and Shabogamo Lake areas, Labrador, 2 reports. Labrador Mining and Exploration Company Limited and Iron Ore Company of Canada. Newfoundland and Labrador Geological Survey, Assessment File LAB/0628, 332 pages.
- Simpson, H.J., Poisson, P. and McLachlan, C. 1985: Assessment report on geological, geochemical and geophysical exploration for 1985 submission on Labrador Mining and Exploration Company Limited blocks 1, 2, 3, 5, 6, 7, 15, 17, 19, 19-1, 19-2, 19-3, 20, 21, 22, 22-4, 22-5, 22-6, 22-9, 22-10, 23 to 38, 41, 42, 51 to 54, 57 to 68, 72 to 76, 82, 84, 85, 86, 88, 89, 90, 92, 99, 101, 102, 111, 112, 116, 118, 121 and 128 in the Labrador City and Schefferville areas, Labrador, 4 volumes. Labrador Mining and Exploration Company Limited. Newfoundland and Labrador Geological Survey, Assessment File LAB/0723, 900 pages.
- Smith, L., Goldner, B. and Sauve, M. 2012: First, fourth, fifth and tenth year assessment report on geophysical exploration for licences 8931M, 10380M, 13954M, 13958M-13962M, 18330M-18332M, 18336M, 18467M, 19361M-19363M and 20499M on claims in the Shabogamo Lake to Green Water Lake area, near Labrador City, Labrador, 2 reports. Rio Tinto Exploration Canada Incorporated, Century Iron Mines Corporation, Labrador Iron Ore Royalty Corporation, Iron Ore Company of Canada and Altius Resources Incorporated. Newfoundland and Labrador Geological Survey, Assessment File LAB/1611, 90 pages.
- Steele, L. 2012: First and second year assessment report on geophysical exploration for licences 17737M, 18381M, 18383M-18384M, 18487M, 18495M, 18540M, 18611M, 18613M-18614M, 18693M-18694M, 19112M, 19114M and 20245M on claims in the Lac Viroit area, western Labrador, 2 reports. Ridgemont Iron Ore Corporation. Mahli, K. and Hicks, D., Newfoundland and Labrador Geological Survey, Assessment File LAB/1698, 68 pages.
- 2013: Second year supplementary and third year assessment report on diamond drilling exploration for licences 17737M, 18381M, 18383M-18384M, 18495M, 18540M, 18611M, 18613M-18614M, 18693M-18694M and 19112M on claims in the Lac Viroit area, western Labrador. Ridgemont Iron Ore Corporation. Mahli, K.



- and Hicks, D., Newfoundland and Labrador Geological Survey, Assessment File LAB/1696, 362 pages.
- Stubbins, J.B.  
 1974: Report of operations for 1973 in Labrador. Labrador Mining and Exploration Company Limited. Newfoundland and Labrador Geological Survey, Assessment File LAB/0261, 39 pages.
- 1975: Report of operations for 1974 in Labrador. Labrador Mining and Exploration Company Limited. Newfoundland and Labrador Geological Survey, Assessment File LAB/0337, 27 pages.
- 1976: Report of operations for 1975 in Labrador. Labrador Mining and Exploration Company Limited. Newfoundland and Labrador Geological Survey, Assessment File LAB/0338, 21 pages.
- 1978a: Report on geochemical sampling and other work on block 65 in the Carol Lake area, Labrador. Iron Ore Company of Canada and Labrador Mining and Exploration Company Limited. Newfoundland and Labrador Geological Survey, Assessment File 23G/02/0160, 10 pages.
- 1978b: Report on geochemical sampling and other work on block 23 in the Labrador City area, Labrador. Iron Ore Company of Canada and Labrador Mining and Exploration Company Limited. Newfoundland and Labrador Geological Survey, Assessment File 23B/0073, 8 pages
- 1978c: Report on geochemical sampling and other work on block 58 in the Labrador City area, Labrador. Iron Ore Company of Canada and Labrador Mining and Exploration Company Limited. Newfoundland and Labrador Geological Survey, Assessment File 23B/0086, 7 pages
- Steele, L.  
 2013: Second year supplementary and third year assessment report on diamond drilling exploration for licences 17737M, 18381M, 18383M-18384M, 18495M, 18540M, 18611M, 18613M-18614M, 18693M-18694M and 19112M on claims in the Lac Virot area, western Labrador. Ridgemont Iron Ore Corporation, Mahli, K. and Hicks, D. Newfoundland and Labrador Geological Survey, Assessment File LAB/1696, 362 pages.
- Thorniley, B.H.  
 1959: Summary report of the geology of the Lorraine No 4 and Wabush No 6 deposits in the Wabush Lake area, Labrador. Iron Ore Company of Canada. Newfoundland and Labrador Geological Survey, Assessment File 23G/0049, 22 pages.
- Tuffy, F.  
 1958: Diamond drilling program, Kissing Lake claim group. Northern Shield Resources Inc., Énergie et Ressources naturelles, Québec, Assessment Report GM 8016, 71 pages.
- 1962: Magnetic profile maps of Wabush No 3, Labrador. Labrador Mining and Exploration Company Limited. Newfoundland and Labrador Geological Survey, Assessment File 23B/0020, 33 pages.
- van Gool, J.A.M.  
 1992: The Grenville Front foreland fold-and-thrust belt in southwestern Labrador: Mid-crustal structural and metamorphic configuration of a Proterozoic orogenic thrust wedge. Unpublished Ph.D. thesis, Memorial University of Newfoundland, St. John's, 372 pages.
- van Gool, J., Calon, T. and Rivers, T.  
 1987: Preliminary report on the Grenville Front Tectonic Zone, Bruce Lake area, western Labrador. *In* Current Research, Part A. Geological Survey of Canada, Paper 87-1A, pages 435-442.
- van Gool, J.A.M., Rivers, T. and Calon, T.  
 2008: Grenville Front Zone, Gagnon terrane, southwestern Labrador: Configuration of a midcrustal foreland fold-thrust zone. *Tectonics*, Volume 27, page TC1004.
- van Nostrand, T.S. and Bradford, W.  
 2014: Geology of the Northeastern Ashuanipi Complex, western Labrador (parts of NTS 1:50 000-scale map areas 23J/6, 7, 10, 11, 14 and 23O/3). *In* Current Research. Government of Newfoundland and Labrador, Department of Natural Resources, Geological Survey, Report 14-1, pages 189-216.
- Viehmann, S., Bau, M., Hoffmannb, J.E. and Münker, C.  
 2015: Geochemistry of the Krivoy Rog Banded Iron Formation, Ukraine, and the impact of peak episodes of increased global magmatic activity on the trace element composition of Precambrian seawater. *Precambrian Research*, Volume 270, pages 165-180.
- Wallace, B.  
 2012a: First year, first year supplementary, fourth year supplementary tenth year and twelfth year assessment report on geophysical exploration for licences 8931M, 9284M, 13958M, 14985M, 16449M-16450M, 18243M, 18467M, 18675M, 18776M, 18778M and 19213M on claims in the Wabush Lake area, Labrador, 4 reports. Iron Ore Company of Canada and Labrador Iron Ore Royalty Corporation. Newfoundland and Labrador Geological Survey, Assessment File LAB/1705, 186 pages.

- 2012b: Tenth year assessment report on aerial photography and diamond drilling exploration for licence 7800M on claims in the Huguette Lake area, near Labrador City, western Labrador. Iron Ore Company of Canada. Newfoundland and Labrador Geological Survey, Assessment File 23B/14/0210, 45 pages.
- 2012c: First year supplementary, third year, fourth year supplementary, ninth and eleventh year assessment report on geophysical exploration for licences 7795M, 10380M, 13959M, 16049M, 18672M, 18674M, 19360M and 19362M on claims in the Julienne Lake area, Labrador, 3 reports. Iron Ore Company of Canada and Labrador Iron Ore Royalty Corporation. Newfoundland and Labrador Geological Survey, Assessment File 23G/02/0311, 130 pages.
- 2012d: Third year assessment file on diamond drilling exploration for licence 15885M on claims in the Wabush Lake area, western Labrador. Iron Ore Company of Canada. Newfoundland and Labrador Geological Survey, Assessment File 23G/02/0305, 32 pages.
- Wallace, B. and Leriche, T.  
2012: Eleventh year assessment report on aerial photography for licence 7799M on claims in the Labrador City area, western Labrador. Iron Ore Company of Canada. Newfoundland and Labrador Geological Survey, Assessment File LAB/1673, 24 pages.
- Wang, C., Zhang, L., Lan, C. and Dai, Y.  
2014: Rare earth element and yttrium compositions of the Paleoproterozoic Yuanjiaocun BIF in the Lüliang area and their implications for the Great Oxidation Event (GOE). *Science China Earth Sciences*, Volume 57, pages 2469-2485.
- Wardle, R.J.  
1979: Geology of the eastern margin of the Labrador Trough. Government of Newfoundland and Labrador, Department of Mines and Energy, Mineral Development Division, Report 78-9, 21 pages.
- Wardle, R.J. and Bailey, D.G.  
1981: Early Proterozoic sequences in Labrador. *In Proterozoic Basins of Canada*. Edited by F.H.A. Campbell. Geological Survey of Canada, Paper 81-10, pages 331-359.
- Wardle, R.J., James, D.T., Scott, D.J. and Hall, J.  
2002: The Southeastern Churchill Province: synthesis of a Paleoproterozoic transpressional orogen: Proterozoic evolution of the northeastern Canadian Shield. *In Lithoprobe Eastern Canadian Shield Onshore-Offshore Transect*. Canadian Journal of Earth Sciences, Volume 39, pages 639-663.
- Wardle, R.J., Ryan, B., Nunn, G.A.G. and Mengel, F.C.  
1990: Labrador segment of the Trans-Hudson Orogen: crustal development through oblique convergence and collision. *In The Early Proterozoic Trans-Hudson Orogen of North America*. Edited by J.F. Lewry and M.R. Stauffer. Geological Association of Canada, Special Paper 37, pages 353-369.
- Wardle, R.J. and van Kranendonk, M.J.  
1996: The Paleoproterozoic southeastern Churchill Province of Labrador-Quebec, Canada: orogenic development as a consequence of oblique collision and indentation. *In Precambrian Crustal Evolution in the North Atlantic Region*. Edited by T.S. Brewer. Geological Society Special Publication (London), No. 112, pages 137-154.
- Wares, R.P. and Goutier, J.  
1990: Deformational style in the foreland of the New Quebec Orogen. *Geoscience Canada*, Volume 17, pages 244-249.
- Way, R., Churchill, R. and Seymour, C.  
2007: First year assessment report on geological and geochemical exploration for licences 10501M, 11927M and 12853M-12854M on claims in the Mills Lake area, western Labrador. Altius Resources Incorporated. Newfoundland and Labrador Geological Survey, Assessment File 23B/0184, 30 pages.
- Zajac, I.S.  
1974: The stratigraphy and mineralogy of the Sokoman Iron Formation in the Knob Lake area, Quebec and Newfoundland. Geological Survey of Canada, Bulletin 220, 159 pages.

## APPENDICES

### **APPENDIX A: Sample Descriptions**

The data are available as a digital comma-separated file (.csv) through this link:

[http://www.nr.gov.nl.ca/nr/mines/geoscience/publications/reports/2019\\_01/Occasional\\_2019\\_01\\_AppendixA.csv](http://www.nr.gov.nl.ca/nr/mines/geoscience/publications/reports/2019_01/Occasional_2019_01_AppendixA.csv)

### **APPENDIX B: Major and Trace Element Data for Outcrop, Drillcore and Pulp Samples**

The data are available as a digital comma-separated file (.csv) through this link:

[http://www.nr.gov.nl.ca/nr/mines/geoscience/publications/reports/2019\\_01/Occasional\\_2019\\_01\\_AppendixB.csv](http://www.nr.gov.nl.ca/nr/mines/geoscience/publications/reports/2019_01/Occasional_2019_01_AppendixB.csv)

### **APPENDIX C: Major-element ICP-OES-FUS Standards and Duplicate Data**

The data are available as a digital comma-separated file (.csv) through this link:

[http://www.nr.gov.nl.ca/nr/mines/geoscience/publications/reports/reports/2019\\_01/Occasional\\_2019\\_01\\_AppendixC.csv](http://www.nr.gov.nl.ca/nr/mines/geoscience/publications/reports/reports/2019_01/Occasional_2019_01_AppendixC.csv)

### **APPENDIX D: Trace-element ICP-OES Standards and Duplicate Data**

The data are available as a digital comma-separated file (.csv) through this link:

[http://www.nr.gov.nl.ca/nr/mines/geoscience/publications/reports/2019\\_01/Occasional\\_2019\\_01\\_AppendixD.csv](http://www.nr.gov.nl.ca/nr/mines/geoscience/publications/reports/2019_01/Occasional_2019_01_AppendixD.csv)

### **APPENDIX E: Trace-element ICP-MS-FUS Standards and Duplicate Data**

The data are available as a digital comma-separated file (.csv) through this link:

[http://www.nr.gov.nl.ca/nr/mines/geoscience/publications/reports/2019\\_01/Occasional\\_2019\\_01\\_AppendixE.csv](http://www.nr.gov.nl.ca/nr/mines/geoscience/publications/reports/2019_01/Occasional_2019_01_AppendixE.csv)

### **APPENDIX F: Exploration Drill-log Database (post-2000)**

The data are available as a digital comma-separated file (.csv) through this link:

[http://www.nr.gov.nl.ca/nr/mines/geoscience/publications/reports/2019\\_01/Occasional\\_2019\\_01\\_AppendixF.csv](http://www.nr.gov.nl.ca/nr/mines/geoscience/publications/reports/2019_01/Occasional_2019_01_AppendixF.csv)





**SITE ADDRESS:**  
NATURAL RESOURCES  
GEOLOGICAL SURVEY  
50 ELIZABETH AVENUE  
ST. JOHN'S, NL, A1A 1W5  
(709)729-3159  
Email: [pub@gov.nl.ca](mailto:pub@gov.nl.ca)  
Website: [www.nr.gov.nl.ca/nr/](http://www.nr.gov.nl.ca/nr/)

